# SYNTHESIS OF $C_2$ SYMMETRIC CYCLOBUTANES AND γ-BUTYROLACTONES VIA PHOTOINDUCED ELECTRON TRANSFER

Michelle Riener

A dissertation submitted to the faculty of the University of North Carolina at Chapel Hill
in partial fulfillment of the requirements for the degree of Doctor of Philosophy in the Department of Chemistry.

Chapel Hill
2014

Approved by:

David A. Nicewicz

Jeff S. Johnson

Wei You

Marcey L. Waters

Alex J. Miller

© 2014
Michelle Riener
ALL RIGHTS RESERVED

# ABSTRACT

Michelle Riener: Synthesis of $C_2$ Symmetric Cyclobutanes and γ–Butyrolactones via Photoinduced
Electron Transfer
(Under the direction of David A. Nicewicz)

## I. Organic Photoredox Catalysis

An overview of the principles concerning photoredox catalysis, alkene oxidation, organic and inorganic photooxidants applied in organic chemistry is discussed.

## II. [2+2] Cycloaddition Reactions of Alkenes *via* Single Electron Transfer Catalysis

A novel method for the diastereoselective synthesis of lignan cyclobutanes via dimerization of simple olefins is presented. Emphasis is on a unique strategy for controlling detrimental cycloreversion and polymerization processes via the use of appropriately tuned electron relays. This method is applied to the direct synthesis of two naturally produced cyclobutane compounds; magnosalin, and pellucidin A, as well as a third natural product, endiandrin A via derivatization.

## III. Synthesis of γ-Butyrolactones via Polar Radical Crossover Cyclization Reactions of Unsaturated Acids And Alkenes

The development of a convergent synthesis of biologically relevant γ-butyrolactone scaffolds by an electron-transfer mediated polar-radical crossover cycloaddition is covered. This transformation proceeds with exquisite regioselectivity and relies on the implementation of a dual-catalyst system. The utility of this method is showcased via the synthesis of two bioactive natural products within the paraconic acid family.

# ACKNOWLEDGEMENTS

First and foremost, I would like to thank my parents for their continuous support and encouragement throughout my graduate career. I would also like to thank my sisters, Romina and Nicole Riener, for their frequent phone calls and texts to check in and keep me sane. I am also very grateful for the support and direction I received from my PI, Dave Nicewicz. From the beginning, Dave knew I had an interest in pursuing a career in industry. I realize this mentality of acceptance is not always present in a PI, so I am genuinely grateful for his open mindedness and help. I would also like to acknowledge Dave Hamilton, Andrew Perkowski, Jean-Marc Granjean, and Tien Nguyen, who with me make up the five 5th years graduating this semester. We started off with no older graduate students to look up to, and had to guide each other from the beginning. I think we have learned a lot about ourselves, and of each other. I am very proud of how far we have come.

I also wanted to acknowledge Mary Zeller, who has also focused her efforts towards the success of the $\gamma$–butyrolactone project. I really appreciate your insight and our frequent discussions on how to improve our method. Additionally, I would like to thank my committee as well as the Alexanian, Johnson, and Crimmins group for granting us access to various chemicals and spectrometers.

# TABLE OF CONTENTS

**LIST OF TABLES** ....... vii

**LIST OF FIGURES** ....... viii

**LIST OF ABBREVIATIONS AND SYMBOLS** ....... xii

**CHAPTER ONE: PHOTOINDUCED ELECTRON TRANSFER** ....... 1

- 1.1 Introduction ....... 1
- 1.2 Background ....... 1
  - 1.2.1 Organic Photosensitizers ....... 5
  - 1.2.2 Alkene Oxidation ....... 8
  - 1.2.3 Co-Catalysts in Photoredox Catalysis ....... 10
  - 1.2.4 Chemical Oxidation ....... 12
- 1.3 Conclusion ....... 12
- 1.4 References ....... 13

**CHAPTER TWO: [2+2] CYCLOADDITION REACTIONS OF ALKENES VIA SINGLE ELECTRON TRANSFER CATALYSIS**

- 2.1 Introduction ....... 15
- 2.2 2+2 Cycloadditions ....... 15
  - 2.2.1 Application to Lignan Natural Products ....... 15
  - 2.2.2 Direct Ultraviolet [2+2] Cycloadditions ....... 19
  - 2.2.3 Radical Anionic Cycloadditions ....... 22
  - 2.2.4 [2+2] via Energy Transfer ....... 25
  - 2.2.5 Electrochemical Cycloadditions ....... 27
  - 2.2.6 Radical Cationic Cycloadditions ....... 31
- 2.3 Synthesis of Lignan Cyclobutanes via an Organic Single-Electron Oxidant Electron-Relay System ....... 41

2.4 Conclusion ... 53

2.5 Experimental ... 55

2.6 References ... 82

## CHAPTER THREE: SYNTHESIS OF γ-BUTYROLACONES *via* POLAR RADICAL CROSSOVER CYCLOADDITION REACTIONS OF UNSATURATED ACIDS AND ALKENES

3.1 Introduction ... 86

3.2 Natural Products: Isolation and Bioactivity ... 87

- 3.2.1 Previous Syntheses of Methylenolactocin and Protolichesterinic Acid ... 88

3.3 Synthesis of γ-Butyrolactones ... 92

- 3.3.1 Methods For The Synthesis of Disubstituted γ-Butyrolactones ... 92
- 3.3.2 Methods For The Synthesis of Trisubstituted γ-Butyrolactones ... 98
- 3.3.3 Synthesis α–Methylene-γ-Butyrolactones ... 104

3.4 Synthesis of γ-Butyrolactones via Polar Radical Crossover Cyclization ... 108

3.5 Results for the Synthesis of Substituted γ-Butyrolactones ... 116

- 3.5.1 Synthesis of Methylenolactocin and Protolichesterinic Acid ... 124

3.6 Conclusion and Outlook ... 126

3.7 Experimental ... 128

3.8 References ... 164

# LIST OF TABLES

Table 2-1 Effect of Electron Relays as an Additive in the [2 + 2] Dimerization of Anethole ........ 44

Table 2-2 Scope of [2 + 2] Dimerization of Aromatic Alkenes via Photoinduced Electron Transfer (part 1) ........ 46

Table 2-3 Scope of [2 + 2] Dimerization of Aromatic Alkenes via Photoinduced Electron Transfer (part 2) ........ 48

Table 2-4 [2 + 2] Dimerization of Terminal Aromatic Alkenes via Photoinduced Electron Transfer ........ 50

Table 3-1 Optimization of Reaction Conditions For Synthesis of γ-Butyrolactones ........ 118

Table 3-2 Reaction Scope For γ-Butyrolactones From β-Methylstyrene and α,β−Unsaturated Acids ........ 119

Table 3-3 Reaction Scope For γ-Butyrolactones From Oxidizable Alkenes and α,β−Unsaturated Acids ........ 121

# LIST OF FIGURES

Figure 1-1 Jablonski Diagram Depicting Fluorescene and Phosphorescence ............................... 3

Figure 1-2 Single Electron Transfer via Light Excitation ........................................................... 4

Figure 1-3 Typical Organic Electron Acceptors ......................................................................... 5

Figure 1-4 Synthesis of TPT and Derivatives ............................................................................. 6

Figure 1-5 Stability of subsequent radical anions for *p*OMe-TPT and *p*F-TPT ............................ 7

Figure 1-6 Oxidation Potentials of Various Alkenes .................................................................... 8

Figure 1-7 Trend in Oxidation Potential of Styrene Derivatives .................................................. 9

Figure 1-8 Photoinduced Nucleophilic Addition of Ammonia and Isopropylamine ................... 10

Figure 1-9 Mechanism for Regeneration of Photooxidant with the Aid of Diazonium **1** ........... 11

Figure 1-10 Common Reductive and Oxidative Co-Catalysts ..................................................... 11

Figure 1-11 Diels Alder Reaction Promoted by Chemical Single Electron Oxidation .................. 12

Figure 2-1 Skeletal Structure of Lignan vs Neolignan ............................................................... 16

Figure 2-2 Lignans Possessing Anti-Inflammatory Properties ................................................... 17

Figure 2-3 Direct Cyclobutane Lignan Synthesis via Photolytic Dimerization .......................... 18

Figure 2-4 Direct Cyclobutane Lignan Synthesis via Photoinduced Electron Transfer .............. 19

Figure 2-5 UV-Promoted Dimerization of N-Substituted Indoles .............................................. 20

Figure 2-6 Key Transformation for the Enantioselective Synthesis of Punctaporonin ............... 20

Figure 2-7 Chiral Hydrogen Template Used to Impart Enantioinduction .................................. 21

Figure 2-8 Lewis Acid Catalysis for the Enantioselective [2+2] Photocycloaddition ................ 22

Figure 2-9 Cathodic Reduction Generating Radical Anions for Cyclization of Bis(enone) ....... 23

Figure 2-10 Chemically-Induced Radical Anion Cyclization of Bis(enone) ............................... 23

Figure 2-11 Ruthenium Catalyzed Radical Anion Photocyclization of Bis(enones) .................... 24

Figure 2-12 Crossed Intermolecular Cycloaddition of Acrylic Enones ....................................... 25

Figure 2-13 Intermolecular Cycloaddition via Energy Transfer .................................................. 26

Figure 2-14 Comparison of Radical Cation vs Energy Transfer Products .................................... 26

Figure 2-15 Electrocatalytic [2+2] Cycloaddition with Enol Ethers And Alkenes ....................... 28

Figure 2-16 Scope For Electrocatalytic [2+2] of Cyclic Enol Ethers And Alkenes ...................... 29

Figure 2-17 Proposed Mechanism For Electrocatalytic [2+2] of Cyclic Enol Ethers

And Alkenes........................................................................................................30

Figure 2-18 Cycloreversion Of Cyclobutanes Via Anodic Oxidation..........................................30

Figure 2-19 Cross Metathesis Reactions Of Enol Ethers And Terminal Alkenes.........................31

Figure 2-20 Proposed Radical Cation Chain Mechanism...........................................................33

Figure 2-21 Dimerization and Cycloreversion of *trans*-Anethole ..............................................34

Figure 2-22 Dimerization of *trans* -Anethole in the Presence of 9-Cyanoanthracene ..................34

Figure 2-23 Dimerization of p-Methoxystyrene in the Presence of Chloranil ..............................35

Figure 2-24 Dimerization of Phenyl Vinyl Ether in the Presence of Photooxidants.....................35

Figure 2-25 Redox Photosensitization for the Dimerization of Indene ........................................36

Figure 2-26 Redox Photosensitization Mechanism Proposed by Sakurai ....................................36

Figure 2-27 Tuning Redox Properties of Ruthenium Complexes ................................................37

Figure 2-28 Optimization of Conditions for Homodimerization of *trans*-Anethole .....................38

Figure 2-29 Scope for the Heterodimerization of Alkenes with *trans*-Anethole ..........................39

Figure 2-30 Scope for the Heterodimerization of Alkenes with 4-Methoxystyrene .....................41

Figure 2-31 Synthesis of $C_2$ Symmetric Cyclobutanes via Photoinduced Electron Transfer .........42

Figure 2-32 Net Stabilization Elucidates Reactivity Pattern of Electron Rich Substituted Styrenes.........................................................................................47

Figure 2-33 X-Ray Crystal Structure of Pellucidin A ..................................................................51

Figure 2-34 Direct [2+2] Synthesis of Magnosalin as a Single Diastereomer ..............................51

Figure 2-35 Elaboration of Anethole Dimer to Furnish Endiandrin A.........................................52

Figure 2-36 Effect of Electron Relay on Cycloreversion ...........................................................52

Figure 2-37 Proposed Mechanism For Photoinduced Dimerization ............................................53

Figure 3-1 Numbering Scheme And Skeletal Structure of γ-Butyrolactones .............................86

Figure 3-2 Biologically Relevant Paraconic Acids....................................................................88

Figure 3-3 Linear Synthesis For Protolichesterinic Acid ..........................................................89

Figure 3-4 Direct Synthesis of γ-Butyrolactone Core: Application to Protolichesterinic Acid ...90

Figure 3-5 Five Step Synthesis For Methylenolactocin.............................................................91

Figure 3-6 Synthesis For Methylenolactocin Arising from Tulipalin .........................................92

Figure 3-7 Lactonization via 4-Hydroxycarbonyl .....................................................................92

Figure 3-8 3,4 Disubstituted γ-Butyrolactones via Aldol Cyclization........................................93

Figure 3-9 3,4 Disubstituted γ-Butyrolactones via NHC Catalysis............................................94

Figure 3-10 2,3,4 Trisubstituted γ-Butyrolactones via NHC Catalysis........................................95

Figure 3-11 3,4 Disubstituted γ-Butyrolactone via (-) Menthol-Derived NHC Catalysis.............96

Figure 3-12 Menthol Derived-Chiral Butenolides........................................................................97

Figure 3-13 Conjugate Addition of Enantiopure Butenolides......................................................98

Figure 3-14 *cis*-3,4-Substituted γ-Lactones With Geminal Dimethyl Substitution.......................99

Figure 3-15 γ-Lactones From Unsymmetrical Ketones and Activated Cyclopropanes..............100

Figure 3-16 γ-Lactones From Symmetrical Ketones and Activated Cyclopropanes...................101

Figure 3-17 2,3,4-Trisubstituted γ-Lactones From Aldehydes and Activated Cyclopropanes....102

Figure 3-18 Synthesis of (-) Dihydropertusaric Acid................................................................103

Figure 3-19 Dreiding-Schmidt Reaction Of α-(Bromomethyl)acrylic Esters With Carbonyls....104

Figure 3-20 Synthesis Of α-Methylene-γ-Butyrolactones From 2-(Hydroxymethyl)acrylates....106

Figure 3-21 Synthesis Of α-Methylene-γ-Butyrolactones From Allylboronates.........................107

Figure 3-22 Comparison Between Standard Substrate Reactivity And Polarity Reversal Reactivity..........................................................................................................108

Figure 3-23 Catalytic anti-Markovnikov Alkene Hydroacetoxylation.......................................109

Figure 3-24 Catalytic Polar Radical Crossover Cycloadditions of Alkenes and Alkenols..........110

Figure 3-25 Partial Substrate Scope Tetrahydrofuran via PRCC...............................................111

Figure 3-26 Proposed Beckwith Transition State Resulting in *cis-trans* Selectivity .................112

Figure 3-27 Synthesis And Proposed Mechanism For Ring Closure of β-Phenylseleno-Crotonates..........................................................................................................112

Figure 3-28 Scope For Ring Closure of β-Phenylseleno-Crotonates and Acyrolates.................113

Figure 3-29 Iridium Catalyzed Photoredox Catalysis................................................................114

Figure 3-30 Proposed Mechanism for Iridium Catalyzed Photoredox Catalysis........................115

Figure 3-31 Comparison of Product Regioselectivity Between Iridium Catalyzed Method and Desired Method For Further Derivatization To Paraconic Acids........116

Figure 3-32 Epimerization of γ-Butyrolactone..........................................................................122

Figure 3-33 Proposed Mechanism for the Synthesis of γ-Butyrolactones via Photoinduced Electron Transfer..............................................................................123

Figure 3-34 Retrosynthesis Analysis of Protolichesterinic Acid ........ 124
Figure 3-35 Synthesis of Protolichesterinic Acid ........ 125
Figure 3-36 Epimerization of Protolichesterinic Acid Intermediate ........ 126
Figure 3-37 Synthesis of Methylenolactocin ........ 126
Figure 3-38 Possible Transformations Derived From Current Work ........ 127

# LIST OF ABBREVIATIONS AND SYMBOLS

| | |
|---|---|
| 2D-NMR | two-dimensional nuclear magnetic resonance |
| 2Me-THF | 2-methyl tetrahydrofuran |
| Å | ångström |
| Ac | acetate |
| AIBN | azobisisobutyronitile |
| Ar | aryl |
| aq | aqueous |
| atm | atmospheres |
| BET | back electron transfer |
| Bn | benzyl |
| br | broad |
| br s | broad singlet |
| $^n$Bu | *normal*-butyl |
| $^t$Bu | *tert*-butyl |
| bpm | bipyrimidine |
| bpy | bipyridine |
| bpz | bipyrazine |
| Bz | benzoyl |
| C# | carbon # |
| $^{13}$C NMR | carbon nuclear magnetic resonance spectroscopy |
| cat | catalytic amount or catalyst |
| conv | conversion |
| COSY | correlated spectroscopy |

| | |
|---|---|
| Cy | cyclohexyl |
| C–C | carbon-carbon bond |
| d | doublet or days |
| DABCO | 1,4-diazabicyclo[2.2.2]octane |
| DBU | 1,8-diazabicyclo[5.4.0]undec-7-ene |
| DCE | 1,2-dichloroethane |
| DCM | dichloromethane |
| dd | doublet of doublet |
| ddt | doublet of doublet of triplets |
| DIBAL | diisobutylaluminum hydride |
| DMAP | 4-*N,N*-dimethylaminopyridine |
| DMF | *N,N*-dimethylformamide |
| DMI | 1,3-dimethylimidazolidinone |
| DMSO | dimethyl sulfoxide |
| dq | doublet of quartet |
| dr | diastereomeric ratio |
| dt | doublet of triplet |
| $E^+$ or El | electrophile |
| *ent* | enantiomeric |
| eq | equation |
| equiv. | equivalents |
| er | enantiomeric ratio |
| Et | ethyl |
| EtOH | ethanol |

| | |
|---|---|
| $Et_3N$ | triethylamine |
| $Et_2O$ | diethyl ether |
| EtOAc | ethyl acetate |
| EWG | electron withdrawing group |
| F | Faraday |
| *fac* | facial |
| $\gamma$ | gamma |
| h | hour |
| $h\nu$ | light |
| $^1$H NMR | proton nuclear magnetic resonance spectroscopy |
| $HCO_2H$ | formic acid |
| HOAc | acetic acid |
| HMDS | 1,1,1,3,3,3-hexamethyldisilazane |
| HRMS | high resolution mass spectroscopy |
| Hz | hertz |
| I | intermediate |
| IR | infrared spectroscopy |
| *J* | coupling constant |
| *k* | reaction rate |
| kcal | kilocalorie |
| $\lambda$ | wavelength |
| L | liter |
| LA | Lewis acid |
| LDA | lithium diisopropylamide |

| | |
|---|---|
| LUMO | lowest unoccupied molecular orbital |
| M | metal or molarity |
| m | multiplet |
| *m* | *meta* |
| mCPBA | m-chloroperoxybenzoic acid |
| Me | methyl |
| MeCN | acetonitrile |
| MeOH | methanol |
| mg | milligram |
| MHz | megahertz |
| min | minutes |
| mL | milliliter |
| mmol | millimole |
| MS | molecular sieves |
| MTBE | methyl *tert*-butyl ether |
| *n* | number of atoms or counterions |
| nm | nanometer |
| NMA | N-mesityl acridinium tetrafluoroborate |
| nOe | nuclear overhauser enhancement |
| NOESY | nuclear overhauser enhancement spectroscopy |
| NR | no reaction |
| Nu | nucleophile |
| *o* | *ortho* |
| *p* | *para* |

| | |
|---|---|
| P | product |
| PET | photoinduced electron transfer |
| PG | protecting group |
| Ph | phenyl |
| Phth | phthalimidyl |
| PMP | *para*-methoxyphenyl |
| PMN | phenylmalononitrile |
| ppm | parts per million |
| ppy | 2-phenylpyridine |
| PPTS | pyridinium *p*-toluenesulfonate |
| PTSA | p-toluenesulfonic acid |
| $^{i}$Pr | *iso*-propyl |
| q | quartet |
| $R_f$ | retention factor |
| *rac* | racemic |
| RCHO | aldehyde |
| Red | reduction |
| rt | room temperature |
| s | singlet |
| S | starting material |
| SCE | saturated calomel electrode |
| $S_N1$ | unimolecular nucleophilic substitution |
| $S_N2$ | bimolecular nucleophilic substitution |
| T | temperature |

| | |
|---|---|
| t | triplet |
| TBAF | tetrabutylammonium fluoride |
| Tf | trifluoromethanesulfonyl |
| TFA | trifluoroacetic acid |
| THF | tetrahydrofuran |
| TLC | thin-layer chromatography |
| TMS | trimethylsilyl |
| Tf/triflate | trifluoromethanesulfonate |
| Ts | *para*-toluenesulfonyl |
| TS | transition state |
| UV | ultraviolet |
| X | anionic ligand, halide, substituent, or number |
| $\delta$ | chemical shift or partial charge |
| $\Delta G$ | change in free energy |
| $\lambda$ | wavelength |
| µL | microliter |
| V | volt |

# CHAPTER ONE: ORGANIC PHOTOREDOX CATALYSIS

## 1.1 1ntroduction

Implementing visible light to catalyze reactions has previously been viewed as ideal yet unrealistic, as many reagents are inert to such long wavelengths. To effect productive chemistry, small molecules require a specific wavelength of light, while irradiation at smaller or larger wavelengths result in compound degradation or no reaction. Yet, there is great reward in creating a class of transformation where light is employed as the energy source. As photocatalyzed reactions proceed via a different reaction mechanism, distinct regio- and stereoselectivities are obtained. This allows for the formation of complex molecules that might not be easily accessible otherwise. If appropriately tuned, organophotoredox catalysis could eliminate the need for high temperatures, pressures, or the use of toxic, expensive, or precious metals. Addressing this problem is the focus of this thesis, whereby the combination of easily synthesized organic catalysts with specific photophysical and redox properties are employed. This development has produced transformations exhibiting exquisite regioselectivity and diastereoselectivity, arising from cheap and commercially available material.

## 1.2 Background

Organic photochemistry is an area of growing interest, rapidly establishing itself as a unique field within organic chemistry. Though initial organo-photochemical discoveries were published in the 1960's, only recently has their utility been explored. Both photoinduced electron transfer and photolytic reactions proceed with the aid of light, however these transformations occur through different mechanisms. To effect a photolytic transformation, ultraviolet light is implemented to forge radical formation via homolytic bond cleavage. This process results in highly reactive intermediates susceptible to fast recombination. Difficulty in controlling photolytic reactions is attributed to the high energy of ultraviolet light, which commonly results in low yields and formation of numerous side products with varying regio- and diastereoselectivity. As opposed to photolytic conditions, photoinduced electron transfer mechanisms are operable with visible light; this controlled process is successful when in the presence of appropriately matched electron donor and acceptor molecules. An electron donor reagent is distinguished by possessing electron-rich groups and is capable of stabilizing a radical cationic charge. Conversely, an electron acceptor molecule possesses electron-deficient groups and is best suited for carrying a radical anionic charge. Due to preferential ionic stability, this produces reactive single-electron species with umpolung character, as an electron donor molecule is transposed to exhibit radical cationic character. This method is appealing, as it affords products not directly accessible via thermal mechanisms.

Depending on the structure of the light-sensitive species, two mechanisms may be invoked. If the donor molecule (D) is sensitive to light, an electron-rich excited species is generated, which serves as a potent single electron reductant. When in the presence of an appropriate substrate, this reductant undergoes single electron transfer to produce a radical anionic substrate. Conversely, if the acceptor molecule (A) is sensitive to light, a similar excited species may be generated; this reagent reacts as a potent single electron oxidant and produces radical cationic species from a suitable electron rich substrate. When in the absence of a donor molecule (D), irradiation of the acceptor molecule (A) results in fluorescence, where the electron promoted to their singlet state ($S_1$) during irradiation is presumed to emit a photon during relaxation to $S_0$ (Figure 1-1). Phosphorescence occurs when the promoted electron at $S_1$ undergoes intersystem crossing to $T_1$ and is followed by photon emission.

**Figure 1-1: Jablonski Diagram Depicting Fluorescene and Phosphorescence**

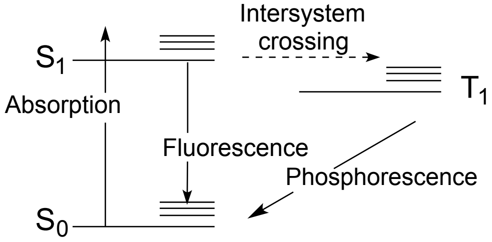

We were interested in utilizing electron transfer to afford radical cations, by employing visible light-sensitive acceptor molecules and light-insensitive donor molecules. Though this process has been understood for decades, the lack of appropriate light-sensitive acceptors capable of catalyzing useful transformations has hindered its development. Only with the recent discovery of visible light-sensitive reagents has this mechanism been exercised and exploited. The excited state energy of an acceptor molecule is correlated to the energy of the photon, and may be quenched in the presence of a donor molecule (D). Though the donor molecule is not directly excitable with visible light, it could undergo electron transfer if it exhibits specific redox properties. As depicted in Figure 1-2, the donor molecule (D) typically possesses a highest occupied molecular orbital (HOMO) that is lower in energy than the lowest unoccupied molecular orbital (LUMO) of the acceptor molecule (A). Therefore in its ground state, the donor molecule (D) is not susceptible to electron transfer, as the process is endergonic and not thermodynamically favorable. When the acceptor molecule (A) is sensitized in the presence of light, a change in electronic configuration occurs; this is depicted by promotion of one electron residing in the HOMO to its lowest lying LUMO. Excitation of the acceptor molecule produces an electron hole in the previously noted HOMO of (A), which lies below the HOMO of (D). Thermodynamics now allow for the exergonic process to occur, where one electron from the donor molecule is transferred to the acceptor molecule. This produces an electron deficient species ($D^{\bullet+}$) and a single electron rich species ($A^{\bullet-}$). This single electron transfer is labeled as the desired process, however if certain parameters of (A) and (D) are not met, back electron transfer (BET) may be observed. This undesired process occurs if the charged species ($D^{\bullet+}$) and ($A^{\bullet-}$) are in close proximity, or if one of the species is severely destabilized.[1]

**Figure 1-2: Single Electron Transfer via Light Excitation**

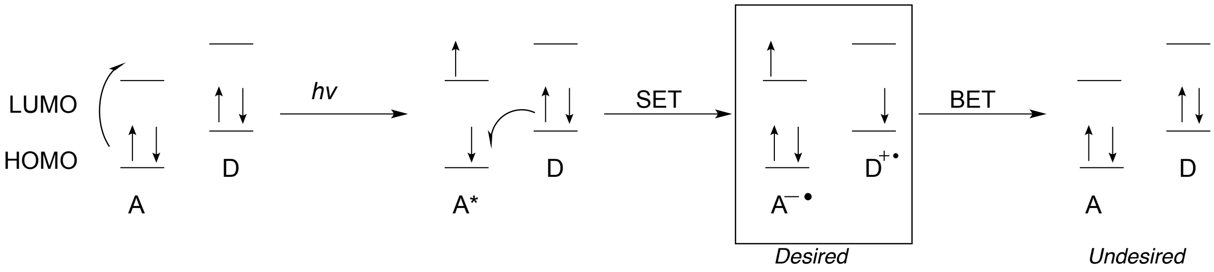

Photoinduced electron transfer may occur from either the single or triplet state of the sensitizer; yet these variants are distinguishable. Electron exchange occurring from the triplet state typically exhibits higher efficiency, and is attributed to a slower rate of back electron transfer (BET). Additionally, the longer-lived triplet state also allows for higher likelihood of reactivity. Though shorter lived, singlet states have higher oxidation capabilities, but are more likely to participate in back electron transfer due to their higher reactivity and resulting instability.[2] For this reason, the choice of sensitizer is extremely important, and can be detrimental to the reaction system if improperly considered.

The likelihood of a reaction partaking in electron transfer can be predicted by considering the simplified Weller equation (equation 1), where the half wave oxidation potential of D ($E_{1/2}^{ox}\ (D)$) and the half wave reduction potential of (A) ($E_{1/2}^{red}\ (A)$) are included. The excitation energy of (A) ($\Delta E_{excit}$) may be combined with the half wave reduction potential of (A) if the excited state reduction potential of the acceptor molecule ($E_{red}^{*}\ (A)$) is known. The coulomb interaction energy $\Delta E_{coul}$ is a calculated variable, and is commonly disregarded when predicting electron transfer (Equation 2).[3] In order to be thermodynamically favorable, Gibbs free energy $\Delta G$ must be equal to or below zero. This may be achieved if the excited state reduction potential of an acceptor molecule ($E_{red}^{*}\ (A)$) is large, and if the half wave oxidation potential of the donor molecule ($E_{1/2}^{ox}\ (D)$) is small.

$$\Delta G = E_{1/2}^{ox}\ (D) - E_{1/2}^{red}\ (A) - \Delta E_{excit}(A) + \Delta E_{coul} \qquad \textit{Equation 1}$$

$$\Delta G = E_{1/2}^{ox}\ (D) - E_{red}^{*}\ (A) \qquad \textit{Equation 2}$$

Solvent polarity is an important variable that can drastically affect the rate and likelihood of electron transfer. This variable plays a role in stabilization and separation of the resulting charged species. Depending on the solvent polarity, various species are proposed to form. In a nonpolar solvent, it is predicted that only an exciplex and contact ion pair are formed (Equation 3). However, if a more polar solvent is used, solvent separated ion pairs and free radical ions are also presumed to form.[3] For these reasons, polar solvents minimize back electron transfer, and induces electron transfer to afford free radical ions.

$$A + D = \left(A^{\delta-}D^{\delta+}\right) \leftrightarrow \left(A^{\cdot-}D^{\cdot+}\right) \leftrightarrow \left(A_s^{\cdot-}D_s^{\cdot+}\right) \leftrightarrow A_s^{\cdot-} + D_s^{\cdot+} \qquad \textit{Equation 3}$$

### 1.2.1 Organic Photosensitizers

Various electron accepting sensitizers including dicyanobenzene (DCB), dicyanonaphthalene (DCN), and dicyanoanthracene (DCA) are depicted in Figure 1-3. These three sensitizers require ultraviolet or near UV for excitation, and are suspected to react solely from their singlet energy state. Regardless of their high oxidizability, these cyanoarenes are not ideal sensitizers for photoinduced electron transfer. This stems from their inability to suppress back electron transfer (BET); which is extremely fast and undesirable (Figure 1-3).

**Figure 1-3: Typical Organic Electron Acceptors[4,5]**

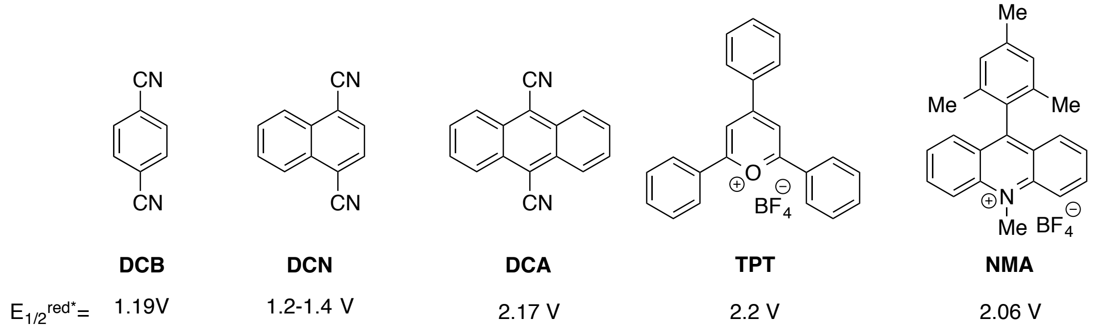

For this reason, great advances in this field transpired when photooxidizing salts were revealed as successful and superior sensitizers. For instance, the use of 2,4,6-triphenylpyrylium tetrafluoroborate (TPT) salt is an excellent sensitizer as it absorbs visible light, and therefore requires less energetic light than other photooxidants. This improvement may aid in decreased formation of byproducts, as only the compound of interest may be sensitized at the long wavelength. Another ideal feature is the subsequent dissociation between the $BF_4^-$ counterion that occurs once the photooxidant and substrate undergo single electron transfer. Net charge separated pairs do not form between the radical anionic acceptor and radical cationic donor species, which results in the minimization of back electron transfer. This in turn enhances free-radical formation.[6] Moreover, photophysical experiments suggest TPT primarily reacts through its triplet state, which correlates to a longer-lived triplet sensitizer.

**Figure 1-4: Synthesis of TPT and Derivatives[7]**

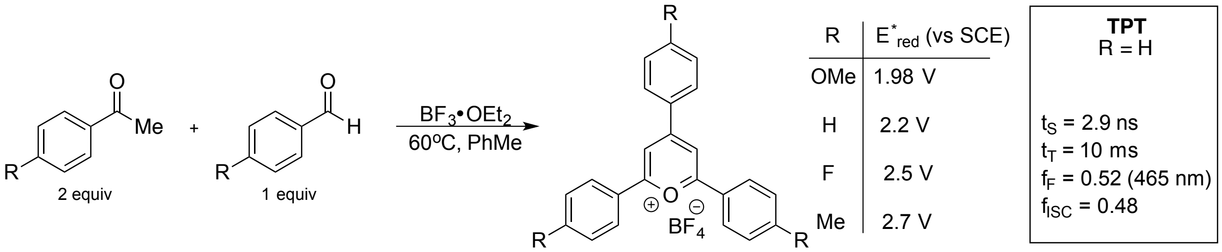

When dissolved in dichloromethane, TPT exhibits two absorption bands at 417 nm and 369 nm. It is suggested that the shorter wavelength absorption is associated to the 4-arylpyrylium moiety, while the longer wavelength is ascribed to the 2,6-diarylpyrylium moiety.[6] From a practical perspective, TPT is an ideal organophotooxidant for its ease in synthesis and derivatization. Not only is TPT commercially available, but the brightly colored photooxidant can be quickly made with two equivalents of acetophenone to one equivalent of benzaldehyde in the presence of $BF_3.OEt_2$. Ease in synthesis allows for rapid and direct derivatization to form sensitizers with various functionality around the aromatic ring. Derivatization produces sensitizers with different absorbance and emission wavelengths, as changing the electron-donating or releasing properties of the aromatic groups has a direct impact on its redox properties (Figure 1-4). If electron rich methoxy groups are appended to the three aromatic rings, the excited state reduction potential of a 2,4,6-trimethoxypyrylium is decreased to +1.98 V. In theory, employing a photooxidant with electron rich substitution may result in faster catalytic turnover since the resulting reduced species possesses electron-donating substituents and cannot fully stabilize the intermediate (Figure 1-5). If an electron withdrawing fluorine atom is appended, the excited state reduction potential is increased to +2.5 V. Theoretically, this photooxidant is capable of reacting with a wider range of substrates; however, a stable radical species is produced following single electron transfer. This radical species may exhibit a rate decrease in subsequent single electron reduction to regenerate the neutral species. This decrease in rate is attributed to increased stability of the intermediate.

**Figure 1-5: Stability of subsequent radical anions for *p*OMe-TPT and *p*F-TPT**

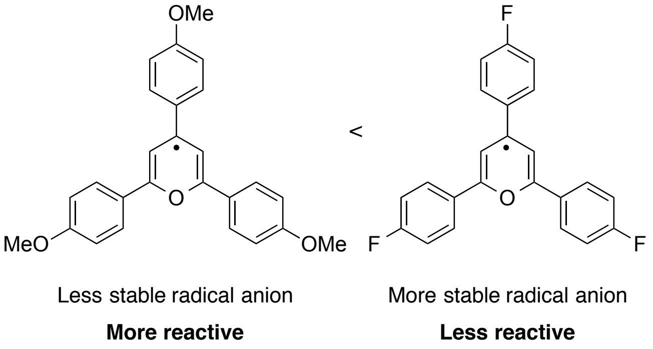

Recently, the Fukuzumi group published a report on a new photooxidant with excellent oxidizing power. 9-Mesityl-10-methylacridinium tetrafluoroborate (NMA) is a robust reagent with a calculated excited state reduction potential of +2.16 V in its locally excited singlet and +1.43 V in its triplet state, respectively.[8] This acridinium is presumed to primarily react via its singlet state, and possesses two absorption bands at 480 nm and 520 nm wavelengths, where the mesityl radical cation moiety is suggested to form with 480 nm light.[9] Similarly to the TPT salts, this mesityl acridinium salt can be simply made in 4 steps from commercially available material. More importantly, NMA is an excellent photooxidant due to its long-lived charge separated state.[10] This extended lifetime is attributed to minimal loss in charge reorganization energy, which was calculated to be +0.79 V. In their ground state, both 9-mesityl-10-methylacridinium tetrafluoroborate and the 2,4,6-trimethoxyoxypyrylium tetrafluoroborate have half wave reduction potentials of −0.36 V and −0.56 V, respectively, and are not capable of alkene oxidation. On the contrary, both are efficient oxidants when in their excited states, ($E^{red*} = +1.97\ V$) and ($E^{red*} = +2.06\ V$), respectively.

### 1.2.2 Alkene Oxidation

Alkenes are a versatile functional group in organic synthesis, and their utility is proven by the numerous methods for further functionalization and derivatization in the literature. They are ideal starting points in a chemical transformation as alkenes are easily synthesized; additionally, many are naturally abundant, commercially available, and cheap. Frequently, oxidation of alkenes refers to dihydroxylation, or diamination, where the number of carbon-oxygen or carbon-nitrogen bonds is increased. In the context of photoinduced electron transfer, alkene oxidation refers to the removal of electrons, which typically originate from a π-orbital. The simplest way to predict alkene oxidation is to consider its oxidation potential.

**Figure 1-6: Oxidation Potentials of Various Alkenes**

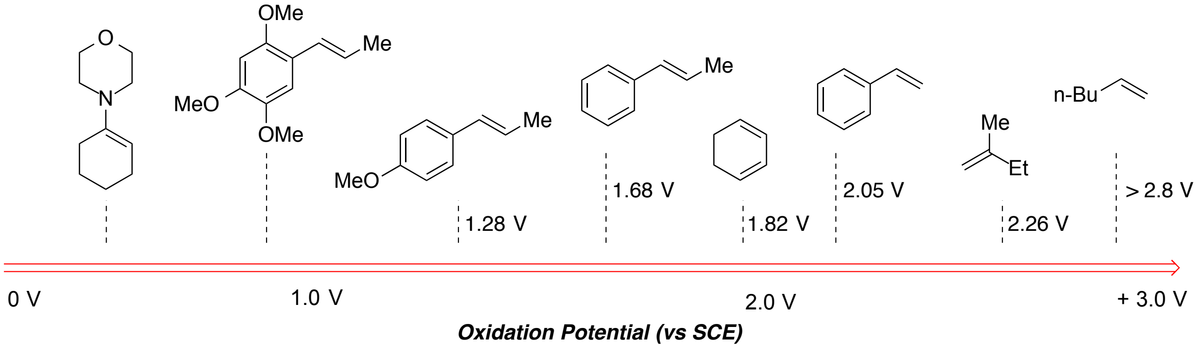

Terminal aliphatic alkenes such as 1-octene have oxidation potentials slightly above +2.8 V, and therefore are difficult substrates to oxidize. However as substitution is increased and conjugation is incorporated, the oxidation potential is decreased. For instance, styrene has a reported half wave oxidation potential of +2.05 V,[11] while 2-methy-l-butene exhibits a half wave oxidation potential of +2.26 V.[12] 1,2-disubstituted conjugated alkenes and those with pendent electron donating groups drastically decrease the oxidation potential, which is due to increased stability of the subsequent radical cation. This is observed by comparing styrene, β-methylstyrene ($E_{1/2}^{ox} = +1.68\,V$), and 4-methoxy-β-methylstyrene (*trans*-anethole) ($E_{1/2}^{ox} = +1.28\,V$). The +0.4 V difference in stability between β-methylstyrene and *t*-anethole suggests that substitution around the aromatic ring has a greater impact at decreasing the oxidation potential than substitution of the alkene. In agreement with this trend, 2,4,5-trimethoxy-β-methylstyrene possesses an oxidation potential below 1.0 V. Enol ether and eneamine substrates are less positive than the alkenes, rendering them extremely susceptible to oxidation, which commonly leads to uncontrolled additions, loss in stereo- and regioselectivity, and polymerization. It is surmised that if an electron-rich aromatic ring is present in the substrate, single electron oxidation occurs from the aromatic system. Via resonance, the radical cation may also reside on the alkene moiety. Reactivity is observed through the alkene portion preferentially, as breaking aromaticity is thermodynamically unfavorable.

Surprisingly, the location of functionality on the aromatic ring has a significant impact on the oxidation potentials of similar substrates (Figure 1-7). This unique tend is observed when *ortho*- *meta*- and *para*-anethole are compared. It was found that increased stability was observed when the electron rich substituent is in the *para* position, as *para*-anethole possesses a half wave oxidation potential of +1.28 V. P*ara*-anethole is significantly easier to oxidize than *meta*-anethole, as the oxidation potential is less positive by +0.38 V. The methoxy group at the *ortho*- position is more stabilizing than at the *meta*, however only by < +0.1 V. The same trend is observed when *ortho-,* *meta*- and *para*-methyl-β-methylstyrene are compared. *Para*-methyl-β-methylstyrene exhibits a half wave oxidation potential of +1.62 V, and is the most oxidizable substrate by over +1.0 V. O*rtho*-methyl-β-methylstyrene has a half wave oxidation potential more positive than the para- derivative, yet is less positive than the *meta* isomer by +0.04 V.[13] Though a similar trend is observed for nucleophilic addition reactions, this observation is unanticipated when solely accounting for the potential required to remove one electron.

**Figure 1-7: Unique Trend in Oxidation Potential of Styrene Derivatives**

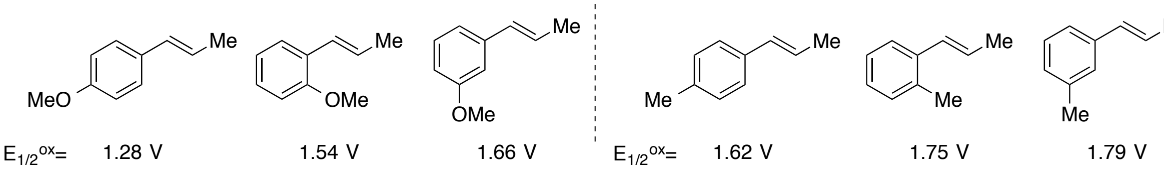

This trend may correlate to a difference in localization of charge-spin density. In 1991, Yamashita and coworkers reported the photoinduced nucleophilic addition of ammonia to electron rich styrene derivatives. Typical addition at the alkene moiety was observed when styrenes possessing electron rich substituents at the *ortho* and *para* positions were subjected to standard conditions; however, when 3,5-dimethoxy-β-methylstyrene was considered, nucleophilic addition occurred at the *ortho* position on the aromatic core. This discrepancy in reactivity was attributed to radical cation localization residing within the aromatic ring. Stabilization *ortho* and *para* to the methoxy substituents is higher in 3,5 dimethoxy-β-methylstyrene than in 3,4 dimethoxy-β-methylstyrene, due to stability overlap. This is presumed to be the longest lived intermediate prior to amine addition for the former case, and results in addition on the aromatic ring (Figure 1-8). [14]

**Figure 1-8: Photoinduced Nucleophilic Addition of Ammonia and Isopropylamine**

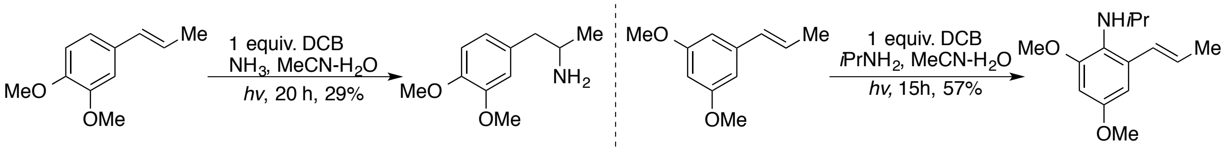

### 1.2.3 Co-Catalysts in Photoredox Catalysis

When rendering a transformation catalytic, it is important to consider the mechanism for photocatalyst regeneration. If a reaction is redox neutral, the photooxidant must undergo single electron reduction with a product intermediate. However, it is also common to include an additive that assists in the regeneration of the photooxidant. The inclusion of an additive or co-catalyst is typical for the regeneration of inorganic photoixdants such as ruthenium$^{III}$ tris(bipyridine) $[Ru(bpy)_3]^{2+}$. This ruthenium complex is a reactive photosensitizer that can serve as a single electron oxidant when excited with visible light. However, early work accomplished by Deronzier demonstrated the necessity of aryldiazonium salts as oxidative quenchers for $[Ru(bpy)_3]^{2+}$.[15] This was showcased for the oxidation of benzylic alcohols to corresponding aldehydes. Deronzier discovered that stoichiometric amounts of diazonium **1** would oxidatively quench the excited state of the ruthenium complex, resulting in the generation of $[Ru(bpy)_3]^{3+}$. Following the loss of nitrogen gas, the diazonium is suspected to undergo hydrogen abstraction, or radical cyclization, affording byproducts **1a** and **1b**. Two equivalents of the reduced ruthenium complex are proposed to undergo a second electron transfer oxidation with the benzylic alcohol, resulting in a two electron transfer. With the assistance of 2,4,6-trimethylpyridine, neutral benzaldehyde is obtained. Single electron reduction resulting in the evolution of nitrogen gas reduced the likelihood of back electron transfer, which is correlated with high efficiency for the regeneration of $[Ru(bpy)_3]^{3+}$.

**Figure 1-9: Mechanism for Regeneration of Photooxidant with the Aid of Diazonium 1**

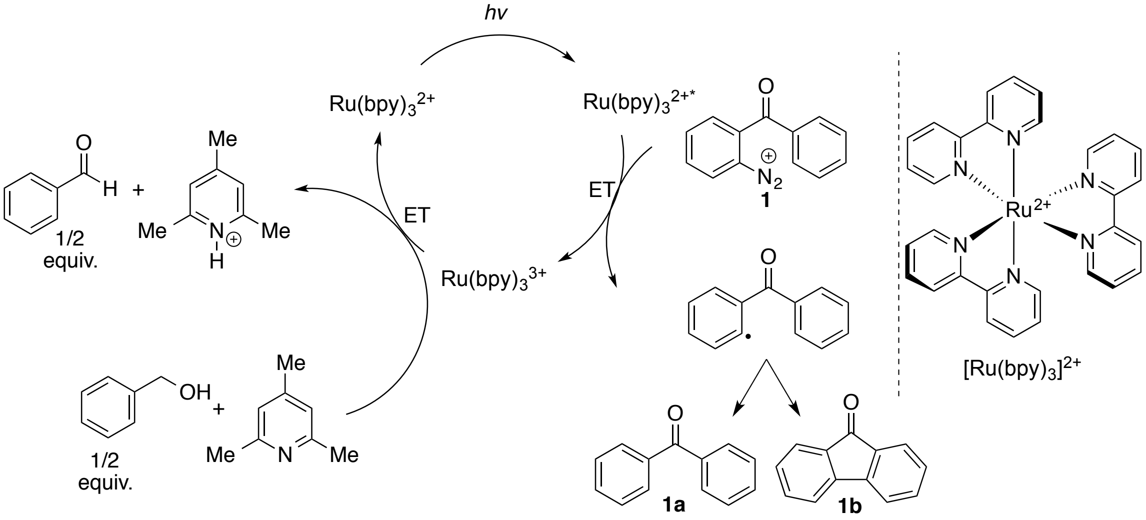
hv
Ru(bpy)3 2+
Ru(bpy)3 2+*
ET
ET
Ru(bpy)3 3+
O
H
+
Me
Me
Me
N
H
1/2
equiv.
OH
+
Me
Me
Me
N
1/2
equiv.
N2
1
1a
1b
[Ru(bpy)3]2+
Ru2+
N

This seminal discovery led to the evaluation of co-catalysts for the reductive or oxidative regeneration of various metal-based photooxidants. Triethylamine and xanthate esters are two common co-catalysts for the single electron reduction of ruthenium (II) (Figure 1-10). Additionally, oxygen, nitroarenes, and methylviologen have been found fruitful in the oxidative regeneration of ruthenium (II) and iridium (II) complexes.[16] These quenchers have been instrumental in catalyst regeneration, resulting in methods with high yields and high efficiency.

**Figure 1-10: Common Reductive and Oxidative Co-Catalysts**

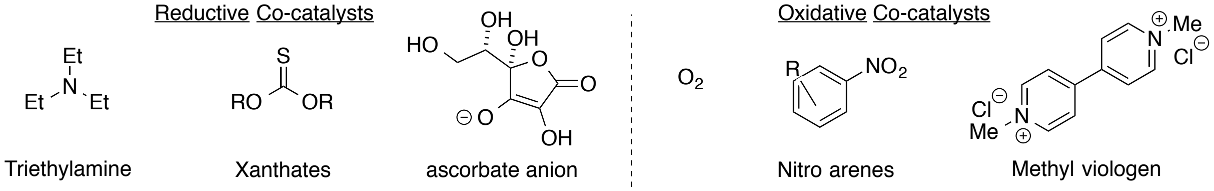
Reductive Co-catalysts
Oxidative Co-catalysts
Et
N
Et
Et
S
RO
OR
HO
OH
OH
O
O
O
OH
O2
R
NO2
Me
N
Cl
Cl
N
Me
Triethylamine
Xanthates
ascorbate anion
Nitro arenes
Methyl viologen

### 1.2.4 Chemical Oxidation

Many electron transfer reactions can also be accomplished with single electron oxidants via chemical oxidation. The most applicable single electron oxidants within this context are triarylaminium hexachloroantimonate complexes ($Ar_3N \bullet SbCl_6^-$). Notable work with single electron transfer with this oxidant was accomplished by Nathan Bauld, where oxidizable substrates were subjected to catalytic amounts of tris(p-bromopheny1)aminium hexachlorostibnate at 0 °C in dichloromethane. When cyclohexadiene was chosen as the oxidizable substrate, the Diels-Alder adduct was obtained in 70% yield (Figure 1-11). If the aminium oxidant was excluded, the same cycloadduct could be obtained in 30% yield; however high temperatures and long reaction times are required.[17] Cyclohexadiene exhibits a half wave oxidation potential of +1.8 V, while tris(p-bromophenyl)aminium hexachlorostibnate has a reported reversible half wave reduction potential of +1.3 V.[18] Surprisingly, this electron transfer occurs while the transformation is +11 kcal/mol endergonic.

**Figure 1-11: Diels Alder Reaction Promoted by Chemical Single Electron Oxidation**

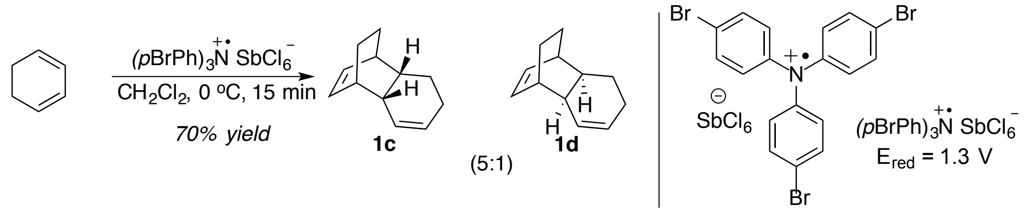

### 1.3 Conclusion

Although the field of photoinduced electron transfer was first developed decades ago, the field is relatively unmapped. Additionally, this unique approach is not commonly utilized for the synthesis of chemically useful substrates, nor typically applied to the synthesis of natural products. Exploration and further development within the field of photoredox catalysis is anticipated, as transformations requiring milder conditions with higher efficiencies are continuously sought after.

# REFERENCES

(1) Ledwith, A. Cation Radicals in Electron Transfer Reactions. *Accounts of Chemical Research* **1972**, *5*, 133–139.

(2) Miranda, M. A.; Izquierdo, M. A.; Pérez-Ruiz, R. Direct Photophysical Evidence for Quenching of the Triplet Excited State of 2,4,6-Triphenyl(Thia)Pyrylium Salts by 2,3-Diaryloxetanes. *J. Phys. Chem. A* **2003**, *107*, 2478–2482.

(3) Mattay, J. Photoinduced Electron Transfer in Organic Synthesis. *Synthesis* **1989**, *1989*, 233–252.

*(4)* H. F. Davis, S. K Chattopadhyay, P. K. Das, *J. Phys, Chem.* **1984***,* 2798-2803.

(5) Blanc, S.; Pigot, T.; Cugnet, C.; Brown, R.; Lacombe, S. A New Cyanoaromatic Photosensitizer vs. 9,10-Dicyanoanthracene: Systematic Comparison of the Photophysical Properties. *Phys. Chem. Chem. Phys.* **2010**, *12*, 11280.

(6) Miranda, M. A.; Garcia, H. 2, 4, 6-Triphenylpyrylium Tetrafluoroborate as an Electron-Transfer Photosensitizer. *Chem. Rev.* **1994**, *94*, 1063–1089.

(7) G, Haucke, P. Czerney, F. Cebulla *Ber. Bunsen-Ges. Phys. Chem.* **1992**, *96*, 880.

(8) Benniston, A. C.; Harriman, A.; Li, P.; Rostron, J. P.; van Ramesdonk, H. J.; Groeneveld, M. M.; Zhang, H.; Verhoeven, J. W. Charge Shift and Triplet State Formation in the 9-Mesityl-10-Methylacridinium Cation. *J. Am. Chem. Soc.* **2005**, *127*, 16054–16064.

(9) Fukuzumi, S.; Kotani, H.; Ohkubo, K.; Ogo, S.; Tkachenko, N. V.; Lemmetyinen, H. Electron-Transfer State of 9-Mesityl-10-Methylacridinium Ion with a Much Longer Lifetime and Higher Energy Than That of the Natural Photosynthetic Reaction Center. *J. Am. Chem. Soc.* **2004**, *126*, 1600–1601.

(10) Ohkubo, K.; Mizushima, K.; Iwata, R.; Souma, K.; Suzuki, N.; Fukuzumi, S. Simultaneous Production of P-Tolualdehyde and Hydrogen Peroxide in Photocatalytic Oxygenation of P-Xylene and Reduction of Oxygen with 9-Mesityl-10-Methylacridinium Ion Derivatives. *Chem. Commun.* **2010**, *46*, 601.

(11) Schepp, N. P.; Johnston, L. J. Reactivity of Radical Cations. Effect of Radical Cation and Alkene Structure on the Absolute Rate Constants of Radical Cation Mediated Cycloaddition Reactions1. *J. Am. Chem. Soc.* **1996**, *118*, 2872–2881.

(12) Neikam, W. C.; Dimeler, G. R.; Desmond, M. M. A Correlation of Electrochemical Oxidation Potential of Organic Compounds with Photoionization Potential. *Journal of the Electrochemical Society* **1964**, *111*, 1190–1192.

(13) Oxidation potentials collected in house by Jean-Marc GranJean.

(14) Yamashita, T.; Yasuda, M.; Isami, T.; Tanabe, K.; Shima, K. Photoinduced Nucleophilic Addition of Ammonia and Alkylamines to Methoxy-Substituted Styrene Derivatives. *Tetrahedron* **1994**, *50*, 9275–9286.

(15) Cano-Yelo, H.; Deronzier, A. Photo-Oxidation of Some Carbinols by the Ru (II) Polypyridyl Complex-Aryl Diazonium Salt System. *Tetrahedron Letters* **1984**, *25*, 5517–5520.

(16) Narayanam, J. M. R.; Stephenson, C. R. J. Visible Light Photoredox Catalysis: Applications in Organic Synthesis. *Chem Soc Rev* **2011**, *40*, 102–113.

(17) Bellville, D. J.; Wirth, D. W.; Bauld, N. L. Cation-Radical Catalyzed Diels-Alder Reaction. *J. Am. Chem. Soc.* **1981**, *103*, 718–720.

(18) Schmittel, M.; Wöhrle, C. Cation Radical Catalyzed Diels-Alder Reaction of Electron-Rich Allenes. *J. Org. Chem.* **1995**, *60*, 8223–8230.

# CHAPTER TWO: [2+2] CYCLOADDITION REACTIONS OF ALKENES VIA SINGLE ELECTRON TRANSFER CATALYSIS[*]

## 2.1 Introduction

The development of a mild, efficient, and 'green' synthetic method has appealed to chemists for some time. Therefore, designing an alternative procedure where the energy of visible light is exploited is a promising approach. Creating a method that reacts by a unique mechanism provides new means for accessing complex structures from architecturally simple material. Visible light is abundant, low energy, and cheap; however, creating a practical method is challenging since most organic small molecules do not absorb visible light. For this reason, the application of light sensitive organic reagents as photoredox catalysts has been instrumental to the progress of this field.

This approach has been applied to the synthesis of cyclobutane lignans; this chemically diverse lignan family features over two-dozen cyclobutane-containing members. Despite the biological importance of this class of compounds, there have been few efforts devoted to the stereoselective synthesis of cyclobutane lignans and lignan analogs. In 2013, we reported a method for the stereoselective synthesis of $C_2$-symmetric cyclobutane alkene dimers that has been applied to the total syntheses of the lignans magnosalin, endiandrin A, and the lignan-like cyclobutane, pellucidin A, of which we propose a revised structure.

## 2.2 [2+2] Cycloadditions

### 2.2.1 Application to Lignan Natural Products

Cyclobutane rings are a basic and prominent structural motif present in numerous natural products including terpenes, fatty acids, lignan and neolignan compounds.[1] The rich family of lignans and neolignans exhibit inhibitory activity against an array of viruses and bacteria, and also display anti-platelet aggregation, and cytotoxicity.[2] Additionally, numerous cyclobutane-containing lignans display useful anti-inflammatory properties via glucocorticoid receptor binding, and inhibition of nitric oxide synthesize.

---

[*] A portion of this chapter previously appeared as an article in Chemical Science. The original citation is as follows: Riener, M.; Nicewicz, D. A. Synthesis of Cyclobutane Lignans via an Organic Single Electron Oxidant–Electron Relay System. *Chem. Sci.* **2013**, *4*, 2625.

Glucocorticoids play a key role in stabilizing stress-related hormones, and also exhibit anti-inflammatory and immunosuppressive properties.[3] Numerous synthetic glucocorticoids have been explored to treat inflammatory conditions such as dermatitis and rheumatoid arthritis. Because they possess non-selective reactivity and resulting in long-term side affects, current glucocorticoids are not ideal for drug therapy. For this reason, the discovery and synthesis of selective glucocorticoids receptor binders may provide an improvement over current treatments. Conversely, overproduction of nitric oxide by *inducible*-nitric oxide synthase (*i*-NOS) is responsible for inflammation and for vasodilation and hypotension associated with septic shock.[4] Therefore, an NOS inhibition assay assists in elucidating new selective inhibitors to *i*-NOS, which may be utilized in drug therapy to prevent these symptoms.

**Figure 2-1: Skeletal Structure of Lignan vs Neolignan**

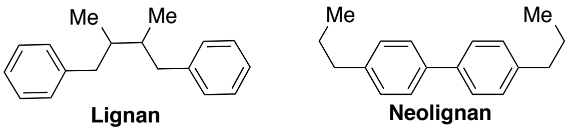

Lignans are so termed for possessing a di-aromatic di-propane subunit, with a bond connecting their β-carbon. Neolignans possess the same skeletal core, but are connected by a bond between the aromatic rings (Figure 2-1). In 2001, Quinn and coworkers discovered a class of lignans isolated from the Australian plant *Endiandra anthropophagorum* that display potent glucocorticoid receptor binding activity (Figure 2-2).[24] Endiandrin A was found as most potent, possessing a concentration of inhibition at 50% ($IC_{50}$) of 0.9 μM. The dimethylated variant of endiandrin A was subjected to the same assay and was also reported to possess binding activity; however, reactivity was significantly diminished when compared to the parent lignan. Nectandrin B was isolated in the same extract and had similar functionality around the aromatic rings, yet possessed a tetrahydrofuran core. Nectandrin B exhibited a glucocorticoid receptor binding $IC_{50}$ of 27 μM, which indicates that this lignan is also less effective than endiandrin A. Due to these results, the authors suggest that the cyclobutane core coupled with the free phenol may be instrumental in glucocorticoid receptor binding activity.

**Figure 2-2: Lignans Possessing Anti-Inflammatory Properties**

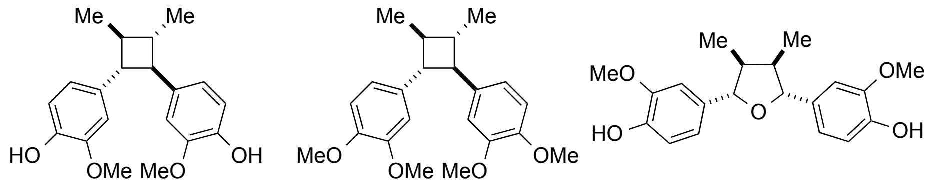

***endiandrin A***
GR binding $IC_{50}$ = 0.9 μM

***di-O-methylendiandrin A***
GR binding $IC_{50}$ =13 μM

***nectandrin B***
GR binding $IC_{50}$ =27 μM

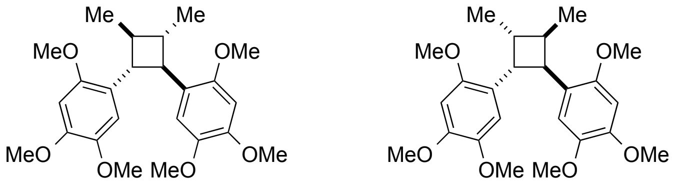

***magnosalin***
NOS inhibition $IC_{50}$ = 5.9 μM

***andamanicin***
NOS inhibition $IC_{50}$ = 53.5 μM

In 2002, Rhu and coworkers isolated lignans magnosalin and andamanicin from the leaves of *Perilla frutescens*.[5] Both cyclobutane lignans possess the same functional groups, head-to-head configuration, and $C_2$ symmetry. Conversely, andamanicin exhibits a *cis-trans-cis* junction around the cyclobutane core, whereas magnosalin displays an all-*trans* connectivity. This subtle difference in stereochemistry has a significant impact on $IC_{50}$ values when each lignan was subjected to a nitric oxide synthase (NOS) inhibition assay. Magnosalin was found to possess an $IC_{50}$ of 5.9 μM; this value is almost ten-fold more potent than andamanicin, which hints that potency arises from the all-*trans* junction.

In 1987, Badheka and coworkers reported the isolation of magnosalin and andamanicin from *piper cubeba*.[6] A third compound, 2,4,5-trimethoxybenzaldehyde was isolated in the same extract, which is proposed to arise from the oxidative cleavage of *trans*-2,4,5-trimethoxy-β-methylstyrene (*E*-

asarone). Though this alkene was not isolated, observation of the benzaldehyde byproduct gives reason to believe formation of this lignan originates from *E*-asarone.

Though simple in structure, lignan cyclobutanes are not trivial to make as single diastereomers. Many propose that these lignan cyclobutanes are naturally produced via a single electron transfer or photolytic [2+2] mechanism. In an isolation report published in 1982, Yamamura and coworkers found evidence to support the latter mechanism; the authors subjected monomer *E*-asarone to direct photolysis in order to elucidate the structure of the isolated compound.[7] Irradiation of *E*-asarone with UV-light and a pyrex filter produced a dimer in 15% yield. Characterization of the synthesized cyclobutane matched with the data for the isolated compound, which verified the structure of Heterotropan. Yamamura also recovered a mixture of *E*- and *Z*- asarones, which suggests that UV-light might be too intense to affect the cyclization in good yields (Figure 2-3).

**Figure 2-3: Direct Cyclobutane Lignan Synthesis via Photolytic Dimerization**

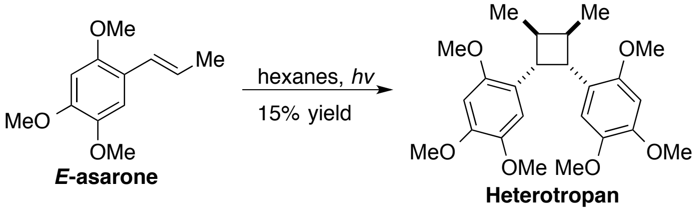

It is important to emphasize the difficulty in elucidating the relative stereochemistry of cyclobutane stereoisomers, as cyclobutanes with various levels of symmetry exhibit similar characterization data. This difficulty is validated, as magnosalin was initially mis-characterized to possess a c*is-trans-cis* junction.[8] Dhar and coworkers did not publish the correct relative stereochemistry of magnosalin and andamanicin until 1993, which was almost a decade after the isolation report.[9] This poses a challenge in identifying the true first syntheses of a particular natural lignan cyclobutane. For instance, in 1987 Kikuchi and coworkers reported the direct synthesis of magnosalin by irradiation of the monomer, *E*-asarone, in the presence of 2 equivalents of pyromellitic acid (Figure 2-4). In this article, the authors report that the cyclobutane was observed in a 6% yield, with a 14% yield of the [4+2] dehydro-adduct, magnoshinin. The mass balance and yields of the cycloadducts are extremely low; less than 10% of the starting monomer was recovered resulting in approximately 70% of material decomposition. The identities of the cycloadducts were proven accurate by matching the spectra of the authentic samples to their acquired characterization. Unfortunately Dhar's report confirms the cyclobutane adduct synthesized by Kikuchi in 1987 is not magnosalin, but instead andamanicin.[10]

**Figure 2-4: Direct Cyclobutane Lignan Synthesis via Photoinduced Electron Transfer**

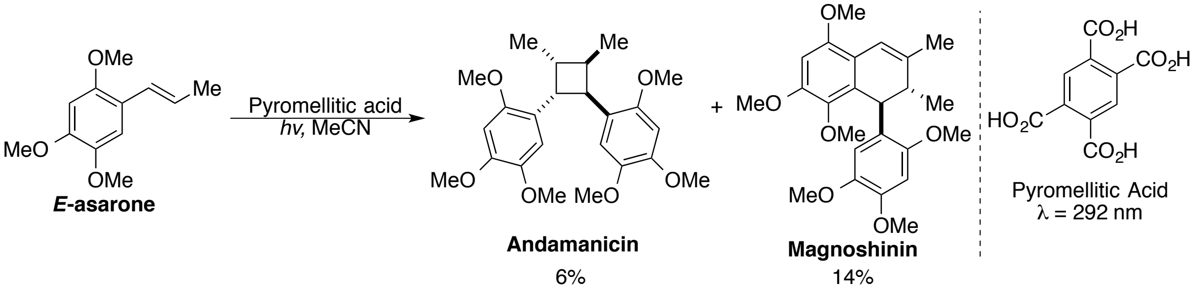

### 2.2.2 Direct Ultraviolet [2+2] Cycloadditions

The field of photochemistry began with the implementation of ultraviolet light (UV light) to mediate transformations. Success of these methods is attributed to high-energy photons, producing 3.1 V to 3.9 V for UV-A (400 nm-315 nm) and 3.9 V – 4.4 V for UV-B (315 nm-280 nm). This immense amount of energy is capable of directly exciting conjugated and aromatic substrates and resulting in alkene isomerization, radical formation, hydrogen abstractions, bond cleavages, and photolytic cyclizations.[11] The development of [2+2] photolytic cyclizations was an important advance, as these cycloadducts could be accessed via thermally promoted [2+2] mechanisms.[12] Unfortunately, even under a UV light-mediated electron transfer mechanism, there is difficultly in controlling the regio- and stereoselectivity. This is demonstrated by Zhang and coworkers, who reported the UV light-promoted [2+2] dimerization of N-acylindoles (Figure 2-5). Zhang observed that dimerization results were enhanced in the presence of acetophenone- a UV light sensitizer. The head-to-head dimer is observed as the major product, however yields are modest and conditions also produce the head-to-tail dimer. Unfortunately, it is unclear if only one diastereomer is formed, or if a total of four compounds are generated.

**Figure 2-5: UV-Promoted Dimerization of N-Substituted Indoles**

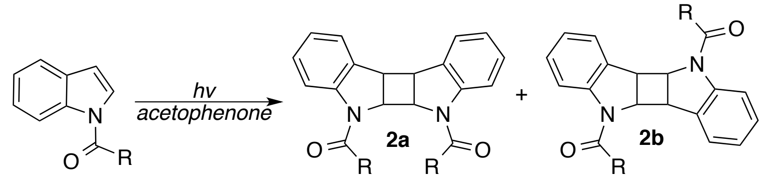

| | | |
|---|---|---|
| R = $OCH_2CH_3$ | 59% | 29% |
| OPh | 56% | 12% |
| Me | 18% | |

Professor Thorsten Bach has been a pioneer in the recent advancement of UV light-promoted cycloadditions resulting in the formation of 4-membered rings. Bach and coworkers have showcased their method in the synthesis of Punctaporonin C by affecting a regio- and stereoselective UV light-promoted [2+2] reaction (Figure 2-6). Cyclobutane formation was proposed to occur when the key intermediate **3** was subjected to ultraviolet light (245 nm). Bach and coworkers discovered that solvent and temperature could be manipulated to provide select dimerization of one alkene over the other, affording desired adduct **3a** in an 89% yield when the reaction was carried out at -75 °C in ethanol.[13]

**Figure 2-6: Key Transformation for the Enantioselective Synthesis of Punctaporonin**

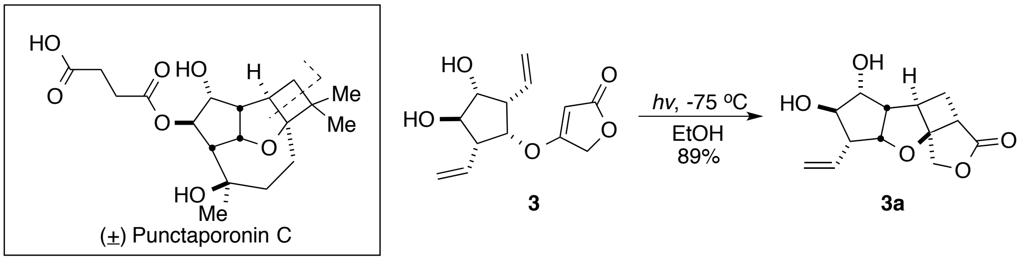

To extend this field, Bach has demonstrated successful intermolecular [2+2] cycloadditions of isoquinolines with good enantiocontrol.[14] This is a tremendous accomplishment, as enantioselective photochemical reactions remain a generally unresolved challenge. The difficulty resides in affecting enantioselectivity purely though non-covalent interactions. Additionally, affecting a regioselective intermolecular cycloaddition is equally difficult while in the presence of such high-energy light. Bach achieved this by creating chiral hydrogen "template" **4**, which is suggested to coordinate with the lactam moiety (Figure 2-7). This template imparts chirality by blocking reactivity from the bottom face, and affects regioselectivity by the choice of solvent and temperature. Polar solvents such as acetonitrile and methanol were most stabilizing of the radical intermediates, which resulted in highest yields for the transformation. However, to minimize formation of fully solvated radical intermediates and selectively impart stereocontrol through the chiral reagent, the reaction must occur in a nonpolar solvent. By reacting isoquinolone **4a** with vinyl phosphonate, vinyl acetate, and *tert*-butyl acrylate in toluene, cyclobutanes **4b**, **4b,** and **4d**, are obtained in greater than 90% yield with good diastereoselectivity and high enantioselectivity for the major isomer. In general, this report showed the first examples of a highly successful enantioselective intermolecular [2+2] reaction between isoquinolone and a range of electron deficient alkenes.

**Figure 2-7: Chiral Hydrogen Template Used to Impart Enantioinduction**

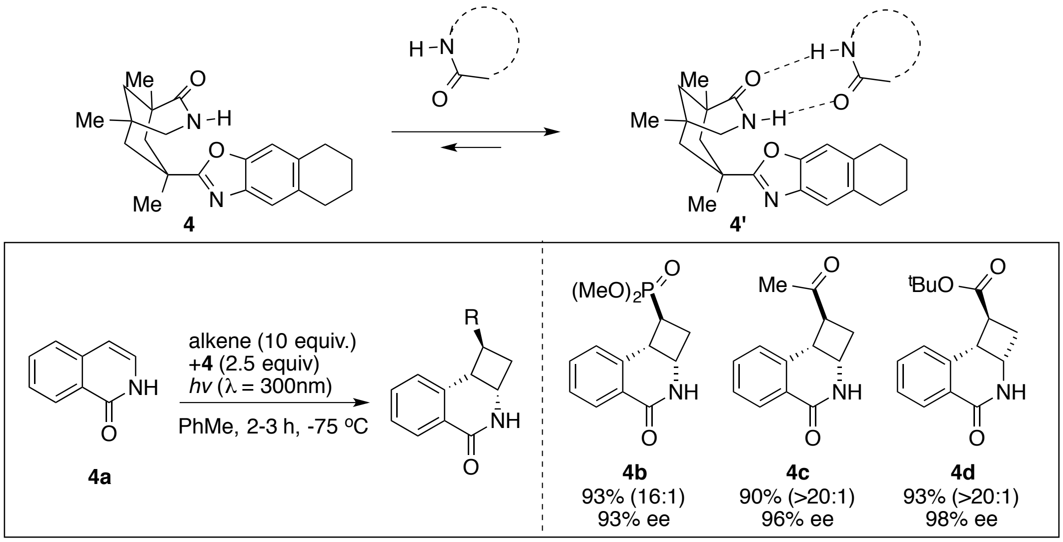

Recently, Bach reported an enantioselective [2+2] photocycloaddition via Lewis acid catalysis. This report focused on the intramolecular dimerization of a unique class of enones, 5,6-dihydro-4-pyridines. Though direct irradiation with λ = 266 nm could affect the intramolecular dimerization, no enantioselectivity would be observed. Bach noted that when Lewis acid **5** was complexed with dihydropyridone substrate **6**, a >50 nm bathochromic shift was observed. This observation led to the creation of an enantioselective intramolecular [2+2] cycloaddition, which required irradiation at 366 nm, and provided cycloadduct **7** in 84% yield with 88% enantioselectivity (Figure 2-8).[15] This is an excellent example of a UV light-mediated transformation that led to a controlled [2+2] dimerization with remarkable selectivity; excitation at a wavelength ideal for sensitization of the complex resulted in formation of enantio-enriched material, while reaction of the free enone **6** was inhibited.

**Figure 2-8: Lewis Acid Catalysis for the Enantioselective [2+2] Photocycloaddition**

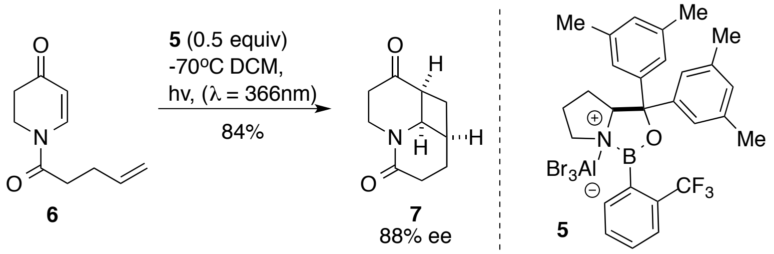

## 2.2.3 Radical Anionic Cycloadditions

Single electron transfer has also proven successful in the regioselective [2+2] cyclization of various alkenes. Contrary to radical cationic methods, very few radical anionic transformations have been reported. In 2002, Krische and Bauld reported the intramolecular anionic cyclodimerization of bis(enones) via electrochemical methods. Krische reported the half wave reduction potential of bis(enone) **8** ($E_{1/2}^{red} = -0.9\ V$). When the substrate is subjected to a potential of −0.9 V in a $LiClO_4$ electrolyte solution in acetonitrile, intramolecular [2+2] cycloaddition was observed in a 36% yield as a mixture of diastereomers **9a** and **9b**. A radical chain mechanism was proposed, wherein collapse of the distonic radical anion intermediate determines *cis:trans* ratio (Figure 2-9). [16]

**Figure 2-9: Cathodic Reduction Generating Radical Anions for Cyclization of Bis(enone)**

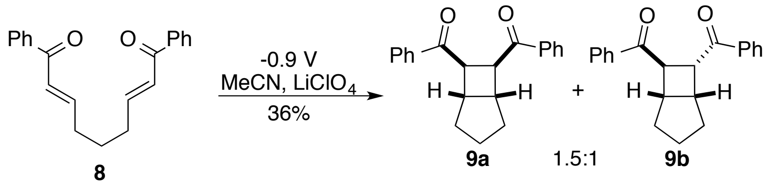

Inspired by the possibility of chemically inducing the same anionic radical cyclization, Krische then considered the inclusion of a pre-formed anion radical to affect intramolecular cyclobutane formation. Krische proposed chrysene anion radical could reduce the bis(enone) **10** to **10a**, resulting in σ-bond formation, producing distonic radical anion species **10b** (Figure 2-10). This intermediate was proposed to undergo a second σ-bond forming step and single electron oxidation, generating desired bicyclic adduct **11c**.[17] The strong *cis* diastereoselectivity was believed to arise from an electrostatic interaction between the carbonyl oxygens and the sodium ion during the transition state. The authors admit that though substoichiometric amounts of crystene are employed (70 mol%), the mechanism of this transformation was not a catalytic radical chain process. It was presumed that tight-ion pairing between the sodium ion with the product ion **10c** caused reaction retardation.

**Figure 2-10: Chemically-Induced Radical Anion Cyclization of Bis(enone)**

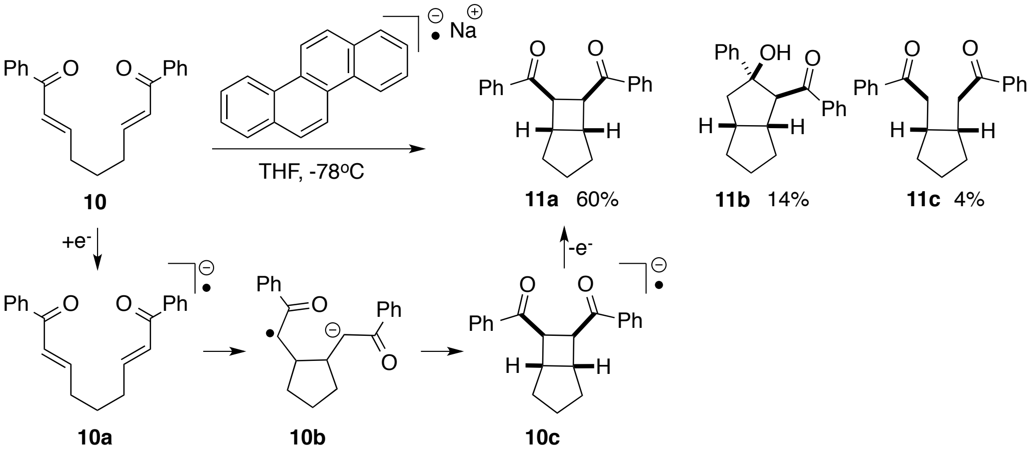

In 2008, Yoon and coworkers broadened the possibilities of radical anion [2+2] cycloadditions by employing visible light-absorbing Ruthenium bypyridyl complexes as photocatalysts. This development prompted the discovery and creation of transformations requiring visible light as the abundant, and nonpolluting energy source. Ruthenium tris-bipyridine (**$Ru(bpy)_3^{2+}$**) has been used extensively as a photocatalyst, and its photophysical properties are well-documented.[18] When excited, these complexes are capable of reacting via energy transfer, and as an excellent single electron oxidant *and* as a single electron reductant. $Ru(bpy)_3^{2+}$ absorbs $\lambda$ = 452 nm, and has a relatively long lifetime in its excited state (~600ns).[19,20] Oxidative quenching of the sensitized ruthenium complex generates Ru(bpy)$_3^{3+}$, a powerful oxidant with a half wave reduction potential of +1.29 V. Respectively, reductive quenching of the same complex provides a strong reductant Ru(bpy)$_3^{+}$, with a half wave oxidation potential of −1.33 V.[21]

Yoon elected to study [2+2] cycloaddition of bis(enones) with Ru(bpy)$_3^{2+}$ as the photoreductant. When bis(enone) **8** was subjected to visible light irradiation in the presence of 5 mol% of Ru(bpy)$_3^{2+}$, 89% of the cycloadduct was isolated. Optimal conditions included stoichiometric amounts of Hünig's base and LiBF$_4$ to reductively quench and generate Ru(bpy)$_3^{+}$, and coordinate with the enone as a Lewis acid, respectively.[8] Yoon also reported the cycloaddition of tethered unsymmetrical bis(enones), which revealed that one aromatic enone must be present to observe reactivity (Figure 2-11). Similar to Krische's report, diastereoselectivities showed preference towards *cis* substitution at the cyclobutane junction. Though a similar effect with coordination of the lithium ion may be at play, the authors do not offer an explanation for this stereoselectivity.

**Figure 2-11: Ruthenium Catalyzed Radical Anion Photocyclization of Bis(enones)**

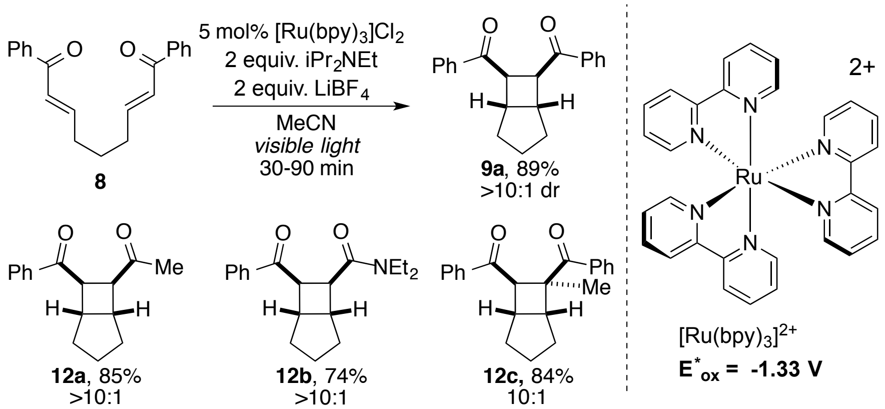

Yoon's extension to this report was the intermolecular [2+2] photocycloaddition of enones with methyl vinyl ketone (Figure 2-12).[22] Aryl enone **13** was proposed to undergo single electron reduction to form the radical anion, which was proposed to react with methyl vinyl ketone via Michael addition. In order to afford good yields and minimize homocoupling, the highly reactive Michael acceptor **13a** was required in excess. Under similar conditions to their previous report, Yoon and coworkers obtained the desired cycloadduct with excellent regioselectivity and modest to good diastereoselectivity.

**Figure 2-12: Crossed Intermolecular Cycloaddition of Acrylic Enones**

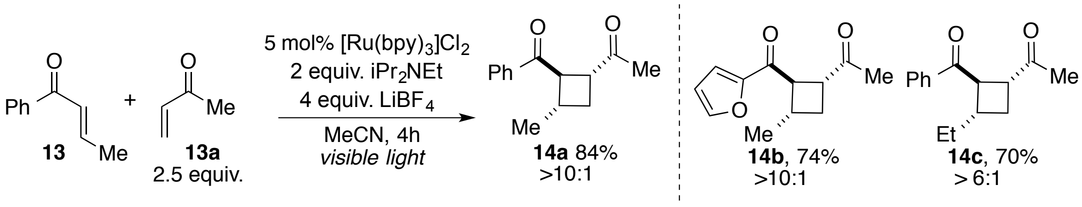

Ph
Me
13
+
Me
13a
2.5 equiv.
5 mol% [Ru(bpy)3]Cl2
2 equiv. iPr2NEt
4 equiv. LiBF4
MeCN, 4h
visible light
Ph
Me
Me
14a 84%
>10:1
Me
Me
14b, 74%
>10:1
Ph
Me
Et
14c, 70%
> 6:1

## 2.2.4 [2+2] via Energy Transfer

Research interests concerning visible light photocatalysis have been extended to consider the energy transfer pathway of photosensitized reagents. As previously mentioned, ruthenium and iridium complexes may react via an energy transfer mechanism to form carbon-carbon bonds. The likelihood of energy transfer occurring is best understood by considering the triplet energy of the complex and substrate. In order for energy transfer to be thermodynamically favorable, the triplet energy of the complex must be higher than that of the substrate. This exergonic process was tested by employing $[Ir(dF(CF_3)ppy)_2(dtbbpy)](PF_6)$, a complex initially discovered by Bernhard in 2005. Bernhard and coworkers observed absorption bands at 310 nm (4.5V) and 380 nm (3.8V) with an emission band at 470 nm.[23] It was also calculated that in its excited state, this iridium complex has an excited state reduction potential of +0.89 V, and an excited state oxidation potential of −1.21 V.

**Figure 2-13: Intermolecular Cycloaddition via Energy Transfer**

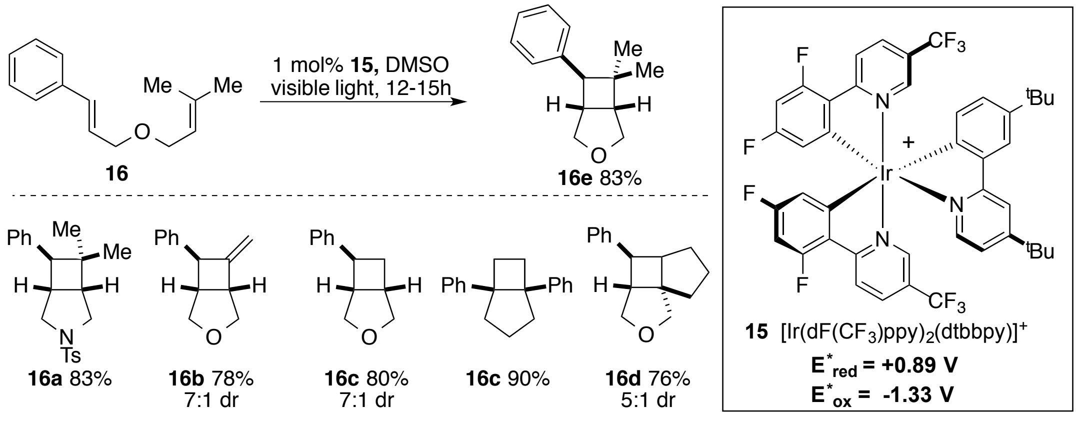

Me
Me
16
1 mol% 15, DMSO
visible light, 12-15h
Me
Me
H
H
16e 83%
Ph
Me
Me
H
H
N
Ts
16a 83%
Ph
H
H
16b 78%
7:1 dr
Ph
H
H
16c 80%
7:1 dr
Ph
Ph
16c 90%
Ph
H
16d 76%
5:1 dr
F
CF3
F
N
+
Ir
tBu
F
N
N
tBu
F
CF3
15 [Ir(dF(CF3)ppy)2(dtbbpy)]+
E*red = +0.89 V
E*ox = -1.33 V

Yoon's approach of cyclodimerization employing iridium complex **15** was one of the first reported methods for the [2+2] cyclobutane formation of electron rich substrates via energy transfer. Styrene-appended ethers were found to efficiently dimerize under their developed conditions, generating the fused bicyclic structure in good yields and acceptable diastereoselectivity (Figure 2-13).[24] To justify the energy transfer mechanism, Yoon reported the half wave oxidation potential of styrene ether **16** ($E_{1/2}^{ox} = +1.42\ V$). As the iridium complex has an excited state reduction potential *below* +1.42 V, electron transfer is not thermodynamically feasible. On the other hand, iridium complex **15** has a triplet energy state ($E_T$) equal to 61 kcal/mol. This is sufficient to undergo energy transfer as most styrenes possess an $E_T$= 60 kcal/mol.[12] As expected with a triplet energy transfer model, the researchers mention no solvent dependence. The scope of this transformation is quite broad, as both α and β substituted styrenes resulted in cyclobutane formation. Aliphatic, non-conjugated alkenes did not undergo cyclization, which is likely attributed to the triplet energy of the alkene exceeding the triplet energy of the iridium complex.

**Figure 2-14: Comparison of Radical Cation vs Energy Transfer Products**

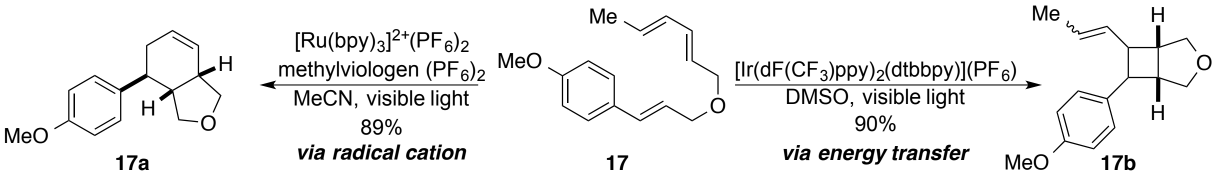

To confidently distinguish the triplet mechanism from an electron transfer mechanism, Yoon subjected diene **17** to two different reaction conditions. Bauld has reported the Diels-Alder cyclization to occur from diene **17**, which was proposed to form via a radical cation mechanism (Figure 2-14).[25] Yoon showed that if substrate **17** was in the presence of the ruthenium complex and methylviologen, the [4+2] product **17a** was efficiently obtained. However, if the iridium complex was employed, the [2+2] cycloadduct **17b** was obtained, which further confirms their reported method reacts through an energy transfer mechanism.

### 2.2.5 Electrochemical Cycloaddition

Electrochemical methods are excellent tools to affect the polarity reversal of a wide range of substrates. Specifically, oxidation of electron rich substrates via anodic oxidative coupling provides a different avenue to access inter- and intramolecular cyclization products that may not be accessible via typical organocatalytic methods. Electrochemical single electron oxidation has been of interest to Chiba and co-workers as an effective method to produce radical cationic species. Their initial focus was on the intermolecular cyclization of two electron rich olefins, affording the cross [2+2] cycloadduct.[26] In this report, an anodic oxidative [2+2] cycloaddition was observed when allyltrimethylsilane **19** was reacted enol ether **18**. To achieve selective anodic oxidation and subsequent radical cationic formation, the enol ether required a 'redox tag', such as *ortho*- or *para*-methoxy benzene. The radical cation of **18** was presumed to undergo nucleophilic attack by allyltrimethylsilane **19**, affording cycloadduct **18a** deficient by one electron. The reaction mechanism was proposed to terminate after single electron reduction of the cyclobutane, affording the neutral adduct. The authors found the purpose of the redox tag was to lower the oxidation potential of the substrate, allowing for reaction to occur in 1.0 M solution of lithium perchlorate/nitromethane. To illustrate the need for a redox tag, the authors showed that cyclization failed to produce **18b** when employing an enol ether lacking a methoxy group on the aromatic ring. (Figure 2-15). Conversely, the reaction was successful for methyl enol ether of *ortho*- methoxyphenyl, delivering cyclobutane **18c** in a 65% yield. Other enol ether reaction partners such as methylenecyclohexene provided cycloadducts **18d**, **18e** in good yields. Lastly, the terminal mono-substituted substrate 1-decene efficiently produced the desired cycloadduct **18g** in a 61% yield.

**Figure 2-15: Electrocatalytic [2+2] Cycloadditionwith Enol Ethers And Alkenes**

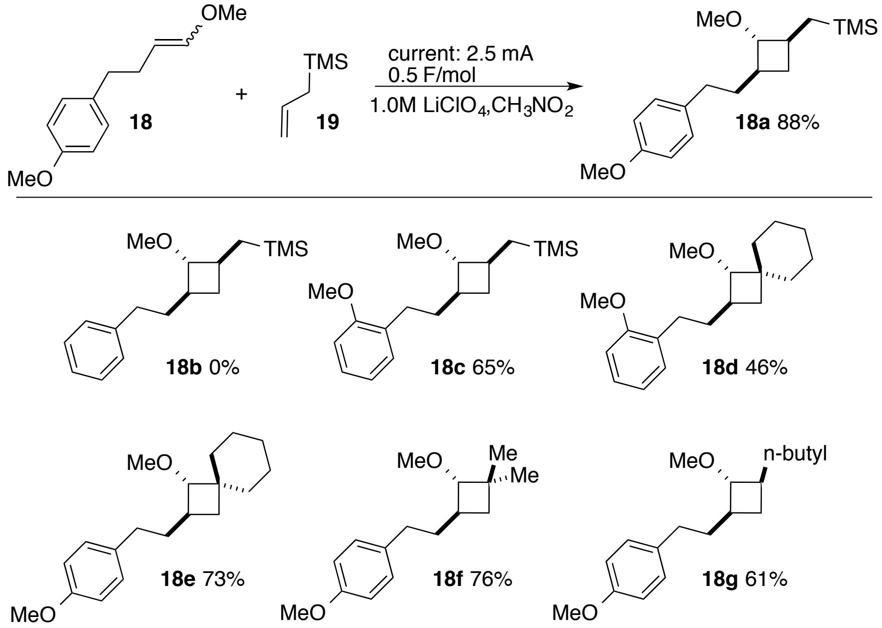
OMe
18
MeO
+
TMS
19
current: 2.5 mA
0.5 F/mol
1.0M LiClO4,CH3NO2
MeO
TMS
18a 88%
MeO
MeO
TMS
18b 0%
MeO
TMS
MeO
18c 65%
MeO
MeO
18d 46%
MeO
18e 73%
MeO
MeO
Me
Me
18f 76%
MeO
MeO
n-butyl
18g 61%
MeO

Overall, the cycloadducts were observed in good yields and as single diastereomers. The high diastereoselectivity was not explained; however, it could be speculated that formation of the radical cation of the enol ether results in the isomerization of the substrate to *trans*. Since only terminally monosubstituted or symmetrical 1,1-disubstituted alkenes were considered in this report, only two diastereomers were likely. High regioselectivity is also observed, which is consistent with the radical cationic mechanism.

Chiba extended this transformation to encompass a slightly wider range of activated aliphatic enol ethers, where dihydrofuran and dihydropyran were found to be competent enol ethers (Figure 2-16). When 3,4-dihydro-2H-pyran **21b** was subjected to standard bulk electrolysis conditions in the presence of 20 equivalents of 4-allylanisole **20**, the desired cycloadduct **20a** was obtained in 94% with a 6:1 diastereomeric ratio favoring the *trans* adduct. Similarly, 3,4-dihydro-2H-furan **21a** was also a competent substrate, producing cyclization product **20d** in 63% yield. Surprisingly, when 4-allylveratrole was chosen as the nucleophilic alkene partner for 3,4-dihydro-2H-pyran, cycloadduct **20b** was only observed in a 10% yield. Due to the less positive oxidation potential of 4-allylveratrole ($E_p^{ox} = +1.37\,V$) compared to 3,4-dihydro-2H-pyran ($E_p^{ox} = +1.45\,V$), the authors believe competitive single electron oxidation of 4-allylveratrole was occurring. In contrast, both 4-allylanisole ($E_p^{ox} = +1.61\,V$) and 2-allylanisole ($E_p^{ox} = +1.56\,V$) possess oxidation potentials more positive than 3,4-dihydro-2H-pyran. These values support the author's hypothesis where selective enol ether oxidation is required to produce the cycloadducts in excellent yields.

**Figure 2-16: Scope For Electrocatalytic [2+2] of Cyclic Enol Ethers And Alkenes**

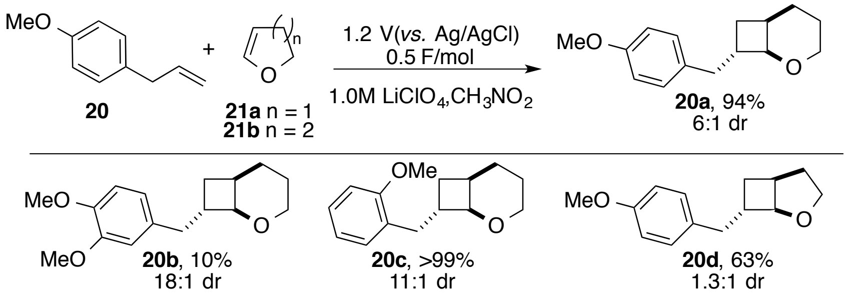

The authors found that no cyclization was observed for either **21a** or **21b** in the presence of allylbenzene. For this reason, the authors propose a mechanism where intramolecular electron transfer from the cyclobutane **22c** to the alkoxylphenyl moiety in **22d** is critical (Figure 2-17). Following intramolecular electron transfer, the cycloadduct **22d** may undergo single electron reduction by two mechanisms; the first occurs with a neutral equivalent of enol ether **22a,** whereas the second occurs via anodic reduction. The regioselectivity is again explained via formation of radical cationic intermediates, where the distonic radical and carbocation are positioned at the most stabilized carbons.

**Figure 2-17: Proposed Mechanism For Electrocatalytic [2+2] of Cyclic Enol Ethers And Alkenes**

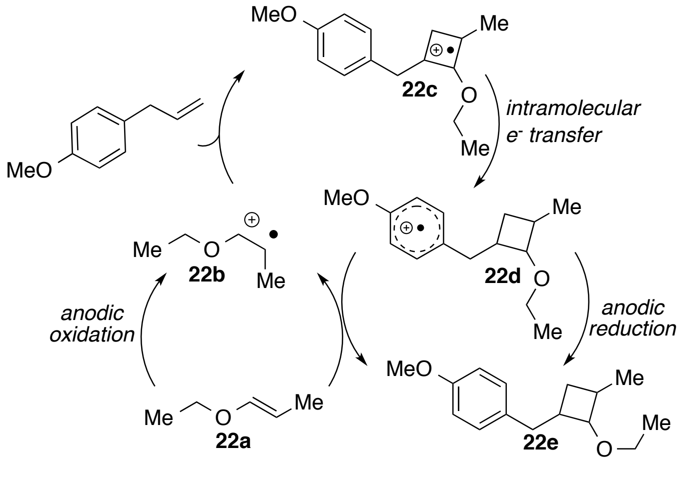
MeO
Me
22c
O
Me
intramolecular
e⁻ transfer
MeO
MeO
Me
22d
O
Me
anodic
reduction
Me
O
22b
Me
anodic
oxidation
MeO
Me
22e
Me
O
Me
O
Me
22a

In a separate report, cycloreversion of the synthesized [2+2] adducts was successfully accomplished by increasing the current to 1.0-5.0 F/mol. This differs from the typical 0.3-0.5 F/mol used for cycloaddition, which relates to 30%-50% of current per mol of substrate.[27] A competition study between cycloreversion of bicyclic compound **23a** in the presence of excess homoallylanisole was reported. When 20 equivalents of homoallylanisole **23b** were included in standard cycloreversion conditions, cycloadduct **23c** was obtained in 29% yield as a mixture of diastereomers. The authors suggest the radical cation is present in the cyclobutane moiety, which releases to recyclize with alkene **23b** present in large excess (Figure 2-18). To confirm this hypothesis, the spin distribution of the radical cation derived from **23a** was calculated, which verified that the charge does reside within the cyclobutyl moiety.

**Figure 2-18: Cycloreversion Of Cyclobutanes Via Aniodic Oxidation**

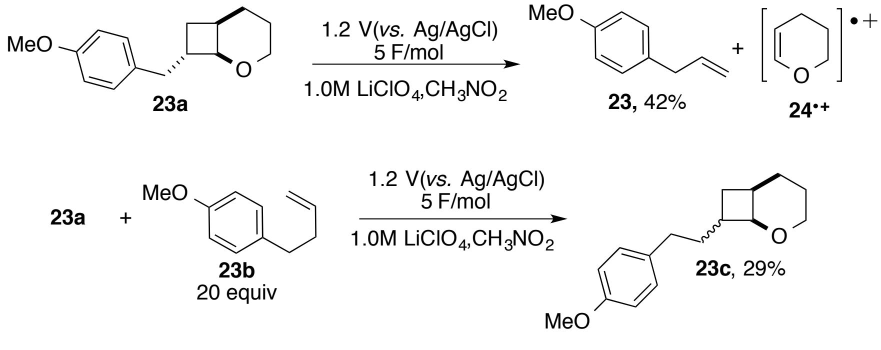
MeO
O
23a
1.2 V(*vs.* Ag/AgCl)
5 F/mol
1.0M LiClO₄,CH₃NO₂
MeO
23, 42%
+
O
24•+
23a
+
MeO
23b
20 equiv
1.2 V(*vs.* Ag/AgCl)
5 F/mol
1.0M LiClO₄,CH₃NO₂
O
23c, 29%
MeO

The ability to manipulate the current present during an electrocatalytic reaction has great utility for the synthesis and cycloreversion of cyclobutanes. An extremely practical extension of this method is to affect cyclization and trigger cycloreversion to afford olefin cross-metathesis products. Such a method would eliminate the need for expensive catalysts and offer a different route for the metathesis of particularly electron rich olefins. Chiba and coworkers have developed a unique method for olefin cross-metathesis of enol ethers resulting in terminal olefins by creating an electrochemical method operating again via a radical cationic mechanism. It was noted that in the presence of 20 equivalents of terminal alkenes such as allylbenzene **25a**, the olefin metathesis adduct of 1-methoxydec-1-ene **25a** delivers 1-decene **25c** in 48% yield. Allylcyclohexane **25d** was also a competent substrate, wherein under the same conditions provided the adduct in a 77% yield (Figure 2-19).[28]

**Figure 2-19: Cross Metathesis Reactions Of Enol Ethers And Terminal Alkenes**

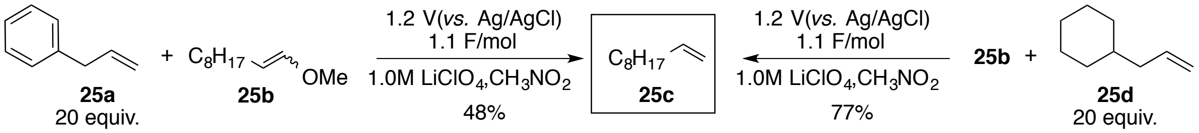

Unfortunately, there are severe drawbacks associated with this process; **25c** was one of two terminal metathesis products achieved. If an internal disubtituted alkene was employed in conjunction with **25b**, a mixture of *E*/*Z* isomers was obtained. Additionally, prohibitive excess of the electron rich alkene was required to afford the metathesis adduct while minimal substrate control was observed. Though cycloadducts were isolated and characterized, product yields were all determined by GC-MS. Still, these significant contributions pave the path for organophotoredox catalysis, and give insight to the possibility of new transformations concerning cycloreversion and olefin metathesis.

### 2.2.6 Radical Cationic Cyclizations

Cyclobutane formation via photoinduced electron transfer dates back to work accomplished by Ellinger in the mid 1960's. Ellinger discovered *N*-vinyl carbazole was susceptible to [2+2] cyclodimerization when in the presence of chloranil and visible light. Following this precedent, Ledwith was interested in producing the dimer with the aid of single electron oxidants. Ledwith elected to study *N*-vinyl carbazole, as it had been known to quantitatively dimerize under single electron transfer mechanisms. To realize photoinduced electron transfer, Ledwith discovered that irradiation with UV light and inclusion of benzophenone ($E_T$= 69.5 kcal/mol) or methylene blue ($E_T$= 33 kcal/mol) produced the desired cyclodimer. As *N*-vinyl carbazole has a triplet energy value *above* benzophenone ($E_T$= 70 kcal/mol), energy transfer mechanisms were ruled out. Instead, a radical cation chain mechanism was suggested, where the reaction was initiated with UV light, resulting in sensitization of benzophenone to its singlet/triplet state (Figure 2-20). Sensitized species **18*** was presumed to undergo single electron oxidation with *N*-vinyl carbazole **27**, delivering **27**$^{\bullet+}$**.** This electron deficient substrate reacts with a second equivalent of neutral carbazole **27**, producing a distonic radical cationic species **27a**, where both charges were stabilized $\alpha$ to the nitrogen. The species was in equilibrium with product **27**$'$, where a weak $\sigma$-bond was proposed. The last propagating step was proposed to occur with a third equivalent of neutral carbazole **27**, producing the desired cycloadduct **28** and regenerating the reactive radical cationic species. Ledwith observed rate enhancement in the presence of oxygen, and for this reason suggests the termination step occurs with oxygen radical.[29]

**Figure 2-20: Proposed Radical Cation Chain Mechanism**

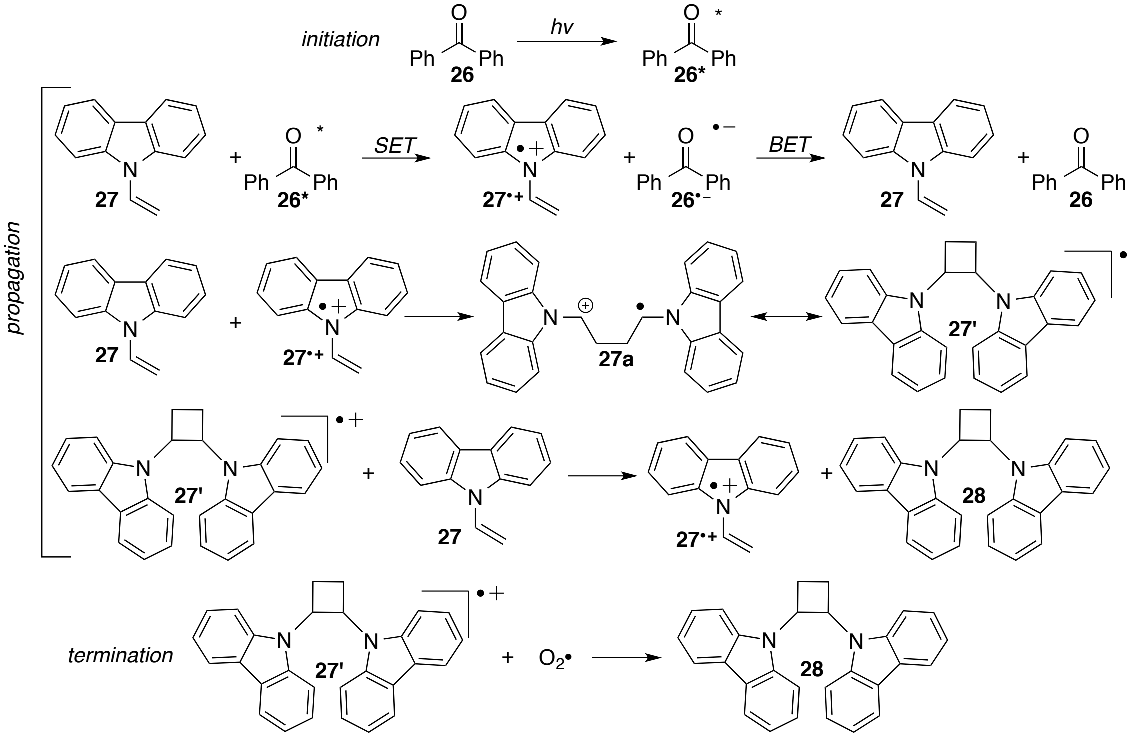

Though significantly more attention has been drawn to the [4+2] photocyclization, Bauld has been a dedicated pioneer in elucidating the scope and limitations of [2+2] photoinduced cycloadditions. His research has predominantly focused on employing *tris*(*p*-bromophenyl)aminium hexachlorostibnate as a single electron oxidant. Admittedly, though the aminium salt is limited to a narrow range of oxidizable substrates, the rapid rate of electron transfer draws appeal to the oxidant. When *trans*-anethole ***t*-29** was subjected to dimerization conditions at -35 °C in the presence of *tris*(*p*-bromopheny1)aminium hexachlorostibnate, the cycloadducts formed retained the *trans*-geometry between the methyl and phenyl moieties. Nonetheless, both *meso* **30a** and $C_2$ symmetric **30b** dimers were observed (Figure 2-21). More intriguing was the observation that cyclobutanes **30a** and **30b** undergo cycloreversion when subjected to standard conditions at a warmer temperature. This result highlights cycloreversion as a prominent and competitive pathway.[30] Additionally, Bauld proposed that formation of the distonic radical cation would not likely produce cycloadducts with high stereospecificity. Instead, the author suggested formation of a long bond, or one-electron bond in cycloadduct **27'**, which was supported by STO-3G level calculations.[15]

**Figure 2-21: Dimerization and Cycloreversion of *trans*-Anethole**

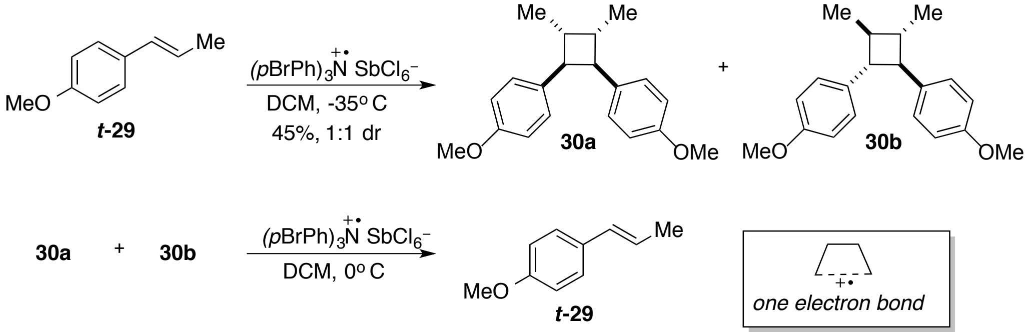

t-29
(pBrPh)3N SbCl6−
DCM, -35° C
45%, 1:1 dr
30a
30b
30a + 30b
(pBrPh)3N SbCl6−
DCM, 0° C
t-29
one electron bond

Lewis also published seminal work achieving photoinduced electron transfer by employing organic photooxidants. After screening a wide range of UV-activated oxidants, Lewis observed highest yields of cyclobutane formation when stoichiometric amounts of the photooxidant 9-cyanoanthracene **CA** were employed (Figure 2-22). The product distribution included *cis*-anethole ***c*-29** and formation of both head-to-head diastereomers **30a** and **30b**; this suggests that photooxidants possessing large excited state reduction potentials may be responsible for olefin isomerization.[31] Additionally, Lewis also observed formation of *p*-anisaldehyde in small amounts, which was attributed to oxidative cleavage of alkenes when in the presence of oxygen.

**Figure 2-22: Dimerization of *trans*-Anethole in the Presence of 9-Cyanoanthracene**

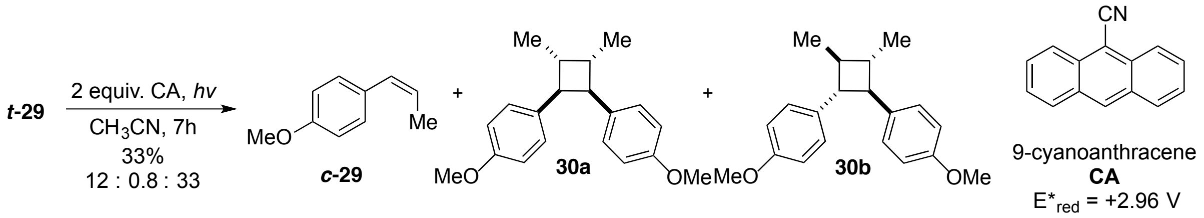

t-29
2 equiv. CA, hv
CH3CN, 7h
33%
12 : 0.8 : 33
c-29
30a
30b
9-cyanoanthracene
CA
E*red = +2.96 V

Following this report, Schepp and Johnston published the dimerization of *p*-methoxystyrene via radical cationic methods. In this report, Johnston subjected methoxystyrene to chloranil as the triplet sensitizer in acetonitrile. Irradiation at 355 nm produced the sensitized species, which was proposed to undergo intersystem crossing, yielding the triplet chloranil sensitizer. Reaction of the activated sensitizer with methoxystyrene delivered the radical cationic species that was suggested to undergo a similar mechanism proposed by Bauld (Figure 2-23). Unfortunately, no yield was reported for this transformation; however, the authors confirm the stereochemistry of cyclobutane **31a** by comparison with literature reports. Product **31b** was also obtained under these conditions, which was formed via the intermolecular [4+2] cycloaddition and followed by rearomatization. It should be noted that this cycloaddition is biased towards the terminal substrate, as no [4+2] adduct was observed when *t*-anethole was subjected to similar conditions. This accomplishment of synthesizing unsubstituted cyclobutane **31a** should not be overlooked. Electron-rich styrenes are subject to uncontrollable polymerization, yet the presented conditions successfully suppressed polymerization and resulted in cyclobutane formation.

**Figure 2-23: Dimerization of *p*-Methoxystyrene in the Presence of Chloranil**

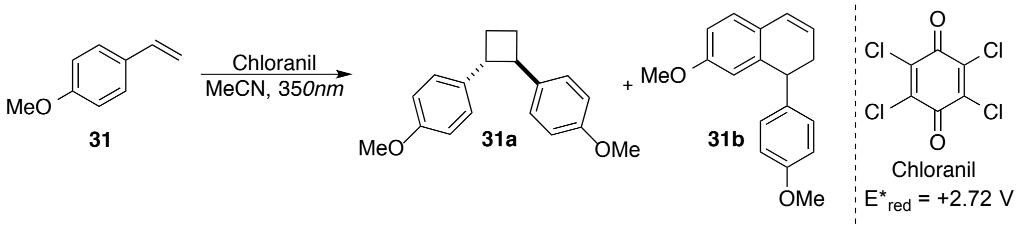

Shigemitsu discovered that phenyl vinyl ether undergoes [2+2] dimerization in the presence of the triplet sensitizer acetophenone.[32] The cycloadduct was observed in 13% yield as a mixture of *cis* and *trans*. However, Mattay found the yield may be increased if 9,10-dicyanoanthracene (DCA) or 2,4,6-triphenylpyrylium tetrafluoroborate (TPT) were used as photooxidants (Figure 2-24). To avoid triplet energy transfer, Mattay irradiated this reaction at wavelengths greater than >400 nm.

**Figure 2-24: Dimerization of Phenyl Vinyl Ether in the Presence of Photooxidants**

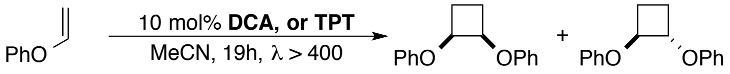

| | | |
|---|---|---|
| **DCA:** | 13% | 24% |
| **TPT:** | 12% | 24% |

Although these conditions produce [2+2] adducts, synthetically useful yields were not observed. If the photooxidant was within range of oxidizing the substrate, low yields were commonly attributed to cycloreversion. Avoiding cycloreversion is challenging, as the cycloadduct created is more reactive than the starting substrate. Moreover, there is the possibility of substrate degradation, or side reactions if oxygen is introduced into the system.

**Figure 2-25: Redox Photosensitization for the Dimerization of Indene**

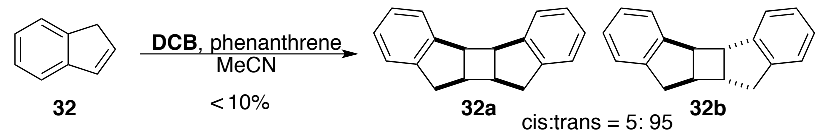

Sakurai and coworkers proposed a noteworthy mechanism for the dicyanobenzene (DCB) photosensitized electron transfer reaction of indene. It was observed that in the presence of dicyanobenzene *and* phenanthrene, dimerization of indene occurred via photoinduced electron transfer (Figure 2-25). Yield of the dimer was less than 10%; however, only the head-to-head regioisomer was observed. This reaction produced cycloadducts **32a** and **32b** with preference for the *trans* dimer (95:5). The diastereomeric preference has been observed previously, and is a distinguishing feature of dimerizations that occur via radical cations.[33] Particularly noteworthy was their proposed mechanism. Sakurai suggested that the aromatic hydrocarbon (**S**) acted as a mediator for electron transfer; direct sensitization of (**S**) resulted in single electron reduction by dicyanobenzene, which was followed by single electron oxidation between electron deficient ($\mathbf{S}^{\bullet+}$) and the neutral substrate (Figure 2-26). This mechanism, coined ‘redox photosensitization’ is different from photoinduced electron-transfer, as sensitization of the aromatic hydrocarbon and not of dicyanobenzene is proposed to occur.

**Figure 2-26: Redox Photosensitization Mechanism Proposed by Sakurai**

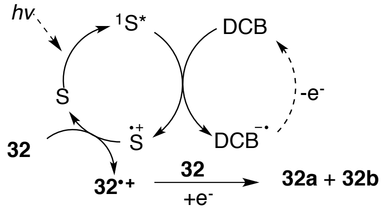

To confirm the mechanism, the reaction was subjected to a triplet sensitizer- benzophenone or acetophenone- instead of dicyanobenzene. No reaction was observed under these conditions, which eliminates the possibility of a triplet energy mechanism, and instead indicates a singlet mechanism.[34] However, it is difficult to fully validate such a mechanism, as intermediates are not isolable.

**Figure 2-27: Tuning Redox Properties of Ruthenium Complexes**

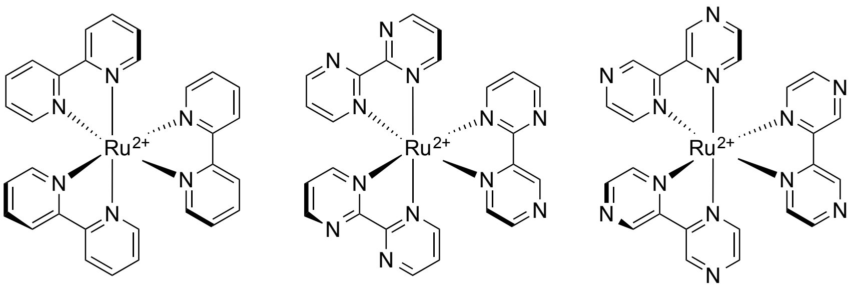

$[Ru(bpy)_3]^{2+}$ **$E^*_{red}$ = 0.77 V**

$[Ru(bpm)_3]^{2+}$ **$E^*_{red}$ = 1.20 V**

$[Ru(bpz)_3]^{2+}$ **$E^*_{red}$ = 1.45 V**

As mentioned earlier, $Ru(bpy)_3^{2+}$ is capable of reacting via numerous mechanisms (i.e. energy transfer, electron transfer, reduction, oxidation). To expand its potential, variations of ruthenium complexes have been synthesized to widen the window for oxidation or reduction. An observable increase in reduction potential is achieved by exchanging the ligands on the ruthenium complex to 2,2' bipyrimidine, or 2,2' bipyrazine. $[Ru(bpz)_3]^{2+}$ has a measured excited state reduction potential of +1.45 V, which has the capability of oxidizing a wider range of alkenes (Figure 2-27). $[Ru(bpm)_3]^{2+}$, with a measured excited state reduction potential of +1.2 V, has also proven useful for alkene oxidation. In particular, Yoon utilized these two complexes to elucidate the limitations of cycloreversion for the cross dimerization of styrenes.[35] Initial investigation focused on the homodimerization of *trans*-anethole ***t*-29**. Unfortunately, no dimer adduct was observed when the solution of ***t*-29** in the presence of a co-oxidant and $Ru(bpy)_3^{2+}$ were irradiated with visible light. This is not surprising as Yoon reported that ***t*-29** possesses a half wave oxidation potential of + 1.1 V, which is more positive than the reduction potential of the ruthenium complex by 0.5 V.[36] Irradiation of the solution with $[Ru(bpz)_3]^{2+}$, a better oxidant than $Ru(bpy)_3^{2+}$ by +0.68 V, and inclusion of air as the co-oxidant did produce desired dimer **25** in 57% yield after 2 hours (Figure 2-28). Unfortunately, prolonged reaction times failed to increase yields. When $[Ru(bpm)_3]^{2+}$ was employed as the photooxidant under standard conditions, the desired cycloadduct **25** was obtained in 72% yield. This reaction was optimized to afford the dimer in an 81% isolated yield by carrying the reaction out at 0 °C. Interestingly, the product was formed as a single diastereomer, where all groups were *trans* to one another. As previously discussed, this diastereomer is the desired one, as the skeletal structure is commonly found in the naturally-occurring and biologically active lignan cyclobutanes.

**Figure 2-28: Optimization of Conditions for Homodimerization of *trans*-Anethole**

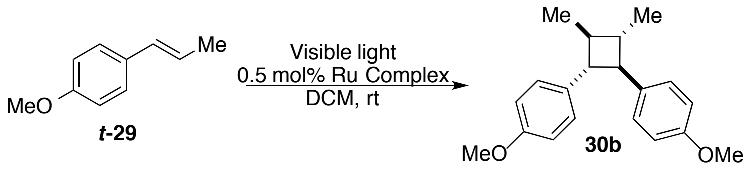

| Ru complex | co-oxidant | time | yield |
|---|---|---|---|
| $[Ru(bpy)_3](BArF)_2$ | $MV(PF_6)_2$ | 24h | 9% |
| $[Ru(bpz)_3](BArF)_2$ | air | 2h | 57% |
| $[Ru(bpm)_3](BArF)_2$ | air | 2h | 72% |
| $[Ru(bpm)_3](BArF)_2$ | air | 2h, 0 °C | 81% |

To explain the unanticipated reactivity pattern of ruthenium complexes, the authors measured the oxidation potential of cycloadduct **30b**. Cycloadduct **30b** was found to possess a half wave oxidation potential of +1.27 V, which is +0.17 V more positive than the oxidation potential of the monomer alkene. $[Ru(bpz)_3]^{2+}$ has an excited state reduction potential capable of oxidizing both the starting alkene as well as the cycloadduct. On the other hand, $[Ru(bpm)_3]^{2+}$ has an excited state reduction potential that lies in between the monomer and the dimer. For this reason, $[Ru(bpm)_3]^{2+}$ was less likely to oxidize the cycloadduct, which allows for the selective single-electron oxidation of *t*-anethole ***t*-29**. In summation, the solution Yoon proposes to impede cycloreversion was by employing a photooxidant possessing an excited state reduction potential that lies between the starting alkene and the cyclobutane adduct. Although effective, this principle is not efficient since a wide range of ruthenium complexes must be synthesized in order to choose a photooxidant with the proper redox properties. This constraint is evident as Yoon's homodimerization of *t*-anethole is the sole example in this report. Due to this limitation, Yoon was unable to apply the methodology for the homodimerization of alkenes, but instead is appropriate for the synthesis of heterodimers. By employing the same principles, heterodimerization between ***t*-29** and other alkenes was affected if the second alkene possesses an oxidation potential more positive than ***t*-29** (Figure 2-29). This requirement allows for selective oxidation of ***t*-29** and results in formation of radical cation ***t*-29**$^{\cdot +}$, while the second alkene is out of range for oxidation by the ruthenium complex and may only react as a nucleophile towards charged species.

**Figure 2-29: Scope for the Heterodimerization of Alkenes with *trans*-Anethole**

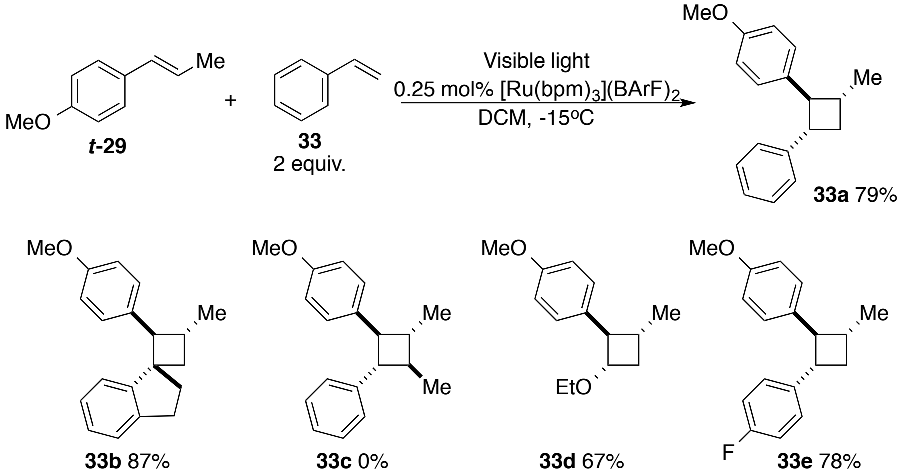

In order to minimize homodimerization, slow addition via syringe pump of ***t*-29** was required. Styrene **33** performed well under standard conditions, as the desired dimer **33a** was obtained in 79% yield when one equivalent of ***t*-29** and two equivalents of the terminal alkene were used. Styrene derivatives with α-substitution were also tolerated, as 1-methylene-2,3-dihydro-1H-indene resulted in formation of the cyclobutane **33b** possessing a quaternary center in 87% yield. The scope of this method was extended to the heterodimerization of ethyl vinyl ether and electron deficient styrenes, providing cyclobutanes **28d** and **28e** in 67% and 78%, respectively. However, reaction of ***t*-29** with β-methyl styrene only resulted in homodimerization of ***t*-29**. The authors speculate that the ruthenium complex may be preferentially oxidizing β-methylstyrene over ***t*-29**. Unfortunately, the discrepancy in this argument is that β-methylstyrene is +0.4 V more positive than ***t*-29**, and therefore out of range of oxidation by the photooxidant.

Yoon extended this method to encompass dimerization of styrene derivatives where 4-

methoxystyrene was employed as the oxidizable olefin (Figure 2-30). While elucidating the scope and limitations of this transformation, a unique trend was discovered. When 4-methoxystyrene **33f** was in the presence of two equivalents of ***t*-29**, desired cycloadduct **33g** was isolated in an excellent 86% yield. However, if a mildly electron donating substituent was *meta* to the alkene substituent on ***t*-29**, a lower yield of the dimer was observed. This trend was observed for *meta*-methyl **33h** and methoxy **33i** cyclobutanes, resulting in 59%, and 29% yields respectively. From these results, it can be concluded that electron-releasing groups in the *meta* position decrease the yield of the cycloadduct. Yoon explains this trend by unselective oxidation of the cycloadduct over the monomer olefin. Unfortunately, this explanation does not rationalize the reactivity trend observed for substrates possessing electron-releasing groups at the *meta* position. This could have been clarified by comparing the yields of cycloadducts possessing the same electron-rich functionality at different positions on the aromatic ring. Moreover, the authors propose two mechanisms to their transformation, which is dependent upon the substrate employed. In order to provide cycloadduct **33g**, the authors suggest the substituted alkene (***t*-29**) undergoes single electron oxidation by the ruthenium complex; this radical cationic intermediate is proposed to react with a neutral equivalent of alkene and is followed by single electron reduction to afford the neutral cycloadduct. Contrary to this mechanism, the authors propose single electron oxidation of the terminal alkene (4-methoxystyrene) by the ruthenium complex initiates the transformation to afford cyclobutanes **33h** and **33i**.

**Figure 2-30: Scope for the Heterodimerization of Alkenes with 4-Methoxystyrene**

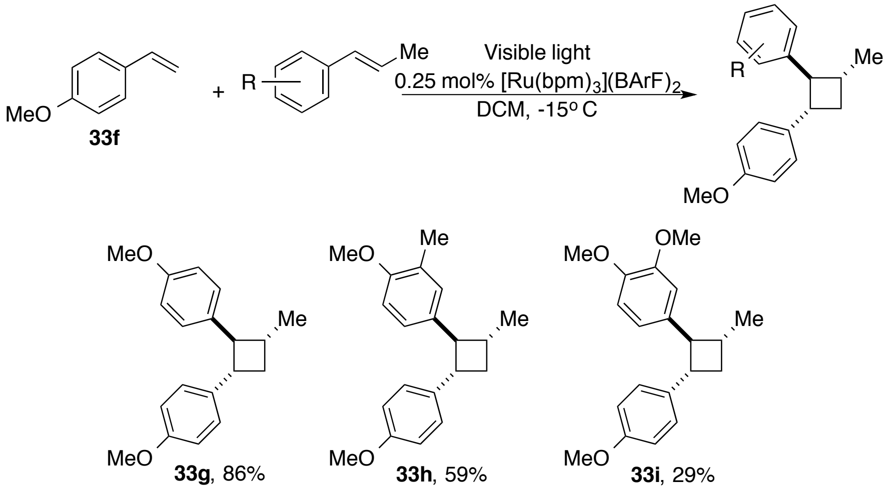

Although successful dimerization methods have been developed using these inorganic photocatalysts, the oxidation and reduction range of ruthenium complexes is still quite narrow. This provides a space of further development. In order to access substrates with more negative reduction potentials or more positive oxidation potentials, a new method is required.

## 2.3 Synthesis of Lignan Cyclobutanes via an Organic Single-Electron Oxidant Electron-Relay System

Given the current limitations of cyclobutane synthesis, we were interested in developing a method based on photoredox catalysis. We hypothesized that a single electron transfer (SET) approach could provide a biomimetic route to the all *trans*-cyclobutane core found in many bioactive lignan natural products (Figure 2-31). To affect dimerization via photoinduced electron transfer, substrates possessing moderately low oxidation potentials, yet capable of affecting nucleophilic addition in its neutral form were necessary. Additionally, a photooxidant able to oxidize electron-rich alkenes while minimizing back electron transfer was desired. For our interests, we wished to focus on organic photooxidants with a direct and simple synthesis, and possessing an absorption band within the visible light range. In the selection of a single electron photooxidant, we focused our attention to triaryloxopyrylium salts as potential candidates due to their excitation in the visible region (*hv* > 400 nm).[37] The use of triaryloxopyrylium salts is also advantageous due to minimization of Coulombic attraction between catalyst and substrate after single electron transfer that can cause unproductive back-electron transfer. As the triarylpyrylium salts possess an excited state reduction potential above than the substrate and the cycloadduct, single electron oxidation of cyclobutane products may occur, as observed by Yoon et. al. (vide supra). In order to remedy this, we proposed that a single photooxidation catalyst could be used in conjunction with an arene or polyarene, acting as an electron relay. The arene would be judiciously selected to match with the oxidation potential of the alkene to avoid significant overpotential. This approach would expand the cycloaddition substrate scope, minimize the need for complex catalyst derivatization, and could allow access to the synthesis of highly oxygenated lignan cyclobutanes.

**Figure 2-31: Synthesis of $C_2$ Symmetric Cyclobutanes via Photoinduced Electron Transfer**

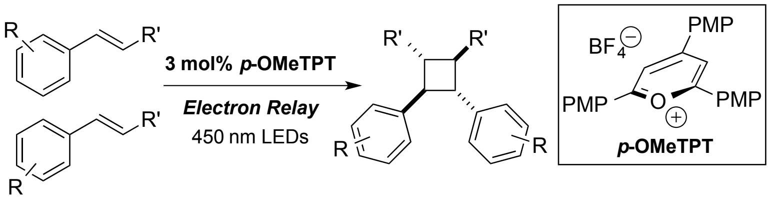

2,4,6-*tris*(4-methoxyphenyl)pyrylium tetrafluoroborate (*p*-OMeTPT) was chosen as the optimal photooxidant as it has an excited state reduction potential of +1.98 V, which is significantly more positive than the styrenes we planned to investigate, and could be attenuated with an appropriate electron relay. We first examined the homodimerization of *trans*-anethole ***t*-29** ($E_{p/2} = +1.29\,V$) as a test case for this proposal. When *trans*-anethole was subjected to 3 mol% of *p*-OMeTPT in acetonitrile in the presence of 450 nm LEDs, only starting material was observed (Table 2-1, entry 1). Since it was certain that the photooxidant was capable of oxidizing ***t*-29**, we hypothesized that cycloreversion may have a faster rate compared to cyclobutane formation. To probe this theory, the effectiveness of triphenylamine ($E_{1/2}^{ox} = +0.91\,V$) and anthracene and ($E_{1/2}^{ox} = +1.21\,V$) as electron relays was considered. As triphenylamine has an oxidation potential that is significantly less positive than ***t*-29**, we would expect direct quenching of the photooxidant resulting in no product formation. On the other hand, anthracene has an oxidation potential value slightly less positive than the monomer. No cycloadduct was observed when 0.25 equivalents of triphenylamine were included (entry 6), while cyclobutane **30b** was observed in a 13% yield when anthracene was employed (entry 2). In the presence of naphthalene ($E_{1/2}^{ox} = +1.61\ V$), appreciable amounts of the cycloadducts were observed (entry 3). As the oxidation potential of naphthalene is closer to the cycloadduct as opposed to the starting monomer, we propose that a competitive oxidation process occurs between naphthalene and the cycloadduct. After some optimization, we found that 0.5 equivalents of the electron relay and longer reaction times (5 days) were required to produce the desired cycloadduct **30b** in 54% yield (entry 5). When the reaction was carried out in the absence of light or when the photooxidant was excluded, no cycloadduct was observed (entry 7 and 8). Similar to Yoon's report, the cycloadduct of ***t*-29** was observed as the single $C_2$-symmetric all *trans* isomer. These observations suggest that the stereochemistry between the methyl group and arene ring of ***t*-29** preferentially retain the *trans* stereochemistry, and that steric effects may explain the relative stereochemistry between the aromatic moieties. To support our mechanistic hypothesis, we calculated the half wave peak potential of cyclodimer **30b** ($E_{p/2} = +1.5\ V$). As we expected, the peak potential of the cycloadduct was found to be more positive than ***t*-29** and similar in value to the electron relay.

**Table 2-1: Effect of Electron Relays as an Additive in the [2 + 2] Dimerization of Anethole**

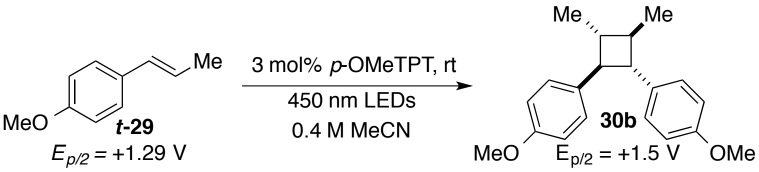

| Entry | Electron Relay[a] | Equivalents | Yield |
|---|---|---|---|
| 1 | none | none | 0% |
| 2 | anthracene (+1.21 V) | 0.25 | 13% |
| 3 | naphthalene (+1.61 V) | 0.25 | 16% |
| 4 | naphthalene | 0.5 | 18% |
| **5[a]** | **naphthalene** | **0.5** | **54%** |
| 6 | $NPh_3$ (+0.91 V) | 0.25 | 0% |
| 7[b] | naphthalene | 0.5 | 0% |
| 8[c] | naphthalene | 0.5 | 0% |

Reactions were carried out for 24 h, unless otherwise noted. $^1$H NMR yields are reported. Peak potentials of electron relay in parenthesis. [a] Reaction time was 5 days. [b] Reaction in the dark. [d]Reaction in the absence of p-OMeTPT.

To distinguish between an electron transfer mechanism and an energy transfer mechanism, the triplet energies of the electron relays were considered. Considering that the triplet energy of the photocatalyst (51 kcal/mol) is below the triplet energy of naphthalene (60 kcal/mol) energy transfer is not likely. For this reason, we propose the polyarenes behave as electron-relays. To test the viability of this method, we next turned our attention to additional styrene derivatives. First, we investigated the oxidative dimerization of 2,4-dimethoxy-β-methylstyrene ($E_{p/2} = +1.19\,V$). The calculated peak potential was exactly +0.1 V less positive than ***t*-29**. By considering the difference between the oxidation potential of ***t*-29** and corresponding dimer **30b**, the oxidation potential of cycloadduct **2.1** could be estimated to be +0.21 V more positive than the monomer ($E_{p/2} \approx +1.4\,V$). The oxidation potential of naphthalene is significantly more positive than cycloadduct **2.1**, and is unable to perform as an electron relay. To better suit this reaction, anthracene was chosen as the electron relay as it exhibits an oxidation potential more positive than the starting monomer and less positive than the suspected oxidation potential of cycloadduct **2.1**. By treating 2,4-dimethoxy-β-methylstyrene to 0.25

equivalents of anthracene in the presence of 3 mol% *p*-OMeTPT and 450 nm light, the all trans $C_2$-symmetric cycloadduct **2.1** was isolated in a 46% yield (Table 2-2, entry 2). If the electron relay was excluded, the background reaction produced the desired cycloadduct in 3% yield, which is described as the parenthetical value. We then considered derivatives of anethole bearing an unconjugated terminal alkene (entry 3). This substrate was found to exhibit a half wave peak potential similar to anethole, suggesting that the aromatic core has the most effect on redox properties. Naphthalene was employed as the electron relay providing 51% yield of **2.2,** where the styrene alkene is selectively dimerized even in the presence of a more accessible alkene. The phthalimide-protected amine (entry 4) also required the same electron relay and successfully dimerized delivering the cyclobutane **2.3** in a 42% yield.

6-Methoxyindene was also considered; unfortunately, standard conditions with the exclusion of an electron relay resulted in polymerization of the material. This unproductive pathway had not been observed in our study previously. To minimize polymerization, the reaction was carried out the reaction at 0 $^{o}$C, and in less polar solvent such as dichloromethane. Though polymerization was reduced, no product formation was observed. Homodimerization of 6-methoxyindene gave the highest yields in the presence of propylene oxide as the additive, producing the desired head-to-head cycloadduct **2.4** in a 72% yield (entry 5). At this time, we do not have definitive mechanistic data to determine the role of the propylene oxide, however it is possible that the epoxide forms a Lewis base complex with the cation radical to prevent polymerization.

**Table 2-2: Scope of [2 + 2] Dimerization of Aromatic Alkenes via Photoinduced Electron Transfer (part 1)**

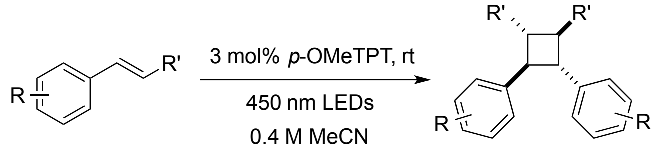

| Entry | Substrate | Electron Relay | Product | Yield[a,b] |
|---|---|---|---|---|
| 1 | 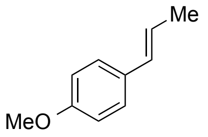 $E_{p/2}$ = +1.29 V | 0.5 equiv. naphthalene | 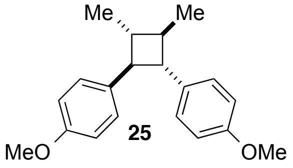 **25** | 54% (0%) |
| 2 | 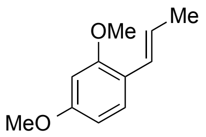 $E_{p/2}$ = +1.19 V | 0.25 anthracene | 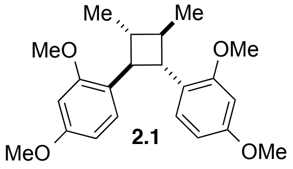 **2.1** | 46% (3%) |
| 3 | 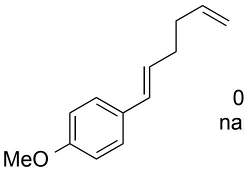 $E_{p/2}$ = +1.33 V | 0.5 equiv. naphthalene | 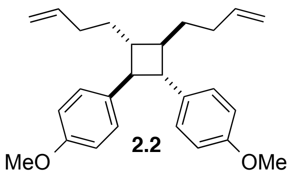 **2.2** | 51% (30%) |
| 4 | 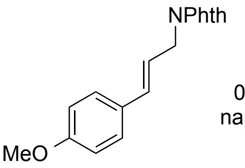 | 0.5 equiv. naphthalene | 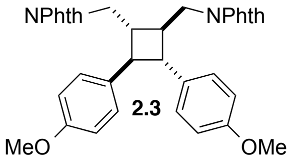 **2.3** | 42% (27%) |
| 5[c] | 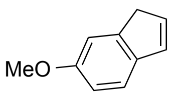 $E_{p/2}$ = +0.99 V | 3 equiv. propylene oxide | 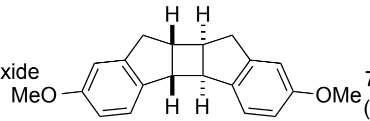 **2.4** | 72% (0%) |

Reactions carried out in 0.4M freeze-pump-thawed acetonitrile. [a] the average of two isolated yields of 100 mg scale [b] reaction was carried out at 0 °C in $N_2$ sparged dichloromethane, [c] reaction was carried out at -10 °C in $N_2$ sparged dichloromethane

7-Methoxy-1,2-dihydronaphthalene (Table 2-3, entry 1) was also found to be susceptible to polymerization when subjected to standard conditions in acetonitrile at room temperature. Following a similar approach, the reaction was out at 0 °C in dichloromethane, yielding the product in 62% as the isolated cycloadduct. These results verified that cyclic alkenes were competent substrates to afford cyclobutane adducts. We then considered 4-hydroxy-3-methoxy-β-methylstyrene and 3,4-

dimethoxy-β-methylstyrene (entry 2, **2.6a** and **2.6b**) as potential substrates. As 2,4-dimethoxy-β-methylstyrene (Table 2-2, entry 2), and 3,4-dimethoxy-β-methylstyrene are constitutional isomers, (Table 2-3, entry 2**, 2.6b**) we expected similar levels of reactivity. Unexpectedly, no cycloaddition was obtained after countless attempts to optimize of the reaction. This lack of reactivity was also observed for the 4-hydroxy-3-methoxy-β-methylstyrene (entry 2b, **2.6a**). As discussed in section 2.2.6, Yoon has also observed a similar reactivity pattern, where electron rich *meta*-substituted monomers exhibit diminished reactivity. Yoon proposed limited reactivity was due to cycloreversion, as the cycloadduct of the di-oxygenated species is now within range of oxidation by the ruthenium complex. Conversely, Yamashita proposed that charge localization resides within the aromatic ring when electron rich *meta* substitution was present (vide supra, Figure 2-32, case 1). When *ortho* and *para* electron rich substituents decorate the aromatic ring, the net stabilization permits for charge delocalization onto the styrenyl alkene (Figure 2-32, case 2).

**Figure 2-32: Net Stabilization Elucidates Reativity Pattern of Electron Rich Substituted Styrenes**

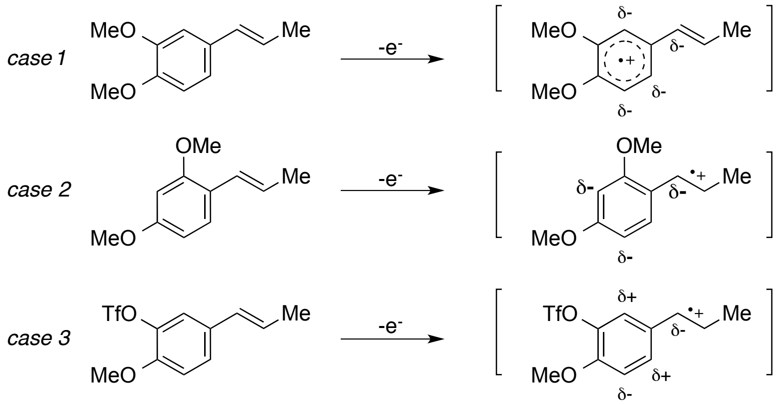

As we were in agreement with Yamashita's argument, we believed charge localization could be manipulated by modifying the electronics of the substrate. To test this hypothesis, we synthesized a substrate possessing an electron withdrawing substituent at the *meta* position and an electron releasing substituent at the *para* position (Figure 2-32, case 3). The trifluoromethanesulfonate (triflate) protected substrate possessed a half wave peak potential of +1.8 V, which suggests that this substrate should be more difficult to oxidize (entry 3). As the oxidation potential of this substrate is closest to the photooxidant, it is plausible that the oxidation potential of the cyclodimer is higher than the photooxidant. This was confirmed as cycloadduct **2.7** was obtained in a 31% yield (entry 3). To complete the substrate scope, we found our transformation effective for the formation of cyclobutanes arising from the carboxybenzyl (Cbz) protected ene-amine, producing product **2.8** in a 78% yield (Table 2-2, entry 4). It should be noted that (1) significantly higher yields of the cyclobutane adducts were obtained in all cases where electron relays were employed and (2) the nature of the electron relay remains unchanged upon completion of the reaction, and is easily removed during purification.

**Table 2-3: Scope of [2 + 2] Dimerization of Aromatic Alkenes via Photoinduced Electron Transfer (part 2)**

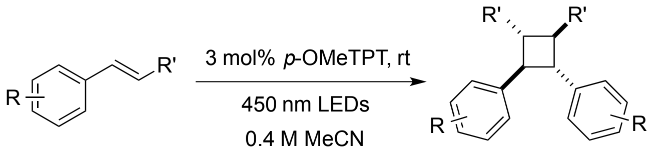

| Entry | Substrate | Electron Relay | Product | Yield[a,b] |
|---|---|---|---|---|
| 1[c] | 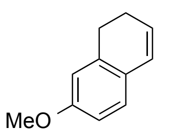 | none | 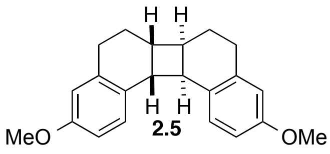 **2.5** | 62% |
| 2 | 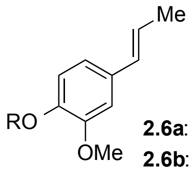 **2.6a**: R=H<br>**2.6b**: R=Me | 0.25 anthracene | 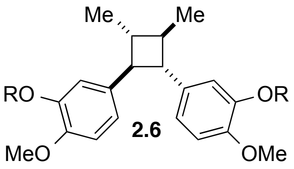 **2.6** | (0%)<br>(0%) |
| 3 | 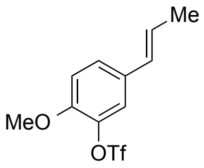 $E_{p/2}$ = +1.8 V | none | 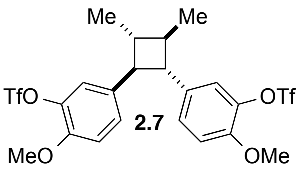 **2.7** | 31% |
| 4[d] | 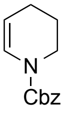 | 0.25 equiv. naphthalene | 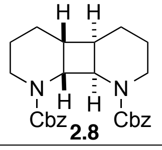 **2.8** | 78%<br>(14%) |

Reactions carried out in 0.4M freeze-pump-thawed acetonitrile. [a] the average of two isolated yields of 100 mg scale, [b] reaction was carried out at 0 °C in $N_2$ sparged dichloromethane, [c] reaction was carried out at -10 °C in acetonitrile, [d] Reaction carried out at 10°C in acetonitrile.

To extend this method, we next considered the head-to-head dimerization of terminal styrenes. This is a challenging feat as electron rich terminal styrenes are common monomers for polymerization, hence extremely susceptible to this detrimental pathway. Not surprisingly, only polymerization was observed when unsubstituted styrenes such as 4-methoxystyrene were subjected to the previously developed conditions (Table 2-4, entry 1). Although not anticipated, this presented the opportunity to create a method where two different deactivating pathways may be thwarted. In an attempt to inhibit the polymerization pathway, we carried out the reactions at cryogenic temperatures. In the absence of an electron relay, polymerization was observed; however, when 0.75 equivalents of anthracene was employed as the electron relay, desired cycloadduct **2.9** was isolated in an excellent 83% yield. 2,4-Dimethoxystyrene possessed a half wave peak potential of +0.99 V, and was also extremely susceptible to polymerization. Anthracene was matched as an ideal electron relay, and resulted in the isolation of head-to-head cycloadduct **2.10** in a 73% yield (entry 2). When 2,4,5-trimethoxystyrene was considered, polymerization could not be thwarted when anthracene was employed. Optimized results for the product formation of 2,4,5-trimethoxystyrene dimer required diethylaniline as the electron relay. This electron relay possesses a half wave oxidation potential of + 0.72 V,[38] which is less positive than the oxidation potential of the monomer. To increase the rate of the transformation, the electron relay was employed in catalytic amounts and the reaction was carried out at room temperature, which produced the desired cycloadduct in a 34% yield (entry 3). Lastly, to compare our method with a common photoinduced electron transfer dimerization adduct, we subjected *N*-vinyl carbazole to standard conditions, and obtained cycloadduct **2.11** in quantitative yield without the need of an electron relay (entry 4).

**Table 2-4: [2 + 2] Dimerization of Terminal Aromatic Alkenes via Photoinduced Electron Transfer**

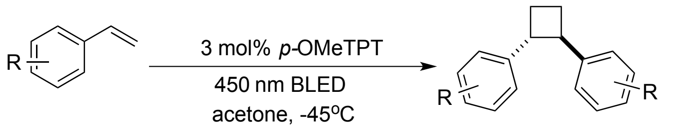

| Entry | Substrate | Electron Relay | Product | Yield[a,b] |
|---|---|---|---|---|
| 1 | 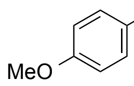 | 0.75 equiv. anthracene | 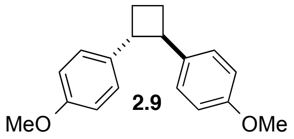 **2.9** | 83%<br>(0%) |
| 2 | 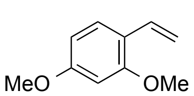 $E_{p/2}$ = + 0.99 V | 0.5 equiv. anthracene | 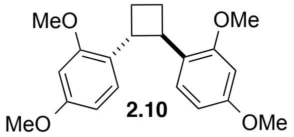 **2.10** | 73%<br>(0%) |
| 3[c] | 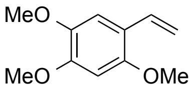 $E_{p/2}$ = + 1 V | 15 mol% diethylaniline | 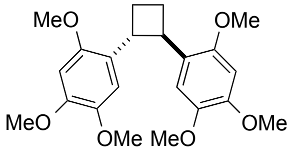 ***pellucidin A*** | 34%<br>(0%) |
| 4[d] | 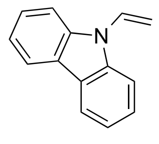 | none | 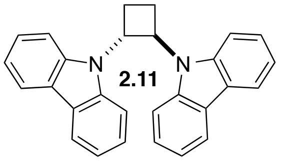 **2.11** | 99% |

[a] Reactions carried out in 0.4 M of sparged acetone. [b] Average of two isolated yields of 100 mg scale. [c] Parenthetical product yield in absence of electron relay. [d] Reaction was carried out at 0°C.

To confirm the stereochemistry around the cyclobutane core, we verified characterization data of the popular N-vinyl carbazole dimer **2.11**. Our data matched identically with the reported characterization, endorsing the *trans* orientation around the cyclobutane core. Dimer (**2.9)** as well as the *meso* dimer been previously studied and characterized by Johnston and Schepp.[39] We were gratified to see confirmation of the *trans* geometry of the aromatic rings. The dimer of the tri-oxygenated substrate (entry 3) had recently been isolated from the herb Peperomia pellucida and characterized by Bamya.[40] The isolation report included isolation of 2,4,5-trimethoxystyrene, which again suggests the cycloadduct might naturally form from monomer dimerization. The authors established the stereochemistry the cycloadduct with 1D and 2D NMR spectroscopy, and concluded that the dimer possessed both aromatic groups *cis* to one another. Though we believed the aromatic groups were *trans* to one another, we found our characterization data matched perfectly with theirs. To solidify the stereochemistry of the cycloadduct, we obtained X-ray quality crystals that unambiguously show the *trans* stereochemistry around the cyclobutane core. With this, we proposed a revised structure of pellucidin A (Figure 2-33).

**Figure 2-33: X-Ray Crystal Structure of Pellucidin A**

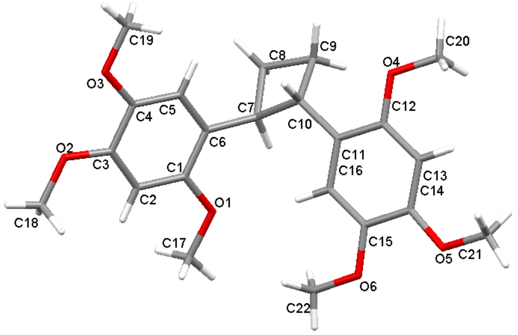
C19
C8
C9
C20
O4
O3
C4
C5
C7
C12
C10
C6
O2
C3
C11
C16
C1
C13
C14
C2
O1
C18
C17
C15
O5
C21
O6
C22

Most importantly, we were able to utilize this method to synthesize two lignan cyclobutane natural products. Treatment of *E*-asarone to the oxidative reaction conditions in the presence of 0.5 equivalents of anthracene furnished magnosalin in 50% yield (Figure 2-34).

**Figure 2-34: Direct [2+2] Synthesis of Magnosalin as a Single Diastereomer**

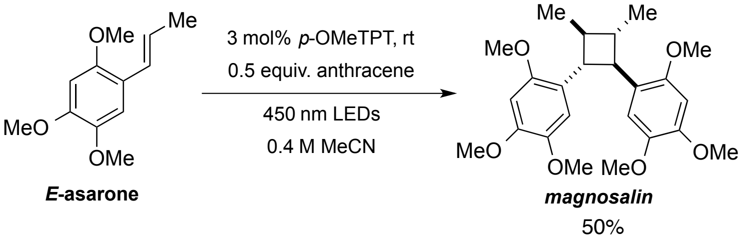
OMe
Me
MeO
OMe
*E*-asarone
3 mol% *p*-OMeTPT, rt
0.5 equiv. anthracene
450 nm LEDs
0.4 M MeCN
Me
Me
MeO
OMe
MeO
OMe
MeO
OMe
***magnosalin***
50%

Unfortunately after several attempts to directly synthesize endiandrin A, no cycloadduct formation was ever observed. This is most likely due to the monomer possessing an electron rich substituent in the *meta* position. However, we were able to further elaborate dimer **30b** by treating the cycloadduct to *ortho*-bromination and demethylation, revealing bromines at the 3-position and the hydroxyls at the 4-position. Lastly, a methoxy-copper coupling was performed on the bromine adduct, which provided endiandrin A in a 59% yield over 3 steps (Figure 2-35). This represents the first synthesis of the bioactive cyclobutane lignan.

**Figure 2-35: Elaboration of Anethole Dimer to Furnish Endiandrin A**

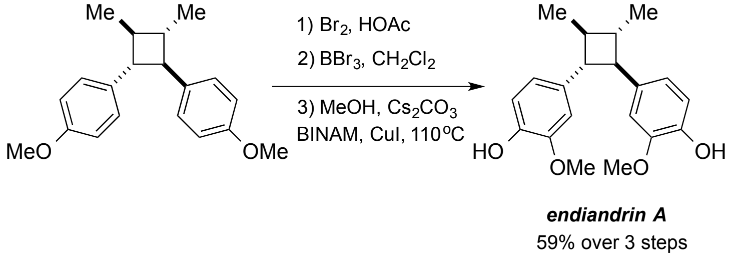
Me
Me
MeO
OMe
1) $Br_2$, HOAc
2) $BBr_3$, $CH_2Cl_2$
3) MeOH, $Cs_2CO_3$
BINAM, CuI, 110°C
Me
Me
HO
OMe MeO
OH
endiandrin A
59% over 3 steps

To probe the role of the electron relay additive and its effect on cycloreversion, we subjected the cyclodimer **2.1** to standard conditions. In the absence of the electron relay, cyclodimer **2.1** was recovered in 65% yield and significant quantities (11%) of the alkene monomer were observed. Low mass balance recovery was suggested to occur due to the formation of the volatile 2,4-dimethoxybenzaldehyde, a product from oxidative cleavage (Figure 2-36).

**Figure 2-36: Effect of Electron Relay on Cycloreversion**

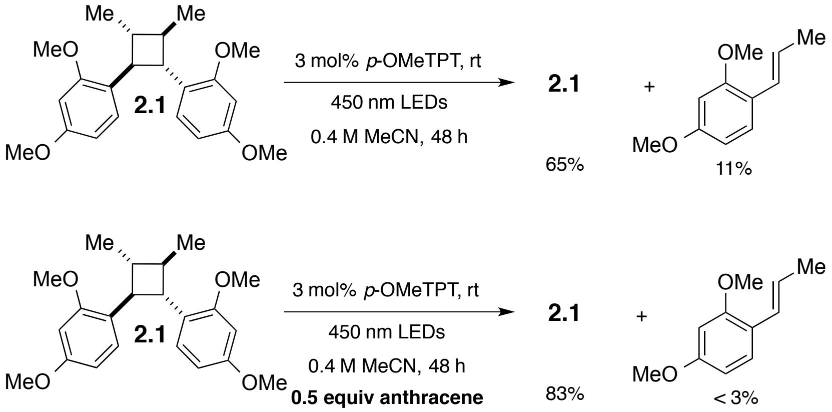
Me
Me
MeO
OMe
2.1
MeO
OMe
3 mol% p-OMeTPT, rt
450 nm LEDs
0.4 M MeCN, 48 h
2.1
65%
+
OMe
Me
MeO
11%
Me
Me
MeO
OMe
2.1
MeO
OMe
3 mol% p-OMeTPT, rt
450 nm LEDs
0.4 M MeCN, 48 h
0.5 equiv anthracene
2.1
83%
+
OMe
Me
MeO
< 3%

If the appropriately matched electron relay was included in the reaction, dimer **2.1** was recovered in an 83% yield, with trace amounts of the alkene present. These results suggest that the presence of anthracene is critical to impeding the cycloreversion process. Based on these results, we propose the following mechanistic hypothesis (Figure 2-37). Initial excitation with visible light provides the excited triarylpyryluim salt, which undergoes single electron oxidation with the electron relay **ER** initially. This delivers the active single electron oxidant **ER***, which in turn accomplishes a second single electron transfer with the alkene substrate. After cycloaddition with another molecule of starting material, the **ER** or the reduced triarylpyrylium salt undergoes single electron reduction with the cyclobutane, furnishing the neutral product. We believe that in the absence of an electron relay, cycloaddition is reversible and most likely due to the reduction potential of the activated triarylpyryluim salt being above the oxidation potential of the cyclobutane. Presently, we propose the electron relay suppresses cycloreversion by shielding the cyclobutane products from oxidative degradation.

**Figure 2-37: Proposed Mechanism For Photoinduced Dimerization**

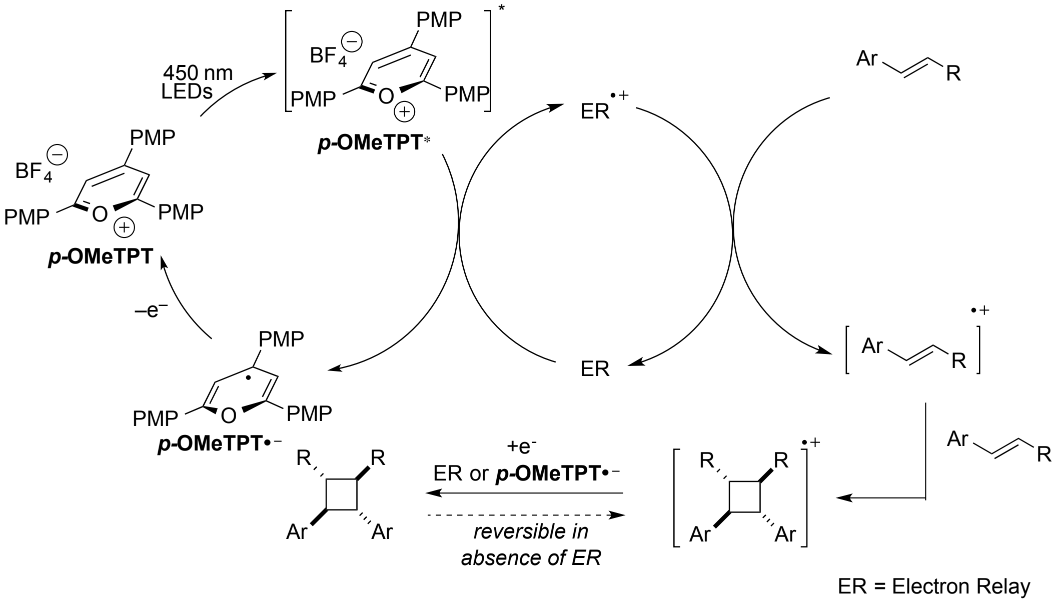

450 nm
LEDs
PMP
BF$_4^{\ominus}$
PMP
PMP
*p*-OMeTPT*
ER$^{\bullet+}$
Ar
R
BF$_4^{\ominus}$
PMP
PMP
PMP
*p*-OMeTPT
–e⁻
PMP
PMP
PMP
*p*-OMeTPT•⁻
ER
Ar
R
•+
Ar
R
+e⁻
ER or *p*-OMeTPT•⁻
reversible in
absence of ER
R
R
Ar
Ar
•+
ER = Electron Relay

## 2.4 Conclusion

We have devised a simple and direct method for the synthesis of $C_2$-symmetric cyclobutanes, which has been applied to the synthesis of magnosalin, various lignan analogs, and 1,1 unsubstituted cyclobutane compounds. By including an electron relay additive, we have offered a protocol for preventing cycloreversion and polymerization of β-substituted styrenes and terminal styrenes, respectively. Additionally, we attempted to best explain the *meta* effect by comparing substrates with oxygenation at different positions around the aromatic ring, and tested the hypothesis of electronic bias by synthesizing a substrate with an electron-withdrawing group in the *meta* position. From this we gathered that the reactivity pattern arises from an electronic effect where the radical cationic charge may be localized within the aromatic ring, but could be delocalized onto the styrenal alkene with the aid of the *meta*-triflate substrate. This method also sheds light on a possible biosynthesis of lignans via a single electron oxidation pathway.

## 2.5 Experimental

**General Methods:** Infrared (IR) spectra were obtained using a Jasco 260 Plus Fourier transform infrared spectrometer. Proton and carbon magnetic resonance spectra (1H NMR and 13C NMR) were recorded on a Bruker model DRX 400, DRX 500, or a Bruker AVANCE III 600 CryoProbe (1H NMR at 400 MHz, 500 MHz or 600 MHz and 13C NMR at 101, 126, or 151 MHz) spectrometer with solvent resonance as the internal standard ($^1$H NMR: $CDCl_3$ at 7.24 ppm; $^{13}$C NMR: $CDCl_3$ at 77.0 ppm). $^1$H NMR data are reported as follows: chemical shift, multiplicity (s = singlet, d = doublet, t = triplet, dd = doublet of doublets, ddt = doublet of doublet of triplets, ddd = doublet of doublet of doublets, dddd = doublet of doublet of doublet of doublets m = multiplet, brs = broad singlet), coupling constants (Hz), and integration. Mass spectra were obtained using a Micromass (now Waters Corporation, 34 Maple Street, Milford, MA 01757) Quattro-II, Triple Quadrupole Mass Spectrometer, with a Z-spray nano-Electrospray source design, in combination with a NanoMate (Advion 19 Brown Road, Ithaca, NY 14850) chip based electrospray sample introduction system and nozzle. Cyclic voltammograms were obtained with a platinum disc working electrode, Ag/AgCl reference electrode, a platinum wire auxillary, and CHI-760 potentiostat using 1 mM solutions of analyte in acetonitrile with 0.1 M tetrabutylammonium perchlorate as supporting electrolyte. Thin layer chromatography (TLC) was performed on SiliaPlate 250 µm thick silica gel plates provided by Silicycle. Visualization was accomplished with short wave UV light (254 nm), aqueous basic potassium permanganate solution, or cerium ammonium molybdate solution followed by heating. Flash chromatography was performed using SiliaFlash P60 silica gel (40-63 µm) purchased from Silicycle. Tetrahydrofuran, diethyl ether, dichloromethane, and toluene were dried by passage through a column of neutral alumina under nitrogen prior to use. Irradiation of photochemical reactions was carried out using a 15W PAR38 blue LED floodlamp purchased from EagleLight (Carlsbad, CA), with borosilicate glass vials purchased from Fisher Scientific. All other reagents were obtained from commercial sources and used without further purification unless otherwise noted.

**Preparation of terminal and β-methyl styrenes**

To an ice-cold mixture of $[Ph_3PCH_3]^+Br^-$ (7.2 g, 20.2 mmol) in THF (155 mL) was added BuLi (in hexanes, 19.4 mmol). The mixture was stirred at the same temperature for 2 h, and a solution of aldehyde (15.5 mmol) in THF (1 mL) was added at -78 $^{o}$C. The mixture was slowly warmed to room temperature over the course of 3 hours. The reaction was diluted with 15 mL of D.I. water. The resulting mixture was extracted with chloroform twice. The combined extracts were dried over $MgSO_4$, and concentrated to leave a solid, which was purified by chromatography on silica gel. The $^{1}$H and $^{13}$C NMR spectrum was identical with that reported. β-methyl substituted styrenes were prepared similarly and then isomerized to the *trans* by known procedures.[41]

**General Procedure A**. To a flame-dried two dram vial equipped with a magnetic stir bar was added the terminal styrene (1.0 equiv.), *p*-OMe TPT (3 mol%), and electron relay (0.25-0.5 equiv). The vial was purged with $N_2$ and sparged acetone was added to achieve a concentration of 0.4 M with respect to substrate, then sealed with a septum screwcap and Teflon tape. The reaction was irradiated with a 450 nm bulb and stirred at the indicated temperature and time period. Upon completion, the reaction was quenched with small amounts of TEMPO, diluted with diethyl ether, and filtered through a short cotton plug. The solution was dry loaded further purified by flash column chromatography with acetone/hexanes as the eluent mixture.

**General Procedure B**. To a flame-dried two dram vial equipped with a magnetic stir bar was added the substituted styrene (1.0 equiv.), p-OMe TPT (3-5 mol%) and electron relay (0.25-0.5 equiv). The vial was purged with $N_2$ and diluted with freeze-pump-thawed acetonitrile to a concentration of 0.4 M with respect to substrate, then sealed with a septum screwcap and Teflon tape. The reaction was irradiated with a 450 nm bulb and stirred the indicated time period. Upon completion, the reaction was diluted with diethyl ether, and filtered through a short cotton plug. The solution was dry loaded further purified by flash column chromatography with acetone/hexanes as the eluent mixture.

**Cycloreversion Procedure C**: To a flame-dried two dram vial equipped with a magnetic stir bar was added the substituted styrene (1.0 equiv.), p-OMe TPT (3 mol%) and electron relay (0.25-0.5 equiv). The vial was purged with $N_2$ and diluted with freeze-pump-thawed acetonitrile to a concentration of 0.4M with respect to substrate, then sealed with a septum screwcap and Teflon tape. The reaction was irradiated with a 450 nm bulb and stirred for 48 hours. Upon completion, yield and mass balance was obtained via $^1$H NMR.

**Cycloreversion Procedure D**: To a flame-dried two dram vial equipped with a magnetic stir bar was added the substituted styrene (1.0 equiv.) and p-OMe TPT (3 mol%). The vial was purged with $N_2$ and diluted with freeze-pump-thawed acetonitrile to a concentration of 0.4M with respect to substrate, then sealed with a septum screwcap and Teflon tape. The reaction was irradiated with a 450 nm bulb and stirred for 48 hours. Upon completion, yield and mass balance was obtained via $^1$H NMR.

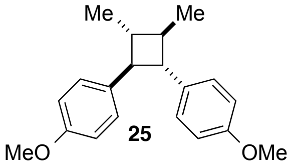

**25**

**4,4'-(3,4-Dimethylcyclobutane-1,2-diyl)bis(methoxybenzene) (25):** The dimer was prepared according to General Procedure **B** using 104 μL of 4-methoxy-β–methylstyrene, 44.8 mg of naphthalene, and 10.2 mg of p-OMe TPT. Reaction was carried out at room temperature and purified via flash chromatography. Reaction time was 5 days. Yield was 56 mg (54%) of the desired adduct as a clear oil. Characterizations matched literature.[42] **$^1$H NMR** (400 MHz, $CDCl_3$) 7.17 (d, 8.8 Hz, 4H), 6.87, (d, *J* = 8.8 Hz, 4H), 9.80 (s, 6H), 2.84 (dd, *J* = 3.2, 5.6 Hz, 2H), 1.88 (m, 2H), 1.22 (d, *J* = 6.0 Hz, 6H). **$^{13}$C NMR** (400 MHz, $CDCl_3$) δ 157.94, 135.92, 127.71, 113.69, 55.23, 52.47, 43.20, 18.86.

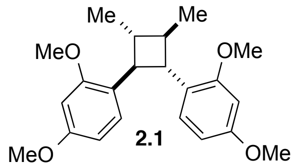

2.1

**4,4'-(3,4-Dimethylcyclobutane-1,2-diyl)bis(1,3-dimethoxybenzene) (2.1):** The dimer was prepared according to General Procedure **B** using 106 mg of 2,4-dimethoxy-β–methylstyrene, 26.7 mg of anthracene, and 8.8 mg of p-OMe TPT. Reaction was carried out at room temperature and purified via flash chromatography. Reaction time was 4 days. Yield was 50 mg (47%) of the desired adduct as a clear oil. $^{1}$**H NMR** (400 MHz, CDCl$_3$) δ 7.21 (d, *J* = 12.0 Hz, 2H), 6.45 (dd, *J* = 2.0, 8.0 Hz, 2H), 6.39 (d, *J* = 2.4 Hz, 2H), 3.78 (s, 6H), 3.690 (s, 6H), 3.26 (dd, *J* = 3.6, 5.6 Hz, 2H), 1.76 (d, 5.2 Hz, 2H), 1.17 (d, *J* = 5.6 Hz, 6H). $^{13}$**C NMR** (400 MHz, CDCl$_3$) δ 158.75, 158.47, 127.74, 125.01, 103.73, 98.20, 55.30, 55.10, 44.88, 43.43, 19.20. **MS** (+ESI) Calculated *m/z* for $[M+H]^+$ = 357.20, Found *m/z* for $[M+H]^+$ = 357.25. **IR** (Thin Film, cm$^{-1}$): 3050, 2998, 2950, 2861, 2851, 1611, 1585, 1506, 1455, 1438, 1294, 1264, 1208. **TLC** 2% acetone/ 98% Hexanes. CAM stains dark blue.

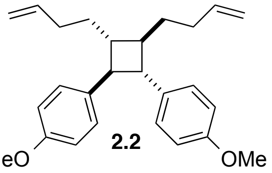

2.2

**4,4'-(3,4-Di(but-3-en-1-yl)cyclobutane-1,2-diyl)bis(methoxybenzene) (2.2):** The dimer was prepared according to General Procedure **B** using 112.8 mg of (*E*)-1-(hexa-1,5-dien-1-yl)-4-methoxybenzene, 38.2 mg of naphthalene, and 14.6 mg of *p*-OMe TPT. Reaction was carried out at room temperature and purified via flash chromatography. Reaction time was 6 days. Yield was 52 mg (42%) of the desired adduct as a clear oil. $^{1}$**H NMR** (400 MHz, CDCl$_3$) δ 7.14 (d, *J* = 6 Hz, 2H) 6.83 (d, *J* = 6 Hz, 2H) 5.81-5.74 (m, 2H), 4.92 (s, 2H), 4.90 (d, *J* = 4 Hz, 2H), 3.78 (s, 6H), 2.81 (dd, *J* = 2.0, 4.0 Hz, 2H), 2.030 (m, 6H), 1.78-1.67 (m, 4H). $^{13}$**C NMR** (400 MHz, CDCl$_3$) δ 157.91, 138.81, 136.01, 127.93, 114.34, 113.61, 55.18, 52.11, 45.37, 35.28, 31.52. **MS** (+ESI) Calculated *m/z* for $[M+H]^+$ = 377.24, Found *m/z* for $[M+H]^+$ = 377.27. **IR** (Thin Film, cm$^{-1}$): 3073, 2997, 2914, 2831, 2547, 2359, 1639, 1611, 1581, 1511, 1455, 1440, 1301, 1247. **TLC** 2% acetone/ 98% Hexanes.

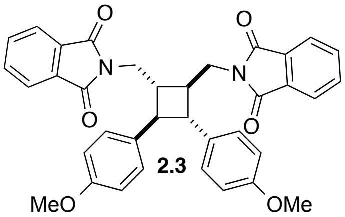
**2.3**

**2,2'-((3,4-Bis(4-methoxyphenyl)cyclobutane-1,2-diyl)bis(methylene))bis(isoindoline-1,3-dione) (2.3)** The dimer was prepared according to General Procedure **B** using 117 mg of (*E*)-2-(3-(4-methoxyphenyl)allyl)isoindoline-1,3-dione, 36 mg of naphthalene, and 6 mg of *p*-OMe TPT. Reaction was carried out at room temperature and purified via flash chromatography. Reaction time was 4 days. Yield was 62 mg (53%) of the desired adduct as a clear oil. **$^1$H NMR** (400 MHz, $CDCl_3$) δ 7.72–7.70 (m, 4H), 7.64-7.62 (m, 4H), 7.12 (d, *J* = 8.8 Hz, 4H), 6.72 (d, *J* = 8.8 Hz, 4H), 3.93-3.82 (dq, *J* = 4.8, 14.0 Hz, 4H), 3.0 (dd, *J* = 3.2, 9.2 Hz, 2H), 2.57 (m, 2H). **$^{13}$C NMR** (400 MHz, $CDCl_3$) δ 168.47, 158.20, 133.68, 132.00, 127.91, 123.08, 113.74, 55.17, 48.38, 43.14, 40.50. **MS** (+ESI) Calculated *m/z* for $[M+H]^+$ = 587.12 Found *m/z* for $[M+H]^+$ = 587.21. **IR** (Thin Film, $cm^{-1}$): 3056, 2933, 2836, 2360, 1771, 1715, 1612, 1513, 1429, 1395, 1265, 1248. **TLC** 20% acetone/ 80% Hexanes. CAM stains dark blue.

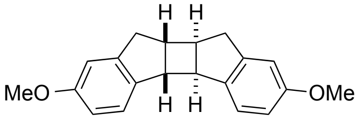
**2.4**

**2,7-dimethoxy-4b,4c,9,9a,9b,10-hexahydrocyclobuta[1,2-*a*:4,3-*a'*]diindene (2.4):** The dimer was prepared according to General Procedure **A** using 140 μL mg of 6-methoxyindene, 210 μL of propylene oxide, and 24 mg of *p*-OMe TPT. Reaction was carried out in sparged dry dichloromethane at –10 °C, and purified via flash chromatography. Reaction time was 24 hours. Yield was 104 mg (71%) of the desired adduct as a clear oil. **$^1$H NMR** (400 MHz, $CDCl_3$) δ 7.33 (d, *J* = 8 Hz, 2H), 6.87 (s, 2H), 6.85 (d, *J* = 8.0 Hz, 2H), 3.85 (s, 6H), 3.64 (d, *J* = 8.0 Hz, 2H), 3.2 (dd, *J* = 16.4, 7.2Hz, 2H), 2.94 (d, *J* = 16.0 Hz, 2H), 2.82-2.79 (m, 2H). **$^{13}$C NMR** (400 MHz, $CDCl_3$) δ 159.11, 145.60, 138.77, 125.61, 113.11, 110.29, 55.38, 53.16, 43.79, 39.51. **MS** (+ESI) Calculated *m/z* for $[M+H]^+$ = 293.15, Found *m/z* for $[M+H]^+$ = 293.16. **IR** (Thin Film, cm-1): 2939, 2905, 2836, 1601, 1579, 1247. **TLC** 2% acetone/ 98% Hexanes. CAM stains dark blue.

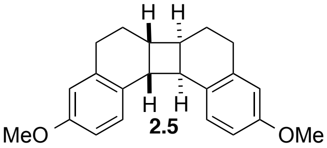
**2.5**

**3,10-dimethoxy-5,6,6a,6b,7,8,12b,12c-octahydrodibenzo[*a,i*]biphenylene (2.5):** The dimer was prepared according to General Procedure **B** using 104 mg of 7-methoxy-1,2-dihydronaphthalene, and 7.3 mg of *p*-OMe TPT. Reaction was carried out in sparged dry dichloromethane at -10°C, and purified via flash chromatography. Reaction time was 7 days. Yield was 65 mg (63%) of the desired adduct as a clear oil. **$^1$H NMR** (400 MHz, $CDCl_3$) δ 6.97 (d, *J* = 8.4 Hz, 2H), 6.77 (dt, *J* = 2.0, 9.6, 17.2 Hz, 4H), 3.82 (s, 6H), 3.20 (dd, *J* = 5.2, 8.0 Hz, 2H), 2.95 (m, 2H), 2.80-2.72 (dt, *J* = 4.4, 9.6, 15.2 Hz, 2H), 2.51 (m, 2H), 1.91-1.86 (m, 2H), 1.79-1.76 (m, 2H) **$^{13}$C NMR** (400 MHz, $CDCl_3$) δ 157.62, 139.51, 132.94, 128.67, 113.88, 111.89, 55.27, 43.88, 35.35, 28.19, 26.81. **MS** (+ESI) Calculated *m/z* for $[M+H]^+$ = 321.16, Found *m/z* for $[M+H]^+$ = 321.17. **IR** (Thin Film, $cm^{-1}$): 3052, 3000, 2924, 2847, 2359, 1608, 1576, 1499, 1265. **TLC** 5% acetone/ 95% Hexanes.

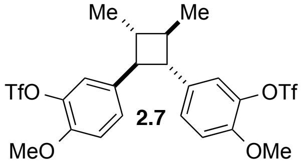
**2.7**

**(3,4-dimethylcyclobutane-1,2-diyl)bis(2-methoxy-5,1-phenylene) bis(trifluoromethanesulfonate) (2.8):** The dimer was prepared according to General Procedure **B** using 118.4 mg of (*E*)-2-methoxy-5-(prop-1-en-1-yl)phenyl trifluoromethanesulfonate, and 5.8 mg of *p*-OMe TPT. Reaction was carried out at room temperature and purified via flash chromatography. Reaction time was 6 days. Yield was 40 mg (34%) of the desired adduct as a clear oil. **$^1$H NMR** (400 MHz, $CDCl_3$) δ 7.12 (dd, *J* = 1.2, 5.6 Hz, 2H), 7.02 (d, *J* = 1.2 Hz, 2H), 6.96 (d, *J* = 5.6 Hz, 2H), 3.89 (s, 6H), 2.76 (dd, *J* = 2.0, 3.6 Hz, 2H), 1.86-1.83 (m, 2H), 1.20 (d, *J* = 4.0 Hz, 6H). **$^{13}$C NMR** (400 MHz, $CDCl_3$) δ 149.74, 138.67, 136.13, 127.21, 120.57, 113.13, 56.24, 52.18, 42.97, 18.60. **MS** (+ESI) Calculated *m/z* for $[M+H_2O]^+$ = 611.53. Found *m/z* for $[M+H_2O]^+$ = 611.03. **IR** (Thin Film, $cm^{-1}$): 3014, 2952, 2923, 2866, 2847, 1621, 1576, 1514, 1455, 1423, 1375, 1294, 1277, 1248, 1211. **TLC** 5% acetone/ 95% Hexanes. CAM stains dark blue.

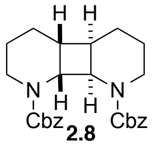

**2.8**

**Dibenzyl octahydrocyclobuta [1,2-*b*:4,3-*b′*] dipyridine-1,8 (8a*H*,8b*H*) -dicarboxylate (2.9):** The dimer was prepared according to General Procedure **B** using 130 mg of benzyl 3,4-dihydropyridine-1(2H)-carboxylate, 19.2 mg of naphthalene, and 8.8 mg of p-OMe TPT. Reaction was carried out in degassed acetonitrile (freeze/pump/thaw method) at –10 °C, and purified via flash chromatography. Reaction time was 4 days. Yield was 104 mg (80%) of the desired adduct as a clear oil. **$^1$H NMR** (400 MHz, $CDCl_3$) δ 7.37-7.33 (m, 10 H), 6.86-6.72 (rotamers, 2 s, 1H), 5.19-5.09, (m, 4H), 4.83 (brs, 1H), 4.06 (br d, *J* = 12.4 Hz, 1H), 3.58 (q, *J* = 5.2, 11.2 Hz, 2H), 2.83 (br t, *J* = 12.4, 24.4 Hz, 1H), 2.03-1.26 (m, 12H). **$^{13}$C NMR** (400 MHz, $CDCl_3$) δ 155.74, 153.63, 152.99, 136.94, 136.43, 128.38, 127.68, 122.25, 121.65, 116.06, 115.39, 67.40, 67. 25, 66.97, 53.52, 42.03, 41.89, 40.13, 25.99, 25.82, 25.52, 25.41, 23.18, 22.93, 21.40, 19.53, 19.37. **MS** (+ESI) Calculated *m/z* for $[M+H]^+$=435.53 Found *m/z* for $[M+H]^+$ = 435.22. **IR** (Thin Film, $cm^{-1}$): 3055, 2939, 2862, 1698, 1455, 1407, 1348, 1311, 1263. **TLC** 5% acetone/ 95% Hexanes. CAM stains dark blue.

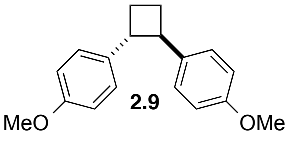

**2.9**

**1,2-Bis(4-methoxyphenyl)cyclobutane (2.9):** The dimer was prepared according to General Procedure **A** using 134 mg of 4-methoxystyrene, 133.5 mg of anthracene, and 14.6 mg of *p*-OMe TPT. Reaction was carried out at –45 °C, and purified via flash chromatography Reaction time was

5.5 days. Yield was 108 mg (80%) of the desired adduct as a clear oil. **$^1$H NMR** (400 MHz, $CDCl_3$) δ 7.18 (d, *J* = 12.0 Hz, 4H), 6.86 (d, *J* = 16.0 Hz, 4H), 3.8 (s 6H), 3.47 (m, 2H), 2.32-2.25 (m, 2H), 2.13-2.07 (m, 2H).**$^{13}$C NMR** (400 MHz, $CDCl_3$) δ 157.98, 136.87, 127.59, 113.72, 55.28, 47.78, 26.03. **MS** (+ESI) Calculated *m/z* for $[M+H]^+$ = 269.15, Found *m/z* for $[M+H]^+$ = 269.07. **IR** (Thin Film, $cm^{-1}$): 2938, 2833, 1611, 1580, 1511, 1462, 1440, 1301, 1247. **TLC** 2% acetone/ 98% Hexanes. CAM stains blue.

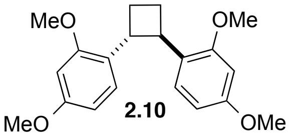

**2.10**

**1,2-Bis(2,4-dimethoxyphenyl)cyclobutane (2.10):** The dimer was prepared according to General Procedure **A** using 115 mg of 2,4-dimethoxystyrene, 62.3 mg of anthracene, and 10.2 mg of *p*-OMe TPT. Reaction was carried out at –45 °C, and purified via flash chromatography. Reaction time was 3 days. Yield was 108 mg (82%) of the desired adduct as a clear oil. **$^1$H NMR** (400 MHz, $CDCl_3$) δ 7.22 (d, *J* = 8.0 Hz, 2H), 6.47 (d, *J* = 2.0 Hz, 2H), 6.44 (s, 2H), 3.87 (br dd, *J* = 8.0, 16.0, 2H), 3.80 (s, 3H), 3.77 (s, 3H), 2.37-2.32 (ddd, *J* = 4.8, 6.8, 11.6 Hz, 2H) 1.96-1.86 (ddd, *J* = 4.0, 8.0, 15.6 Hz, 2H). **$^{13}$C NMR** (400 MHz, $CDCl_3$) δ 158.91, 158.12, 127.48, 125.64, 103.66, 98.24, 55.29, 55.21, 39.95, 27.17. **MS** (+ESI) Calculated *m/z* for $[M+H]^+$ = 329.17, Found *m/z* for $[M+H]^+$ = 329.12. **IR** (Thin Film, $cm^{-1}$): 2936, 2866, 2834, 2360, 2341, 2065, 1613, 1585, 1506, 1456, 1437, 1290, 1260, 1208. **TLC** 5% acetone/ 95% Hexanes. CAM stains dark blue.

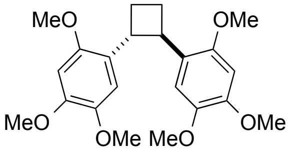

***pellucidin A***

**1,2-Bis(2,4,5-trimethoxyphenyl)cyclobutane (Pellucidin A):** The dimer was prepared according to General Procedure **A** using 116 mg of 2,4,5-trimethoxystyrene, 14 μL of diethylaniline, and 8.8 mg of *p*-OMe TPT. Reaction was carried out at room temperature, and purified via flash chromatography. Reaction time was 5 days. Yield was 42.3 mg (36%) of the desired adduct as a white solid. **$^1$H NMR**

(400 MHz, $CDCl_3$) δ 6.98 (s, 2H), 6.48 (s, 2H), 3.86 (s, 6H), 3.85 (s, 6H), 3.75 (s, 6H), 2.32-2.27 (m, 2H), 1.96-1.92 (m, 2H). **$^{13}$C NMR** (400 MHz, $CDCl_3$) δ 151.11, 148.60, 143.11, 124.64, 111.88, 97.81, 56.61, 56.56, 56.23, 40.47, 27.04. **MS** (+ESI) Calculated *m/z* for $[M+H]^+$ = 389.17, Found *m/z* for $[M+H]^+$ = 389.17. **IR** (Thin Film, $cm^{-1}$): 2988, 2935, 1715, 1523, 1462, 1440, 1349, 1227. **TLC** **1**5% acetone/ 85% Hexanes. CAM stains dark blue. X-ray level crystals were obtained by dissolving 20mg of material in 1.5mL acetone and layering 10 mL hexanes overtop. **Crystal Data**: $C_{22}H_{24}O_6$, M = 384.41, 0.4 × 0.05 × 0.05mm$^3$, tricyclic, space group P-1, *a*=5.0348(4), *b*=14.3242(9), *c*= 15.1715(10) Å, α= 115.546(5) β= 90.919(6) , γ= 98.363(6)°, V= 972.89(12) Å$^3$, Z= 2, T =100 K, 8212 reflections collected, 3264 unique [$R_{int}$ = 0.0934]. The refinement (259 variables, 0 restrictions) based on $F^2$ converged with R = 0.0622, $R_w$ = 0.1319, and GOF= 1.010 using 3264 independent reflections with [I>=2σ (I)].

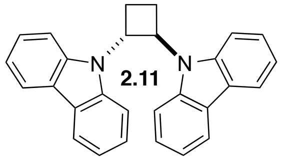

**2.11**

**1,2-Di(9*H*-carbazol-9-yl)cyclobutane** (**Table 2, Entry 4)** The dimer was prepared according to General Procedure **A** using 154 mg of N-vinyl carbazole, and 11.7 mg of p-OMe TPT. Reaction was purified via filtration through a short plug of silica. No future purification was required, Reaction time was 15 hours. Yield was 150 mg of the desired adduct as a white solid. (97%). Analytical data for N-vinyl carbazole dimer matches literature reports:[43] **$^1$H NMR** (400 MHz, $CDCl_3$) δ 8.07 (d, *J* = 8.0 Hz, 4H), 7.576 (d, *J* = 8.4 Hz, 4H), 7.38 (t, *J* = 7.2 Hz, 15.6 Hz, 4H), 7.20 (t, *J* = 8.0, 14.8 Hz, 4H), 6.29 (dd, J = 8.4 Hz, 17.2 Hz, 2H), 3.12 (m, 2H), 2.74 (m, 2H) **$^{13}$C NMR** (400 MHz, $CDCl_3$) δ 139.94, 125.76, 123.58, 120.49, 119.33, 109.65, 54.45, 20.89. **IR** (Thin Film, $cm^{-1}$): 3049, 1623, 1595, 1482, 1451, 1334, 1264, 1210.

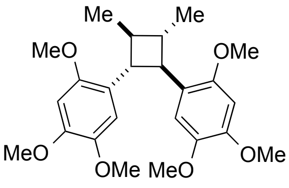

*magnosalin*

**2,4,5-trimethoxy-β–methylstyrene Dimer (magnosalin):** The dimer was prepared according to General Procedure **B** using 104 mg of 2,4,5-trimethoxy-β–methylstyrene, 22 mg of anthracene, and 7.3 mg of p-OMe TPT. Reaction was carried out at room temperature and purified via flash chromatography. Reaction time was 4 days. Yield was 52 mg (50%) of the desired adduct as a white solid. **$^1$H NMR** (400 MHz, $CDCl_3$) δ 6.94 (s, 2H), 6.46 (s, 2H), 3.86 (s, 6H), 3.85 (s, 6H), 3.69 (s, 6H), 3.27 (dd, *J* = 3.2, 8.8 Hz, 2H), 1.77 (dd, *J* = 5.2, 16.4 Hz, 2H), 1.18 (d, *J* = 5.2 Hz, 6H). **$^{13}$C NMR** (400 MHz, $CDCl_3$) δ 151.67, 147.53, 143.11, 123.90, 112.22, 97.85, 56.74, 56.60, 56.21, 45.38, 43.51, 19.11. **MS** (+ESI) Calculated *m/z* for $[M+H]^+$ = 416.22, Found *m/z* for $[M+H]^+$ = 417.26. **IR** (Thin Film, $cm^{-1}$): 3055, 2951, 2832, 2359, 1669, 1608, 1508, 1464, 1438, 1396, 1371, 1318, 1266, 1206. **TLC** 10% acetone/ 90% Hexanes. CAM stains dark blue.

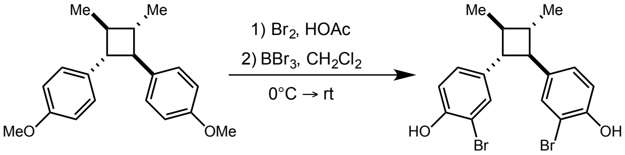

Bromination[44] and demethylation[45] were conducted according to literature procedures. Anethole dimer was stirred in acetic acid at 0 °C. $Br_2$ was added dropwise and the reaction was stirred at room temperature for 30 minutes. The reaction was quenched with $Na_2S_2O_5$, extracted with DCM, washed with brine, dried over $MgSO_4$, and concentrated *in vacuo*. The crude material was then stirred in anhydrous DCM at 0 °C. $BBr_3$ was added dropwise and the reaction was stirred at 0 °C for 2 h. The reaction was then allowed to stir overnight. Upon completion of the reaction, the mixture was cooled to 0 °C, quenched with $H_2O$, extracted with DCM, washed with brine, dried over $MgSO_4$, and concentrated *in vacuo*. The crude material was purified by column chromatography yielding 128 mg, (80% yield) over two steps. **$^1$H NMR** (400 MHz, $CDCl_3$) δ 7.27 (d, *J* = 2.0 Hz, 2H), 7.03 (dd, *J* = 2.0,

8.4 Hz, 2H), 6.93 (d, J = 8.4 Hz, 2H), 5.69 (s, 2H), 2.72 (dd, *J* = 3.6, 6.0 Hz, 2H), 1.81 (dd, *J* = 1.2, 1.6 Hz, 2H), 1.17 (d, *J* = 5.6 Hz, 6H). **$^{13}$C NMR** (400 MHz, $CDCl_3$) δ 150.60, 136.99, 129.94, 127.63, 115.92, 110.18, 52.23, 43.19, 18.67. **TLC** 20% acetone/ 80% Hexanes. CAM stains dark blue.

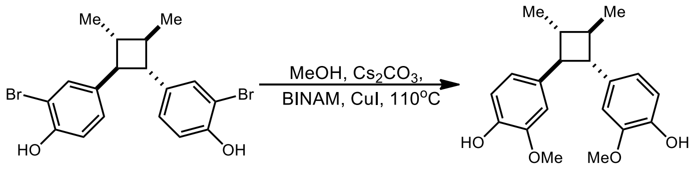

***endriandin A***

**Endiadrin A**: The copper-catalyzed methoxylation was conducted using a modified literature procedure[46] as follows: a scintillation vial was charged with the substrate (158 mg, 1 eq), $Cs_2CO_3$ (0.481g, 4 eq), CuI (28 mg, 0.4 eq), and BINAM (42 mg, 0.4 eq) in a glove box. To the vial was added sparged MeOH (2.5 mL, 0.15M) and the reaction mixture was stirred at 110 °C for 40 hours. The reaction mixture was allowed to cool to room temperature and the crude mixture was diluted with water and quenched with 3M HCl at 0 °C. The aqueous layer was then extracted with DCM multiple times and the organics were dried over $MgSO_4$, and concentrated. The crude product was purified by column chromatography to yield 93 mg (77%) of the desired product as a yellow oil. **$^1$H NMR** (400 MHz, $CDCl_3$) δ 6.89 (d, *J* = 8.0 Hz, 2H), 6.77 (dd, *J* = 1.6, 8.4 Hz, 2H), 6.71 (s, 2H), 5.55 (s, O-H, 2H), 3.86 (s, 6H), 2.80 (dd, *J* = 3.2, 5.6 Hz, 2H), 1.86 (d, *J* = 4.8 Hz), 1.22 (d, *J* = 5.6 Hz, 6H). **$^{13}$C NMR** (400 MHz, $CDCl_3$) δ 146.31, 143.87, 135.77, 119.28, 114.16, 109.38, 55.79, 53.16, 42.94, 18.82. **MS** (+ESI) Calculated *m/z* for $[M+H]^+$= 329.17 Found *m/z* for $[M+H]^+$ = 329.13. **IR** (Thin Film, $cm^{-1}$): 3525, 3055, 3004, 2946, 2918, 2862, 2061, 1856, 1611, 1514, 1463, 1452, 1431, 1371, 1264, 1239, 1208. **TLC** 20% acetone/ 80% Hexanes. CAM stains dark blue.

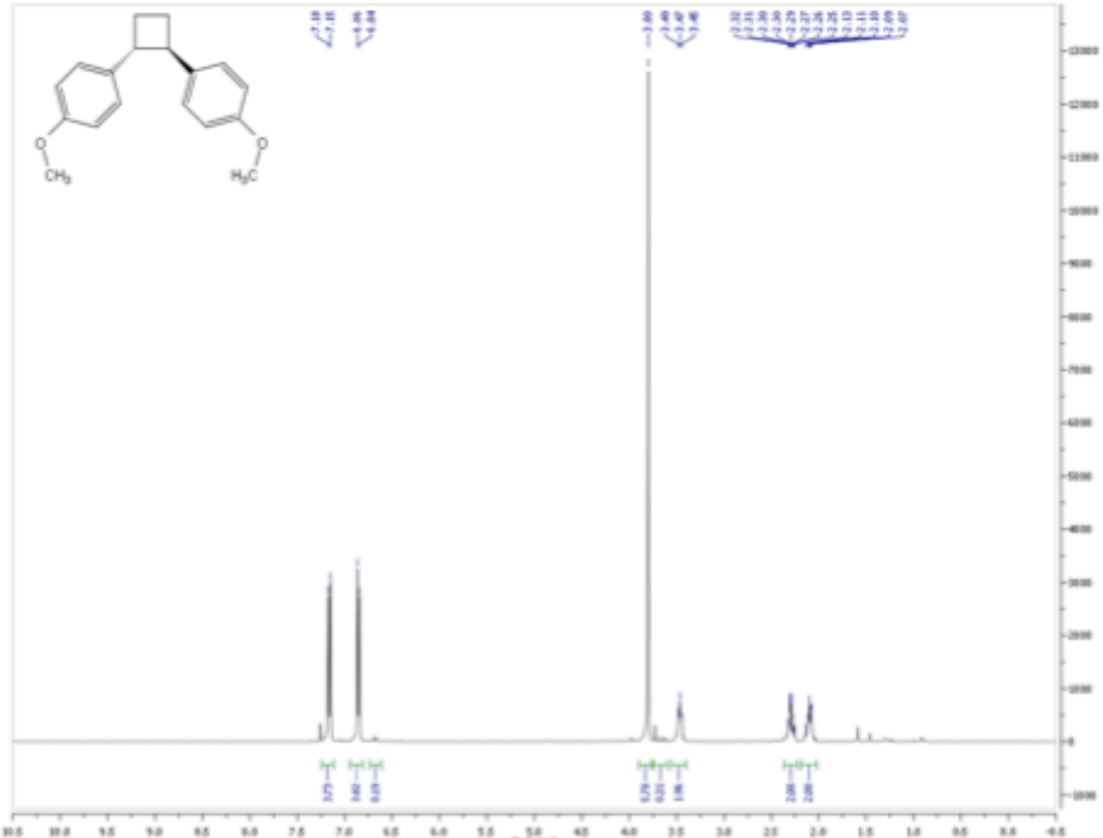
CH3
H3C

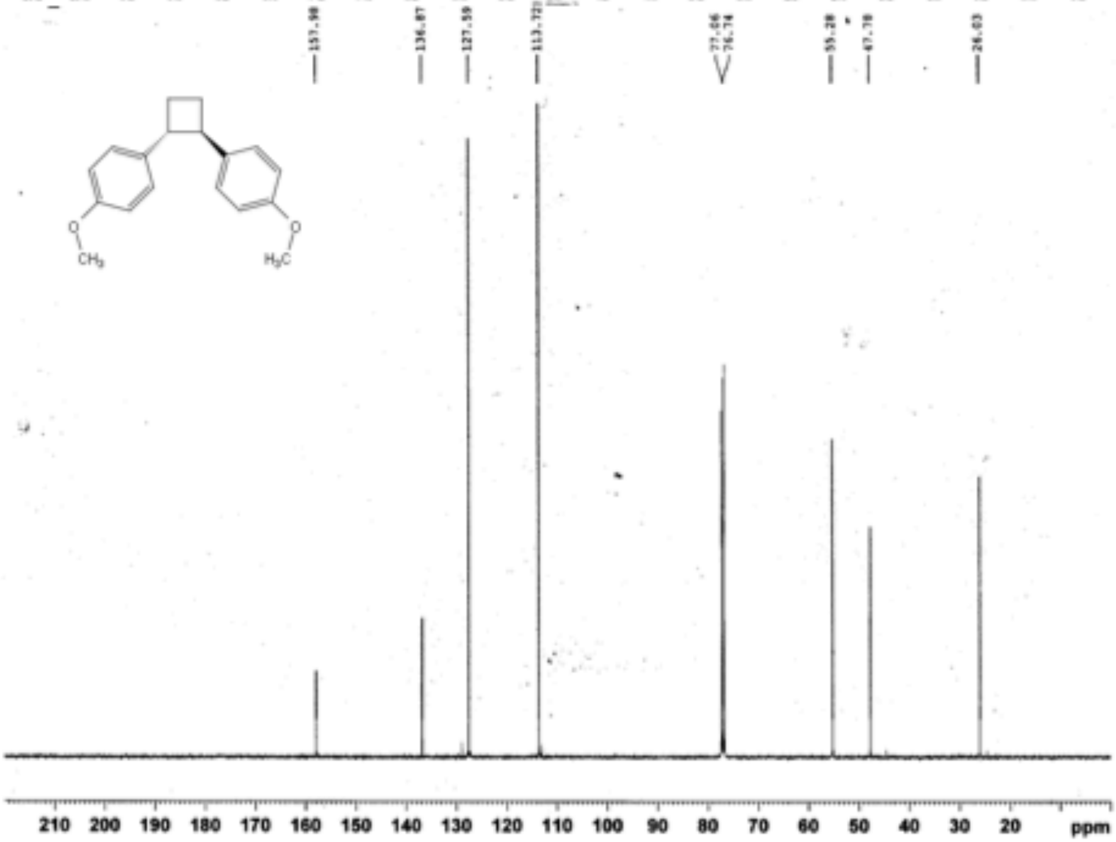
157.98
136.87
127.59
113.72
77.06
76.74
55.28
47.70
26.03
CH3
H3C
210
200
190
180
170
160
150
140
130
120
110
100
90
80
70
60
50
40
30
20
ppm

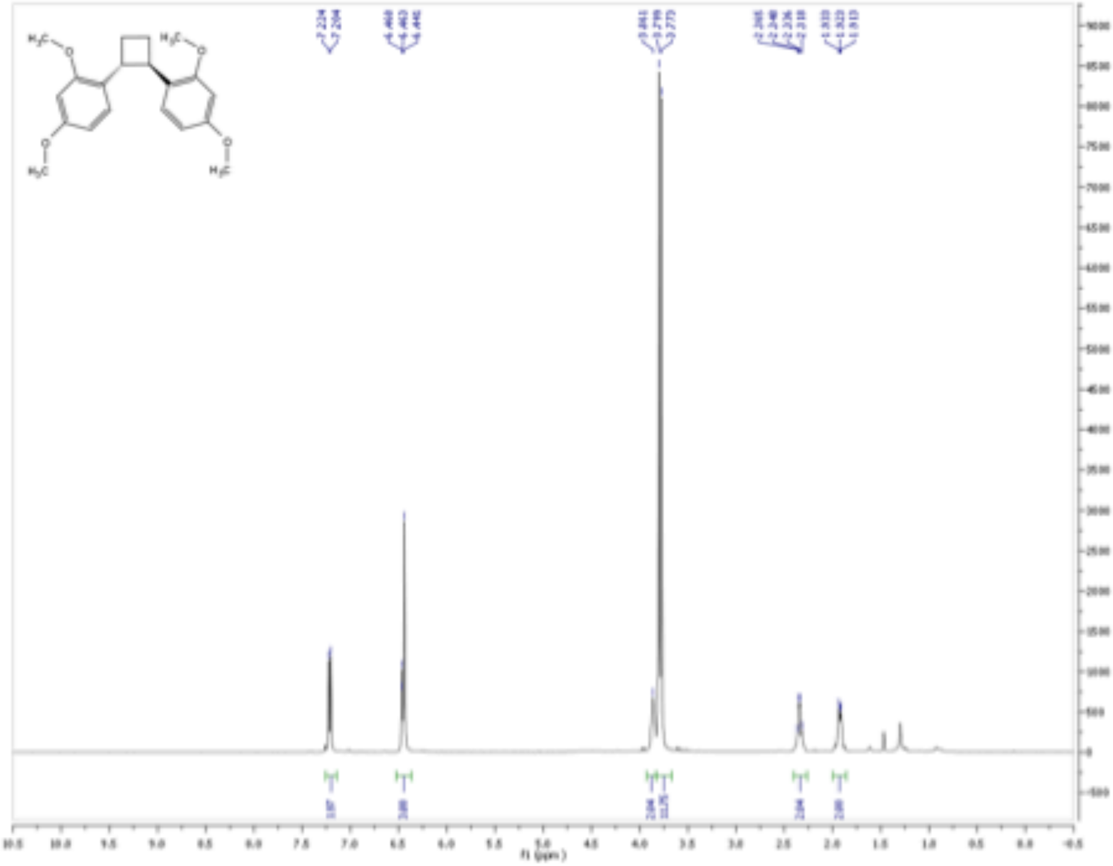
7.224
7.204
6.460
6.452
6.445
3.843
3.795
3.773
2.265
2.246
2.236
2.218
1.933
1.922
1.913
H3C
O
f1 (ppm)

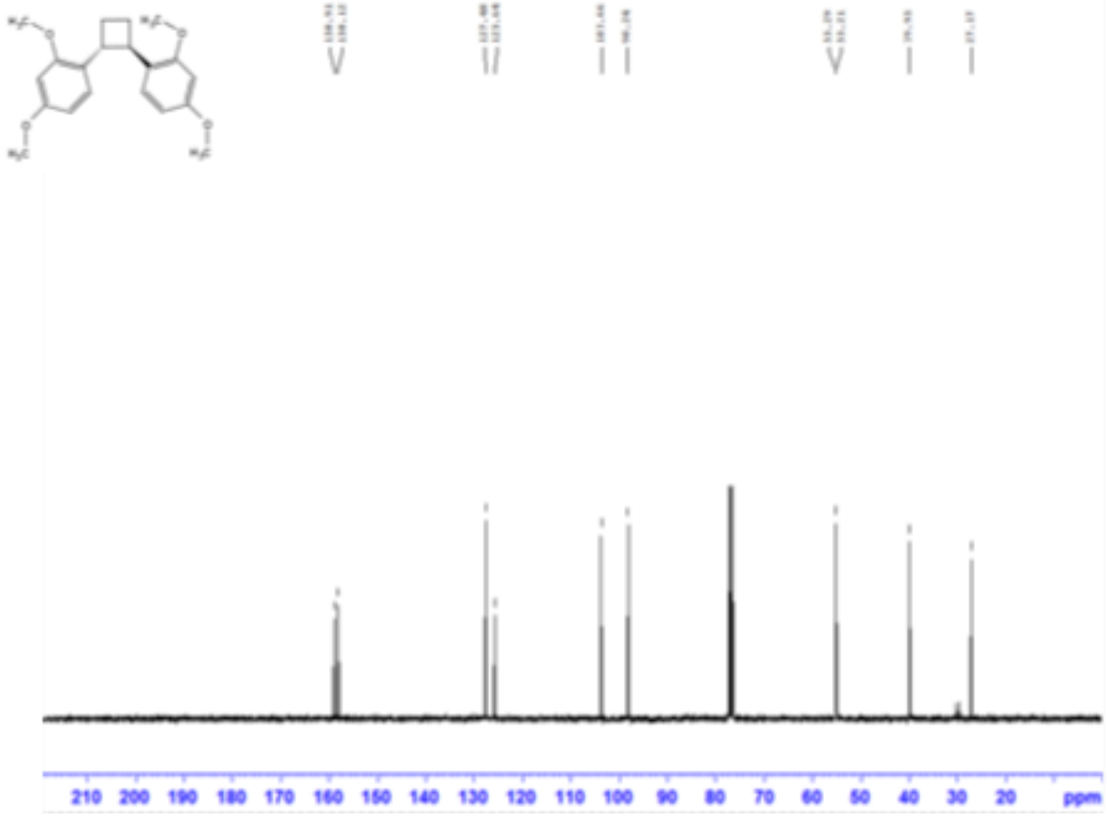
158.93
158.12
127.80
125.08
103.66
98.28
55.29
55.01
39.93
27.17
H3C
O
210
200
190
180
170
160
150
140
130
120
110
100
90
80
70
60
50
40
30
20
ppm

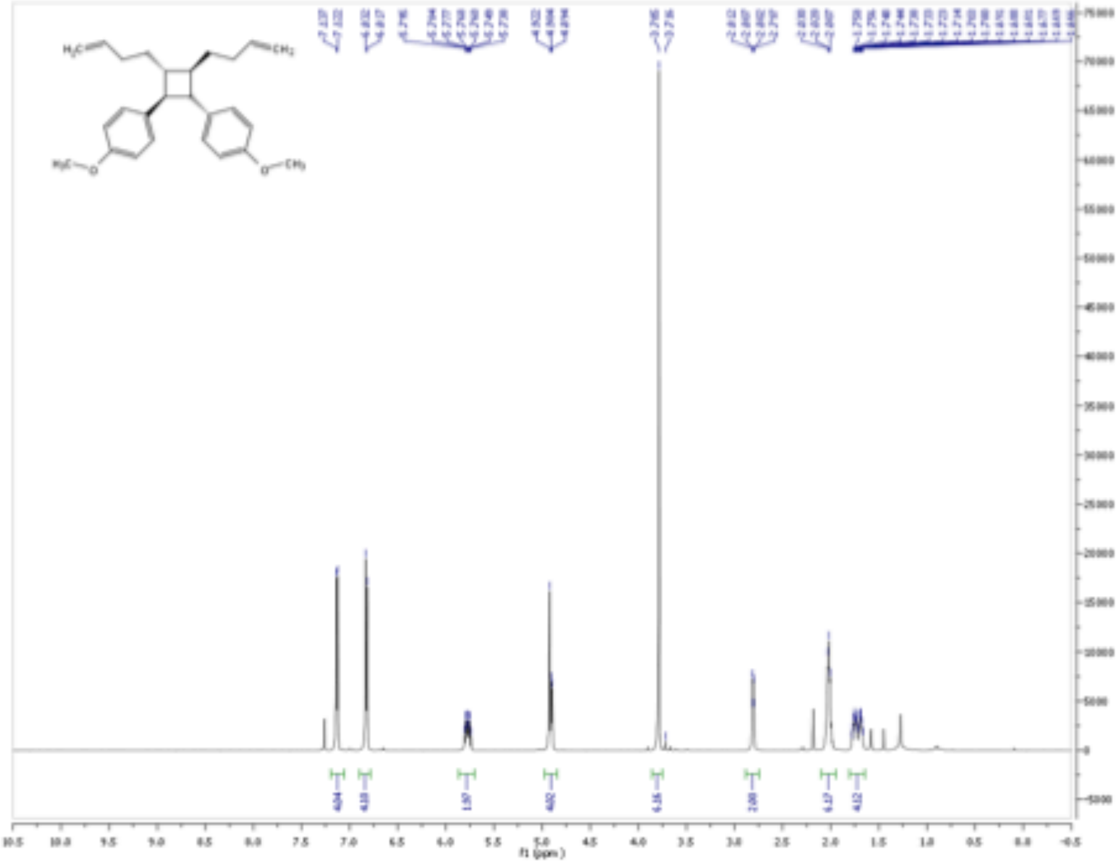
H₂C
CH₂
H₃C
O
CH₃
4.04
4.10
1.97
4.02
6.16
2.00
4.17
4.12
10.5
10.0
9.5
9.0
8.5
8.0
7.5
7.0
6.5
6.0
5.5
5.0
4.5
4.0
3.5
3.0
2.5
2.0
1.5
1.0
0.5
0.0
-0.5
f1 (ppm)
75000
70000
65000
60000
55000
50000
45000
40000
35000
30000
25000
20000
15000
10000
5000
0
-5000

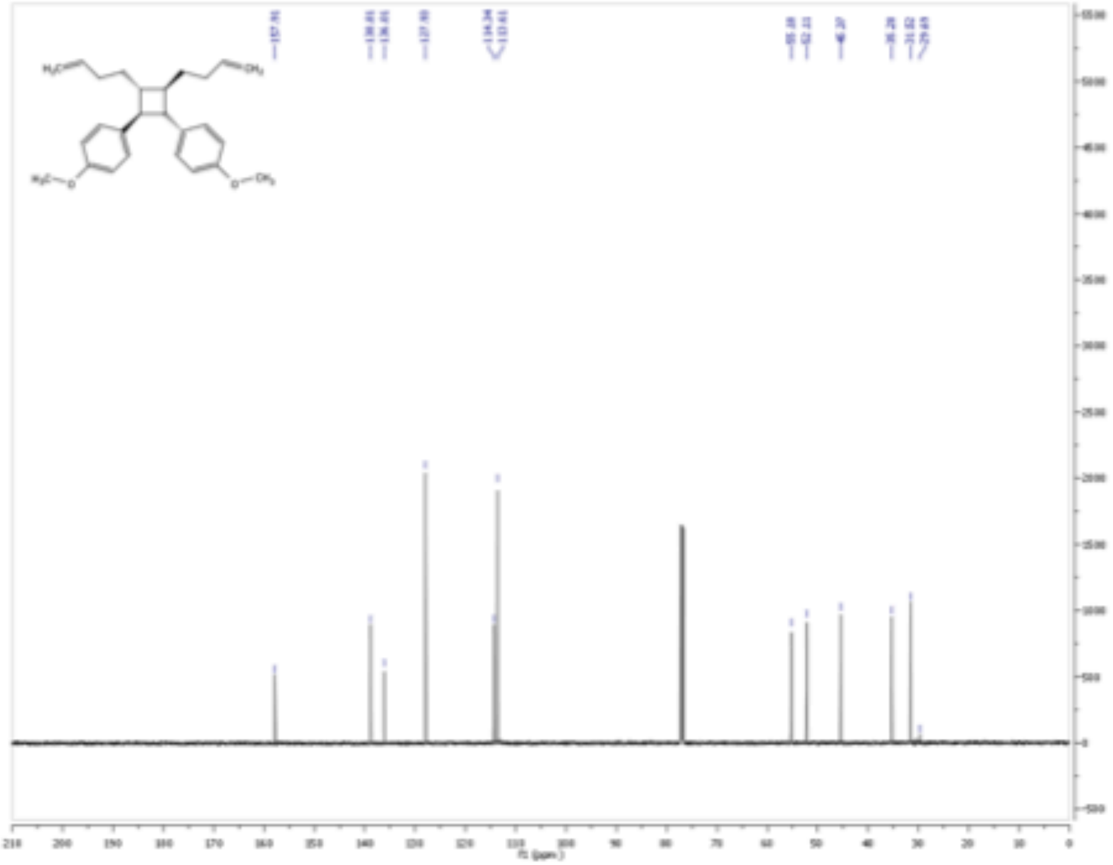
H₂C
CH₂
H₃C
O
CH₃
210
200
190
180
170
160
150
140
130
120
110
100
90
80
70
60
50
40
30
20
10
0
f1 (ppm)
5500
5000
4500
4000
3500
3000
2500
2000
1500
1000
500
0
-500

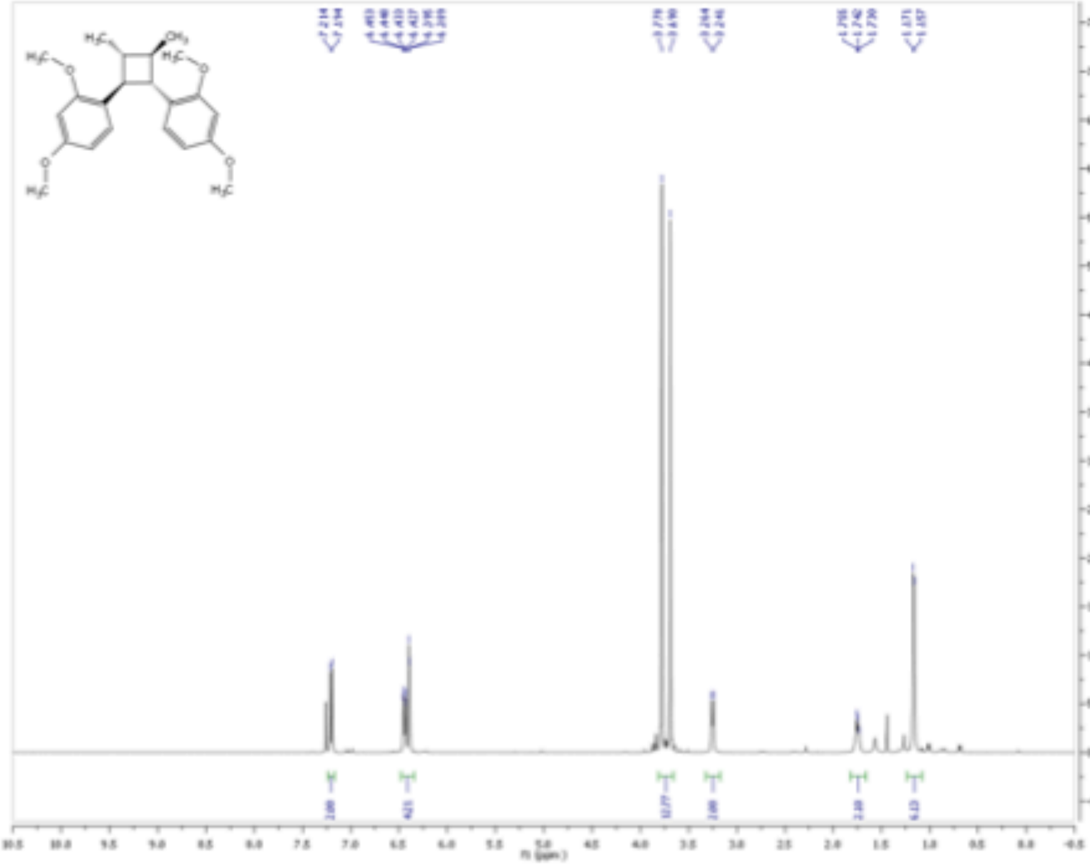
7.214
7.194
6.453
6.448
6.433
6.427
6.395
6.389
3.779
3.690
3.264
3.246
1.755
1.742
1.730
1.171
1.157
H₃C
CH₃
H₃C
O
2.00
4.21
12.77
2.00
2.10
6.13
f1 (ppm)

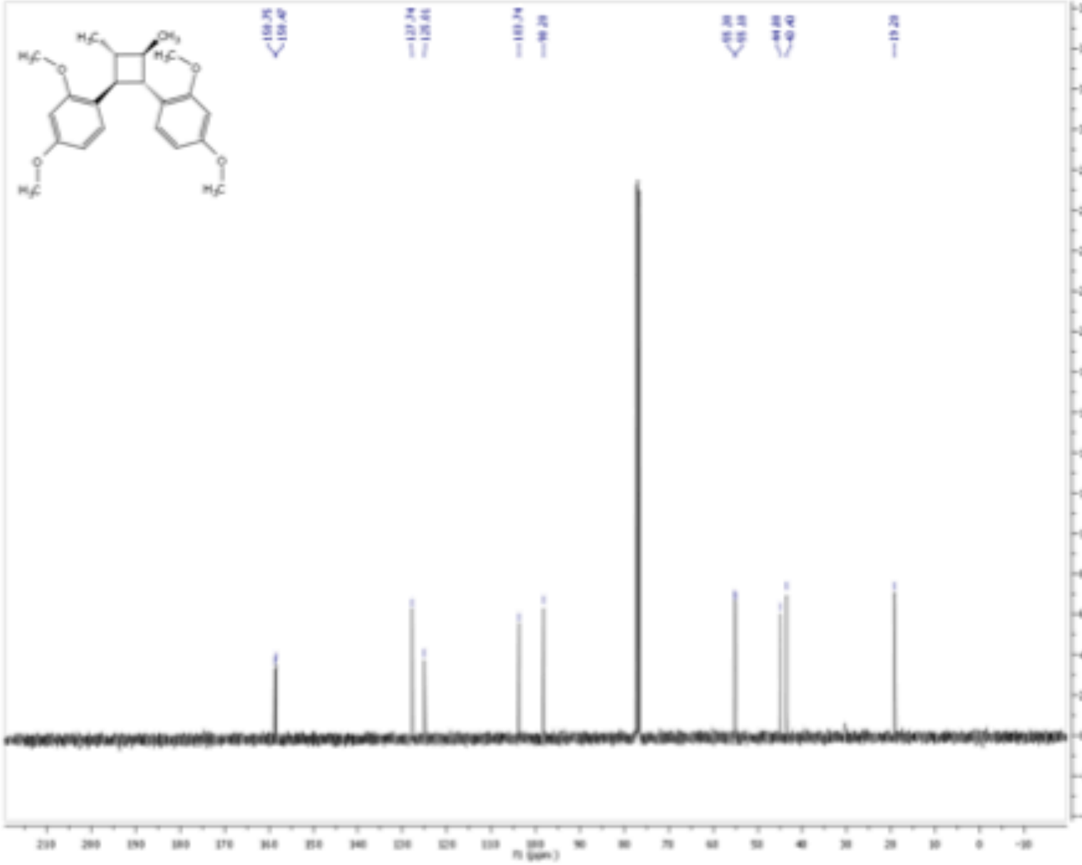
159.75
158.47
127.74
125.01
103.74
98.28
55.26
55.18
44.88
43.42
19.28
H₃C
CH₃
O
f1 (ppm)

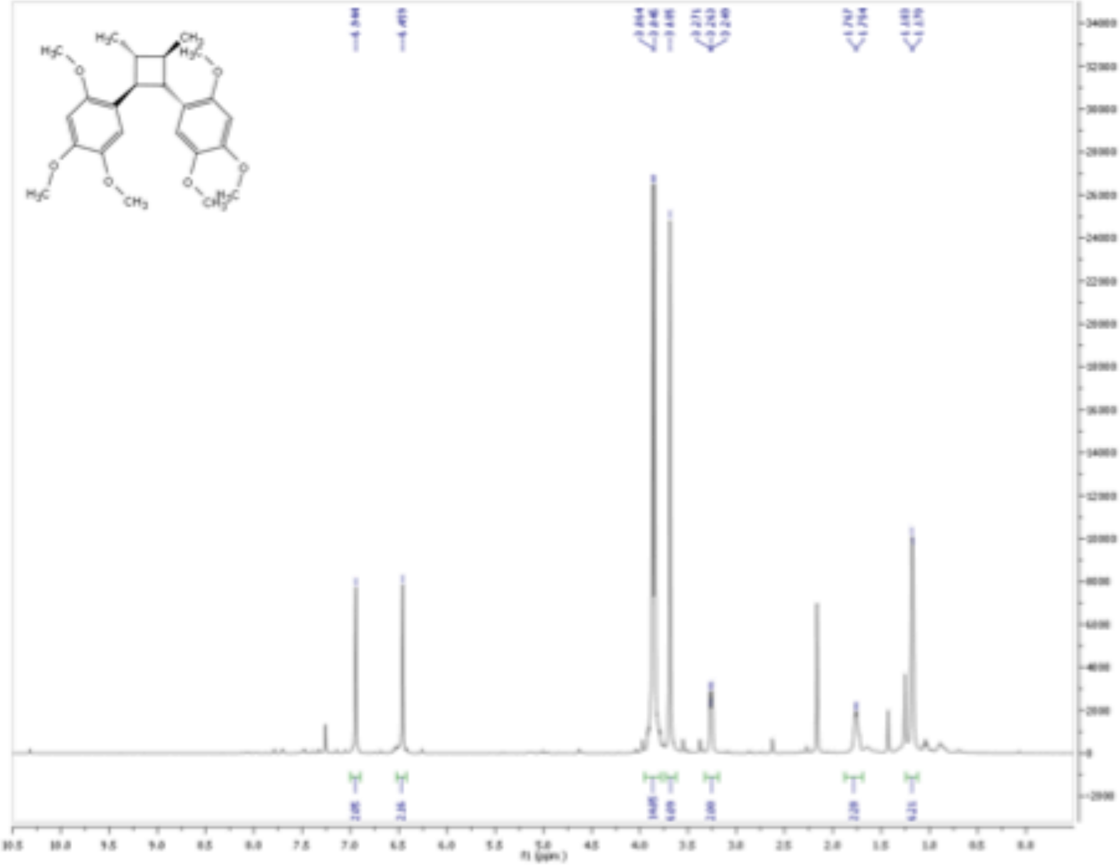

6.944
6.459
3.854
3.846
3.695
3.271
3.263
3.249
1.767
1.754
1.183
1.170
2.05
2.16
14.05
6.09
2.00
2.09
6.21
10.5
10.0
9.5
9.0
8.5
8.0
7.5
7.0
6.5
6.0
5.5
5.0
4.5
4.0
3.5
3.0
2.5
2.0
1.5
1.0
0.5
0.0
f1 (ppm)

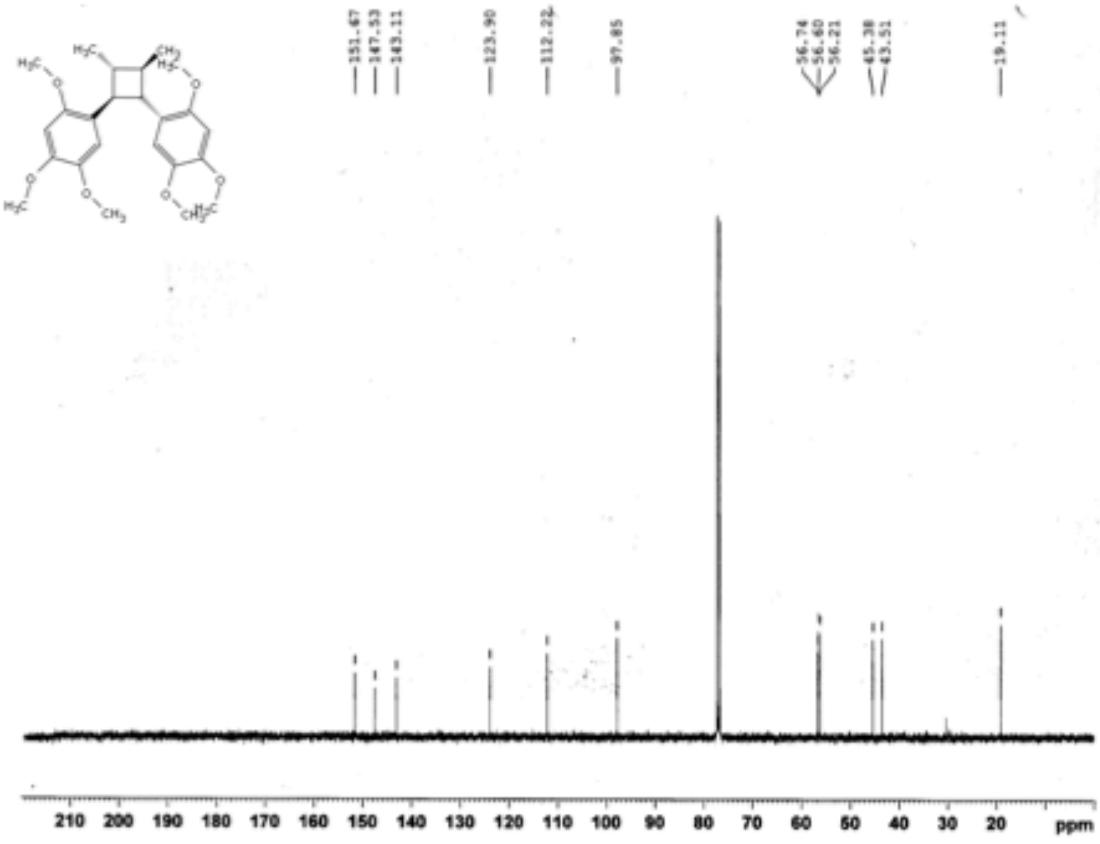

151.67
147.53
143.11
123.90
112.22
97.85
56.74
56.60
56.21
45.38
43.51
19.11
210
200
190
180
170
160
150
140
130
120
110
100
90
80
70
60
50
40
30
20
ppm

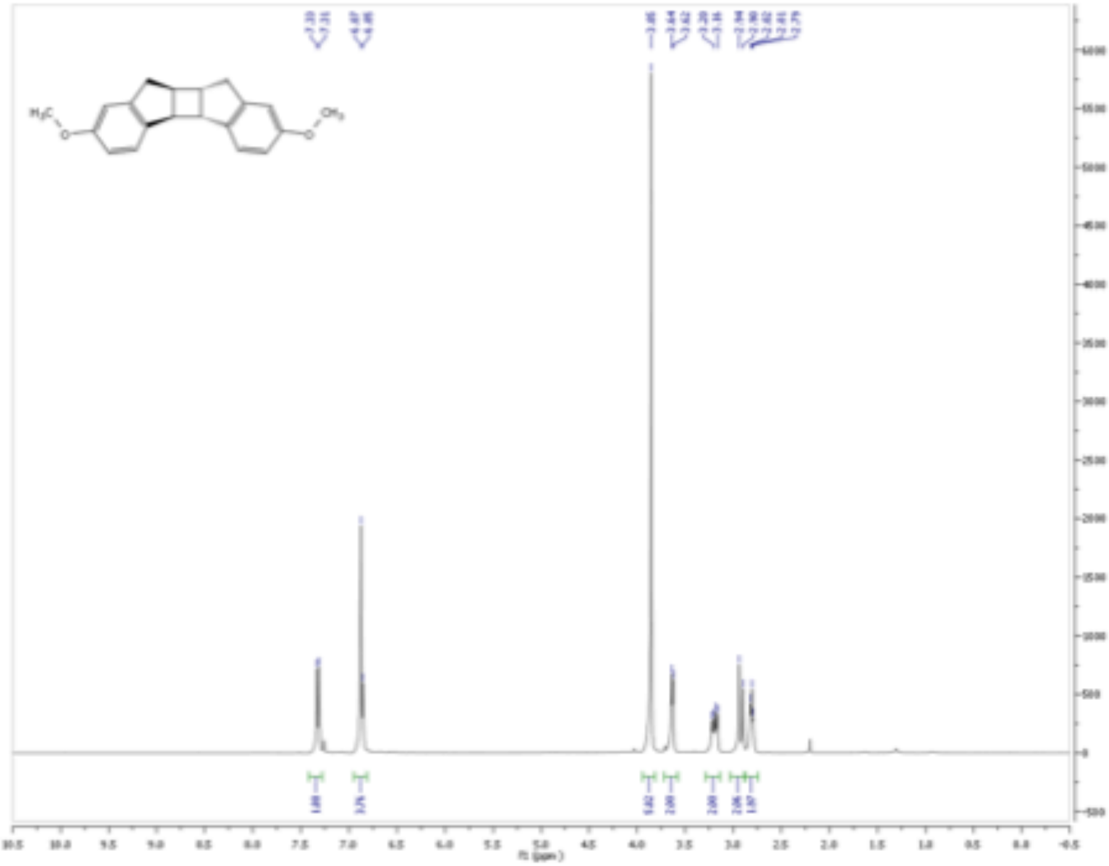
7.33
7.31
6.87
6.85
3.86
3.64
3.62
3.20
3.16
2.94
2.90
2.82
2.81
2.79
$H_3C$
O
$CH_3$
f1 (ppm)

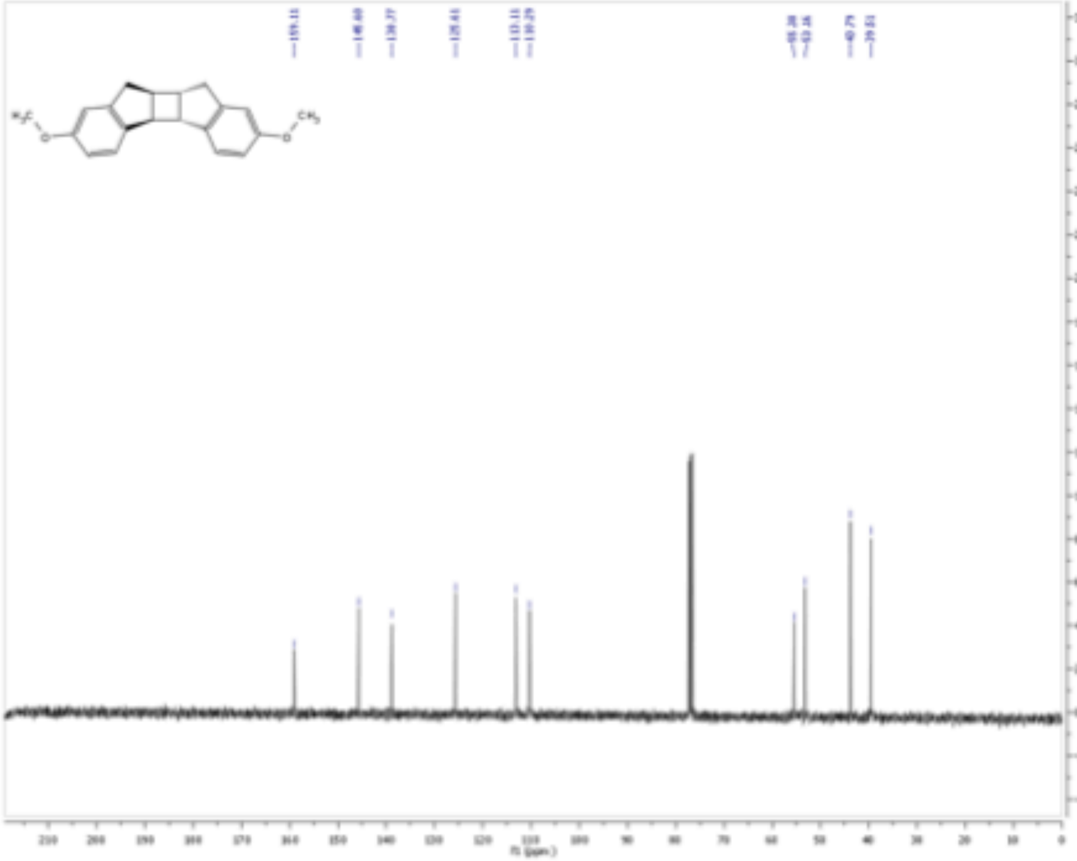
159.11
146.40
138.77
125.61
113.11
110.29
55.38
53.16
43.75
39.51
$H_3C$
O
$CH_3$
f1 (ppm)

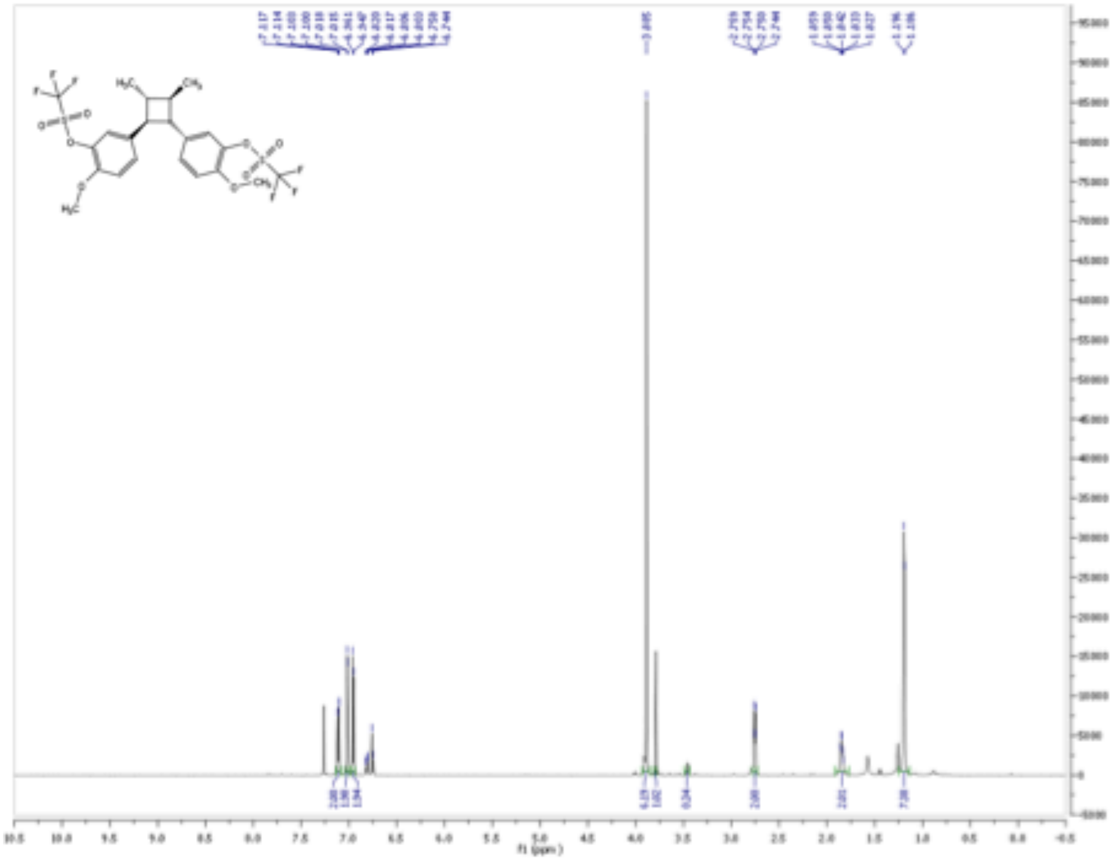

7.117
7.114
7.103
7.100
7.018
7.015
6.961
6.947
6.833
6.817
6.806
6.803
6.759
6.744
3.885
2.759
2.754
2.750
2.744
1.859
1.850
1.842
1.833
1.827
1.176
1.166
2.00
1.98
1.94
6.15
1.02
0.24
2.00
2.01
7.28
F
O
S
H3C
CH3
f1 (ppm)

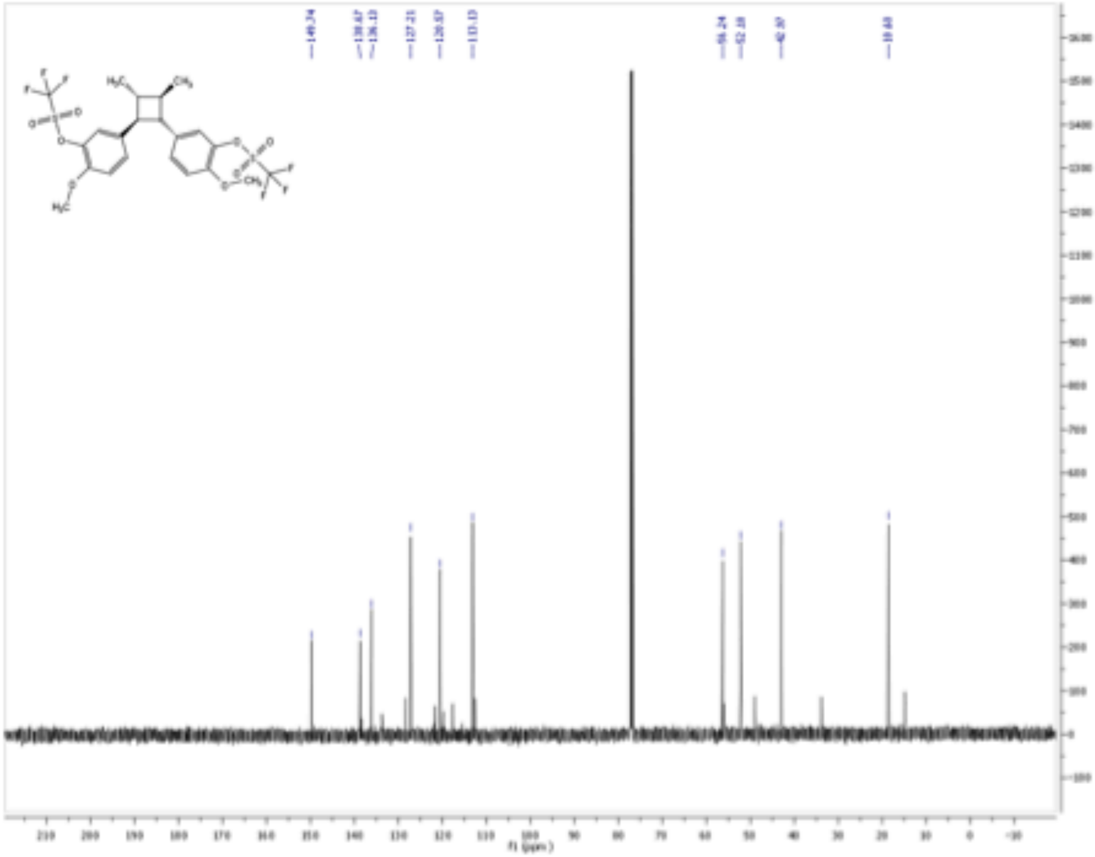

149.74
138.47
136.13
127.21
120.57
113.13
56.24
52.18
42.97
18.68
F
O
S
H3C
CH3
f1 (ppm)

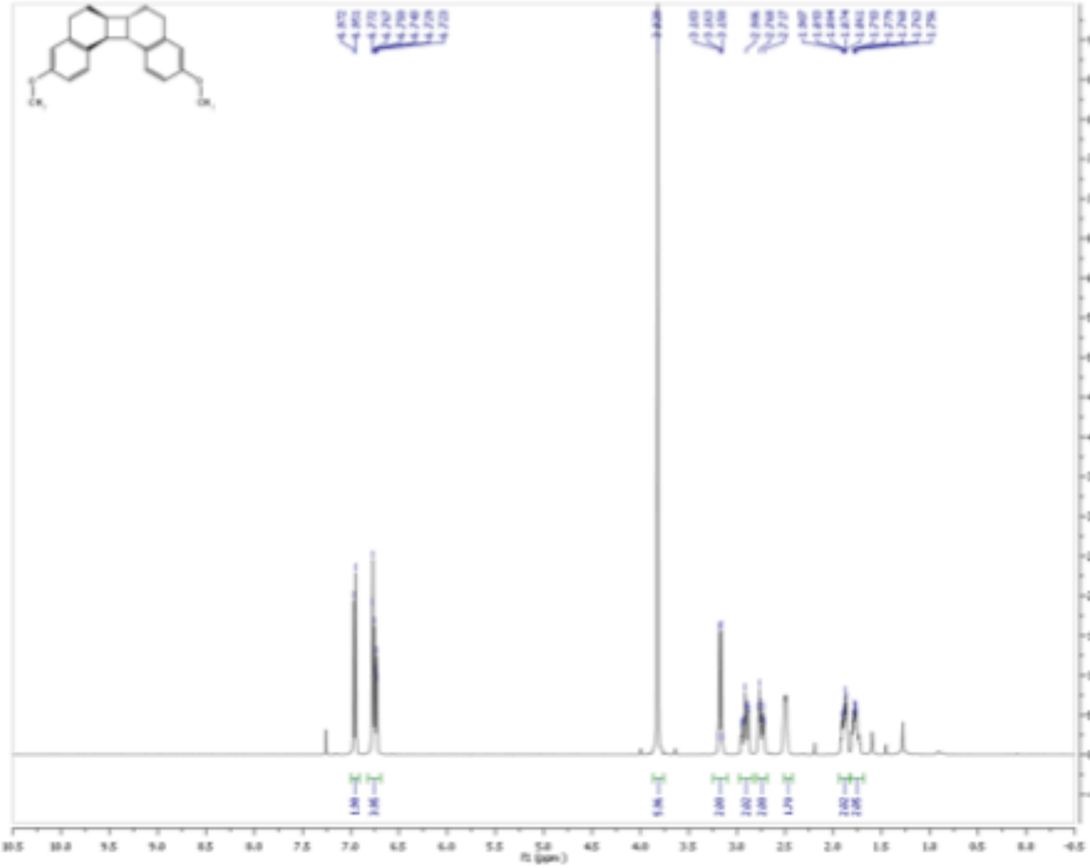

f1 (ppm)
10.5
10.0
9.5
9.0
8.5
8.0
7.5
7.0
6.5
6.0
5.5
5.0
4.5
4.0
3.5
3.0
2.5
2.0
1.5
1.0
0.5
0.0
-0.5

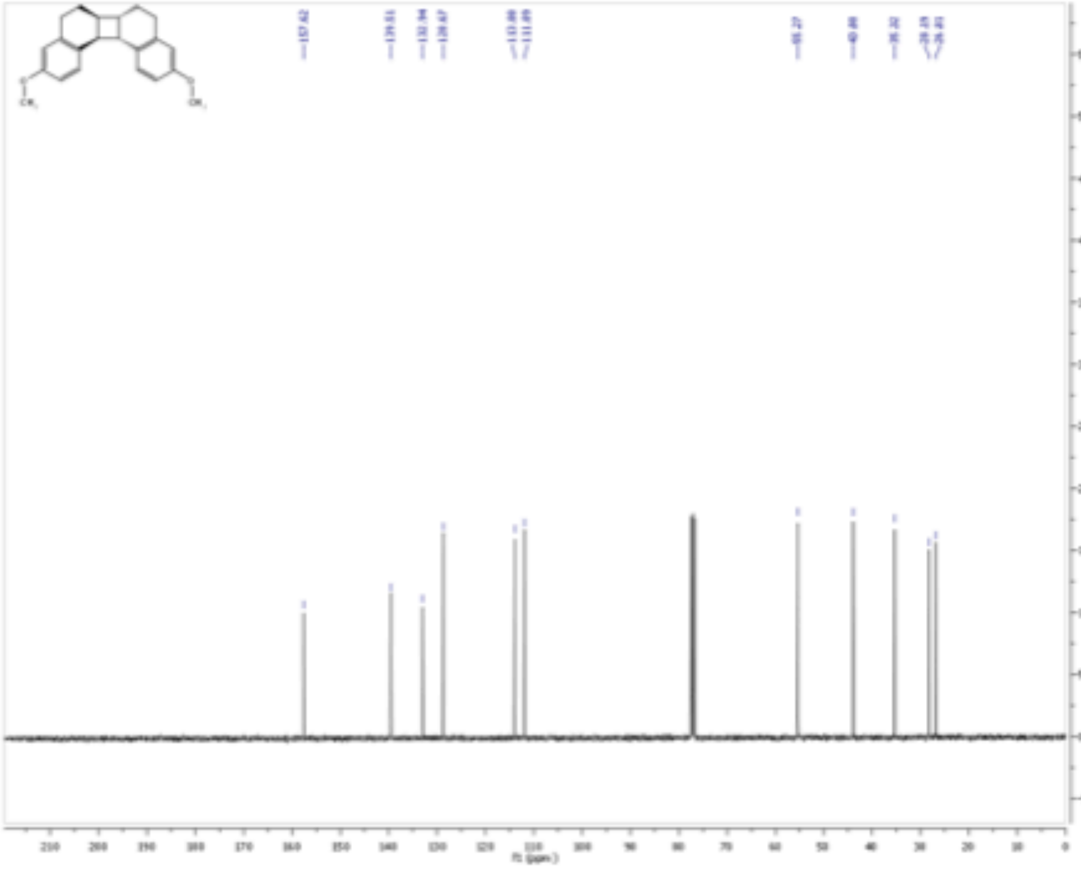

157.62
139.51
132.94
128.67
113.80
111.65
55.27
43.86
35.32
28.25
26.83
f1 (ppm)
210
200
190
180
170
160
150
140
130
120
110
100
90
80
70
60
50
40
30
20
10
0

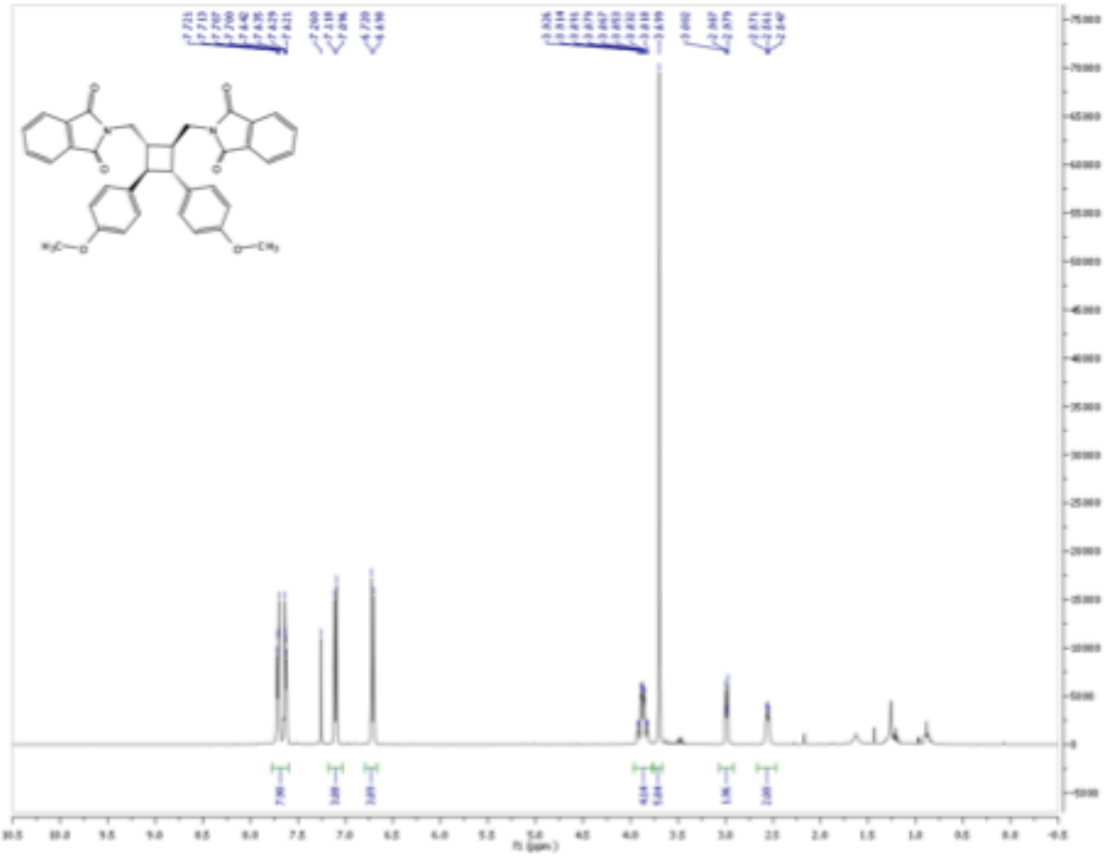

O
N
H₃C—O
O—CH₃
f1 (ppm)
10.5
10.0
9.5
9.0
8.5
8.0
7.5
7.0
6.5
6.0
5.5
5.0
4.5
4.0
3.5
3.0
2.5
2.0
1.5
1.0
0.5
0.0
-0.5
75000
70000
65000
60000
55000
50000
45000
40000
35000
30000
25000
20000
15000
10000
5000
0
-5000

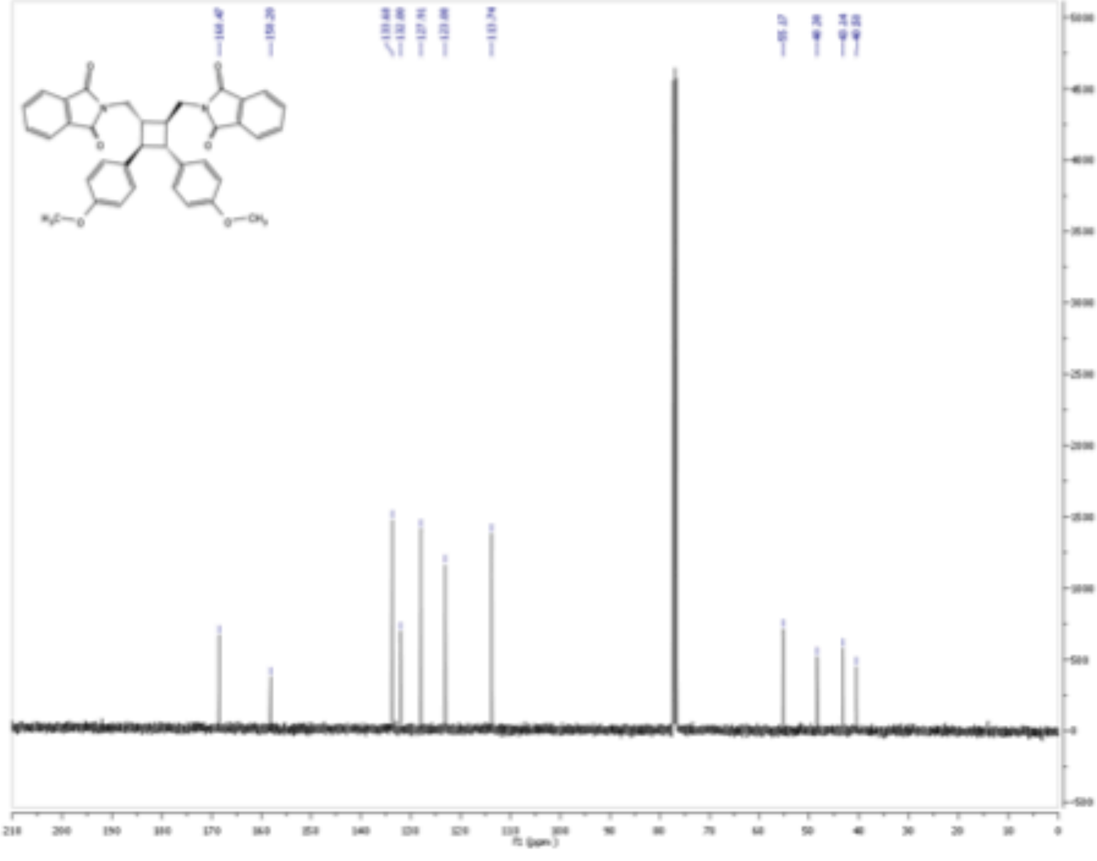

168.47
158.29
113.74
55.17
O
N
H₃C—O
O—CH₃
f1 (ppm)
210
200
190
180
170
160
150
140
130
120
110
100
90
80
70
60
50
40
30
20
10
0
5000
4500
4000
3500
3000
2500
2000
1500
1000
500
0
-500

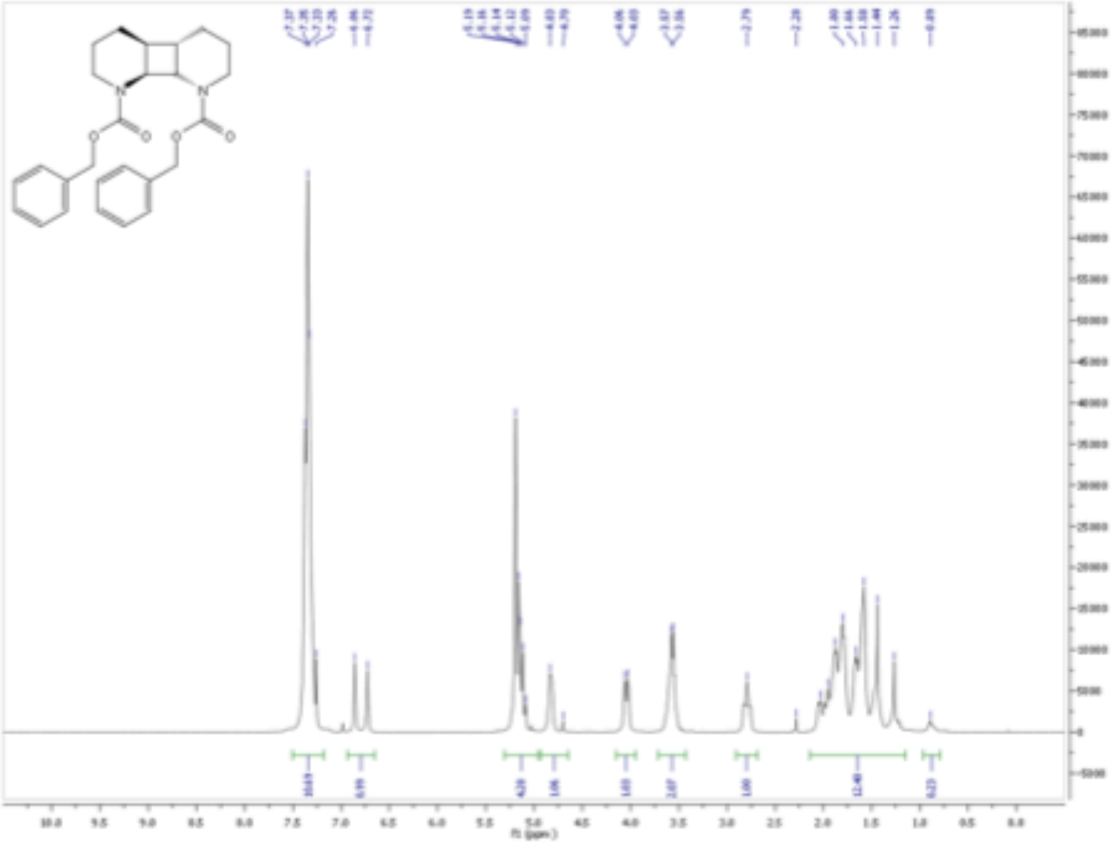

N
O
O
N
O
O
10.0
9.5
9.0
8.5
8.0
7.5
7.0
6.5
6.0
5.5
5.0
4.5
4.0
3.5
3.0
2.5
2.0
1.5
1.0
0.5
0.0
f1 (ppm)

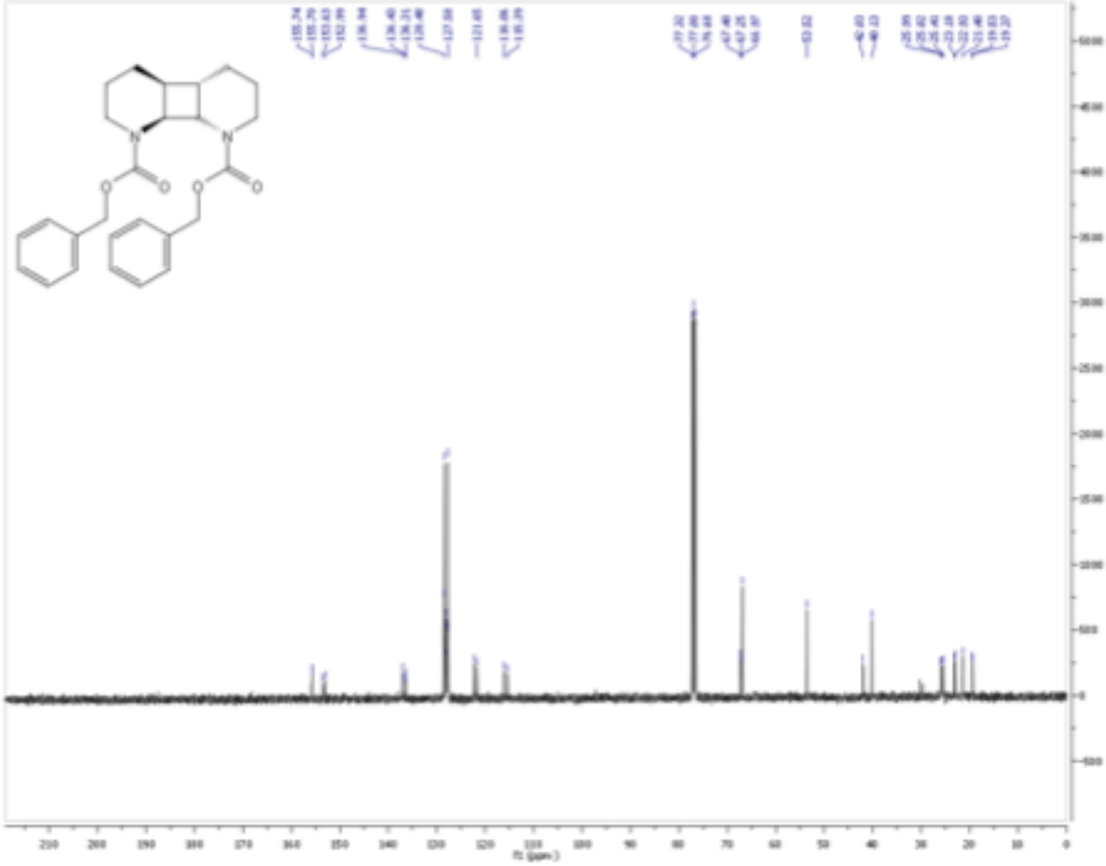

N
O
O
N
O
O
210
200
190
180
170
160
150
140
130
120
110
100
90
80
70
60
50
40
30
20
10
0
f1 (ppm)

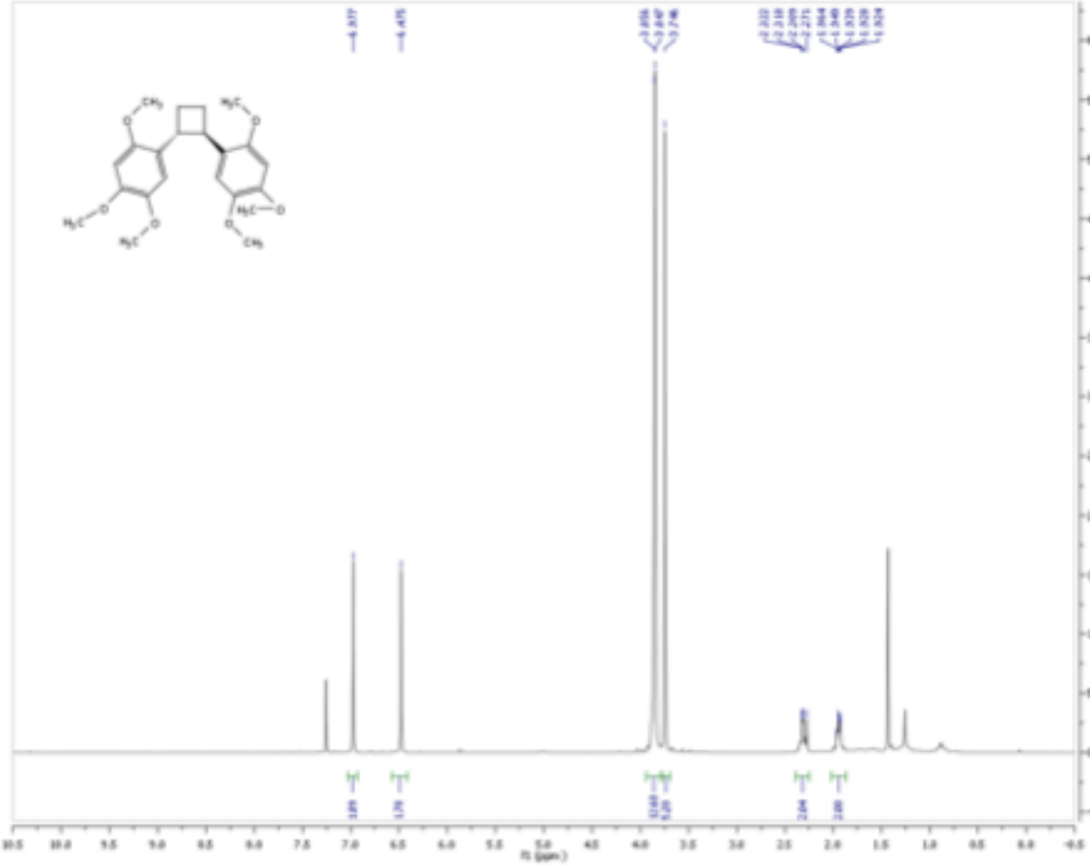
CH3
H3C
O
f1 (ppm)
10.5
10.0
9.5
9.0
8.5
8.0
7.5
7.0
6.5
6.0
5.5
5.0
4.5
4.0
3.5
3.0
2.5
2.0
1.5
1.0
0.5
0.0
-0.5

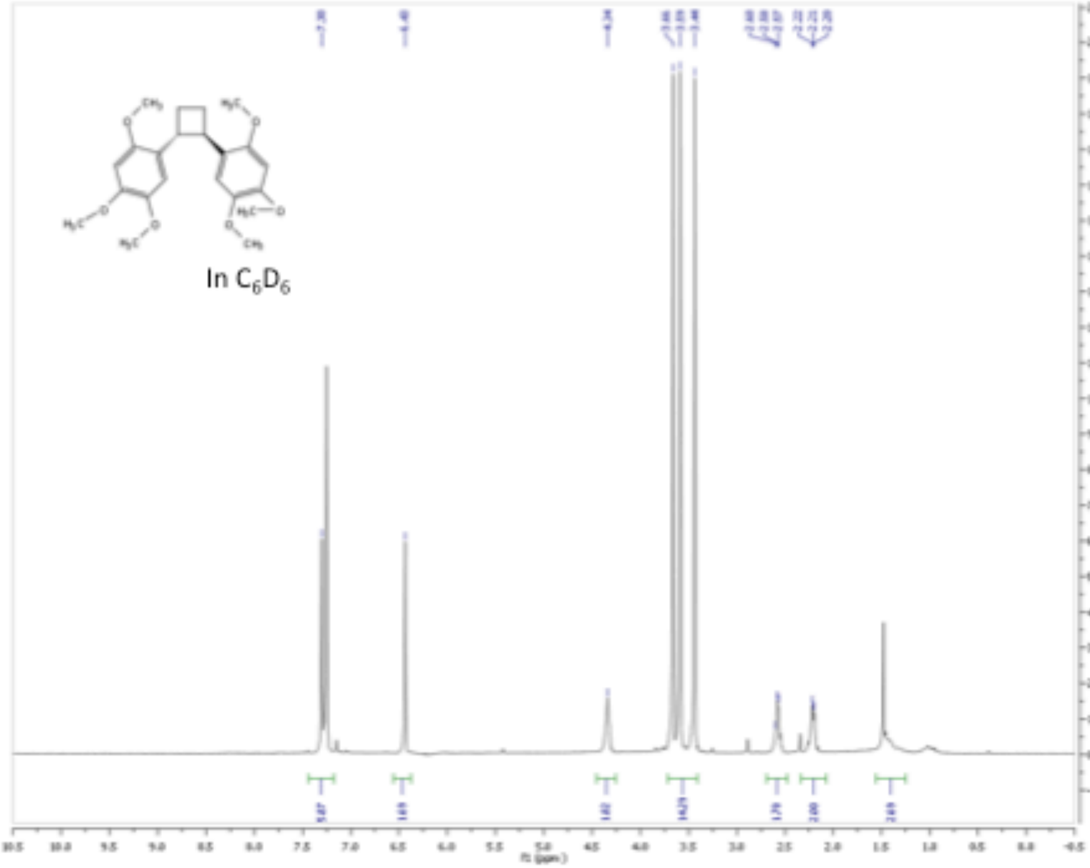
In $C_6D_6$
CH3
H3C
O
f1 (ppm)
10.5
10.0
9.5
9.0
8.5
8.0
7.5
7.0
6.5
6.0
5.5
5.0
4.5
4.0
3.5
3.0
2.5
2.0
1.5
1.0
0.5
0.0
-0.5

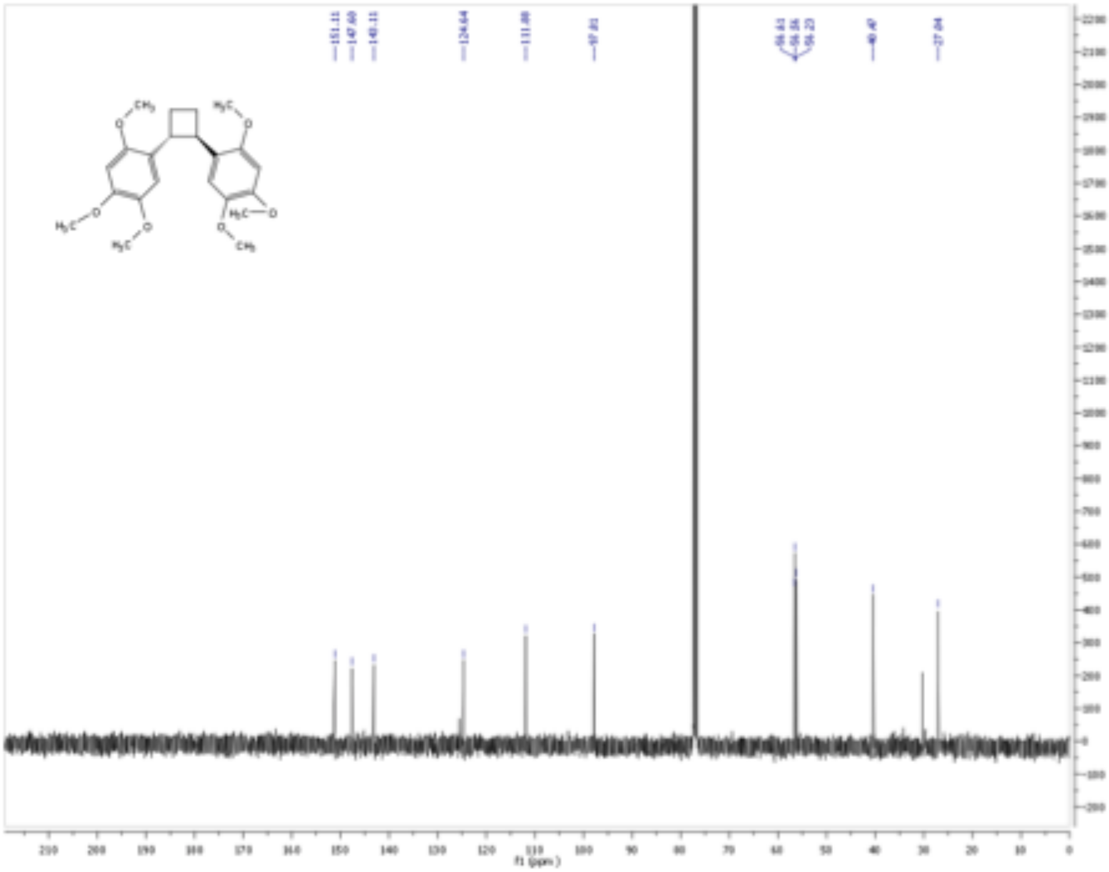
151.11
147.60
143.11
124.64
111.88
97.81
56.63
56.56
56.23
40.47
27.04
CH3
H3C
O
H3C
H3C
CH3
f1 (ppm)
210
200
190
180
170
160
150
140
130
120
110
100
90
80
70
60
50
40
30
20
10
0
2200
2100
2000
1900
1800
1700
1600
1500
1400
1300
1200
1100
1000
900
800
700
600
500
400
300
200
100
0
-100
-200

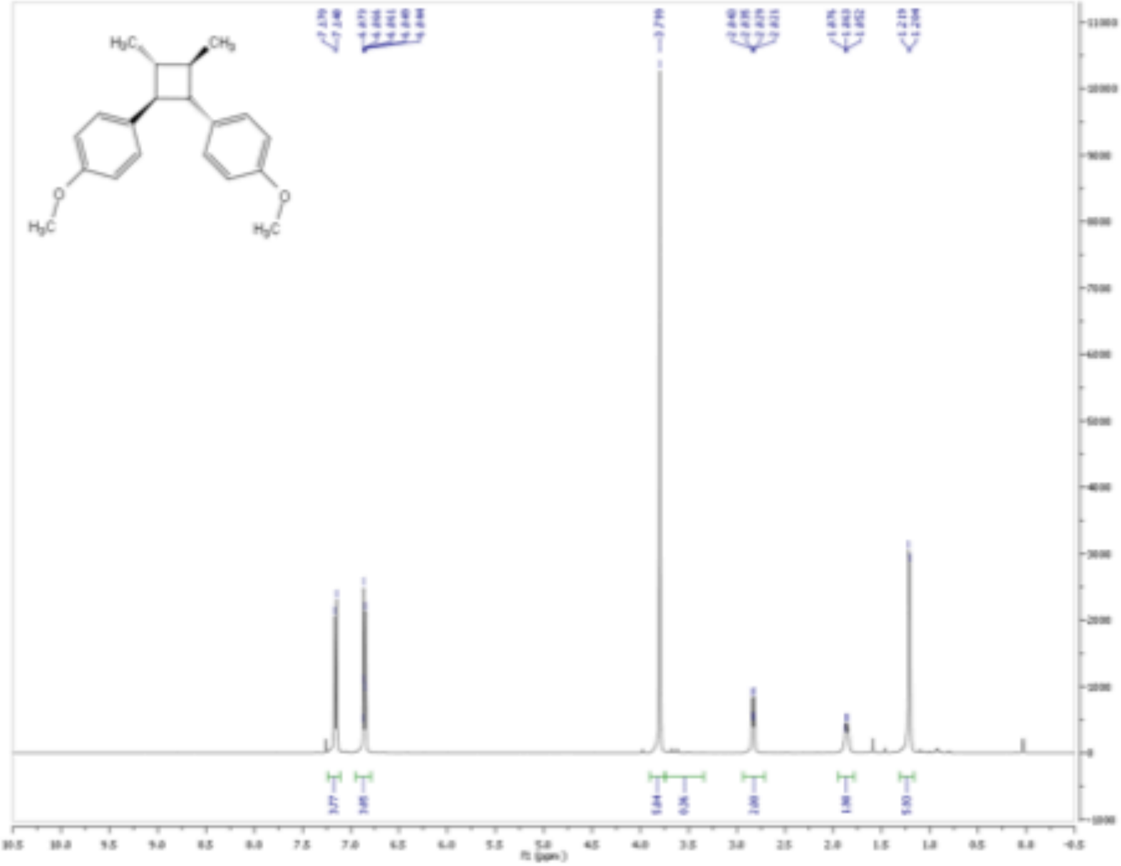
H3C
CH3
O
H3C
O
H3C
7.170
7.148
6.873
6.866
6.861
6.849
6.844
3.799
2.840
2.835
2.829
2.821
1.875
1.863
1.852
1.219
1.204
3.77
3.85
5.64
0.26
2.00
1.98
5.93
10.5
10.0
9.5
9.0
8.5
8.0
7.5
7.0
6.5
6.0
5.5
5.0
4.5
4.0
3.5
3.0
2.5
2.0
1.5
1.0
0.5
0.0
-0.5
f1 (ppm)
11000
10000
9000
8000
7000
6000
5000
4000
3000
2000
1000
0
-1000

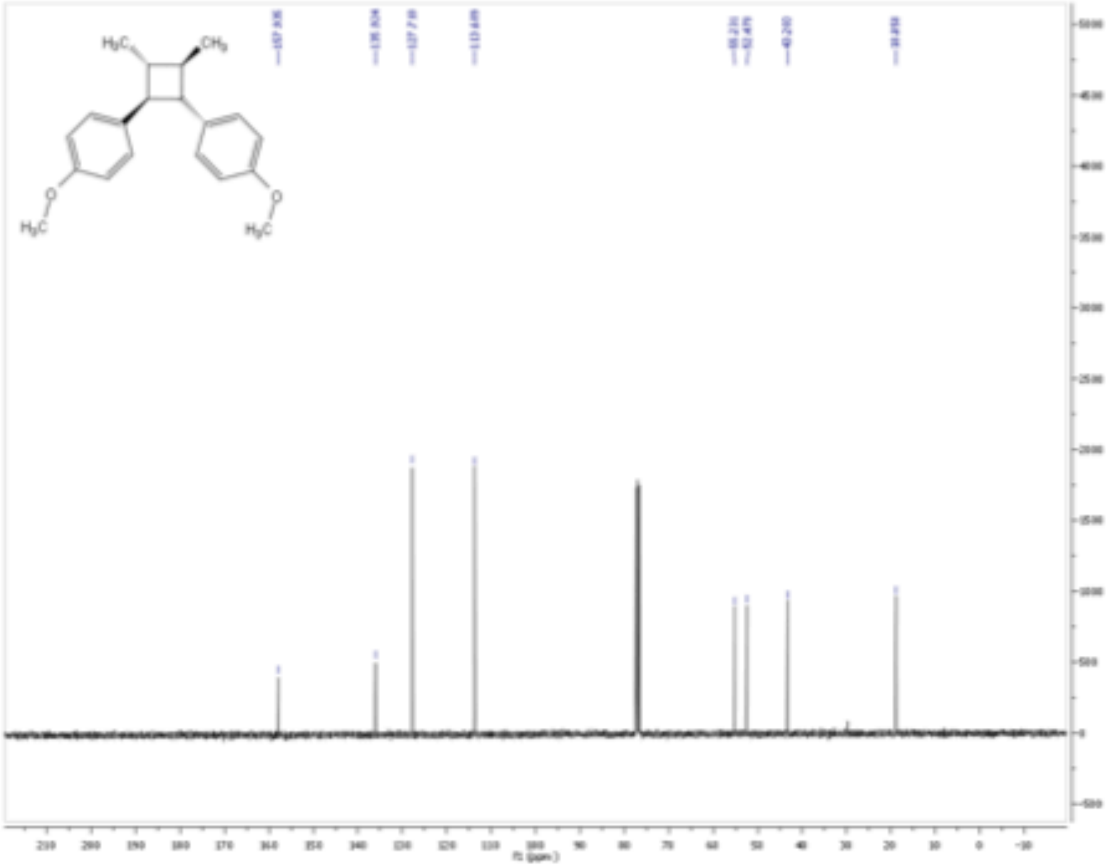
H3C
CH3
O
H3C
O
H3C
157.936
135.824
127.718
113.695
55.231
52.475
43.240
18.858
210
200
190
180
170
160
150
140
130
120
110
100
90
80
70
60
50
40
30
20
10
0
-10
f1 (ppm)
5000
4500
4000
3500
3000
2500
2000
1500
1000
500
0
-500

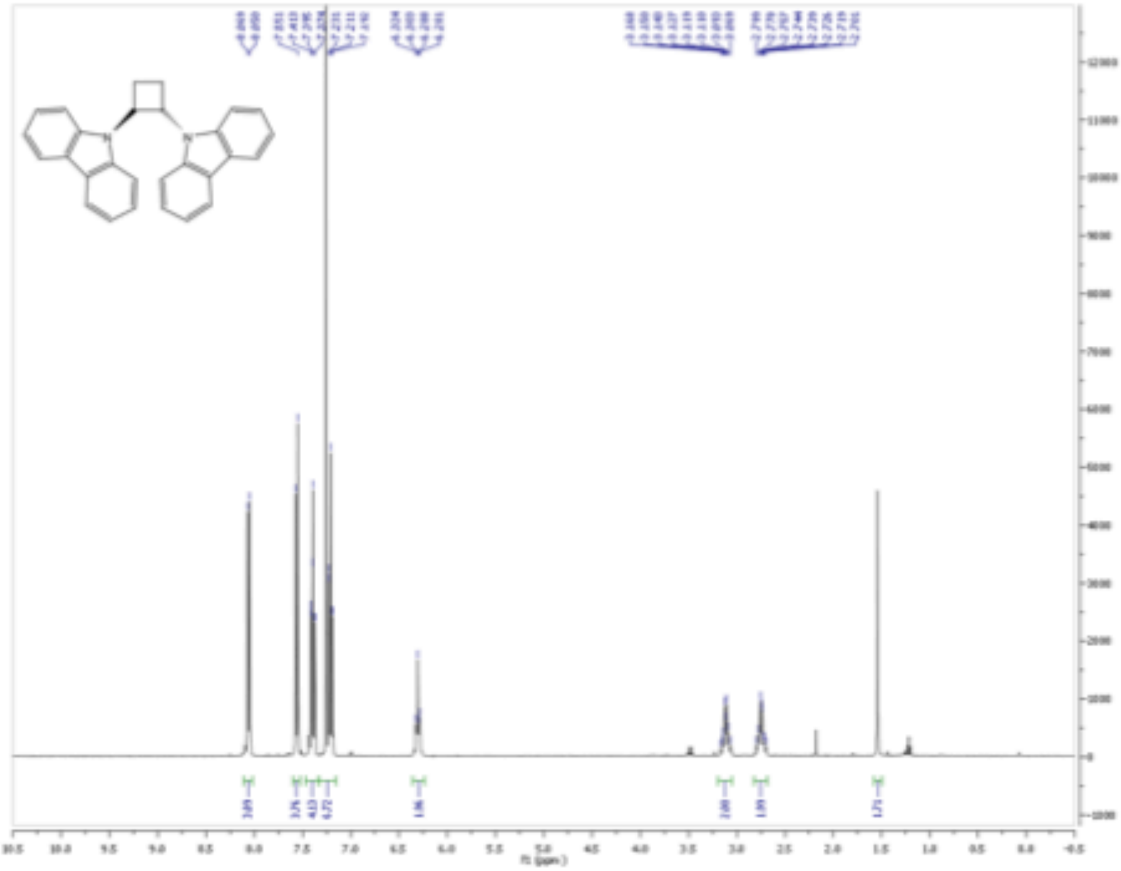
f1 (ppm)

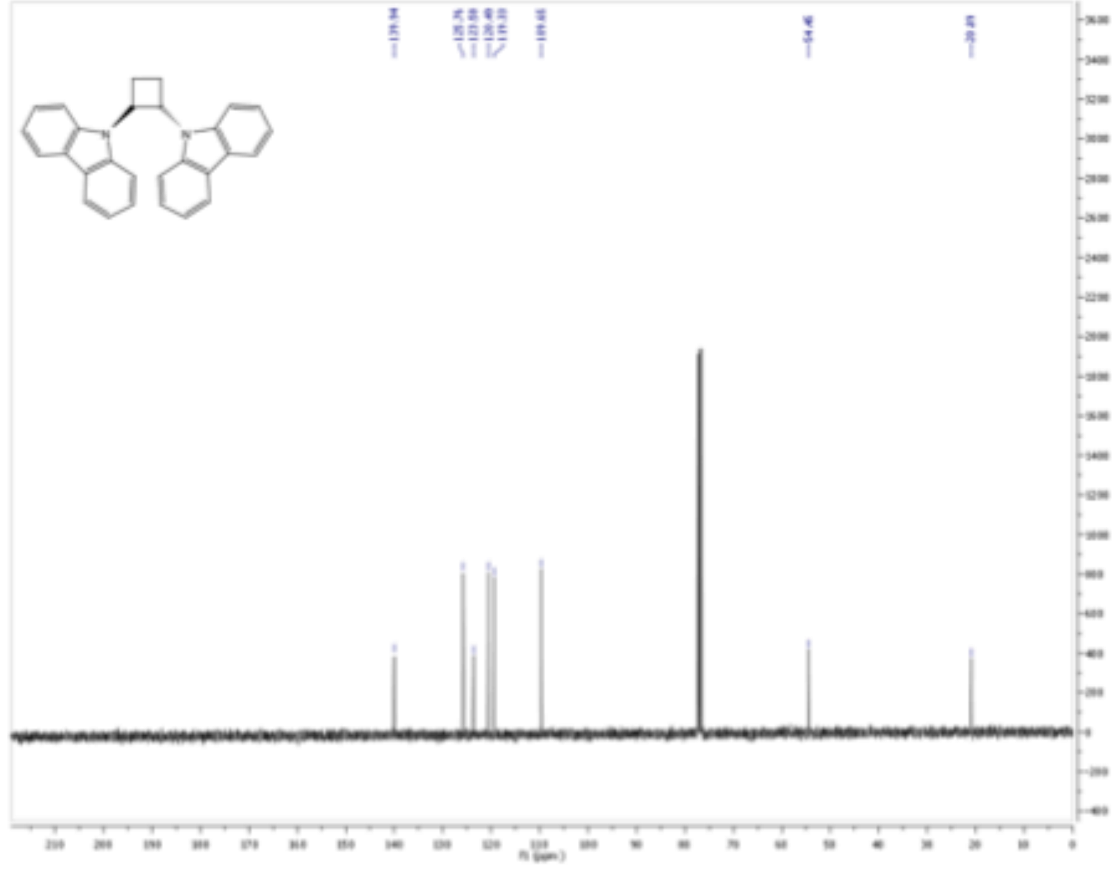
f1 (ppm)

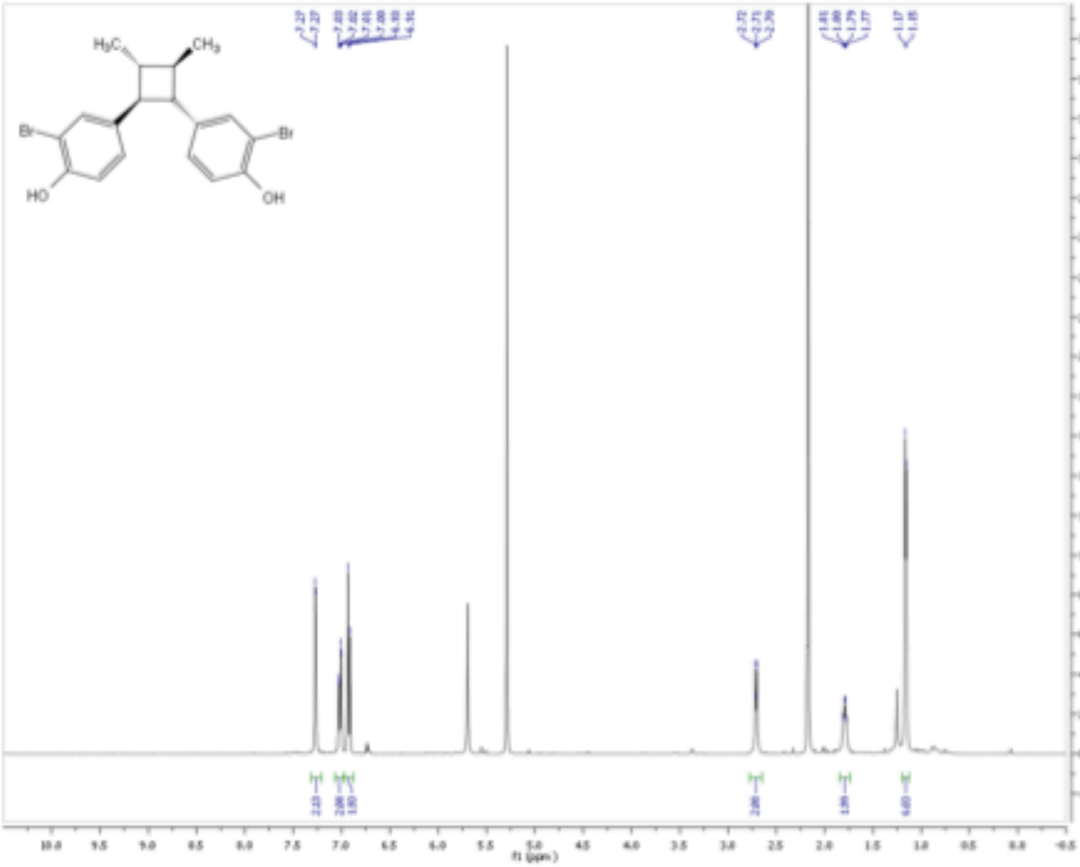

H3C
CH3
Br
Br
HO
OH
7.27
7.27
7.03
7.02
7.01
7.00
6.93
6.91
2.72
2.71
2.70
1.81
1.80
1.79
1.77
1.17
1.15
2.03
2.00
2.02
2.00
1.95
6.03
f1 (ppm)

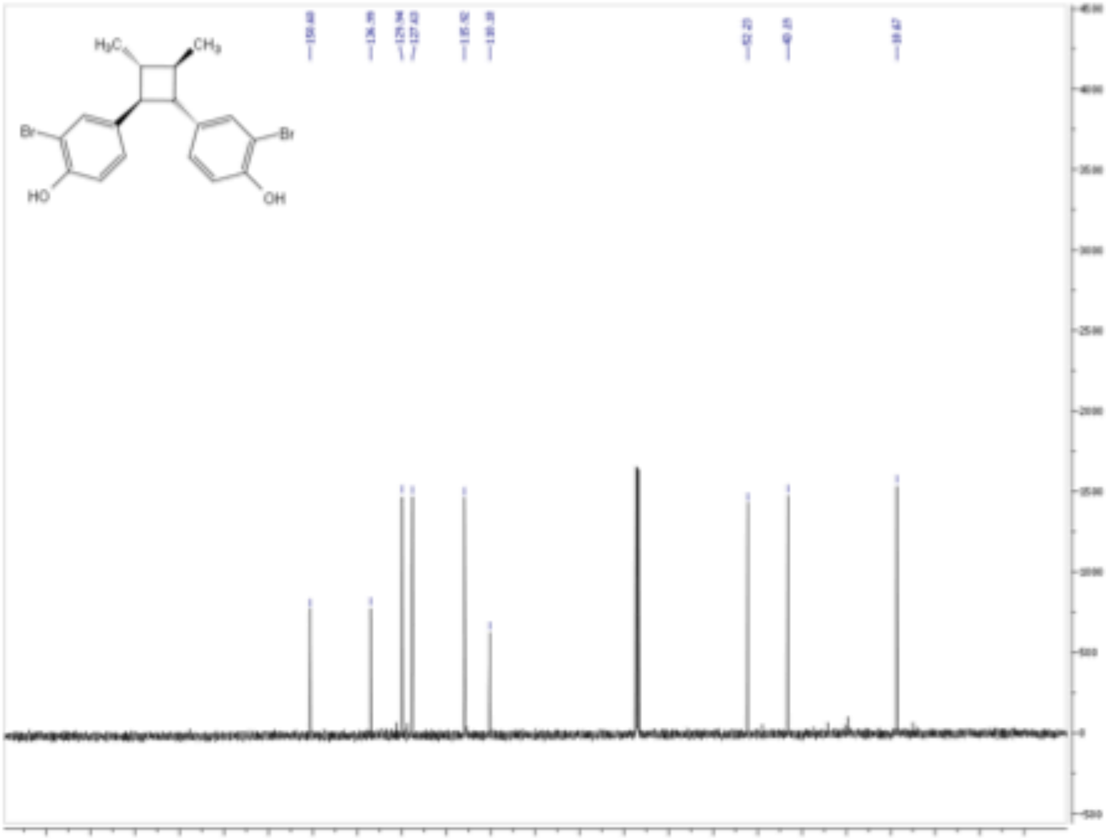

H3C
CH3
Br
Br
HO
OH
150.60
136.95
129.94
127.63
115.92
110.19
52.23
43.05
18.67
f1 (ppm)

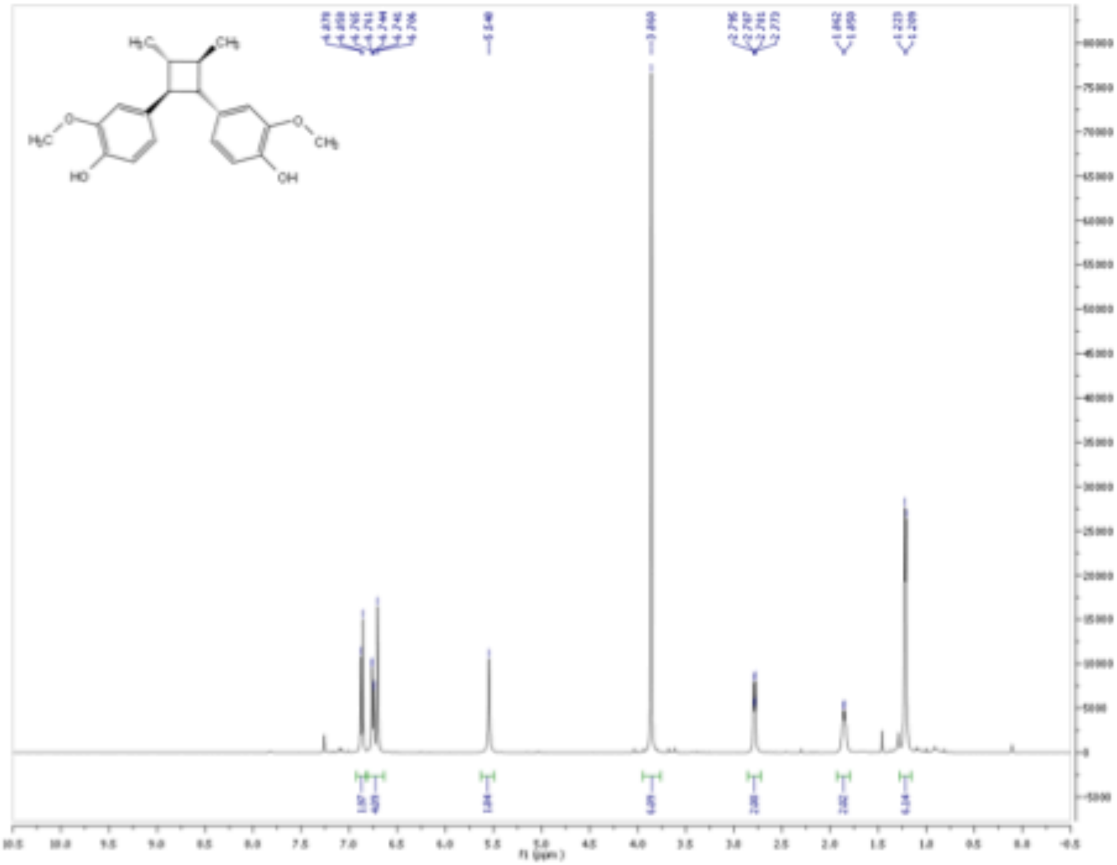
H₃C
CH₃
H₃C
O
CH₃
HO
OH
f1 (ppm)

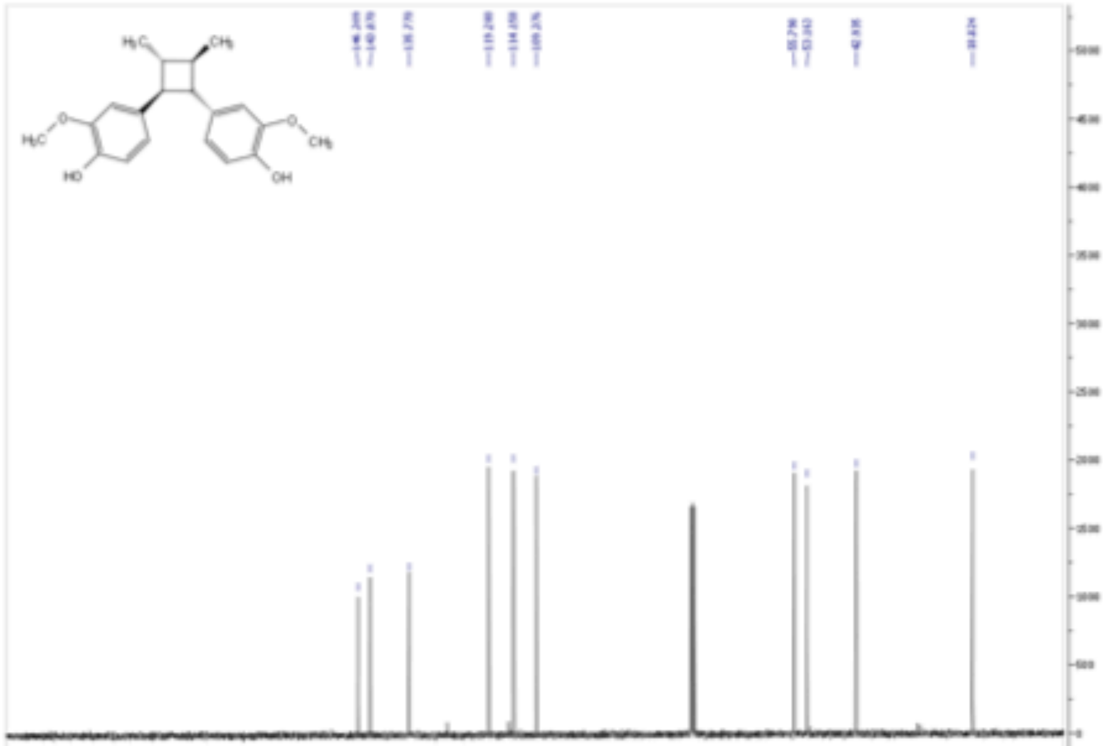
H₃C
CH₃
H₃C
O
CH₃
HO
OH
f1 (ppm)

# REFERENCES

(1) Sergeiko, A.; Poroikov, V. V.; Hanus, L. O.; Dembitsky, V. M. Cyclobutane-Containing Alkaloids: Origin, Synthesis, and Biological Activities. *Open Med Chem J* **2008**, *2*, 26–37.

(2) Dembitsky, V. M. Bioactive Cyclobutane-Containing Alkaloids. *J. Nat. Med.* **2007**, *62*, 1–33.

(3) Davis, R. A.; Carroll, A. R.; Duffy, S.; Avery, V. M.; Guymer, G. P.; Forster, P. I.; Quinn, R. J. Endiandrin a, a Potent Glucocorticoid Receptor Binder Isolated From the Australian Plant Endiandraanthropophagorum. *J. Nat. Prod.* **2007**, *70*, 1118–1121.

(4) Ryu, J.-H.; Son, H. J.; Lee, S. H.; Sohn, D. H. Two Neolignans From Perilla Frutescens and Their Inhibition of Nitric Oxide Synthase and Tumor Necrosis Factor-Alpha Expression in Murine Macrophage Cell Line RAW 264.7. *Bioorg. Med. Chem. Lett.* **2002**, *12*, 649–651.

(5) Kilbourn, R. G.; Gross, S. S.; Jubran, A.; Adams, J.; Griffith, O. W.; Levi, R.; Lodato, R. F. NG-Methyl-L-Arginine Inhibits Tumor Necrosis Factor-Induced Hypotension: Implications for the Involvement of Nitric Oxide. *Proceedings of the National Academy of Sciences* **1990**, *87*, 3629–3632.

(6) Badheka, L. P.; Prabhu, B. R.; Mulchandani, N. B. Lignans of Piper Cubeba. *Phytochemistry* **1987**, *26*, 2033–2036.

(7) Yamamura, S.; Niwa, M.; Terada, Y.; Nonoyama, M. The Isolation and Structures of Novel Neolignans and Neosesquilignans From Heterotropa Takaoi M. *Bulletin of the Chemical Society of Japan* **1982**, *55*, 3573–3579.

(8) Kikuchi, T. Kadota, S. Yanada, K. Tanaka, K. Watanabe, K. Yoshizaki, M. Yokoi, T. Shingu T. Isolation and Structure of Magnosalin and Magnoshinin, New Neolignans From Magnolia Saliciforia Maxim. *Chemical & pharmaceutical bulletin* **1983**, *31*, 1112–1114.

(9) Mahindru, R. N.; Taneja, S. C.; Dhar, K. L.; Brown, R. T. Reassignment of Structures of the Neolignans, Magnosalin and Andamanicin. *Phytochemistry* **1993**, *32*, 1073–1075.

(10) Kadota, S.; Tsubono, K.; Makino, K.; Takeshita, M.; Kikuchi, T. Convenient Synthesis of Magnoshinin, an Anti-Inflammatory Neolignan. *Tetrahedron Letters* **1987**, *28*, 2857–2860.

(11) Anslyn, Eric V., and Dennis A. Dougherty. *Modern Physical Organic Chemistry*. Sausalito, CA: University Science, 2006. Print.

(12) Laue, Thomas, and Andreas Plagens. *Named Organic Reactions*. Hoboken, NJ: Wiley, 2005. Print.

(13) Fleck, M.; Bach, T. Total Synthesis of Punctaporonin C by a Regio- and Stereoselective [2+2]-Photocycloaddition. *Chem. Eur. J.* **2010**, *16*, 6015–6032.

(14) Coote, S. C.; Bach, T. Enantioselective Intermolecular [2+2] Photocycloadditions of Isoquinolone Mediated by a Chiral Hydrogen-Bonding Template. *J. Am. Chem. Soc.* **2013**, *135*, 14948–14951.

(15) Brimioulle, R.; Bach, T. Enantioselective Lewis Acid Catalysis of Intramolecular Enone [2+2] Photocycloaddition Reactions. *Science* **2013**, *342*, 840–843.

(16) Roh, Y.; Jang, H.-Y.; Lynch, V.; Bauld, N. L.; Krische, M. J. Anion Radical Chain Cycloaddition of Tethered Enones: Intramolecular Cyclobutanation and Diels−Alder Cycloaddition. *Org. Lett.* **2002**, *4*, 611–613.

(17) Yang, J.; Felton, G. A. N.; Bauld, N. L.; Krische, M. J. Chemically Induced Anion Radical Cycloadditions: Intramolecular Cyclobutanation of Bis(Enones) via Homogeneous Electron Transfer. *J. Am. Chem. Soc.* **2004**, *126*, 1634–1635.

(18) Juris, A.; Balzani, V.; Barigelletti, F.; Campagna, S.; Belser, P. L.; Zelewsky, Von, A. Ru (II) Polypyridine Complexes: Photophysics, Photochemistry, Eletrochemistry, and Chemiluminescence. *Coordination Chemistry Reviews* **1988**, *84*, 85–277.

(19) De Cola, L.; Barigelletti, F.; Balzani, V.; Belser, P.; Zelewsky, Von, A.; Voegtle, F.; Ebmeyer, F.; Grammenudi, S. Ruthenium(II)-Polypyridine Cage Complexes: Luminescence and Photochemical Properties. *J. Am. Chem. Soc.* **1988**, *110*, 7210–7212.

(20) Ischay, M. A.; Anzovino, M. E.; Du, J.; Yoon, T. P. Efficient Visible Light Photocatalysis of [2+2] Enone Cycloadditions. *J. Am. Chem. Soc.* **2008**, *130*, 12886–12887.

(21) Narayanam, J. M. R.; Stephenson, C. R. J. Visible Light Photoredox Catalysis: Applications in Organic Synthesis. *Chem Soc Rev* **2011**, *40*, 102–113.

(22) Du, J.; Yoon, T. P. Crossed Intermolecular [2+2] Cycloadditions of Acyclic Enones via Visible Light Photocatalysis. *J. Am. Chem. Soc.* **2009**, *131*, 14604–14605.

(23) Lowry, M. S.; Goldsmith, J. I.; Slinker, J. D.; Rohl, R.; Pascal, R. A.; Malliaras, G. G.; Bernhard, S. Single-Layer Electroluminescent Devices and Photoinduced Hydrogen Production From an Ionic Iridium(III) Complex. *Chem. Mater.* **2005**, *17*, 5712–5719.

(24) Lu, Z.; Yoon, T. P. Visible Light Photocatalysis of [2+2] Styrene Cycloadditions by Energy Transfer. *Angew. Chem. Int. Ed.* **2012**, *51*, 10329–10332.

(25) Kim, T.; Mirafzal, G. A.; Liu, J.; Bauld, N. L. Is Hole Transfer Involved in Metalloporphyrin-Catalyzed Epoxidation *J. Am. Chem. Soc.* **1993**, *115*, 7653–7664.

(26) Chiba, K.; Miura, T.; Kim, S.; Kitano, Y.; Tada, M. Electrocatalytic Intermolecular Olefin Cross-Coupling by Anodically Induced Formal [2+2] Cycloaddition Between Enol Ethers and Alkenes. *J. Am. Chem. Soc.* **2001**, *123*, 11314–11315.

(27) Okada, Y.; Nishimoto, A.; Akaba, R.; Chiba, K. Electron-Transfer-Induced Intermolecular [2 + 2] Cycloaddition Reactions Based on the Aromatic "Redox Tag" Strategy. *J. Org. Chem.* **2011**, *76*, 3470–3476.

(28) Okada, Y.; Chiba, K. Electron Transfer-Induced Four-Membered Cyclic Intermediate Formation: Olefin Cross-Coupling vs. Olefin Cross-Metathesis. *Electrochimica Acta* **2011**, *56*, 1037–1042.

(29) Ledwith, A. Cation Radicals in Electron Transfer Reactions. *Accounts of Chemical Research* **1972**, *5*, 133–139.

(30) Bauld, N. L.; Pabon, R. Cation Radical Catalyzed Olefin Cyclodimerization. *J. Am. Chem. Soc.* **1983**, *105*, 633–634.

(31) Lewis, F. D.; Kojima, M. Electron Transfer Induced Photoisomerization, Dimerization, and Oxygenation of Trans-and Cis-Anethole: the Role of Monomer and Dimer Cation Radicals. *J. Am. Chem. Soc.* **1988**, *110*, 8664–8670.

(32) Kuwata, S.; Shigemitsu, Y.; Odaira, Y. Photosensitized Cyclodimerization of Phenyl Vinyl Ethers. *J. Org. Chem.* **1973**, *38*, 3803–3805.

(33) Farid, S.; Shealer, S. E. Radical Cations: Photochemical and Ferric Ion-Induced Formation and Reactions of Indene Radical Cation. *J. Chem. Soc., Chem. Commun.* **1973**, 677.

(34) Majima, T.; Pac, C.; Nakasone, A.; Sakurai, H. Redox-Photosensitized Reactions. 7. Aromatic Hydrocarbon-Photosensitized Electron-Transfer Reactions of Furan, Methylated Furans, 1,1-Diphenylethylene, and Indene with *p*-Dicyanobenzene. *J. Am. Chem. Soc.* **1981**, *103*, 4499–4508.

(35) Ischay, M. A.; Ament, M. S.; Yoon, T. P. Crossed Intermolecular [2 + 2] Cycloaddition of Styrenes by Visible Light Photocatalysis. *Chem. Sci.* **2012**, *3*, 2807.

(36) Variation of oxidation potential of substrates between publications is due to the difference in solution concentration when subjected to cyclic voltammetry. For clarity, values from the papers are used in reference to other values within the same paper.

(37) Miranda, M. A.; Garcia, H. 2, 4, 6-Triphenylpyrylium Tetrafluoroborate as an Electron-Transfer Photosensitizer. *Chem. Rev.* **1994**, *94*, 1063–1089.

(38) Satpati, A. K.; Nath, S.; Kumbhakar, M.; Maity, D. K.; Senthilkumar, S.; Pal, H. Bimolecular Electron Transfer Reactions in Coumarin–Amine Systems: Donor–Acceptor

Orientational Effect on Diffusion-Controlled Reaction Rates. *Journal of Molecular Structure* **2008**, *878*, 84–94.

(39) Schepp, N. P.; Johnston, L. J. Nanosecond and Picosecond Dynamics of the Radical Cation Mediated Dimerization of 4-Methoxystyrene. *J. Am. Chem. Soc.* **1994**, *116*, 6895–6903.

(40) de C Bayma, J.; Arruda, M. S. P.; Müller, A. H.; Arruda, A. C.; Canto, W. C. A Dimeric ArC 2 Compound From Peperomia Pellucida. *Phytochemistry* **2000**, *55*, 779–782.

(41) Green, I. R.; October, N. Role of the Methoxy Group in Product Formation via $TiCl_4$ Promoted 4-Phenyldioxolane Isomerizations. *ARKIVOC: Online Journal of Organic Chemistry* **2010**.

(42) Nozaki, H.; Otani, I.; Noyori, R.; Kawanisi, M. Photochemical Reactions of Trans-Anethole. *Tetrahedron* **1968**, *24*, 2183–2192.

(43) Ostrauskaite, J.; Voska, V.; Grazulevicius, J. V. Synthesis and Properties of Glass-Forming Hydrazones II [1]. Hydrazones Containing Bicarbazolyl Units. *Monatshefte für Chemie/Chemical Monthly* **2002**, *133*, 599–607.

(44) Tripathi, S.; Chan, M.-H.; Chen, C. An Expedient Synthesis of Honokiol and Its Analogues as Potential Neuropreventive Agents. *Bioorg. Med. Chem. Lett.* **2012**, *22*, 216–221.

(45) Hille, U. E.; Hu, Q.; Vock, C.; Negri, M.; Bartels, M.; MUller-Vieira, U.; Lauterbach, T.; Hartmann, R. W. Novel CYP17 Inhibitors: Synthesis, Biological Evaluation, Structure-Activity Relationships and Modeling of Methoxy- and Hydroxy-Substituted Methyleneimidazolyl Biphenyls. *European Journal of Medicinal Chemistry* **2009**, *44*, 2765–2775.

(46) Naidu, A. B.; Sekar, G. An Efficient Intermolecular BINAM–Copper(I) Catalyzed Ullmann-Type Coupling of Aryl Iodides/Bromides with Aliphatic Alcohols. *Tetrahedron Letters* **2008**, *49*, 3147–3151.

# CHAPTER THREE: SYNTHESIS OF γ-BUTYROLACONES *via* POLAR RADICAL CROSSOVER CYCLOADDITION REACTIONS OF UNSATURATED ACIDS AND ALKENES

## 3.1 Introduction

The γ-butyrolactone subunit is a prevalent structural feature in numerous natural products displaying a vast range of bioactivity. Many natural compounds of this class are defined by the substitution pattern around the butyrolactone core. Within the butyrolactone class exist structures with an α-methylene-γ-butyrolactone motif. This motif is common to a number of natural products with biologically relevant properties including anticancer, antibacterial, antiviral, anti-inflammatory, and antifungal.[1] Numerous paraconic acids, a class of γ-butyrolactone natural products distinguished by their β-carboxylic acid, also possess this α-methylene feature (Figure 3-1). For these reasons, the γ-butyrolactone core has captivated the attention of numerous groups resulting in the development of several synthetic methods devoted to its construction.

**Figure 3-1: Numbering Scheme And Skeletal Structure of γ-Butyrolactones**

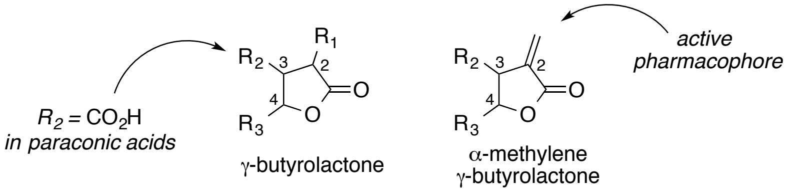

Methods for the construction of 2,3,4-trisubstituted γ-butyrolactones are less frequently reported, while methods focusing on γ-butyrolactones with 2,3 and 3,4-substitution are more commonly described. In addition, only a handful of methods have been applied to the synthesis of biologically relevant natural products. The α-methylene motif has been distinguished to be the active pharmacophore amongst the paraconic acids, providing increased activity when compared to α-methyl variants.[2] With this increased reactivity comes a more structurally challenging compound to synthesize, prone to Michael addition side reactions. With this in mind, we sought to develop a method for the synthesis of di- and trisubstituted γ-butyrolactones, which may be directly applied to the synthesis of bioactive natural products possessing the α-methylene moiety. We report the direct organocatalytic synthesis of γ-butyrolactones from simple alkene and unsaturated acid starting materials. The cycloadducts synthesized include γ-butyrolactones with aliphatic, aromatic, heteroaromatic, α-alkylidine, and masked α-methylene functionality. Our method allows for further product derivatization, providing the diastereoselective synthesis of two paraconic acids, methylenolactocin and protolichisterinic acid, in a total of 3 steps.

## 3.2 Natural Products: Isolation and Bioactivity

In the early 1940's, *Cetraria islandica* (L.) Ach., also known as Iceland moss, was commonly used as a classical remedy for treatment of throat irritation, cough, gastritis, and relief of certain types of ulcers.[3] Due to interest in its bioactivity, research was carried out to better understand the biological reactivity of the active component in the moss. In a study carried out in the 1950's, protolichesterinic acid was isolated from the plant and was found to exhibit antibacterial properties against *Streptococcus* and *Staphlyococcus*.[4] More recently, protolichesterinic acid has been found to display antitumor activity against solid-type Ehrlich carcinoma, affect inhibition against DNA polymerase activity in HIV-1 reverse transcriptase,[5] exhibit antifungal activity and inhibitory activity towards HCT-116 (coloncarcinoma), [6,7] and affect apoptosis to cancer cells.[8] Additionally, this active compound was found to exhibit modest radical scavenging activity, which was correlated to antioxidant activity.[9] A report within the last decade announced that protolichesterinic acid reached anti-proliferative maximal effective concentration at 50% ($EC_{50}$) values in human cancer cell lines at 4 μg/mL, which is within the "criteria limit for compounds worthy of further investigation."[10] For these reasons, this active γ-butyrolactone has appealed to synthetic chemists and health science researchers, resulting in several studies for both its direct synthesis and extended bioactivity.

**Figure 3-2: Biologically Relevant Paraconic Acids**

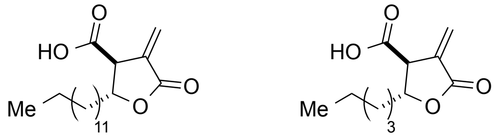

***Protolichesterinic acid*** ***Methylenolactocin***

In 1988, Park and coworkers published the isolation of methylenolactocin produced in the culture filtrate of a *penicilium* strain originating from a soil sample in Japan. The authors isolated this ingredient due to its reactivity in an antitumor antibiotics assay, which was based on a Michael addition reaction. Following chemical investigation, the structure of methylenolactocin was correctly identified as α-methylene γ-butyrolactone with a pendent carboxylic acid at C3, and aliphatic 5-carbon chain at C4.[11] In this seminal report, the authors found methylenolactocin to be active against gram-positive bacteria and possess antitumor activity against Ehrlich carcinoma. At this time, the absolute stereochemistry was not identified, yet was elucidated by various research groups including Yoshihara and coworkers.[12] Reports on structure elucidation launched an overwhelming number of publications regarding the bioactivity of the small molecule.

### 3.2.1 Previous Syntheses of Methylenolactocin and Protolichesterinic Acid

Several examples of racemic and enantioselective syntheses have been reported for both of these paraconic acids. One of the early reported syntheses of (±) protolichesterinic acid was published by Watts and Johnson in the early 70's.[13] This transformation began with free radical addition of *n*-tetradecanal with dimethyl maleate, affording methyl 3-methoxycarbonyl-4-oxoheptadecanoate in a 68% yield (Figure 3-3). To affect formation of the γ-butyrolactone core, acyclic intermediate **33b** was subjected to hydride delivery, which promoted lactonization and provided **33c** in an 86%. Raney Nickel reduction provided lactone **33d** in 20% yield. When methyl ester lactone **33d** was subjected to methyl magnesium carbonate (Stiles' reagent), no product was observed, however when monoacid lactone **33e** was then treated with Stiles' reagent, the racemic diacid **33f** was isolated in 92.5% yield.[14] The diacid was then reacted with formaldehyde and diethylamine, where the evolution of carbon dioxide provided protolichesterinic acid as the sole adduct.

**Figure 3-3: Linear Synthesis For Protolichesterinic Acid**

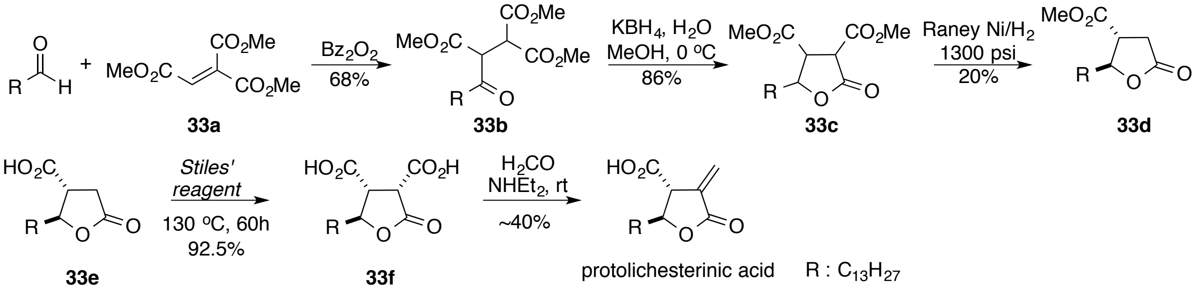

In 1998, Roy reported a transition metal catalyzed radical cyclization for the synthesis of substituted tetrahydrofurans arising from alkynyl epoxides (Figure 3-4). Roy and coworkers showed the utility of their method by applying it to the synthesis of (±) methylenolactocin, and (±) protolichesterinic acid.[15] Initial efforts were devoted to converting tetrahydrofuran **34b** directly to each paraconic acid. However, double oxidation of **34b** resulting in formation of the desired lactone proved unsuccessful (crossed arrow, Figure 3-4). Instead, a linear synthesis was devised, wherein free alcohol **34b** was protected prior to lactone formation, and was then deprotected and oxidized. Though a mixture of **34e** diastereomers were employed in this transformation, isomerization to the more stable conformer was observed following a Jones oxidation, resulting in the isolation of pure methylenolactocin and protolichesterinic acid in similar yields. As *trans* substitution produced a more stable conformer during their key intramolecular cyclization reaction, the desired diasteroselectivity was obtained. Additionally, preference for a 5–*exo* cyclization over 6-*endo* is verified according to Bauldwin's rules.[16]

**Figure 3-4: Direct Synthesis of γ-Butyrolactone Core: Application to Protolichesterinic Acid**

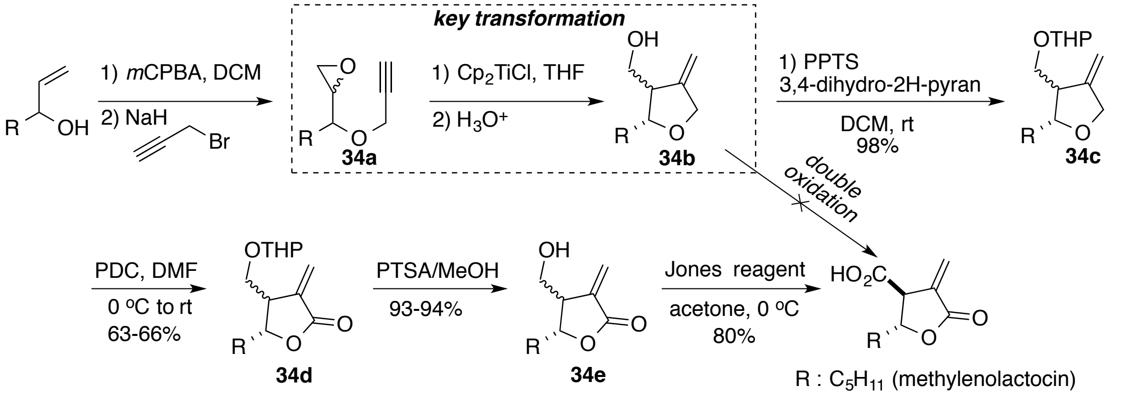
key transformation
1) mCPBA, DCM
2) NaH
Br
34a
1) Cp2TiCl, THF
2) H3O+
34b
1) PPTS
3,4-dihydro-2H-pyran
DCM, rt
98%
34c
double oxidation
PDC, DMF
0 °C to rt
63-66%
34d
PTSA/MeOH
93-94%
34e
Jones reagent
acetone, 0 °C
80%
OTHP
OH
HO2C

R : $C_5H_{11}$ (methylenolactocin)
R : $C_{13}H_{27}$ (protolichesterinic acid)

The continuous refinement of syntheses for these two natural products has persisted throughout the last few decades. Many concise syntheses have been published,[17] including work accomplished by Loh and Lye in 2001. The authors believed the α-methylene γ-butyrolactone core could be directly formed via an indium-mediated allylation reaction arising from *Z*-allyl bromide **35b:*Z*** (Figure 3-5).[18] The allyl bromide reagent was easily synthesized in two steps starting from the Baylis Hillman reaction between methyl acrylate and methyl glyoxylate. Alkenol **35a** was provided in 52% yield, which was then brominated with $PBr_3$ affording a mixture of *Z* and *E* isomers **35b** (95:5, *Z*:*E*) in excellent yield. The isomers were easily separated and the major isomer **35b:*Z*** was subjected to their key transformation in the presence of hexanal. Using stoichiometric indium after three days resulted in formation of lactone **35c** accompanied by uncyclized **35d** in 85% yield. Though not initially anticipated, the authors discovered methylenolactocin could also be formed by treating uncyclized product **35d** with TFA, followed by acid hydrolysis. This allowed adducts **35c** and **35d** to be taken on directly to the natural product. Though this method required stoichiometric amounts of indium, this protocol allows for the synthesis of methylenolactocin and other paraconic acids with similar functionality.

**Figure 3-5: Five Step Synthesis For Methylenolactocin**

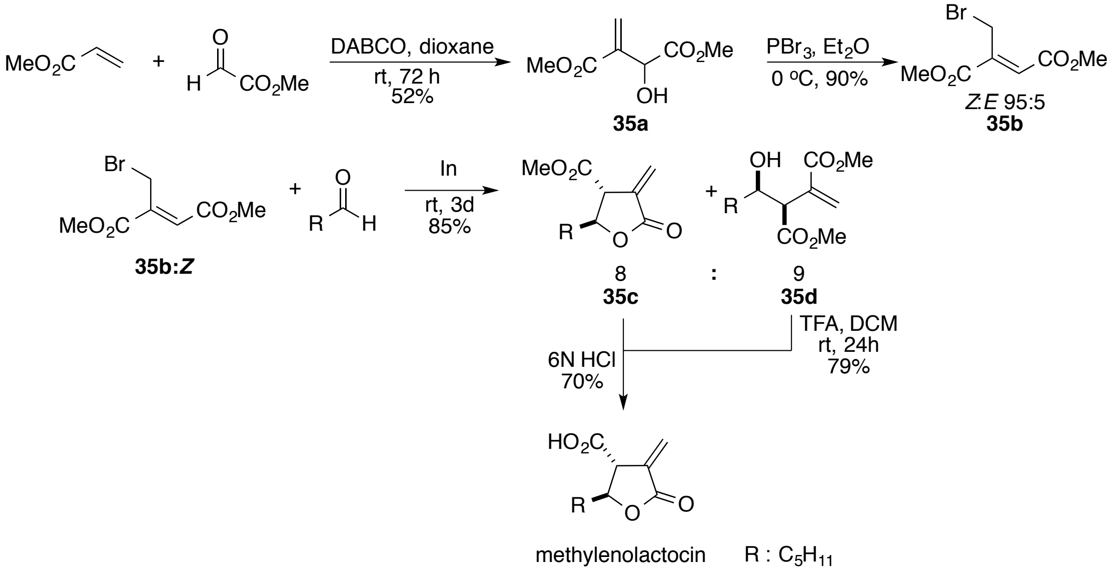
MeO2C
+
O
H
CO2Me
DABCO, dioxane
rt, 72 h
52%
MeO2C
CO2Me
OH
35a
PBr3, Et2O
0 °C, 90%
Br
MeO2C
CO2Me
Z:E 95:5
35b
Br
MeO2C
CO2Me
35b:Z
+
O
R
H
In
rt, 3d
85%
MeO2C
R
O
O
8
35c
:
+
OH
CO2Me
R
CO2Me
9
35d
TFA, DCM
rt, 24h
79%
6N HCl
70%
HO2C
R
O
O
methylenolactocin
R : C5H11

Hodgson and Clark recently reported the concise racemic synthesis for methylenolactocin, where the key transformation converted bromolactone **36a** to 2-substituted α-methylene butyrolactone **36b** via chromium catalysis (Figure 3-6).[19] Bromolactone **36a** was synthesized in 55% yield over two steps with one purification from tulipalin. Following the screening of several catalysts, optimal conditions for this Barbier-type coupling were found by employing a modified method developed by Shi for Nozaki-Hiyama-Kishi reactions.[20] Butyrolactone **36b** was subjected to *trans*-lactonization with catalytic amounts of *p*-toluenesulfonic acid, affording **36c** in 84% yield. Lastly, disubstituted lactone **36c** was treated with Jones reagent to afford methylenolactocin in 72% yield. Their key transformation exhibited excellent diastereoselectivity (99:1), which was rationalized by the transition state depicted in Figure 3-6. The authors propose metal coordination with the oxygen of the aldehyde occurred as a 6-membered transition state, which oriented the R group on the aldehyde away from the butyrolactone moiety. Other substrates in this report show the high diastereoselectivity was maintained, and forged the desired cycloadduct in 65-94% yields.

**Figure 3-6: Synthesis For Methylenolactocin Arising from Tulipalin**

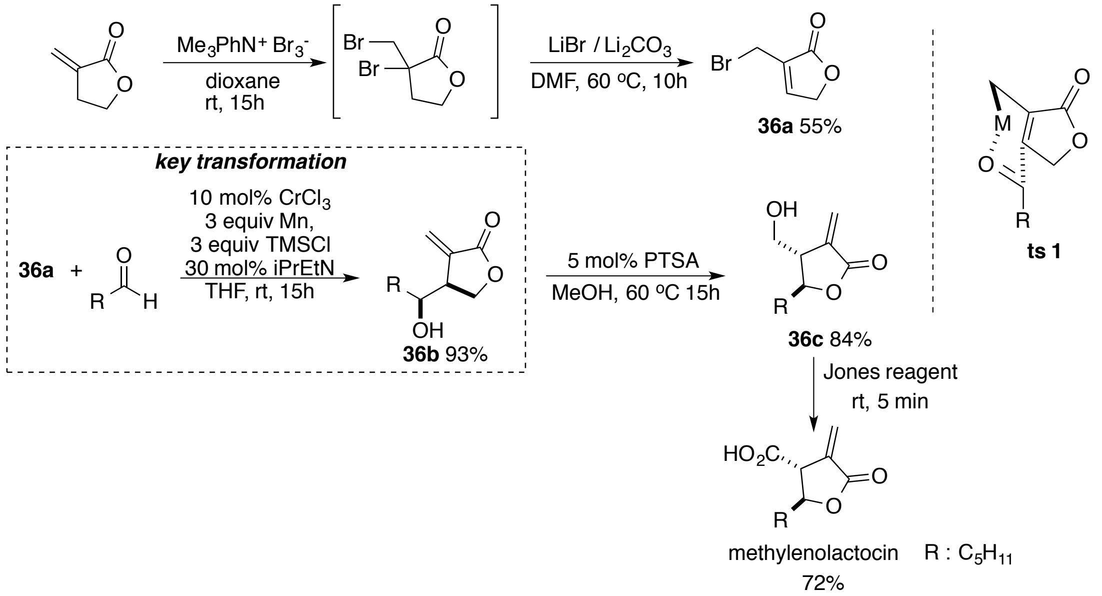
Me3PhN+ Br3-
dioxane
rt, 15h
LiBr / Li2CO3
DMF, 60 °C, 10h
36a 55%
ts 1
key transformation
10 mol% CrCl3
3 equiv Mn,
3 equiv TMSCl
30 mol% iPrEtN
THF, rt, 15h
36b 93%
5 mol% PTSA
MeOH, 60 °C 15h
36c 84%
Jones reagent
rt, 5 min
methylenolactocin R : C5H11
72%

After considering the procedures reported for the syntheses of methylenolactocin and protolichesterinic acid, we were fascinated by the possibility of developing a more concise method, which would encompass synthesis of γ-butyrolactones with application to natural product synthesis. Though numerous enantioselective examples for the synthesis γ-butyrolactones exist,[21] methods to construct di- and trisubstituted γ-butyrolactones are discussed (*vide infra*) to better understand the limitations present in each method. Attention is brought to seminal work in the field as well as to novel and innovative methods that have previously been used.

## 3.3 Synthesis of γ-Butyrolactones

### 3.3.1 Methods For The Synthesis of Disubstituted γ-Butyrolactones

**Figure 3-7: Lactonization via 4-Hydroxycarbonyl**

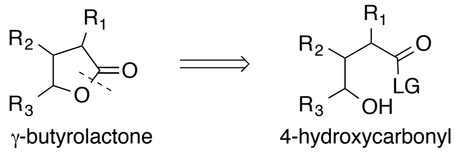
R1
R2
R3
γ-butyrolactone
LG
OH
4-hydroxycarbonyl

When considering a direct retrosynthesis, a disconnection of the lactone is evident via formation and cyclization from the requisite acyclic 4-hydroxycarbonyl intermediate (Figure 3-7).

The challenge in this approach is substrate instability, where uncontrolled self-condensation commonly results.[22] While the difficulty of controlling the homoaldol reaction as been accepted by many, a significant advancement was realized by Hoppe and coworkers by the development of a novel aldehyde allylation strategy (Figure 3-8). Hoppe believed γ-butyrolactones could be constructed in a linear fashion arising from carbamate **37a**. Deprotonation and equilibration between the negatively charged species of **37a** are then treated with $Ti(O^iPr)_4$, to give the allyl titanate **37b**, which was obtained as a single diastereomer via crystallization. In the presence of isobutyroaldehyde, **37b** underwent addition to afford aldol adduct **37c** in an excellent yield (90%). Mercury-assisted methanolysis followed, producing the intermediate **37e**, which was then subjected to oxidizing conditions, giving disubstituted lactone **37d** in 89% yield over two steps. Though successful, a chiral reagent was required to obtain the *trans* selectivity between substituents, resulting in a very linear approach.

**Figure 3-8: 3,4 Disubstituted γ-Butyrolactones via Aldol Cyclization**

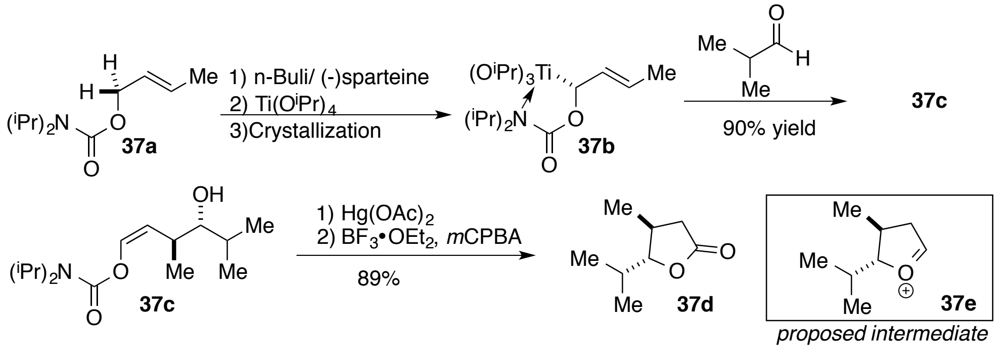

With recent advances in nucleophilic carbene catalysis, homoenolates may be generated from the condensation of α,β-unsaturated aldehydes, which in turn may be reacted with a second aldehyde to affect lactone formation. This approach was considered by Bode and Glorius, where polarity reversal of electrophilic α,β-unsaturated aldehydes was achieved with the aid of imidazolium derived *N*-heterocyclic carbene (NHC) catalysts.[23,24] The resulting nucleophilic species can react with aromatic aldehydes or ketones to give 3,4- and 3,4,4-substituted γ-butyrolactones. Glorius found 1,3-dimesityl-2,3-dihydro-1H-imidazol-2-ylidene (IMes) to be a competent catalyst for this transformation (Figure 3-9). Optimal conditions required slight excess of the benzaldehyde derivative to the α,β-unsaturated aldehyde, 5 mol% of the *N*-heterocyclic carbene catalyst, 5 mol% of 1,8-Diazabicyclo[5.4.0]undec-7-ene (DBU) at room temperature in polar solvents.

**Figure 3-9: 3,4 Disubstituted γ-Butyrolactone via NHC Catalysis**

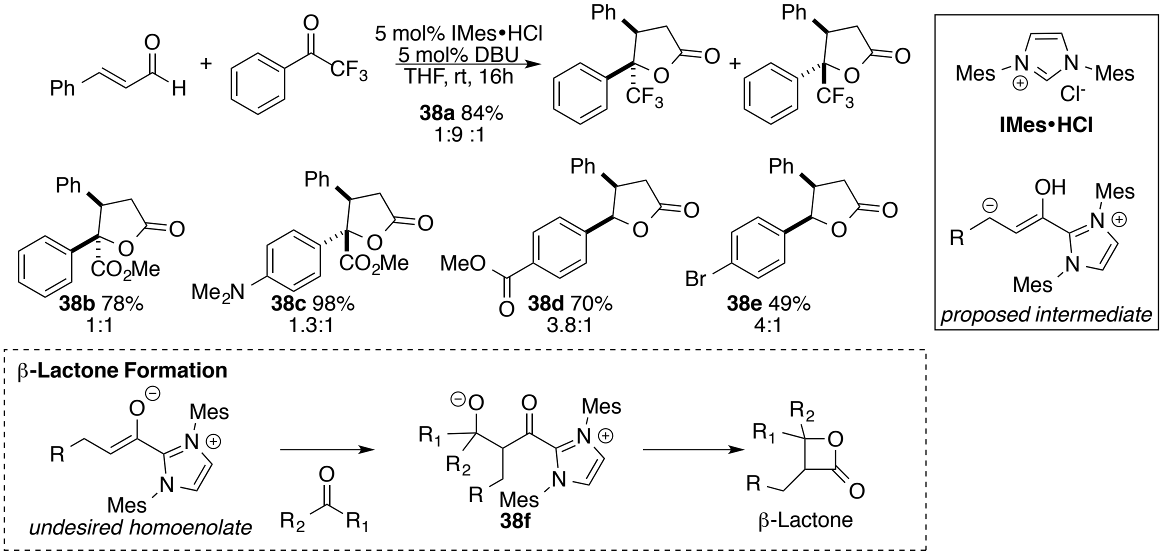
5 mol% IMes•HCl
5 mol% DBU
THF, rt, 16h
38a 84%
1:9 :1
38b 78%
1:1
38c 98%
1.3:1
38d 70%
3.8:1
38e 49%
4:1
IMes•HCl
proposed intermediate
β-Lactone Formation
undesired homoenolate
38f
β-Lactone

These conditions proved successful for the reaction of electron-rich and electron-poor aromatic ketones, as tetrasubstituted lactones **38a**, **38b** and **38c** were obtained in good to excellent yields. A wide scope for the formation of γ-butyrolactones arising from the reaction of aromatic aldehydes and cinnamic acids was developed. However unique solvent, stoichiometry, and reaction times were required for each transformation. Production of γ-butyrolactones **38d** and **38e** verified that electron-withdrawing aldehydes are within the scope of this reaction. Glorius and coworkers discovered that when less polar solvents and cooler temperatures were employed, β-lactone formation was observed as the major product. The authors predict byproduct formation occurred by the reaction of an aromatic aldehyde and the *undesired homoenolate* depicted in Figure 3-9; adduct **38f** is proposed to undergo intramolecular cycloaddition expelling **IMes** and producing β-lactones. To extend this work, the umpolung reaction of α-methylcinnimaldehyde was investigated, providing α–substituted γ–butyrolactones. Trisubstituted γ-butyrolactone **39a** was formed in 83% yield as a mixture of four diastereomers (Figure 3-10). In general, this method of polarity reversal is an excellent approach to produce cyclic adducts arising from the coupling of two electrophilic substrates.

**Figure 3-10: 2,3,4 Trisubstituted γ-Butyrolactone via NHC Catalysis**

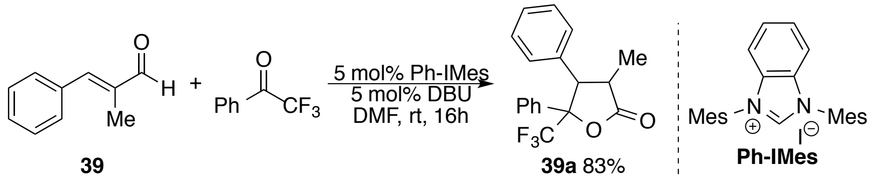

Typical *N*-heterocyclic carbene catalysis is restricted to large spatial bisarylimidazolium salts and aryl-substituted triazolium salts. These salts commonly require multistep syntheses arising from expensive materials. Additionally, yields for the catalysts are typically low and require oxygen-free conditions.[25] These limitations were recently considered by the Yu group, who reported the conjugate umpolung of α,β–unsaturated acids for the stereoselective synthesis of γ-butyrolactones via imidazolium chiral ionic liquids.[26] An ionic liquid is composed of positive and negatively charged ions in the liquid state; implementing chiral salts as ionic liquids results in a chiral medium. Efforts were focused on the synthesis of (-) menthol-derived imidazoliums possessing various *N*-substitution and counteranions. This class of catalyst has a direct and moderately high yielding 3-step synthesis, easy separation, and allows for catalyst recycling at the conclusion of the transformation. *n*-Butyl substitution with the $PF_6^-$ counteranion proved most successful (Figure 3-11). Moderate yields were observed with benzaldehyde derivatives possessing electron releasing groups such as methyl (**40a**), and electron-withdrawing groups such as fluoro, bromo, and methyl ester (**40b**, **40c**, and **40d,** respectively). A very modest level of enantioselectivity was reported for the *cis* and *trans* γ-butyrolactones, where 22% ee for *cis* **40d** was the highest reported value. On the other hand, successful catalyst recyclability experiments showed consistent reactivity of the chiral catalyst after 6 reaction cycles. This report is an excellent example for the polarity reversal of electrophilic α,β–unsaturated substrates, which are rendered nucleophilic with the aid of N-heterocyclic carbene catalysis.

**Figure 3-11: 3,4 Disubstituted γ-Butyrolactones via (-) Menthol-Derived NHC Catalysis**

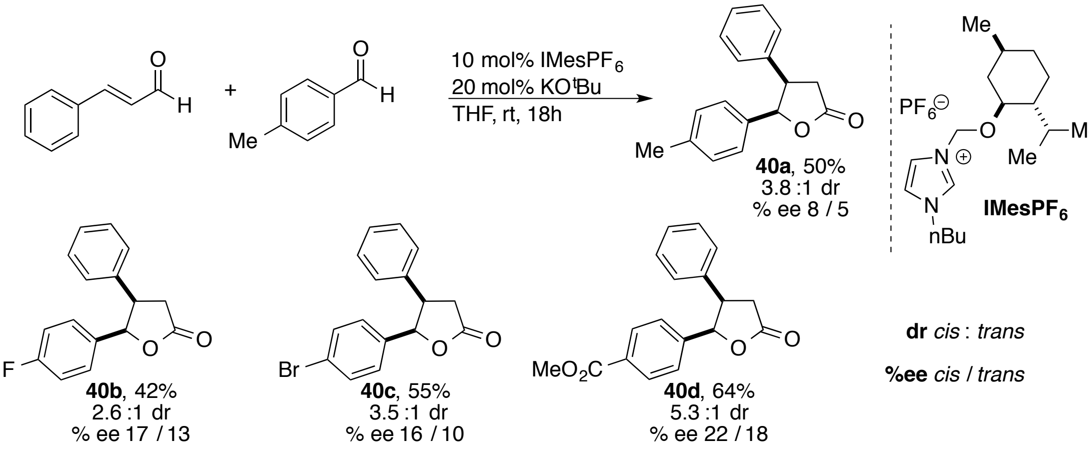
10 mol% IMesPF6
20 mol% KOtBu
THF, rt, 18h
40a, 50%
3.8 :1 dr
% ee 8 / 5
IMesPF6
40b, 42%
2.6 :1 dr
% ee 17 / 13
40c, 55%
3.5 :1 dr
% ee 16 / 10
40d, 64%
5.3 :1 dr
% ee 22 / 18
dr cis : trans
%ee cis / trans

Synthesizing γ-butyrolactones from butenolides has also become a popular approach, as butenolides are a versatile building block for the synthesis of monocyclic or polycyclic butyrolactones. Additionally, butenolides are often natural products themselves, which opens the possibility to approaching γ-butyrolactones in a biomimetic fashion. Chiral butenolides have played a key role in natural product synthesis as they can be easily derived from L-glutamic acid and D-mannitol.[27] This ideal chiral synthon was developed by Feringa and Jong in 1989 for the synthesis of mono and bicyclic lactones. Racemic butenolide **41** was subjected to 1.5 equivalents of *l*-menthol under thermal conditions (Figure 3-12). A mixture of enantiomers **41b** and **41c** were provided, where menthol-derived butenolide **41b** preferentially crystallized out of solution. With this approach, the authors provided three examples of substituted and unsubstituted chiral butenolides **41ba**, **41bb**, and **41bc**. Though the alkene in the butenolide was not used for further functionality, disubstituted lactones were produced via the palladium on carbon reduction, producing **41baa, 41bba,** and **41bca**.

**Figure 3-12: Menthol Derived-Chiral Butenolides**

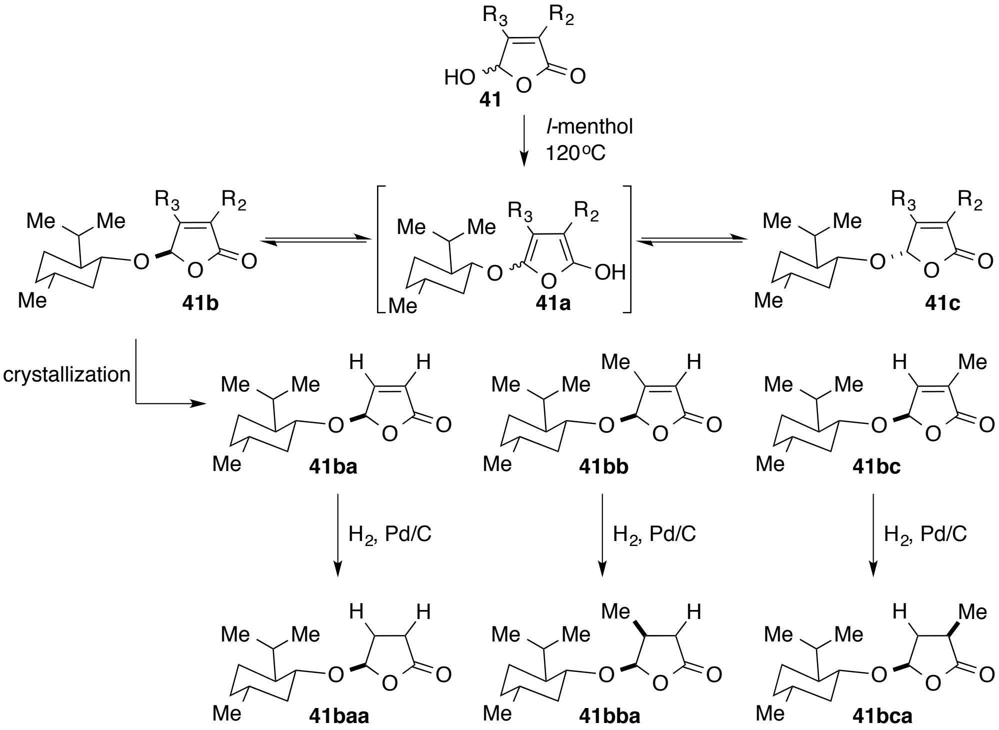

One limitation associated with this process is the loss of product **41c**, as only one enantiomer may be crystallized out of solution. This could be rectified by promoting a dynamic kinetic asymmetric transformation (DYKAT), converting racemic material to enantiopure products. The chiral butenolide could also be subjected to conjugate addition via the α,β double bond, which would further expand its utility. These two prospects were recently considered by Trost and coworkers, where enantiomerically pure γ–aryloxybutenolides were constructed via a palladium catalyzed asymmetric allylic alkylation under DYKAT conditions.[28] When the racemic butenolide was subjected to palladium-catalyzed conditions, and in the presence of a chiral ligand, tetrabutylammonium chloride and 2-naphthol, butenolide **42** was obtained in 84% yield and 96% ee (Figure 3-13). Numerous nucleophiles are known to stereoselectively undergo Michael addition of stabilized electrophiles. An example of this is presented, where good facial selectivity was observed when dimethyl malonate in the presence of base undergoes conjugate addition to *ent*-**42**, providing adduct **43b** in 77% yield. Other stabilized nucleophiles such as 2-nitropropane also underwent conjugate addition with *ent*-**42**, delivering **43a** in 93% yield. Once the desired transformation was complete, the chiral auxiliary could be easily reduced with sodium borohydride, providing the enantiomerically pure monosubstituted γ-butyrolactone. The efficiency of the naphthoxy moiety to affect diastereocontrol was explored by the authors, where excellent levels of enantioselectivity was obtained. Unfortunately, this method does not allow for a general application to synthesize a class of natural products due to its linear approach. Additionally, only products excluding substitution at the 2-position may be obtained.

**Figure 3-13: Conjugate Addition of Enantiopure Butenolides**

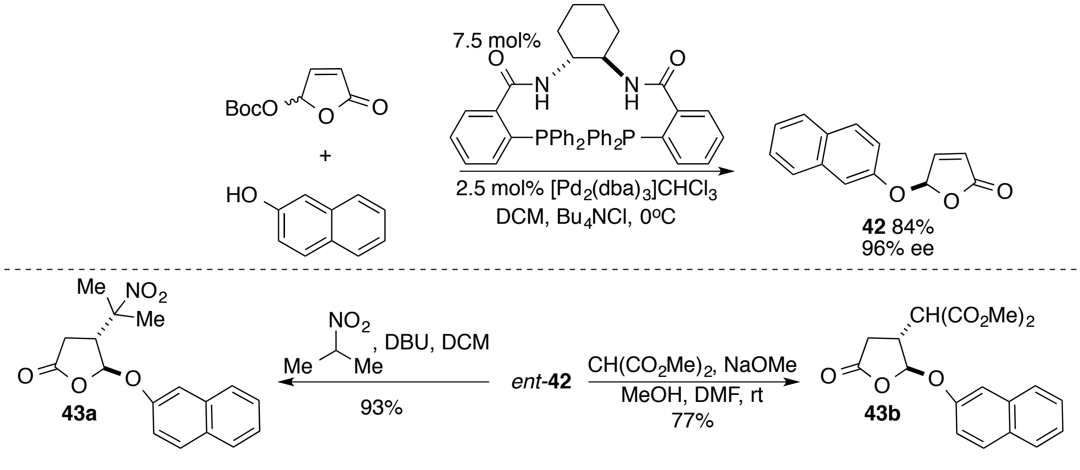

### 3.3.2 Methods For The Synthesis of Trisubstituted γ-Butyrolactones

As previously mentioned, 2,3,4-trisubstituted γ-butyrolactones are prevalent structures in natural products, chiefly within the paraconic acids. The majority of these naturally-produced compounds possess three different functional groups with varying stereochemistry. Methods for the synthesis of trisubstituted lactones are rare, as the challenge for controlling the diastereoselectivity of the transformation is increased. In an attempt to transition to the diastereoselective synthesis of trisubstituted γ-butyrolactones, Shimada and Saigo attempted the synthesis of 3,4 disubstituted lactones with a geminal dimethyl moiety at the 2-position.[29] The authors achieved this by the Lewis acid-promoted cyclization of 2,2-dialkoxycyclopropanecarboxylic esters with aldehydes or unsymmetrical ketones. The selection of 2,2-dialkoxycyclopropanecarboxylic esters enabled ring-opening reactions, as these activated cyclopropanes possess electron-withdrawing and electron-donating substituents. Such cyclopropanes exhibit stability similar to 1,3 zwitterions, rendering them versatile building blocks in organic synthesis. Consequently, vicinal donor-acceptor substituted cyclopropanes may react with both nucleophiles and electrophiles. Following the screening of various Lewis acids, the authors found $TiBr_4$ as a competent stoichiometric reagent to provide butyrolactones with a *cis* 3,4 relationship. Activated cyclopropane **44** and 3-phenylpropanal in the presence of $TiBr_4$ at cryogenic temperatures delivered the desired lactone **44a** in 87% yield and 5.6:1 d.r. (Figure 3-14). Higher diastereoselectivies were observed when benzaldehyde and isopropylaldehyde were employed, resulting in excellent yields for **44b (**91%, 46:1 dr) and **44e** (87%, 19:1 dr). *trans*-Cinnimaldehyde was also found to be a viable substrate, generating lactone **44c** in an 89% yield and 3.5:1 dr. The authors propose 1,3 zwitterion **45** reacts stoichiometrically with the Lewis acid, resulting in the formation of activated intermediate **46**, which cyclizes with the aldehyde of interest. The moderate *cis* selectivity is attributed to the bidentate coordination of titanium, which suggests the reaction is proceeding via a cyclic transition state (*vide infra*). As the bond length of the titanium oxygen bond is short relative to other Lewis acids screened, there is more steric repulsion between itself and pendent functionality. Therefore, smaller groups prefer to occupy the axial position, resulting in the generation of cis γ-lactone. This is depicted in transition state **ts 2** in Figure 3-15.

**Figure 3-14: *cis* 3,4-Substituted γ-Lactones With Geminal Dimethyl Substitution**

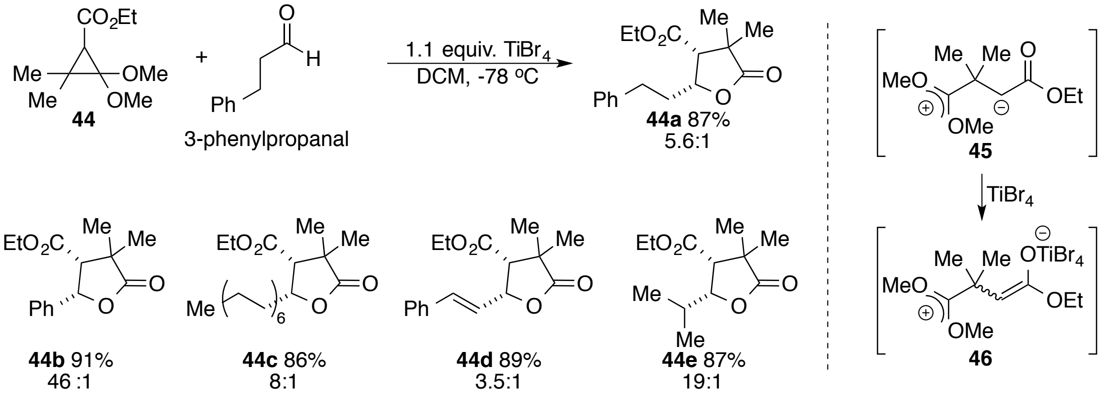

TiBr$_4$ was also found as a successful Lewis acid for the transformation of activated cyclopropanes and unsymmetrical ketones to γ-butyrolactones. One distinction of this transformation was the formation of acyclic intermediate **47** as the major adduct (Figure 3-15). The authors found that subjecting the crude material to catalytic amounts of *p*-toluenesulfonic acid at elevated temperatures produced the desired adduct, rendering the two step sequence optimal for the transformation. Methyl ketones such as methyl isobutyl ketone and methyl isopropyl ketone were competent substrates for the formation of γ-butyrolactones with a quarternary center at the 4-position, providing **44g** and **44h** in 93% and 82% yield, respectively. Excellent diastereoselectivity was observed for methyl isopropyl ketone, while modest diastereoselectivities were reported for other substrates. Methyl vinyl ketone, a reactive substrate prone to Michael addition, was also found as a viable substrate giving γ−lactone **44i** in a 70% yield.

**Figure 3-15: γ-Lactones From Unsymmetrical Ketones and Activated Cyclopropanes**

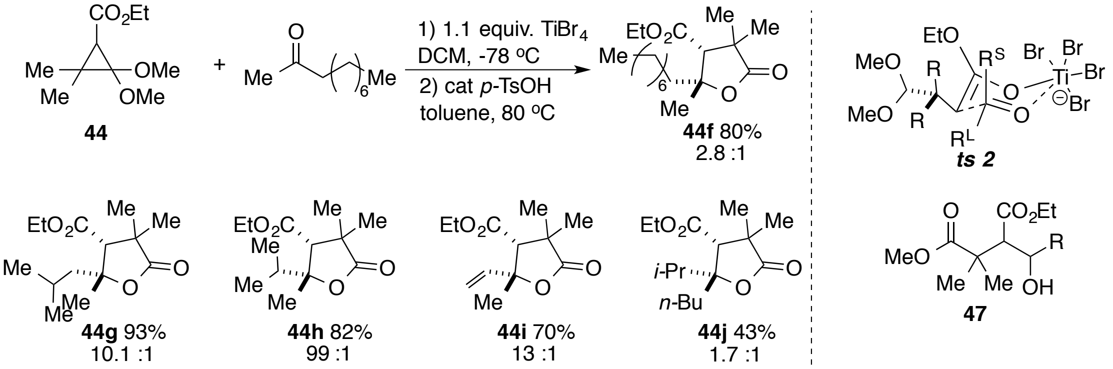

One requirement to achieve modest diastereoselectivies was to employ a ketone with distinguishable “small” and “large” substituents. This limitation was observed when *n*-butyl isopropyl ketone produced desired cycloadduct **44j** in a modest yield and with minor diastereoselectivity. Work was extended to encompass *cis* 2,3-disubstituted γ-butyrolactones arising from a modified cyclopropane and symmetrical ketones (Figure 3-16).[30] This was achieved by subjecting activated cyclopropanes **48a** or **48b** to standard conditions in the presence of TiCl$_4$. Surprisingly, the order of addition and solvent polarity were found to have a profound effect on the diastereoselectivity of the transformation. For this reason, two sets of standard conditions (Method A and B) are presented. Method A produced lactones with higher diastereoselectivity and was achieved when the reaction solution was added to a mixture of the cyclopropane and $TiCl_4$, and carried out at -45 $^{o}$C in acetonitrile. Method B proved to be higher yielding but with a marked decrease in diastereoselectivity. This required the addition of $TiCl_4$ to a mixture of the cyclopropane and ketone, and carrying out the transformation at -78 $^{o}$C in dichloromethane. The difference in methods was exemplified by considering γ-butyrolactone **44k** arising from cyclopropane **48a** and 4-heptanone. A diastereoselective ratio of 16:1 favoring the *cis* isomer was observed when the reaction was carried out with method A, yet a higher yield is observed when method B is employed (90%). Similar results were obtained when cyclohexanone was reacted as the symmetrical ketone for the formation of lactone **44l**. This solvent dependence on the diastereoselectivites was attributed to the solvation of the cationic substituent. If the transformation occurs in a polar solvent, the Newman projection of the titanium enolate depicted in Figure 3-16 was favorable, as separation of charges results in minimizing electronic repulsion. However, when the transformation occurred in a nonpolar solvent such as dichloromethane, the difference in energy barriers between conformations was minimal, resulting in lower diastereoselectivity.

**Figure 3-16: γ-Lactones From Symmetrical Ketones and Activated Cyclopropanes**

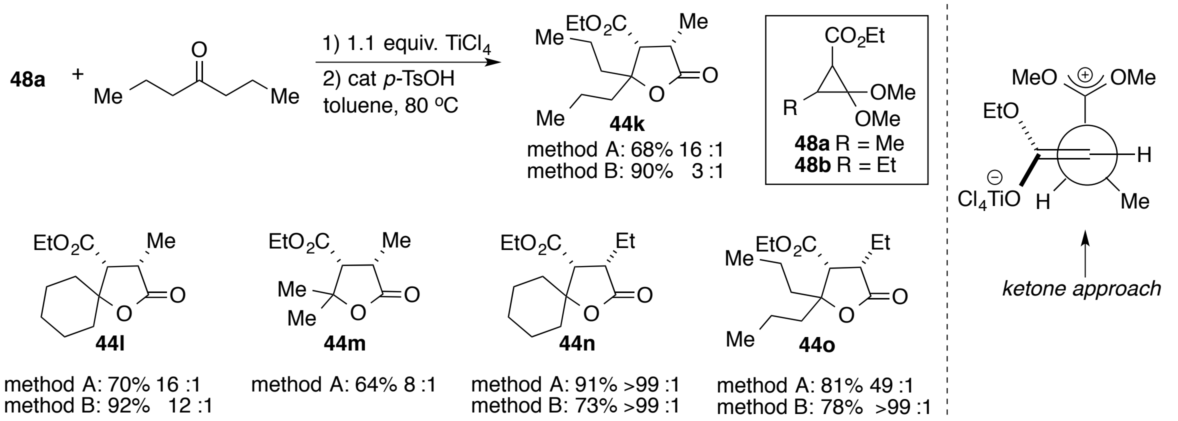
48a
+
O
Me
Me
1) 1.1 equiv. TiCl4
2) cat p-TsOH
toluene, 80 °C
EtO2C
Me
Me
O
O
Me
44k
method A: 68% 16 :1
method B: 90% 3 :1
CO2Et
R
OMe
OMe
48a R = Me
48b R = Et
MeO
OMe
EtO
Cl4TiO
H
H
Me
ketone approach
EtO2C
Me
O
O
44l
method A: 70% 16 :1
method B: 92% 12 :1
EtO2C
Me
Me
Me
O
O
44m
method A: 64% 8 :1
EtO2C
Et
O
O
44n
method A: 91% >99 :1
method B: 73% >99 :1
Me
EtO2C
Et
O
O
Me
44o
method A: 81% 49 :1
method B: 78% >99 :1

To better understand the reactivity and diastereoselectivity, variations of the cyclopropane were investigated. The ethyl cyclopropane derivative **48b** had superior reactivity than the methyl cyclopropane **48a** when subjected to similar reaction conditions; this was clear when considering the results for **44l** and **44n**. Excellent diastereoselectivites were observed with both methods for **44n**, where method A delivered the lactone in a 91% yield while method B resulted in a 73% yield. This pattern was also observed when lactones **44k** and **44o** were compared; higher overall diastereoselectivity was observed when cyclopropane **48b** was employed. Increased yields for transformations with cyclopropane **48b** were explained by increased steric bulk of ethyl vs methyl groups, which increased the likelihood of conjugate addition occurring via the depicted model in Figure 3-16.

This work culminated with a last report by the same authors for the diastereoselective synthesis of 2,3,4-trisubstituted γ-butyrolactones occurring from 2,2-dialkoxycyclopropanecarboxylicesters and carbonyl compounds.[31] When activated cyclopropanes were treated with aldehydes under previously developed conditions, a mixture of 4 diastereomers was obtained. Following a Lewis acid screening, the authors discovered zirconium tetrachloride ($ZrCl_4$) exhibited highest selectivity for the *cis-trans* isomer. When the same cyclopropylester **48a** was subjected to newly developed conditions with *n*-hexylaldehyde, the desired lactone **44p** was observed in an 89% yield with major diastereomer possessing a *cis-trans* geometry (Figure 3-17). When **48b** was employed with *n*-hexanal, the desired adduct **44q** was observed in a 90% yield with the same major diastereomer. Surprisingly, minimal improvement in diastereoselectivity was observed when *t*-butylaldehyde and benzaldehyde were chosen as substrates.

**Figure 3-17: 2,3,4-Trisubstituted γ-Lactones From Aldehydes and Activated Cyclopropanes**

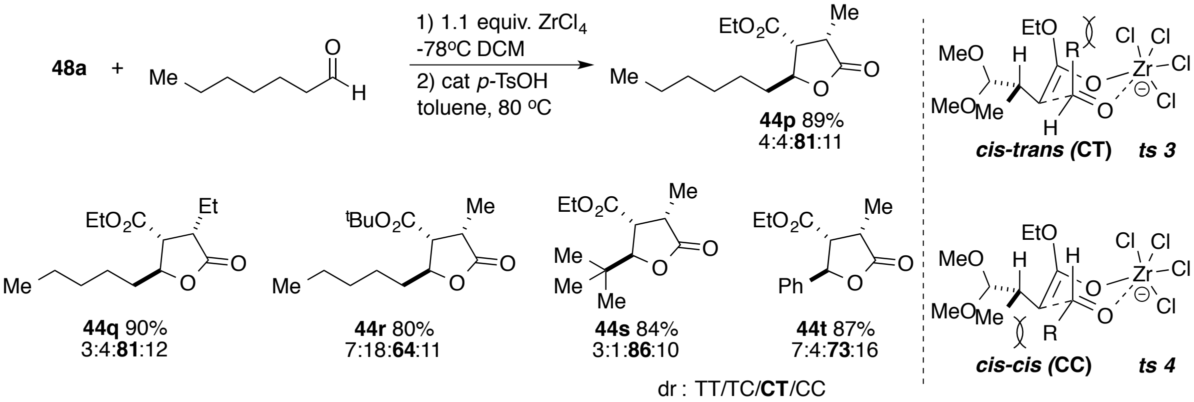

The stereochemistry was justified by first considering the *cis* selectivity at C2 and C3. The geometry of the chiral center next to the enolate dictates the stereochemistry at C2 and C3, where the hydrogen is preferred axial. The orientation of the methyl group pseudo equatorial is ideal in order to minimize steric clash between itself and the ethyl enolate. Next, the orientation of the aldehyde was considered to explain the trans selectivity at the 3,4 position. By studying **ts 3** in Figure 3-17, the *cis-trans* selectivity required the aldehyde to position the R group axial, which resulted in steric repulsion with the ethyl enolate. Though seemingly disfavored, this orientation possesses less steric repulsion compared to the counterpart **ts 4.** This transition state was attainable with $ZrCl_4$ as the Zr-O bond length is longer than the Ti-O bond length, which was previously described. The utility of this method was showcased in the synthesis of the paraconic acid (-) Dihydropertusaric acid, which possesses *cis-trans* stereochemistry around the γ-butyrolactone core (Figure 3-18). Synthesis of the paraconic acid was accomplished by subjecting 2,2-dialkoxycyclopropanecarboxylicester **48c** and the thioacetate protected aldehyde to standard cyclization conditions. The desired diastereomer was isolated in a 65% yield, with small amounts of the undesired isomers formed. Following optical resolution, (-) **49** was deprotected with treatment of NBS and subjected to acid hydrolysis, furnishing the desired adduct in a 79% yield. The completion of this synthesis revealed that initial characterization of the natural product was incorrect, where dihydropertusaric acid was originally proposed to exhibit *trans-cis* stereochemistry. The subtle characterization difference was discerned by comparing the coupling constants of the proton appended to C4 on the isolated natural product to the *trans-cis* and *cis-trans* lactones formed in Figure 3-17. This simple mis-assignment highlights the difficulty in correctly identifying the relative stereochemistry in 5 membered lactones. Though impressive methods have been developed via the aid of Lewis acids, these examples show the necessity of employing $TiCl_4$, $TiBr_4$, and $ZrCl_4$ in stoichiometric amounts.

**Figure 3-18: Synthesis of (-) Dihydropertusaric Acid**

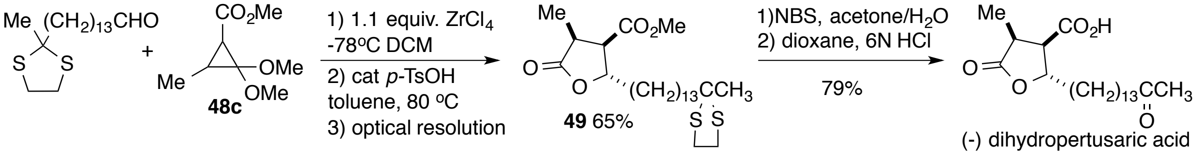

### 3.3.3 Synthesis of α-Methylene-γ-Butyrolactones

The reactivity of naturally derived and chemical analogues of α-methylene γ-butyrolactones has broad bioactivity and unique application.[32] For this reason, the synthesis of these biologically relevant natural products and derivatives has attracted significant attention. Though α-methylene lactones possessing minimal substitution have been found to be biologically relevant as well,[33] for the purpose of this thesis, only seminal work and methods for the synthesis α-methylene butyrolactones with 3,4-disubstitution will be discussed.

In 1970, Dreiding and Schmidt independently developed a method for the synthesis of α-methylene-γ-butyrolactones. This Reformatsky-type reaction accessed the cycloadduct by subjecting α-(bromomethyl) acrylic ester **50** and an aldehyde or ketone to zinc$^0$.[34] In one step, the cycloadduct was obtained in modest to good yields. Figure 3-19 includes the results published by Schmidt, as no substrate scope was included in Dreiding's initial report. Excellent yields were obtained for the cyclization of α-(bromomethyl) acrylic ester **50** and phenyl substituted aldehydes and ketones. Unfortunately, no direct trend was observed between aldehyde and ketone reactivity, as both benzaldehyde and acetophenone provided the butyrolactones **50d** and **50e** in quantitative yields. Though this initial report did not allow for the synthesis of γ-butyrolactones with substitution at the 3-

position, this method has been further extended to affect the enantioselective synthesis of 3,4-disubstituted α-methylene γ-butyrolactones.[35]

**Figure 3-19: Dreiding-Schmidt Reaction Of α-(Bromomethyl)acrylic Esters With Carbonyls**

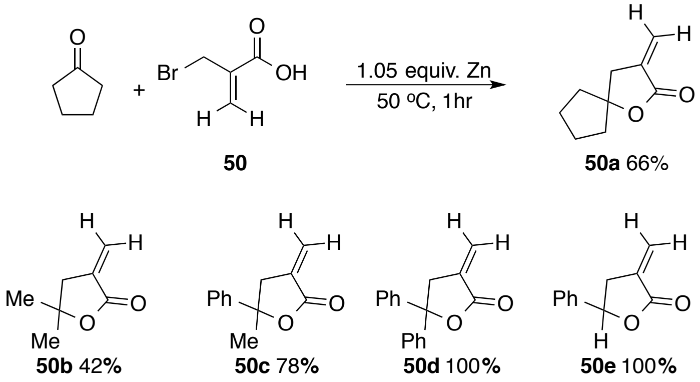

Another convergent method for the synthesis of γ-butyrolactones occurs through the palladium catalyzed allylation of 2-(hydroxymethyl)acrylates to aldehydes. Prior to this report, the Dreiding-Schmidt method using 2-(bromomethyl)acrylates was considered a good candidate for the metal-mediated allylation of aldehydes. Unfortunately, a challenging synthesis and instability of this acrylate is a significant hindrance to this approach. Masuyama and Kurusu believed 2-alkoxycarbonyl-allylating reagents offered similar reactivity with the advantage of stability and ease in synthesis, making them superior to 2-(bromomethyl)acrylates.[36] The method developed by these authors required equimolar amounts of acrylate to aldehyde, stoichiometric amounts of $SnCl_2$, and was carried out in 1,3-dimethylimidazolidinone (DMI) and water at 80 °C. The authors obtained the *syn* adduct as the major isomer with excellent diastereocontrol, and attribute this to an acyclic transition state, depicted in Figure 3-20. Formation of the π-allyl palladium complex of **52a** was proposed to be susceptible to alkene isomerization and reaction with $SnCl_2$, providing intermediate **52b**. Due to chelation between the ester carbonyl and the tin moiety, addition was proposed to occur via the acyclic transition state depicted in the Newman projection. This provided the addition *syn* adduct **52c**, which cyclized to the *syn* cycloadduct **52d**. Though excellent diastereoselectivity was observed, low yields ranging from 18% - 40% were obtained. Additionally, the necessity of stoichiometric tin is a drawback to this method due to toxicity.

**Figure 3-20: Synthesis Of α-Methylene γ-Butyrolactones From 2-(Hydroxymethyl)acrylates**

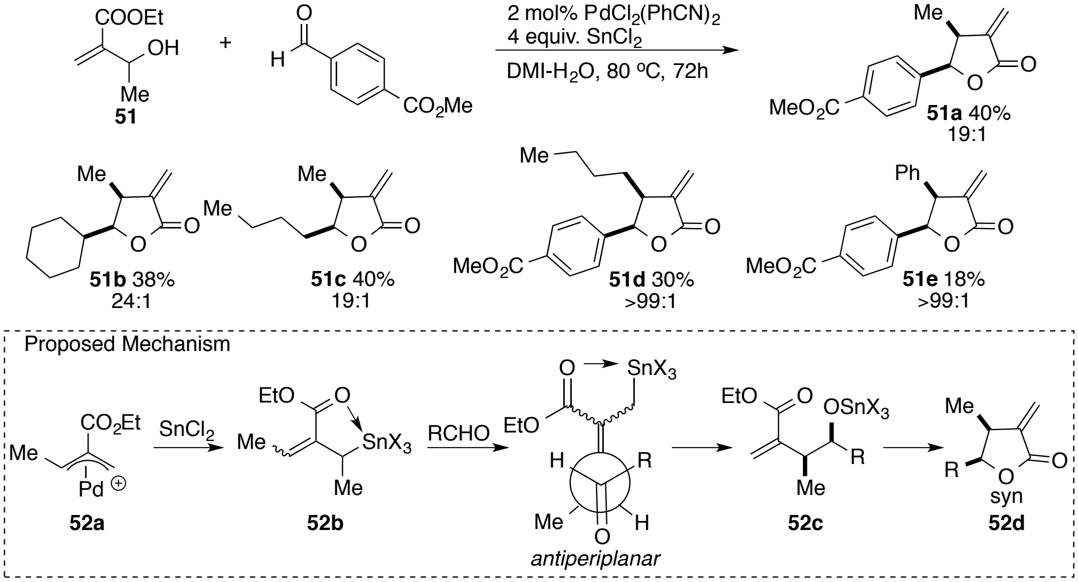
COOEt
OH
Me
51
+
H
O
CO2Me
2 mol% PdCl2(PhCN)2
4 equiv. SnCl2
DMI-H2O, 80 °C, 72h
Me
O
O
MeO2C
51a 40%
19:1
Me
51b 38%
24:1
Me
Me
51c 40%
19:1
Me
MeO2C
51d 30%
>99:1
Ph
MeO2C
51e 18%
>99:1
Proposed Mechanism
CO2Et
Me
Pd ⊕
52a
SnCl2
EtO
O
Me
SnX3
Me
52b
RCHO
O → SnX3
EtO
H
R
Me
H
O
antiperiplanar
EtO
O
OSnX3
R
Me
52c
Me
R
O
O
syn
52d

There are numerous examples of butyrolactone syntheses via palladium catalysis; however, other substrate limitations are still present. For instance, Gargnier and coworkers forged dimethyl- and phenyl-alkylidine γ-butyrolactones, where lactones with substitution on the 4-position were obtained. However, this work could not be extended to α-methylene γ-butyrolactones, or lactones with 3,4 disubstitution.[37] Few examples exist for the synthesis of 3,4 disubstituted α-methylene-butyrolactones, and organocatalytic methods are scarce. Creating a synthetic method for this class of small molecules via organic catalysis is appealing as these catalysts typically are more affordable to synthesize, and are air and bench top stable. The Hall group created one of the earliest organocatalytic methods that commenced the transition between metal-catalyzed methods to organic catalysis; this was accomplished by developing the transformation for α-methylene-γ-butyrolactones with quaternary centers arising from tetrasubstituted allylboronates and aldehydes.[38] This work was inspired by research accomplished by Hoffmann and Schlapbach that demonstrated allylboronates provide stereodefined quaternary carbon centers.[39] Initial research focused on the addition of activated allylboronates to aldehydes with the exclusion of Lewis acids. Though the transformation proved successful and acceptable yields were obtained, elevated temperatures and reaction times of up to two weeks were required. The authors then considered the possibility of rate acceleration with the inclusion of Sc(OTf)$_3$ as a Lewis acid. The addition of 10 mol% of Sc(OTf)$_3$ increased the rate of the reaction by 35 times, and allowed the reaction to proceed at room temperature (Figure 3-21). When allyl boronate **53** was reacted with one equivalent of an aromatic aldehyde, the desired product was generated in modest yields, but with greater than 20:1 *syn* selectivity. Aliphatic aldehydes depicted in the second row of Figure 3-21 were viable substrates; however, 1.5 equivalents of the aldehydes were required to obtain modest yields, albeit with excellent *syn* diastereoselectivity. The authors presume the origin of selectivity occurs from the cyclic transition state ***ts*** **5**, where coordination of the metal with the ester carbonyl and axial oxygen appended to boron orients the substrate. The authors propose that the aldehyde approaches with the hydrogen positioned axial to minimize steric repulsion.

**Figure 3-21: Synthesis Of $\alpha$-Methylene-$\gamma$-Butyrolactones From Allylboronates**

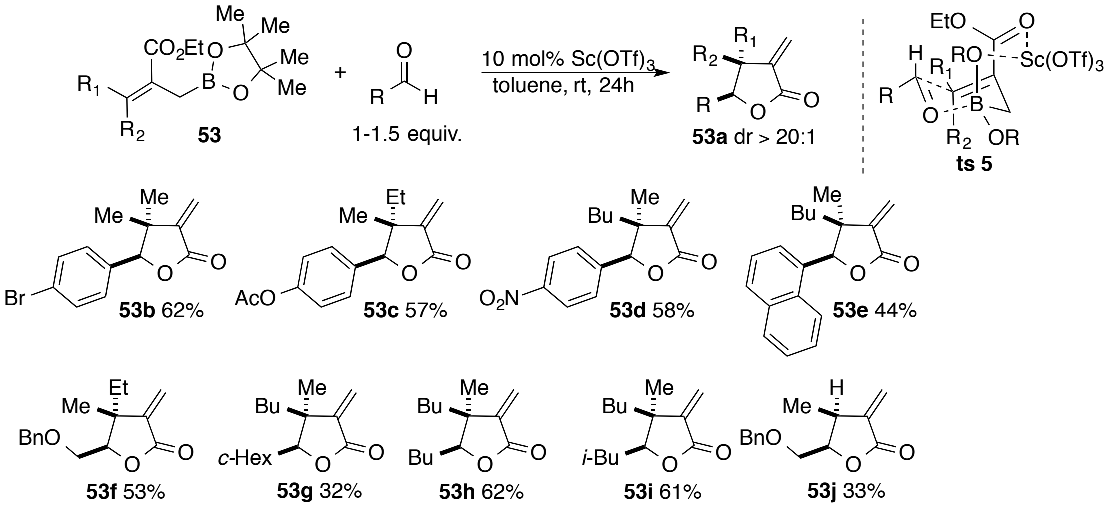

Even with modest yields, the simplicity of this transformation is appealing. The main limitation is due to the challenging synthesis of allyl boronate **53** and derivatives that exhibit high *E/Z* selectivity. The authors have recognized this drawback and have focused their effort on refining the method. Hall recently reported a method to arrive at allylboronates with high stereocontrol via a two-step sequence involving cuprate addition to alkynyl esters, followed by the addition of an iodomethane boronate.[40]

### 3.4 Synthesis of γ-Butyrolactones via Polar Radical Crossover Cycloaddition

Traditionally, electron-rich alkenes are considered nucleophiles as they may undergo nucleophilic addition when in the presence of an appropriate electrophile (Figure 3-22). Conversely, α,β-unsaturated acids are active Michael acceptors, as they are electrophilic at the β-position. A direct coupling of these two reagents could provide rapid access to the desired motif. However, in order to provide the butyrolactone, we required polarity reversal of both the alkene and the unsaturated acid, and also desired cycloaddition with very specific regioselectivity. Organophotoredox catalysis is precedented to carry out reactions via polarity reversal, and we saw this as an opportunity to create a direct method with this novel approach. We saw electron-rich alkenes reacting as electrophiles prone to nucleophilic attack by the acidic moiety of the α,β-unsaturated acid, resulting in lactone formation.

**Figure 3-22: Comparison Between Standard Substrate Reactivity And Polarity Reversal Reactivity**

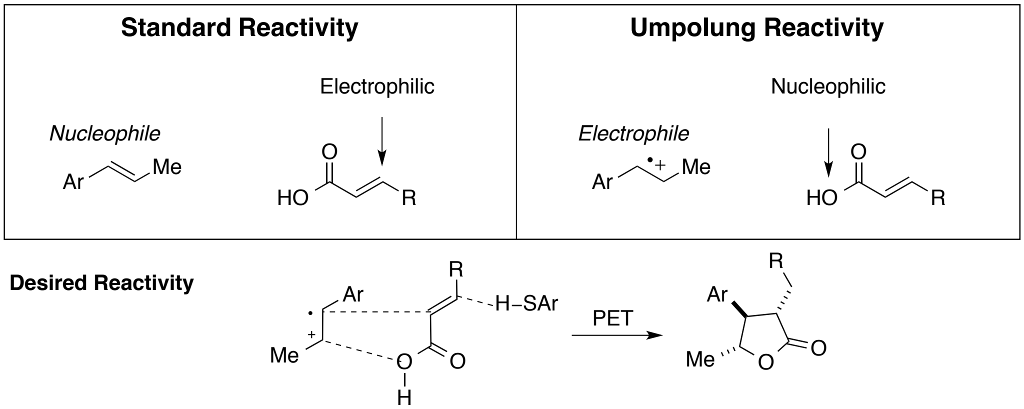

Seminal work for polarity reversal via organophotoredox catalysis by our group gave us confidence that this approach would be successful. In particular, Perkowski and Nicewicz recently published the anti-Markovnikov addition of carboxylic acids to alkenes, demonstrating that electron-rich alkenes are easily rendered electrophilic by single electron oxidation (Figure 3-23).[41] We reported that 1) catalytic base could increase the nucleophilicity of the acid, improving both yield and rate, and 2) benzenesulfinic acid and thiophenol used in catalytic quantities were viable hydrogen atom sources. More importantly, this report also showed that acetic acid could act as a nucleophile in the presence of oxidizable alkenes. This transformation was accomplished by subjecting the alkene to the single electron oxidant 9-mesityl-10-methylacridinium tetrafluoroborate (NMA), which affected single electron oxidation of the alkene. The regioselectivity obtained from hydroacetoxylation is ideal, as we required acid addition to occur at the β-carbon in order to afford the desired γ–butyrolactones.

**Figure 3-23: Catalytic anti-Markovnikov Alkene Hydroacetoxylation**

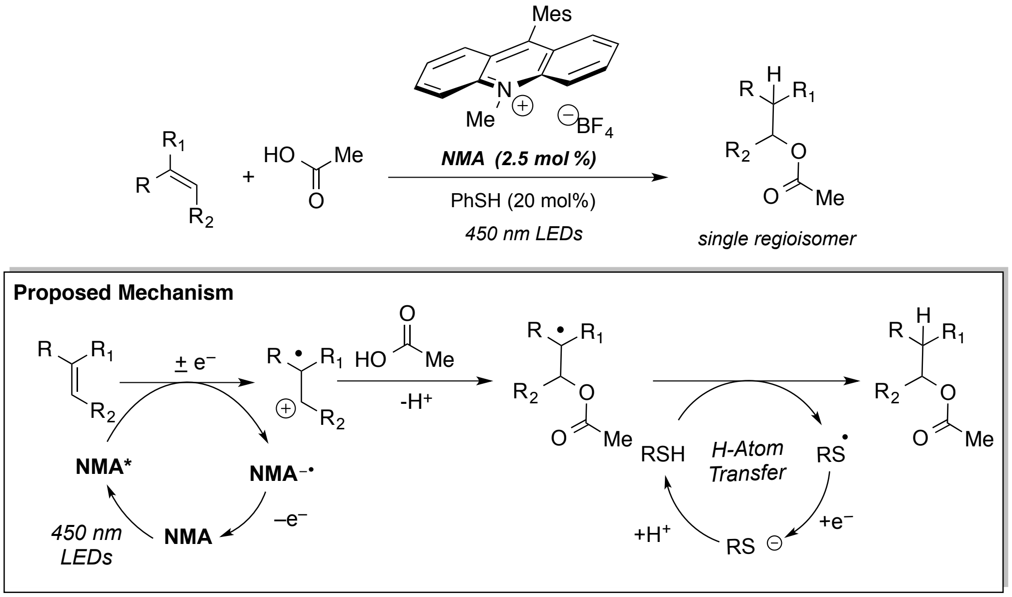

Another important precedent from our group was published by Grandjean and Nicewicz in 2013, where allyl alcohols and electron-rich alkenes were subjected to photoredox catalysis to afford highly substituted tetrahydrofuran products. [42] To successfully affect the transformation, the polar-radical crossover cycloaddition (PRCC) sequence was applied. This two-step process takes advantage of both reaction vectors common to radical cation species; an initial polar reaction occurs at the cationic carbon and is followed by a 5-*exo* radical cyclization step. As depicted in Figure 3-24, the proposed mechanism for the reaction with β-methylstyrene and allyl alcohol initiates with the single electron oxidation of an alkene resulting in the radical cationic species. Allyl alcohol then undergoes nucleophilic attack with the radical cationic substrate in the "polar step". Following this, a radical cyclization ensues in a 5-*exo* cyclization, and terminates with hydrogen atom transfer.

It is important to note that the cycloadduct may only be obtained if nucleophilic addition by allyl alcohol precedes hydrogen transfer. The challenge in affecting the transformation relies on the radical cyclization: in order to obtain tetrahydrofurans, the cyclized product possessing a primary radical must preferentially exist in solution over the uncyclized radical intermediate. Though the radical cyclization may be reversible, efforts were focused on developing a method to drive the equilibrium to the cyclized product. The authors achieved this by including a redox-active hydrogen atom source with specific characteristics. In order to serve as an effective hydrogen atom source, the reagent must 1) possess an X-H bond with a bond dissociation energy (BDE) between 70-80 kcal/mol, 2) be susceptible to single electron reduction in order to regenerate the photooxidant and 3) possess a pKa high enough to regenerate the hydrogen atom source. Additionally, a basic anion would also minimize the presence of acid in the reaction mixture, therefore regulating the pH of the solution, and affecting a redox neutral transformation. All of these characteristics affect the rate of reactivity for the hydrogen atom source, which must be matched perfectly to the rate of the reaction. Grandjean and Nicewicz found that phenylmalononitrile fit those requirements exquisitely when used in stoichiometric amounts; phenylmalononitrile possesses a bond dissociation energy of 77 Kcal/mol, a half wave reduction potential of +0.19 V, and a pKa of 4.2.

**Figure 3-24: Catalytic Polar Radical Crossover Cycloadditions of Alkenes and Alkenols**

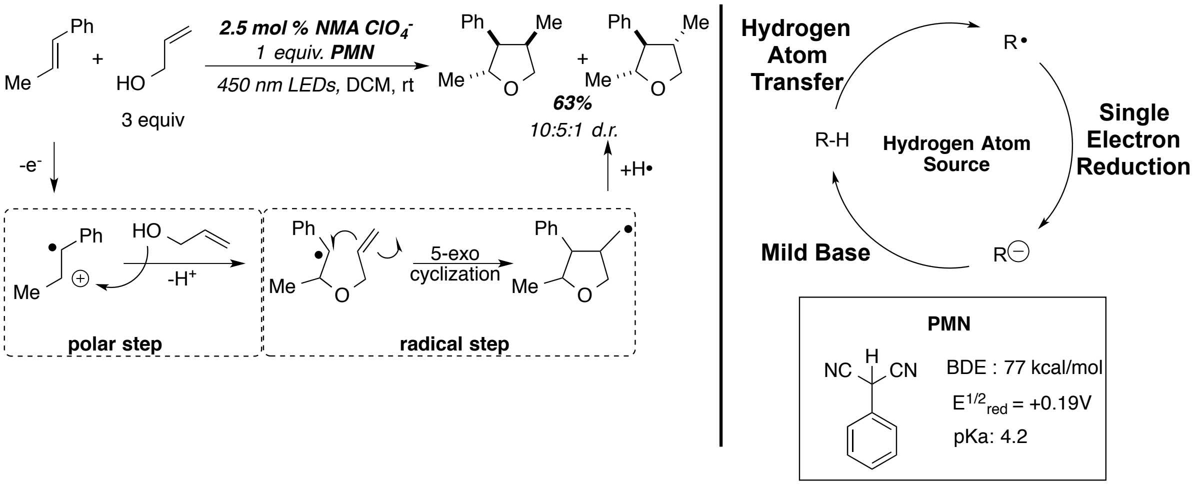
Ph
Me
+
HO
3 equiv
2.5 mol % NMA ClO4-
1 equiv. PMN
450 nm LEDs, DCM, rt
Ph
Me
Me
O
+
Ph
Me
Me
O
63%
10:5:1 d.r.
-e-
+H•
Ph
Me
HO
-H+
polar step
Ph
Me
O
5-exo
cyclization
Ph
Me
O
radical step
Hydrogen Atom Transfer
R•
Single Electron Reduction
R-H
Hydrogen Atom Source
Mild Base
R⊖
PMN
NC
H
CN
BDE : 77 kcal/mol
E1/2red = +0.19V
pKa: 4.2

Standard conditions included 3 equivalents of allyl alcohol, stoichiometric amounts of the hydrogen atom source, and catalytic amounts of the photooxidant in DCM in the presence of 450 nm LED lamps. The authors found this transformation to be general for the reaction of allyl alcohol with various substituted styrene derivatives including indene, 1-phenylcyclohexene, 3-phenylprop-2-enol, and 2-methyl-2-butene (Figure 3-25). All yields reported for cycloadducts were of the amount isolated except for **56d**, as a yield for the highly volatile compound could only be accurately measured by GC-MS. Yields ranged between 40-95%, with modest diastereoselectivity. Interestingly, the authors observed the major isomer to possess a *trans-cis* relationship. This was confirmed by NOE NMR experiments, which revealed a *cis* relationship between C3 and C4. The relationship between C1 and C2 was consistently *trans*, which is attributed to the isomerization to the *trans* when the radical cationic species is produced.

**Figure 3-25: Partial Substrate Scope of Tetrahydrofuran Synthesis via PRCC**

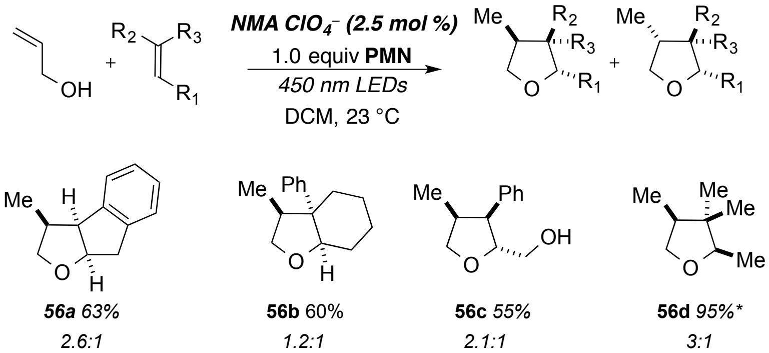

The relative stereochemistry was determined by comparison of the $^1$H NMR of tetrahydrofuran adducts to a report by Kelly and Lambert, where tetrahydrofuran synthesis also occurs via a 5-*exo* cyclization.[43] Preference for *trans-cis* stereochemistry is explained by considering the Beckwith model, where the envelope-type conformation of **pseudo eq** is proposed as the lowest energy conformer. Subsequently, 5-*exo* cyclization proceeds with the alkene in the equatorial position and results in formation of the *trans-cis* diasteromer (Figure 3-26).

**Figure 3-26: Proposed Beckwith Transition State Resulting in *cis-trans* Selectivity**

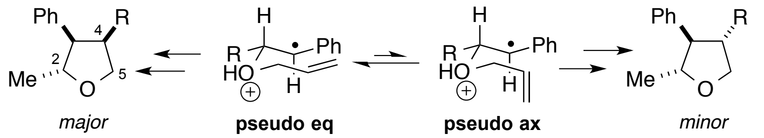

We envisioned extending the methodology developed by both Perkowski and Grandjean to develop a concise method to synthesize γ-butyrolactones, where further derivatization to α-methylene-γ-butyrolactones was possible. Key precedent by Clive and coworkers described the synthesis of γ-butyrolactones via 5-*exo* radical cyclizations.[44] Clive creatively approached the cyclization to arise from the homolytic cleavage of a carbon-selenium (C-Se) bond. This C-Se bond was strategically positioned in close proximity to an α,β–unsaturated ester, where a 5-*exo*-cyclization could occur. It is well precedented that C-Se bond cleavage can result in radical formation when treated with Ph$_3$SnH and azobisisobutyronitrile (AIBN).

The activated selenide **54b** was synthesized by reacting phenyl selenium chloride (PhSeCl) with the alkene of choice (Figure 3-27). Silver-mediated substitution of the alkyl chloride resulted in the formation of ester **54b**. With the aid of the radical initiator and in the presence of $Ph_3SnH$ as the hydrogen atom donor, the secondary radical **54c** was generated, which was proposed to quickly cyclize to form the bicyclic radical intermediate **54d**. Hydrogen atom transfer from $Ph_3SnH$ terminated the transformation, delivering lactone **55**.

**Figure 3-27: Synthesis And Proposed Mechanism For Ring Closure of β-Phenylseleno-Crotonates**

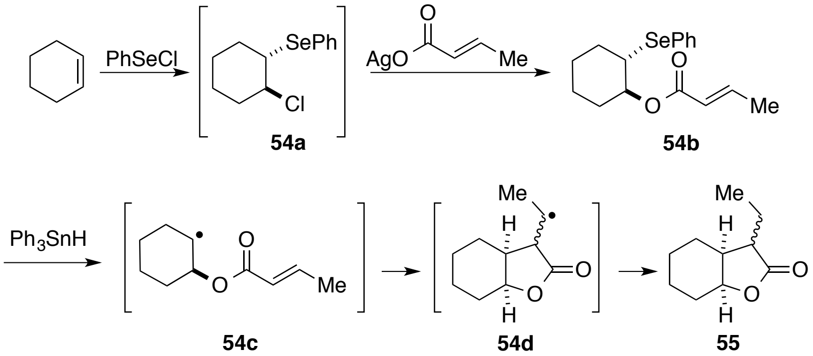

Optimal conditions included slow addition of stoichiometric and catalytic amounts of $Ph_3SnH$ and AIBN, respectively, to the refluxing mixture. While the ring junction possessed *cis* stereochemistry, the major adduct exhibited *trans* substitution between C2 and C3. When crotonate was employed as the α,β-unsaturated ester, modest yields were obtained for lactone **55a** (Figure 3-28). However, the unsubstituted acrylate derivative offered **55b** in poor yield. Similar yields were obtained for formation of the [6.5.0] bicycle **55a** verses [5.5.0] **55c**. Lastly, the authors tested the radical cyclization on an acyclic substrate, where conformation of the radical intermediate was no longer constrained. *cis* 2-Methylbutene was subjected to similar conditions, affording the active substrate **55d** (Figure 3-28). Under standard conditions, the authors noted formation of all four diastereomers, where the major isomer **55g** exhibited all *trans* stereochemistry. The second isomer formed in large quantities was the all *cis* lactone **55e**. To verify that the radical intermediate does not retain any stereochemical information upon formation, the authors synthesized **epi-55d**. Not surprisingly, the same all-*trans* isomer **55g** was formed as the major adduct, with *cis* **55e** as the minor diastereomer.

**Figure 3-28: Scope For Ring Closure of β-Phenylseleno-Crotonates And Acyrolates**

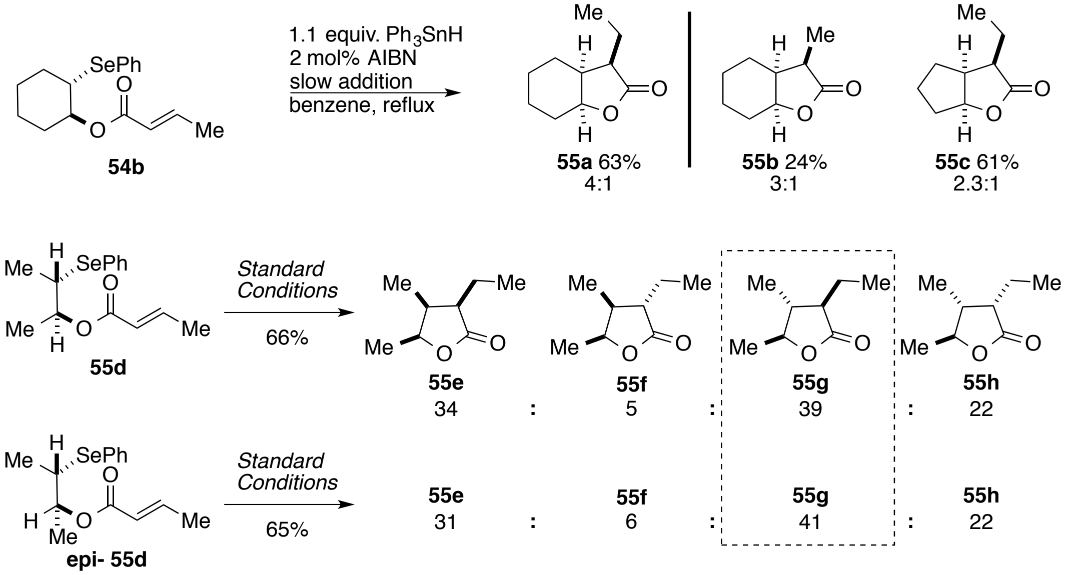
SePh
O
O
Me
54b
1.1 equiv. Ph3SnH
2 mol% AIBN
slow addition
benzene, reflux
Me
H
O
O
H
55a 63%
4:1
H
Me
O
O
H
55b 24%
3:1
Me
H
O
O
H
55c 61%
2.3:1
Me
H
SePh
O
Me
O
H
Me
55d
Standard Conditions
66%
Me
Me
Me
O
O
55e
34
:
55f
5
:
55g
39
:
55h
22
Me
H
SePh
O
H
O
Me
Me
epi- 55d
Standard Conditions
65%
55e
31
:
55f
6
:
55g
41
:
55h
22

Though typical radical addition to an α,β–unsaturated ester is proposed to occur at the β–carbon, the authors reason the 5-*exo* cycloadduct was observed due to a kinetic and steric preference. We believed this seminal report provided excellent precedent for the feasibility of developing a direct method for the synthesis of γ–butyrolactones via radical cyclization. Additionally, as the reported yields are modest and all four diastereomers are formed, we envisioned a method that could produce a single diastereomer with higher levels of selectivity.

During the course of this project, Wei and Liu reported an interesting method for the synthesis of γ-butyrolactones via photoredox catalysis.[45] The authors presented an iridium (III) catalyzed method where α-bromoesters react with electron-rich alkenes to afford butyrolactone adducts. Ideal reaction conditions were found to be a 4:1 solution of acetonitrile to water, stoichiometric amounts of $LiBF_4$ for carbonyl activation, and catalytic amounts of *fac*-$Ir(PPy)_3$ in the presence of 450 nm light. After the screening of various α-bromoesters, the highest yields were observed when α-bromoester **57** was employed. This transformation was amenable to substituted and terminal styrenes as depicted in Figure 3-29. Though excellent yields were obtained, marginal diastereoselectivity was observed. In the case of **57f**, the d.r. was not reported.

**Figure 3-29: Iridium Catalyzed Photoredox Catalysis**

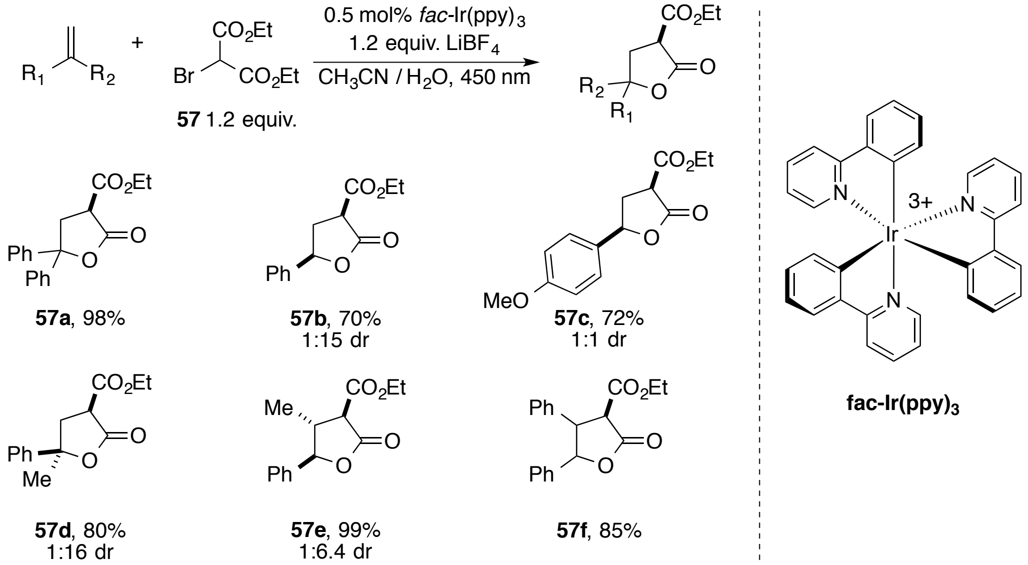

R1
R2
+
CO2Et
Br
CO2Et
57 1.2 equiv.
0.5 mol% fac-Ir(ppy)3
1.2 equiv. LiBF4
CH3CN / H2O, 450 nm
CO2Et
R2
R1
O
O
CO2Et
Ph
Ph
57a, 98%
CO2Et
Ph
57b, 70%
1:15 dr
CO2Et
MeO
57c, 72%
1:1 dr
CO2Et
Ph
Me
57d, 80%
1:16 dr
Me
CO2Et
Ph
57e, 99%
1:6.4 dr
Ph
CO2Et
Ph
57f, 85%
N
3+
N
Ir
N
fac-Ir(ppy)3

The mechanism of this novel transformation is proposed to begin with single electron transfer between α-bromoester **57** and the iridium complex, resulting in formation of a carbon centered radical and loss of bromine. This activated radical species undergoes addition with diphenylethylene, providing the trisubstituted radical intermediate **58b.** In order to regenerate the iridium complex, single electron oxidation of the substrate occurred with the oxidized complex, which provided carbocation intermediate **58c**. This intermediate is proposed to react with water to afford the hydrated species. Alcohol **58d** undergoes lactonization furnishing the neutral γ–butyrolactone. The authors confirmed the lactone oxygen arrived from water by caring out oxygen-18 ($^{18}$O) labeling studies. Additionally, it was verified that the α-bromoester was inert to disproportionation in the presence of 450 nm when the iridium catalyst was excluded, therefore supporting a photoredox mechanism.

**Figure 3-30: Proposed Mechanism for Iridium Catalyzed Photoredox Catalysis**

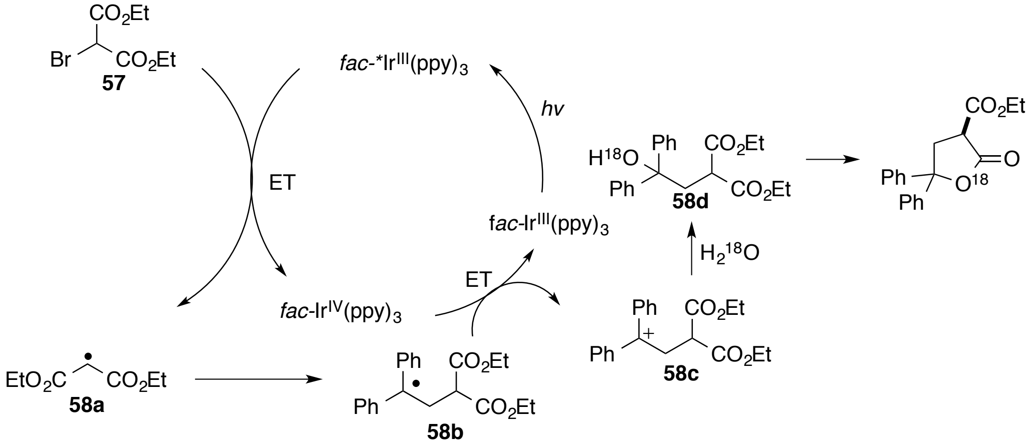

57
fac-*Ir^III(ppy)3
hv
ET
fac-Ir^III(ppy)3
fac-Ir^IV(ppy)3
ET
58a
58b
58c
58d
H2^18O
O^18

It is important to note the distinction between this method and our efforts: this transformation occurs with the aid of a single electron reductant iridium complex, where carbon-oxygen bond formation occurs at the more substituted carbon. On the other hand, we were interested in achieving the transformation with an organic single electron oxidant, where radical addition results in carbon-carbon bond formation at the most stable position. The products of our proposed transformation possess opposite regioselectivity, which is evident by comparing lactone **57e** to the model substrate in Figure 3-31. Though successful, it is difficult to envision using this iridium-catalyzed method for the synthesis of the paraconic acids, as the formed γ-butyrolactones do not map onto the natural products. For this reason, we believed a method complimentary to the one presented would have broad applicability.

**Figure 3-31: Comparison of Product Regioselectivity Between Iridium Catalyzed Method and Desired Method For Further Derivitization To Paraconic Acids**

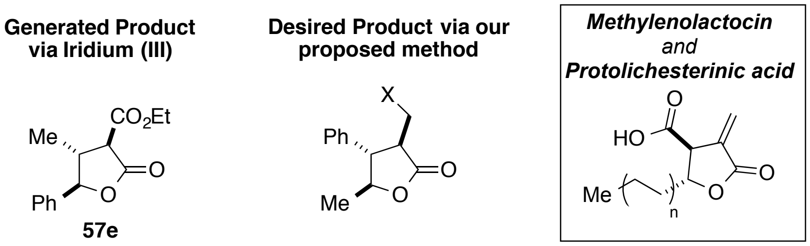

Generated Product via Iridium (III)
57e
Desired Product via our proposed method
Methylenolactocin and Protolichesterinic acid

## 3.5 Results for the Synthesis of Substituted γ-Butyrolactones

Similar to the tetrahydrofuran report, we believed success of this transformation was contingent upon the careful selection of an appropriate redox-active hydrogen atom source. To improve upon the previous report, we wished to use substoichiometric amounts of the hydrogen atom source resulting in a redox neutral and organocatalytic method. We began our efforts by investigating the reaction between crotonic acid and β-methylstyrene. By applying the conditions for tetrahydrofuran synthesis, we were pleased to see formation of the desired cycloadduct in 20% yield (Table 3-1). Unfortunately, two byproducts were formed during the course of this reaction; though phenylmalononitrile displays ideal properties to affect a cyclization, the enhanced electrophilic nature of the crotonic acid resulted in substantial Michael addition byproduct formation. Additionally, significant amounts of the uncyclized adduct was concurrently produced. We believed the ratio of product to uncyclized byproduct could be manipulated by modifying the hydrogen atom source. Modification of this variable is ideal as numerous hydrogen atom sources with varying bond dissociation energies and acidities are available. The screen of redox active hydrogen atom sources included 9-cyanofluorene **59a** and aromatic thiols **59b** and **59c**. When crotonic acid and β−methylstyrene were subjected to standard conditions in the presence of stoichiometric amounts of 9-cyanofluorene **59a**, a Michael addition byproduct was obtained. When thiophenol **59b** was chosen as the hydrogen atom source, the uncyclized byproduct dominated the reaction. After a wide optimization screen, only a trace amount of the desired cycloadduct was obtained with crotonic acid (entry 3). Though not ideal, formation of the uncyclized byproduct validates that single electron oxidation of β-methylstyrene and subsequent nucleophilic addition by crotonic acid was occurring. Therefore, we speculated that slow 5-*exo* cyclization could be due to radical destabilization and concurrent byproduct formation. While hydrogen atom abstraction is proposed to be a fast process, radical cyclization could be reversible; therefore, we believed the uncyclized byproduct was favored due to the benzylic radical preferentially existing in solution (Figure 3-33).

By adjusting the polarity of the unsaturated acid, we proposed that the equilibrium could be altered to lie in favor of the radical species post cyclization. We discovered that hydrogen atom sources requiring carbon-hydrogen bond cleavage were needed in stoichiometric amounts, but those resulting from heteroatom-hydrogen bond cleavage could be used substoichiometrically. Optimization with mono-*tert*-butyl fumarate accomplished by Mary Zeller showed formation of the desired adduct in 62% yield in the presence of 20 mol% of thiophenol. This confirmed that uncyclized byproducts could be minimized by matching a thiol hydrogen atom donor with an unsaturated acid bearing a radical stabilizing group. We found the requirement of base was dependent on the nucleophilicity of the α,β–unsaturated acid; therefore optimal conditions for the cyclization of β-methylstyrene and mono-tert-butyl fumarate include 10 mol% of 2,6-lutidine (entry 5).

**Table 3-1: Optimization of Reaction Conditions For Synthesis of γ-Butyrolactones**

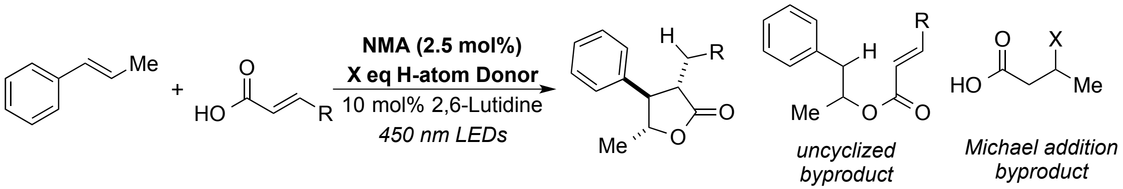
Me
+
HO
O
R
NMA (2.5 mol%)
X eq H-atom Donor
10 mol% 2,6-Lutidine
450 nm LEDs
H
R
O
Me
O
R
H
Me
O
O
uncyclized byproduct
O
X
HO
Me
Michael addition byproduct

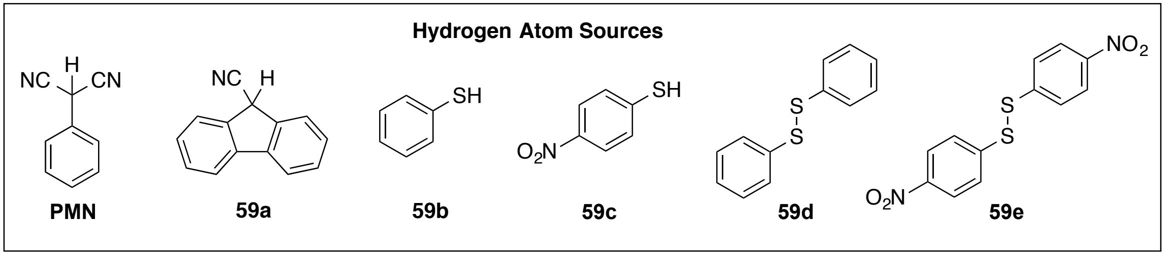
Hydrogen Atom Sources
NC
H
CN
PMN
NC H
59a
SH
59b
SH
O2N
59c
S
S
59d
NO2
S
S
O2N
59e

| Entry | R | Conditions | Conversion | % Yield [b] (% uncyclized) |
|---|---|---|---|---|
| 1 | Me | 1 eq **PMN**[a] | 96% | 20% (34%) |
| 2 | Me | 1 eq **59a**[a] | 88% | 18% (20%) |
| 3 | Me | 20 mol% **59b** | 63% | 2% (44%) |
| 4 | H | 20 mol% **59b** | 50% | 2%(43%) |
| 5 | $CO_2tBu$ | 20 mol% **59b** | 80% | 62% |
| 6 | $CO_2tBu$ | 20 mol% **59c** | 100% | 64% |
| 7 | $CO_2tBu$ | 10 mol% **59d** | 99% | 79% |
| 8 | $CO_2tBu$ | 10 mol% **59e** | 100% | 64% |
| 9 | $CO_2tBu$ | 10 mol% **59e**, no base | 100% | 64% |

Reactions carried out on a 0.3 mmol scale in $N_2$ sparged dichloromethane [0.15], at room temperature. Unless otherwise noted, 1.1:1 acid:alkene for 24 hours, [a] 4 days, 5:1 acid: alkene, [b] all yields by $^1H$ NMR against $TMS_2O$

The catalytic cycle for a thiol hydrogen atom source is proposed to initiate with hydrogen atom abstraction, resulting in production of a thiyl radical, which then undergoes single electron reduction. Following this, the thiyl anion acts a base where reprotonation results in reestablishment of the hydrogen atom source (*vide infra*). As thiyl radicals are prone to dimerize, we considered the possibility of *in situ* disulfide formation. This was verified by experimental work done by a fellow graduate student in the Nicewicz group: phenyl disulfide was isolated as a byproduct when thiophenol was used as a hydrogen atom source. As thiophenol may be formed from the homolytic bond cleavage, we considered disulfides as hydrogen atom surrogates. When 10 mol% of phenyl disulfide was chosen as the hydrogen atom surrogate, the desired γ-butyrolactone was formed in 79% yield (entry 7). To verify the reaction was occurring via photoinduced electron transfer, two control reactions were conducted: no product was observed when 1) the reaction was carried out in the dark, or when 2) the photooxidant was excluded.

**Table 3-2: Reaction Scope For γ-Butyrolactones From β-Methylstyrene and α,β–Unsaturated Acids**

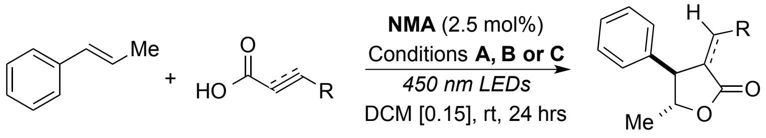

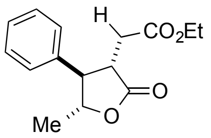
**3.1** 66% 2.2:1
Condition A

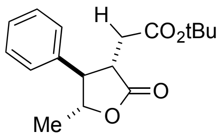
**3.2** 74% 2.3: 1
Condition A

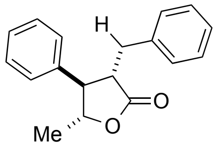
**3.3** 81% 4.7: 1
Condition B

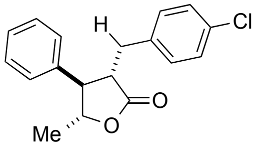
**3.4** 80% 5.2:1
Condition B

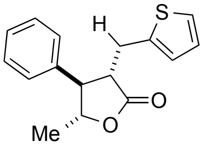
**3.5**[ab] 55% 2.7: 1
Condition B

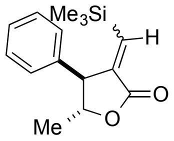
**3.6**[a] 85% 1.3: 1
Condition B

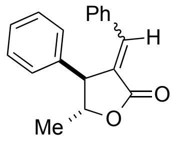
**3.7**[a] 41% 1.4:1
Condition C

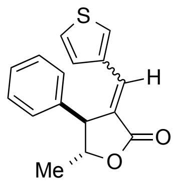
**3.8**[a] 44% 2.3: 1
Condition C

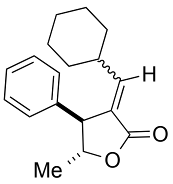
**3.9**[a] 83% 1: 1
Condition C

Reactions carried out in 0.15 M of sparged dichloromethane, average of two isolated yields on 100mg scale. **Condition A**: 1:1.1 alkene: acid, 10 mol% 2,6-Lutidine, 10 mol% $Ph_2S_2$, **Condition B**: 3:1 alkene: acid, 15 mol% $Ph_2S_2$ **Condition C:** 2-3:1 alkene: acid, 10 mol% 2,6-Lutidine, 15 mol% $Ph_2S_2$ carried out for 2-4 days. [a] trans: trans ratio, [b] reaction carried out for 48 h.

With standard conditions identified, we next considered the reaction scope with respect to α,β–unsaturated acids (Table 3-2). Reaction conditions were designed for three classes of substrates; Condition A was ideal for α,β-unsaturated acids which required base to increase nucleophilicity, and

Condition B worked well for nucleophilic α,β-unsaturated acids where base was not necessary. Condition C was designed for alkynyl acids, which were found to require catalytic amounts of base and longer reaction times. The reaction of β-methylstyrene with commercially available mono ethyl fumarate furnished the expected adduct **3.1** in a 66% yield, with a small 2.2:1 diastereomeric ratio. As observed with the tetrahydrofuran method, the selectivity between the phenyl and methyl groups was consistently *trans* due to radical cation isomerization and increased stability. The major isomer was observed to possess the all *trans* stereochemistry, which was also witnessed by Clive and coworkers.[41]

*Trans*-cinnamic acid was found to be a viable substrate, providing lactone **3.3** in 81% yield with 4.7:1 dr without the need for base. The electron-poor derivative of cinnamic acid also proved successful and furnished lactone **3.4** in comparable yield with slightly higher d.r. (5.2:1). The α,β-unsaturated heteroaromatic acid (Z)-3-(thiophen-2-yl)acrylic acid, was found to react significantly slower and required extended reaction times. Under standard conditions over the course of 48 hours, desired cycloadduct **3.5** was isolated in 55% yield. We then turned our attention to the use of propiolic acid with the hope of directly forging α-methylene-γ-butyrolactones. Unfortunately, only trace quantities of the α-methylene-γ-butyrolactone were obtained (data not shown). We speculated that the radical cyclization was again the problematic step in this process as we observed varying quantities of the uncyclized product. We then considered silyl-protected alkynyl acids in hopes of further derivatizing the lactone for the synthesis of α−methylene γ-butyrolactones. We were pleased to see that 3-(trimethylsilyl)propiolic acid was activated enough to produce lactone **3.6** as a mixture of *cis* and *trans* in an 85% yield under Condition B. Other alkynyl acids considered include 3-phenylpropiolic acid, 3-(thiophen-2-yl)propiolic acid, which afforded lactones **3.7** and **3.8** in 41% and 44% yields, respectively. Cyclization with 3-cyclohexylpropiolic acid produced lactone **3.9** in 83%, which demonstrates that aromaticity is not required to stabilize the $sp^2$ radical post cyclization.

**Table 3-3: Reaction Scope For γ-Butyrolactones From Oxidizable Alkenes and α,β–Unsaturated Acids**

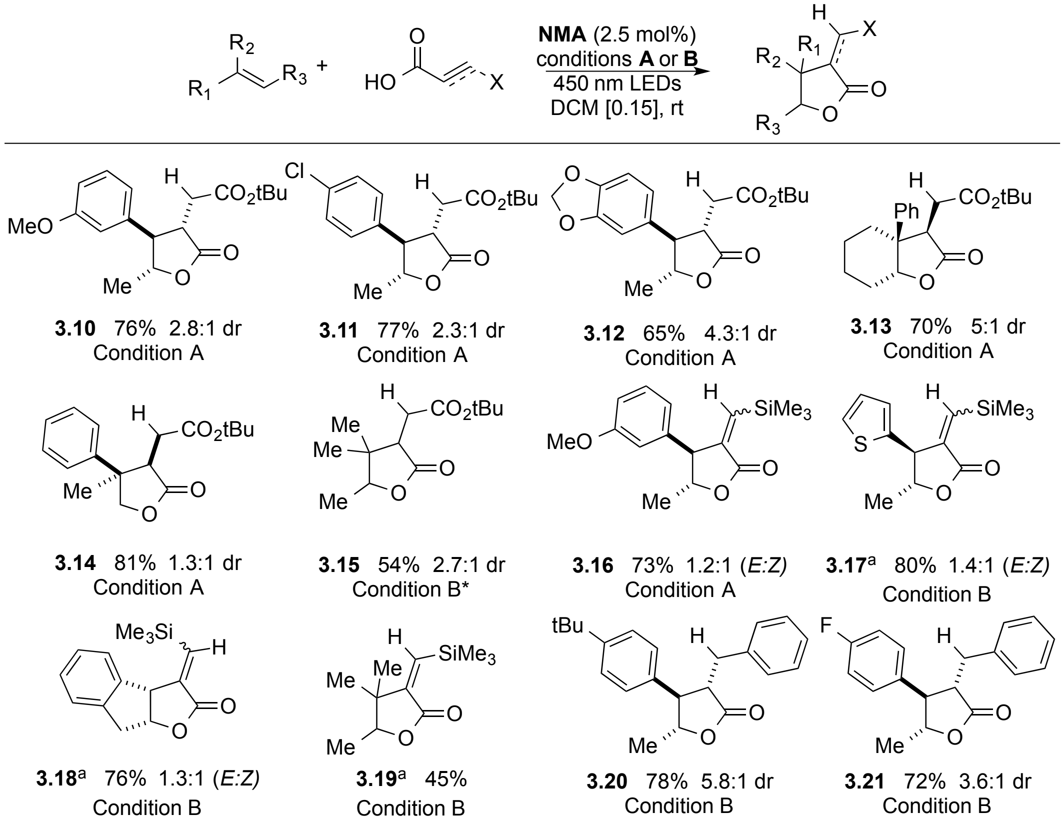

**3.10** 76% 2.8:1 dr
Condition A

**3.11** 77% 2.3:1 dr
Condition A

**3.12** 65% 4.3:1 dr
Condition A

**3.13** 70% 5:1 dr
Condition A

**3.14** 81% 1.3:1 dr
Condition A

**3.15** 54% 2.7:1 dr
Condition B*

**3.16** 73% 1.2:1 (*E:Z*)
Condition A

**3.17**[a] 80% 1.4:1 (*E:Z*)
Condition B

**3.18**[a] 76% 1.3:1 (*E:Z*)
Condition B

**3.19**[a] 45%
Condition B

**3.20** 78% 5.8:1 dr
Condition B

**3.21** 72% 3.6:1 dr
Condition B

Reactions carried out in 0.15 M of sparged dichloromethane, average of two isolated yields on 100mg scale, followed by dr ratio. **Condition A**: 1:1.1 alkene: acid, 10 mol% 2,6-Lutidine, 10 mol% $Ph_2S_2$, **Condition B***: 3:1 alkene:acid,10 mol% 2,6-Lutidine, 5 mol% *p*$NO_2$PhSH. **Condition B**: 3:1 alkene:acid, 15 mol% $Ph_2S_2$ [a] trans:cis ratio.

We then considered the scope of oxidizable alkenes in conjunction with either mono-*tert*-butyl fumarate, 3-(trimethylsilyl)propiolic acid, or *trans*-cinnamic acid for the synthesis of γ-butyrolactones. Mono-*tert*-butyl fumarate, in combination with β-methylstyrene derivatives (Table 3-3, entries 3.10-3.12) of varying electron density, forged the expected lactones in good yields and moderate diastereoselectivity. Trisubstituted alkenes such as 1-phenylcyclohexene and 2-methyl-2-butene gave lactones **3.13** and **3.15** in acceptable yields. We were pleased to see that α–methylstyrene, a 1,1-disubstituted alkene, was an acceptable substrate and provided lactone **3.14** in 81% yield. 3-(Trimethylsilyl)propiolic acid was found to be slightly less reactive compared to mono-*tert*-butyl fumarate, which is obvious when comparing the yields for lactones **3.15** and **3.19**.

Nevertheless, this alkynyl acid reacted well with electron-rich substrates and heteroaromatic alkenes (**3.16**, **3.17**). Similar reactivity with cinnamic acid was observed when reacted with electron-rich and electron-poor substituted styrenes (**3.20**, **3.21**). In order to directly compare the reactivity between alkene and alkyne variants, 3-(trimethylsilyl)acrylic acid was synthesized and subjected to various conditions. Unfortunately, only trace amounts of the cycloadduct were ever obtained. This dissimilar reactivity was surprising to us; however we reasoned it might be correlated to the α-silicon effect, which inevitably destabilizes the α−position to the silicon group. We reasoned this effect is not observed when the alkyne variant was used, as the required alignment of d-orbitals is no longer possible. Differentiating the relative stereochemistry of major and minor diastereomers proved challenging for lactones possessing quaternary stereocenters; the stereochemistry for **3.13** and **3.14** were confirmed by the apparent anisotropy between the C1 hydrogen and the aromatic group observed in the $^1$H NMR spectra. Unfortunately, the major and minor diasteromers could not be distinguished for **3.15**. All lactones derived from alkynyl acids were produced as a mixture of cis:trans isomers except for **3.19**. When 3-(trimethylsilyl)propiolic acid was used with 2-methyl-2-butene, only the *E*-stereoisomer of **3.19** was observed. It is plausible that the fleeting vinyl radical intermediate equilibrates to relieve non-bonding interactions between the neighboring gem-dimethyl group and the TMS-group.

**Figure 3-32: Epimerization of γ-Butyrolactone**

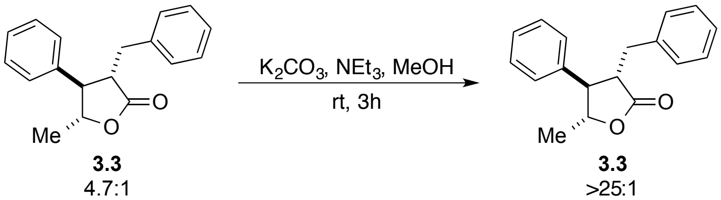

As diastereocontrol between C2 and C3 was modest, we investigated the possibility of epimerization to upgrade the diastereoselectivity. Epimerization of a 4.7:1 diastereomeric mixture of lactone **3.3** to the more thermodynamically-stable *trans-trans* isomer was readily accomplished by treatment with triethylamine and potassium carbonate in methanol (Figure 3-32). Epimerizations similar to this have been accomplished before,[26] which further confirms the stereochemistry of the major product is the all *trans* isomer. This simple protocol allows for the isolation of lactone adducts with higher than >25:1 diastereoselectivity.

**Figure 3-33: Proposed Mechanism for the Synthesis of γ-Butyrolactones via PhotoInduced Electron Transfer**

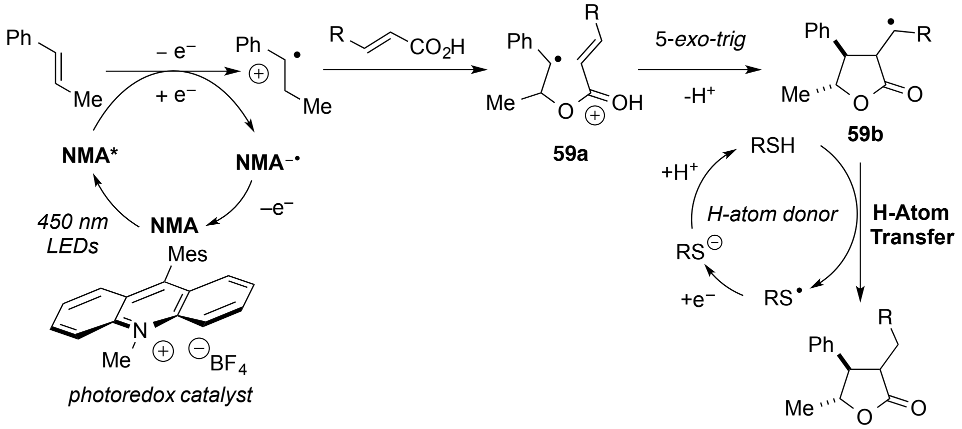

We propose the following mechanism for the synthesis of butyrolactones arising from oxidizable alkenes and unsaturated acids: single electron oxidation between the mesityl photooxidant (NMA) affords the radical cationic species of the alkene, which is susceptible to nucleophilic addition (Figure 3-33). The radical and cationic character of the activated species is interchangeable; however when in the presence of an α,β–unsaturated acid, the stability of the radical dictates addition. Nucleophilic addition by the acid oxygen occurs at the carbon alpha to the methyl group, giving **59a** bearing a stabilized benzylic radical. A 5-*exo* cyclization produces intermediate **59b,** which quickly undergoes hydrogen atom transfer with the hydrogen atom source. Though phenyl disulfide was employed as the hydrogen atom surrogate, we believe thiophenol is the active hydrogen atom source. This sequence forms the neutral butyrolactone, and generates an equivalent of thiyl radical. The thiyl radical is presumed to undergo single electron transfer with the electron-rich photocatalyst, producing the thiyl anion and regenerating the active photoredox catalyst. Though it is unclear how thiophenol is generated from phenyl disulfide, recent findings by our group suggest direct photolysis with 450 nm light results in homolytic bond cleavage of the sulfur-sulfur bond (unpublished data).

### 3.5.1 Synthesis of Methylenolactocin And Protolichesterinic Acid

**Figure 3-34: Retrosynthesis Analysis of Protolichesterinic Acid**

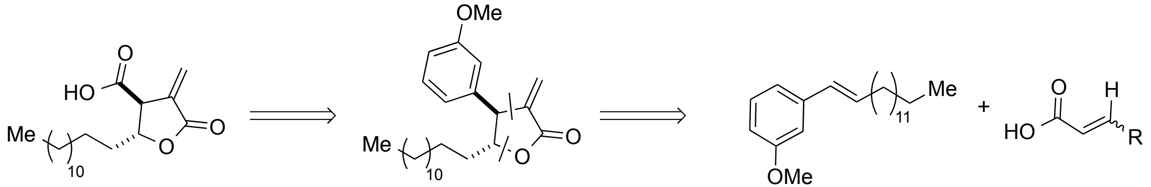

***Protolichesterinic acid***

We believed our method could be applied to the direct synthesis of paraconic acids with α−methyl or α−methylene subunits. However, success of this transformation was contingent upon selecting the appropriate unsaturated acid and alkene. First, we considered acrylic acid as the unsaturated substrate for our transformation (Figure 3-34). Similarly to propiolic acid, only uncyclized and Michael addition byproducts were formed. This result is not surprising, as we recognized the 5-*exo* cyclization requires a radical stabilizing group appended to the acid. Next, we considered the lactone product **3.6** arising from 3-(trimethylsilyl)propiolic acid and β−methylstyrene. We proposed desilylation of the vinyl TMS and oxidation of an electron-rich aromatic to a carboxylic acid with a $RuCl_3/NaIO_4$ system, which would afford the skeletal structural we desired.[46] After several attempts to desilyate with various fluorine sources, α-methylene products were never obtained. Instead unreacted *E*-isomer and alkene isomerization of the desilylated *Z*-isomer to the internal position were obtained. These unsuccessful attempts led us to consider β-haloacrylic acids as reaction partners to construct the *exo* methylene moiety. When *trans* chloroacrylic acid was employed in combination with β-substituted styrenes, poor yields of the major isomer were obtained. As observed with crotonic acid, Michael addition byproducts dominated the reaction. We then considered employing *cis:trans* mixtures of the chloroacrylic acid, which resulted in increased yields of the lactone. After numerous reaction condition manipulations, we transitioned to commercially availably *cis* chloroacrylic acid as the unsaturated nucleophile. To our surprise, the Michael addition adduct was suppressed when the *cis* variant was used. This permitted *cis* chloroacrylic acid to undergo nucleophilic addition and 5-*exo* cyclization with **3.22**, affording desired lactone **3.24** in acceptable yields (Figure 3-34). After fine-tuning the reaction conditions, we found that 10 mol% 2,6-lutidine, 1.1 equiv. *cis* chloroacrylic acid, 2.5 mol% of NMA, and 15 mol% of phenyl disulfide were optimal. The reaction was irradiated for 24 hours and the desired product **3.24** was isolated in 66% yield as a mixture of major and minor isomers. Arene oxidation using catalytic amounts of $RuCl_3$ and stoichiometric amounts of $NaIO_4$ furnished lactone **3.25**. Unfortunately, bicycle **3.26** was observed in modest yield, which we believe is formed via intramolecular nucleophilic substitution of the minor isomer. The crude reaction mixture was subjected to elimination conditions providing protolichesterinic acid in 47% with 2 purification steps beginning from our key intermolecular transformation.

**Figure 3-35: Synthesis of Protolichesterinic Acid**

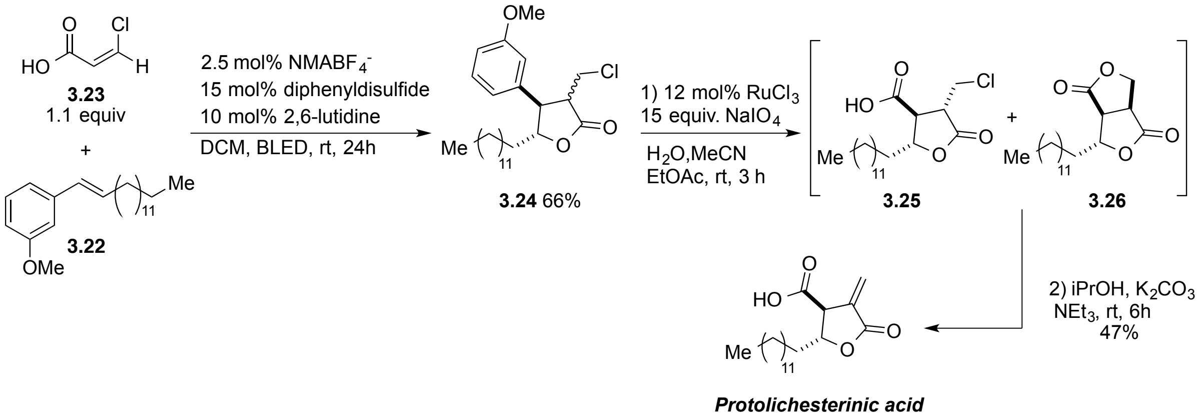

3.23
1.1 equiv
+
3.22
2.5 mol% NMABF$_4^-$
15 mol% diphenyldisulfide
10 mol% 2,6-lutidine
DCM, BLED, rt, 24h
3.24 66%
1) 12 mol% RuCl$_3$
15 equiv. NaIO$_4$
H$_2$O,MeCN
EtOAc, rt, 3 h
3.25
3.26
2) iPrOH, K$_2$CO$_3$
NEt$_3$, rt, 6h
47%
Protolichesterinic acid

We speculated epimerization of lactone **3.24** to the all *trans* isomer might eliminate formation of the bicycle byproduct. When subjected to epimerization conditions, lactone **3.24** was quantitatively converted to methoxy adduct **3.27** (Figure 3-36). Initially, we found this pathway promising as oxidation of the aromatic ring smoothly resulted in lactone **3.28**. The crude material was then subjected to a range of unsuccessful elimination conditions with the intention of forming the *exo* methylene. De-methoxylation proved more challenging than expected; the desired adduct along with isomerization byproducts were consistently obtained in low and indiscernible yields.

**Figure 3-36: Epimerization of Protolichesterinic Acid Intermediate**

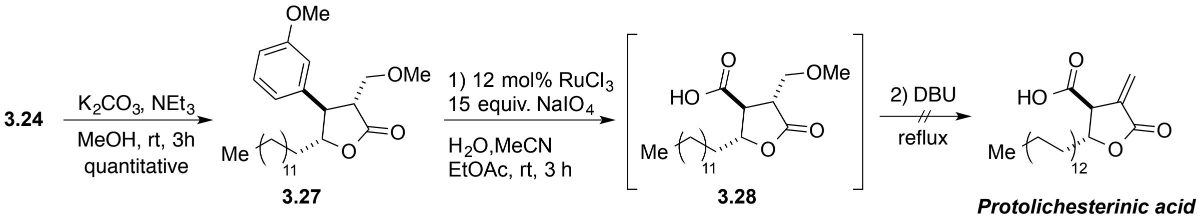
3.24
$K_2CO_3$, $NEt_3$
MeOH, rt, 3h
quantitative
OMe
OMe
Me
11
O
3.27
1) 12 mol% $RuCl_3$
15 equiv. $NaIO_4$
$H_2O$,MeCN
EtOAc, rt, 3 h
O
HO
OMe
Me
11
O
3.28
2) DBU
reflux
O
HO
Me
12
O
Protolichesterinic acid

We next applied our successful synthetic method for protolichesterinic acid to the synthesis of methylenolactocin. This work, accomplished by Mary Zeller in the Nicewicz group, followed the same protocol and yielded the paraconic acid in a 14% overall yield (Figure 3-37).

**Figure 3-37: Synthesis of Methylenolactocin**

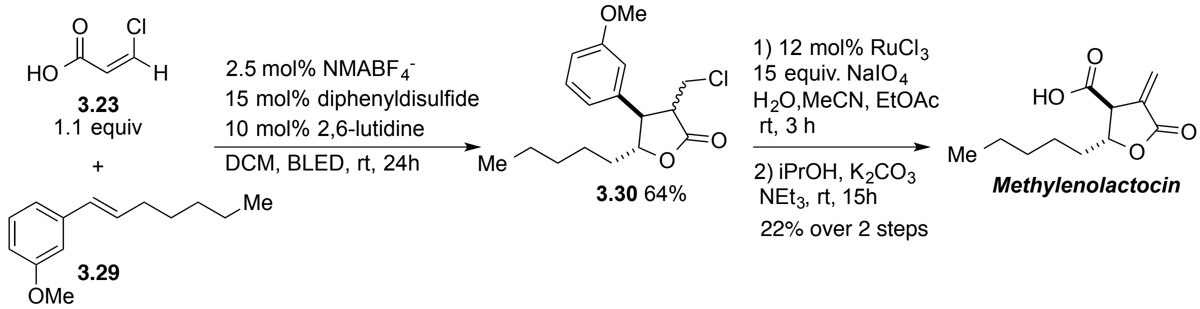
O
Cl
HO
H
3.23
1.1 equiv
+
Me
3.29
OMe
2.5 mol% $NMABF_4^-$
15 mol% diphenyldisulfide
10 mol% 2,6-lutidine
DCM, BLED, rt, 24h
OMe
Cl
Me
O
3.30 64%
1) 12 mol% $RuCl_3$
15 equiv. $NaIO_4$
$H_2O$,MeCN, EtOAc
rt, 3 h
2) iPrOH, $K_2CO_3$
$NEt_3$, rt, 15h
22% over 2 steps
O
HO
Me
O
Methylenolactocin

## 3.6 Conclusion and Outlook

In summary, our method provides a modular approach to the synthesis of γ-butyrolactones, rapidly producing complexity from a variety of simple, often commercially available, oxidizable olefins and unsaturated acids. With only small variations in conditions, a large variety of α,β–unsaturated acids can be used. The method has been applied to the synthesis of α-methylene and α-alkylidine lactones with acids possessing aliphatic, aromatic, and heteroaromatic substituents. It has also been applied to a highly diastereoselective synthesis of the α-methylene paraconic acids methylenolactocin and protolichesterinic acid. This method has shown that mildly nucleophilic unsaturated acids react favorably with the radical cation species and undergo 5-*exo* cyclization.

**Figure 3-38: Possible Transformations Derived From Current Work**

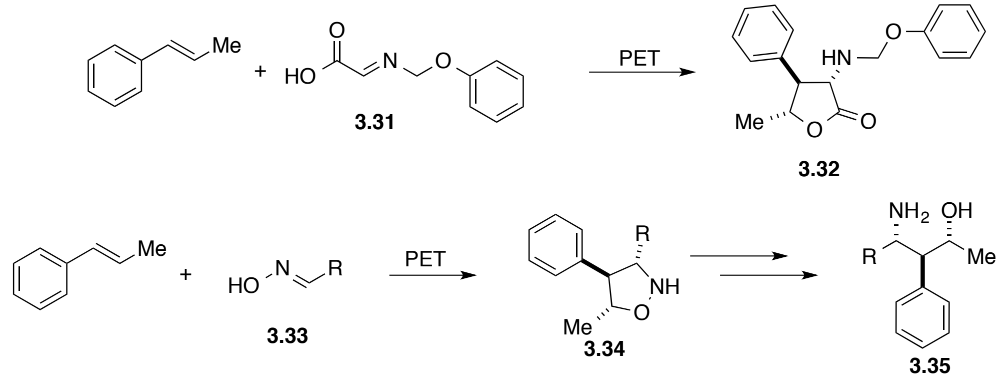

An extension of this project wherein oximino acids react with oxidizable olefins is now underway (Figure 3-38, top). Work accomplished by Clive and coworkers suggests similar reactivity may be obtained with oximino acids; this extension would encompass the scope of substituted γ-butyrolactones with various nitrogen-substituted groups.[47] Additionally, another interesting transformation worth investigating is the use of oxime acids in combination with oxidizable alkenes (Figure 3-38, bottom). Affecting this 3+2 cyclization may offer an alternate route to isoxazolidine **3.34** with the propensity of forming 1,3-amino alcohols in a stereoselective manner.

## 3.7 Experimental

### General Methods

Infrared (IR) spectra were obtained using a Jasco 260 Plus Fourier transform infrared spectrometer. Proton and carbon magnetic resonance spectra (1H NMR and 13C NMR) were recorded on a Bruker model DRX 400, DRX 500, or a Bruker AVANCE III 600 CryoProbe (1H NMR at 400 MHz, 500 MHz or 600 MHz and 13C NMR at 101, 126, or 151 MHz) spectrometer with solvent resonance as the internal standard ($^1$H NMR: $CDCl_3$ at 7.26 ppm; $^{13}$C NMR: $CDCl_3$ at 77.0 ppm). $^1$H NMR data are reported as follows: chemical shift, multiplicity (s = singlet, d = doublet, t = triplet, dd = doublet of doublets, ddt = doublet of doublet of triplets, ddd = doublet of doublet of doublets, dddd = doublet of doublet of doublet of doublets m = multiplet, brs = broad singlet), coupling constants (Hz), and integration. Mass spectra were obtained using a Micromass (now Waters Corporation, 34 Maple Street, Milford, MA 01757) Quattro-II, Triple Quadrupole Mass Spectrometer, with a Z-spray nano-Electrospray source design, in combination with a NanoMate (Advion 19 Brown Road, Ithaca, NY 14850) chip based electrospray sample introduction system and nozzle. Cyclic voltammograms were obtained with a platinum disc working electrode, Ag/AgCl reference electrode, a platinum wire auxillary, and CHI-760 potentiostat using 1 mM solutions of analyte in acetonitrile with 0.1 M tetrabutylammonium perchlorate as supporting electrolyte. Thin layer chromatography (TLC) was performed on SiliaPlate 250 μm thick silica gel plates provided by Silicycle. Visualization was accomplished with short wave UV light (254 nm), aqueous basic potassium permanganate solution, or cerium ammonium molybdate solution followed by heating. Flash chromatography was performed using SiliaFlash P60 silica gel (40-63 μm) purchased from Silicycle. Tetrahydrofuran, diethyl ether, dichloromethane, and toluene were dried by passage through a column of neutral alumina under nitrogen prior to use. Irradiation of photochemical reactions was carried out using a 15W PAR38 blue LED floodlamp purchased from EagleLight (Carlsbad, CA), with borosilicate glass vials purchased from Fisher Scientific. All other reagents were obtained from commercial sources and used without further purification unless otherwise noted.

### Preparation of 3-(trimethylsilyl)propiolic acid

To a flame dried round bottom containing MeMgBr was added a solution of trimethylsilylalkyne in THF at 0°C under $N_2$, and was stirred for two hours. Carbon dioxide was then bubbled through the reaction at -5 $°C$ for one hour and then at room temperature for two hours. Dilute aqueous hydrochloric acid was slowly added at 0°C to the mixture, which was extracted with light petroleum. Organic extract was washed with brine, dried over $MgSO_4$, evaporated, and distilled.

**General Procedure A.** This method was carried out by Mary Zeller, and can be found in the supplementary information for the published report.

**General Procedure B**. To a flame-dried two dram vial equipped with a magnetic stir bar was added the alkene (2-3 equiv.), α,β-unsaturated acid (1 equiv.), *NMA* $BF_4^-$ (2.5 mol%), and phenyl disulfide (15 mol%). The vial was purged with $N_2$ and sparged dichloromethane was added to achieve a concentration of 0.15 M with respect to substrate, and sealed with a septum screwcap and Teflon tape. The reaction was irradiated with a 450 nm lamp and stirred at room temperature for the indicated time period. Upon completion, the reaction was dry loaded and further purified by flash column chromatography with acetone/hexanes as the eluent mixture.

**General Procedure C**. To a flame-dried two dram vial equipped with a magnetic stir bar was added the alkene (2-3 equiv.), α,β-unsaturated acid (1 equiv.), *NMA* $BF_4^-$ (2.5 mol%), 2,6-lutidine (10 mol%) and phenyl disulfide (15 mol%). The vial was purged with $N_2$ and sparged dichloromethane was added to achieve a concentration of 0.15 M with respect to substrate, and sealed with a septum screwcap and Teflon tape. The reaction was irradiated with a 450 nm lamp and stirred at room temperature for the indicated time period. Upon completion, the reaction was dry loaded and further purified by flash column chromatography with acetone/hexanes as the eluent mixture.

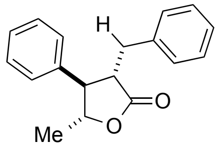

**3.3** 81% 4.7: 1
Condition B

**3-benzyl-5-methyl-4-phenyldihydrofuran-2(3H)-one (3.3)** The lactone was prepared according to General Procedure B using 194 μL of β–methylstyrene, 74 mg of cinnamic acid, 16 mg of phenyl disulfide, and 5 mg of NMA $BF_4^-$. Reaction was carried out at room temperature for 24 hours and purified via flash chromatography. Yield was 108 mg (81%, 4.7:1 dr) of the desired adduct as a clear oil. Characterizations include major and minor diastereomers. **$^1$H NMR** (600 MHz, $CDCl_3$) δ major: 7.27–6.78 (m, 10H), 4.3 (dq, *J* = 9.67, 6.61 Hz, 1H) 3.17 (m, 1H), 3.04 (ddd, J=4.8, 5.4, 14.4 Hz, 1H), 2.89 (dd, J =5.9, 14.3 Hz, 1H), 2.74, (dd, J=9.5, 12.1 Hz, 1H), 1.18 (d J=6.6 Hz, 3H). Minor: 7.27–6.78 (m, 10H), 4.71, (dq, J=1.8, 6.6 Hz, 1H), 3.30-3.2 (m, 3H), 2.28, (dd, J= 9.9, 14.7 Hz, 1H) 1.42 (d, J = 6.6 Hz, 3H). **$^{13}$C NMR** (600 MHz, $CDCl_3$) δ177.71, 176.74, 138.57, 137.19, 136.80, 129.64, 127.76, 126.56, 126.34, 81.25, 81.08, 54.25, 50.39, 49.41, 33.50, 31.59, 20.39, 18.46. **MS** (GC-MS) Calculated *m/z* for $[M]^+$ = 266, Found *m/z* for $[M]^+$ = 266. **IR** (Thin Film, $cm^{-1}$): 3062, 3029, 2976, 2923, 1770, 1602, 1496.

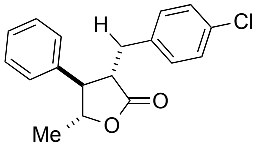

**3.4** 80% 5.2:1
Condition B

**3-(4-chlorobenzyl)-5-methyl-4-phenyldihydrofuran-2(3H)-one (3.4)**: The lactone was prepared according to General Procedure B using 155 µL of β−methylstyrene, 73 mg of p-chlorocinnamic acid, 13 mg of phenyl disulfide, and 4 mg of NMA $BF_4^-$. Reaction was carried out at room temperature for 24 hours and purified via flash chromatography. Yield was 98 mg (82%, 5.2 : 1dr) of the desired adduct as a clear oil. Characterizations include major and minor diastereomers. **$^{1}$H NMR** (600 MHz, $CDCl_3$) δ major: 7.34-7.0 (m, 9H), 4.4 (dq, 6, 12.6 Hz, 1H), 3.22-3.186 (m, 1H), 3.07 (dd, J=4.8, 14.4 Hz, 1H), 2.9 (5.9, 14.3 Hz, 1H), 2.7 (dd, J =9.9, 12.1 Hz, 1H), 1.25 (d J=6.6 Hz, 3H). Minor: 7.27−6.78 (m, 9H), 4.76 (dq, J = 8.8 Hz, 1H), 3.3 -3.0 (m, 3H), 2.31( dd, J= 9,14.4 Hz, 1H), 1.48 (d, J= 6.6 Hz, 3H). ). **$^{13}$C NMR** (600 MHz, $CDCl_3$) δ177.43, 136.38, 135.68, 132.41, 130.98, 130, 129.05, 128.88, 128.41, 128.38, 127.91, 127.85, 127.70, 81.07, 50.39, 44.70, 31.12, 30.92, 30.24, 29.65, 20.40. **MS** (GC-MS) Calculated *m/z* for $[M]^+$ = 300, Found *m/z* for $[M]^+$ = 300. **IR** (Thin Film, $cm^{-1}$): 3063, 3030, 2977, 2928, 2359, 1771, 1600, 1491.

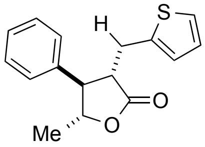

**3.5**[ab] 55% 2.7: 1
Condition B

**5-methyl-4-phenyl-3-(thiophen-2-ylmethyl)dihydrofuran-2(3H)-one (3.5)**: The lactone was prepared according to General Procedure B using 155 µL of β-methylstyrene 61.6mg of (E)-3-(thiophen-2-yl)acrylic acid, 13 mg of phenyl disulfide, and 4 mg of NMA $BF_4^-$. Reaction was carried out at room temperature for 2 days and purified via flash chromatography. Yield was 69 mg (63%, 2.7:1) of the desired adduct as a yellow oil. **$^{1}$H NMR** (600 MHz, $CDCl_3$) δ *major*: 7.39-7.09 (m, 7H), 6.91 (dd, J= 3.3, 5.1 Hz, 1H), 6.81 (d, J = 3.3 Hz, 1H), 4.48, (m 1H), 3.39 (dd, J= 4.6, 15.2 Hz, 1H), 3.21 (dt, J = 5, 12.1 Hz, 1H), 3.1 (dd, J= 5.5, 15 Hz, 1H), 2.92 (dd, J = 9.9, 12.1 Hz, 1H), 3.54 (d, J = 6.24 Hz, 3H). *minor*: 7.36- 7.25 (m, 3H) 7.15 (dd, J=1.10, 5.14 Hz, 1H), 7.09 (m, 2H), 6.89 (dd, J=3.3, 5.14 Hz, 1H), 6.57 (d, J=3.3 Hz, 1H), 4.92 (dq, J =1.7, 6.5 Hz, 1H), 3.39 (m, 2H), 3.25 (dd, J = 3.9, 15.6 Hz, 1H), 2.55 (dd, J= 9.9, 15.4 Hz, 1H), 1.53 (d, J = 6.6 Hz, 3H). **$^{13}$C NMR** (600 MHz,

$CDCl_3$) *major:* 176.29, 138.69, 136.74, 129.35, 129.08, 127.40, 126.93, 124.48, 80.96, 53.63, 49.84, 27.33, 20.45. *minor:* 176.98, 141.22, 138.34, 128.89, 127.91, 127.74, 126.74, 125.52, 123.70, 81.47, 50.49, 45.26, 26.20, 20.48. **MS** (GC-MS) Calculated *m/z* for $[M]^+$ = 272, Found *m/z* for $[M]^+$ = 272. **IR** (Thin Film, $cm^{-1}$): 3734, 3648, 3055, 2980, 2925, 2359, 2341, 1770, 1732, 1716, 1652, 1558, 1507, 1455.

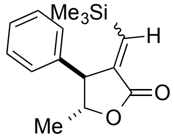

**3.6**[a] 85% 1.3: 1
Condition B

**(E/Z)-5-methyl-4-phenyl-3-((trimethylsilyl)methylene)dihydrofuran-2(3H)-one (3.6)**: The lactone was prepared according to General Procedure B using 194 μL of β-methylstyrene, 71 mg of 3-(trimethylsilyl)propiolic acid, 16 mg of phenyl disulfide, and 5 mg of NMA $BF_4^-$. Reaction was carried out at room temperature for 24 hours and purified via flash chromatography. Yield was 101 mg (78%, 1.3 :1 trans:cis) of the desired adduct as a clear oil. Characterizations include *cis* and *trans* products. **$^1$H NMR** (600 MHz, $CDCl_3$) δ trans: 7.34-7.15 (m, 5H), 4.41 (dq, J= 4.5, 6.3Hz, 1H), 3.77 (dd, J= 2.8, 4.3 Hz, 1H), 1.47 (d, J = 6.3 Hz, 3H), -0.13 (s, 9H). cis: 7.40-7.32 (m, 3H), 7.18-7.17 (m, 2H), 6.13 (d, J=2.93 Hz, 1H), 4.49 (dq, J= 6.17, 7.89 Hz, 1H), 3.69 (dd, J= 2.93, 8.07 Hz, 1H), 1.45 (d, J= 6.2 Hz, 3H), 0.20 (s, 9H). **$^{13}$C NMR** (600 MHz, $CDCl_3$) trans: δ169.99, 143.96, 143.73, 141.75, 129.07, 127.88, 127.58, 82.23, 52.70, 21.42, -1.49. cis: δ169.98, 143.71, 141.70, 129.04, 127.85, 82.22, 52.63, 21.39, -1.52. **MS** (GC-MS) Calculated *m/z* for $[M]^+$ = 260, Found *m/z* for $[M]^+$ = 260. **IR** (Thin Film, $cm^{-1}$): 3058, 3030, 2957, 2360, 2341, 1750, 1455, 1266, 1249, 1194.

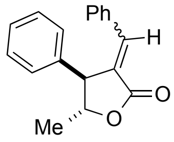

**3.7**[a] 41% 1.4:1
Condition C

***trans*-3-((Z/E)-benzylidene)-5-methyl-4-phenyldihydrofuran-2(3H)-one (3.7):** The lactone was prepared according to General Procedure C using 103.6 μL of β-methylstyrene 58.4 mg of 3-phenylpropiolic acid, 13 mg of phenyl disulfide, 4.7 μL of 2,6-lutidine, and 4 mg of NMA $BF_4^-$. Reaction was carried out at room temperature for 4 days and purified via flash chromatography. Yield was 53 mg (49%, 1.56:1) of the desired adduct as a yellow oil. **$^1$H NMR** (600 MHz, $CDCl_3$) δ *cis*: 7.83, (m, 2H), 7.44-7.27 (m, 9H), 6.59, (d, J = 2.6 Hz, 1H), 4.61-4.58 (m, 1H), 3.92 (dd, J = 2.9, 8.1 Hz, 1H), 1.5 (d, J = 6.2 Hz, 3H). δ *trans:* 7.8 (d, J = 2.6 Hz, 1H), 7.28 (m, 11H), 4.57 (qd, J = 3.5, 6.3 Hz, 1H), 4.17, (t, J = 2.8 Hz, 1H), 1.52 (m, 3H). **$^{13}$C NMR** (600 MHz, $CDCl_3$) *cis:* 168.29, 141.30, 138.90, 133.40, 130.81, 130.28, 129.70, 129.21, 128.82, 128.10, 127.96, 80.94, 57.44, 19.81. *trans:* 172.02, 139.79, 139.77, 133.41, 130.50, 129.91, 129.22, 128.46, 127.52, 127.19, 82.61, 52.14, 21.84. **MS** (GC-MS) Calculated *m/z* for $[M]^+$ = 264, Found *m/z* for $[M]^+$ = 264. **IR** (Thin Film, $cm^{-1}$): 3734, 3648, 3566, 2359, 1771, 1716, 1698, 1683, 1670, 1558, 1540, 1507.

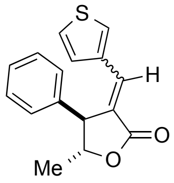

**3.8**[a] 44% 2.3: 1
Condition C

***trans*-3-(Z/E)-5-methyl-4-phenyl-3-(thiophen-3-ylmethylene)dihydrofuran-2(3H)-one (3.8):** The lactone was prepared according to General Procedure C using 103.6 μL of β-methylstyrene, 60.4 mg of 3-(thiophen-2-yl)propiolic acid, 13 mg of phenyl disulfide, 4.7 μL of 2,6-lutidine, and 4 mg of NMA $BF_4^-$. Reaction was carried out at room temperature for 4 days and purified via flash chromatography. Yield was 48 mg (44%, 1.56:1) of the desired adduct as a clear oil. **$^1$H NMR** (600

MHz, $CDCl_3$) δ *cis*: 8.24, (m, 1H), 7.64, (dd, J = 5.14, 1.10 Hz, 1H), 7.22-7.45, (m, 8H), 6.43 (d, J = 2.93 Hz, 1H), 4.55 (dq, J = 6.13, 8.02 Hz, 1H), 3.87 (dd, J = 2.57, 8.07 Hz, 1H), 1.43-1.49 (m, 3H). δ *trans:* 7.87 (s, 1H), 7.37-7.19 (m, 8H), 6.9 (m, 1H), 4.56-4.53 (m, 1H), 4.08 (m, 1H), 1.55 (m, 3H). **$^{13}$C NMR** (600 MHz, $CDCl_3$) *cis:* 168.81, 135.37, 133.69, 131.42, 129.21, 128.81, 125.05, 81.14, 57.17, 19.87. *trans*: 172.10, 140.04, 135.83, 133.10, 130.23, 129.40, 126.90, 126.20, 82.53, 52.00, 22.05. **MS** (+ESI) Calculated *m/z* for $[M+H]^+$= 271.07, Found *m/z* for $[M+H]^+$ = 271.12. **IR** (Thin Film, $cm^{-1}$): 3085, 3054, 2985, 2305, 1748, 1636, 1558, 1540, 1519, 1265.

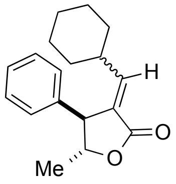

**3.9**$^a$ 83% 1: 1
Condition C

***trans-3*-(Z/E)-3-(cyclohexylmethylene)-5-methyl-4-phenyldihydrofuran-2(3H)-one (3.9):** The lactone was prepared according to General Procedure C using 103.6 μL of β-methylstyrene, 60.8 mg of 3-cyclohexylpropiolic acid, 13 mg of phenyl disulfide, 4.7 μL of 2,6-lutidine, and 4 mg of NMA $BF_4^-$. Reaction was carried out at room temperature for 4 days and purified via flash chromatography. Yield was 99 mg (92%, 1:1) of the desired adduct as a clear oil. **$^1$H NMR** (600 MHz, $CDCl_3$) δ *cis:* 7.41-7.15 (m, 5H), 5.68, (dd, J = 2.6, 9.9 Hz, 1H), 4.40 (m, 1H), 3.67 (dd, J = 2.57, 8.07 Hz, 1H), 2.51 (m, 1H), 1.66 (m, 5H), 1.41 (m, 3H), 1.35 (m, 2H), 1.11 (m, 1H), 0.99 (m, 1H). *trans*: 7.38-7.20 (m, 5H), 6.75-6.70 (dd, J = 2.75, 10.45 Hz, 1H), 4.56-4.47 (m, 1H), 3.78 (dd, J = 2.93, 5.14 Hz, 1H), 1.89 (m, 1H), 1.73-1.50 (m, 4H), 1.48 (d, J = 6.24 Hz, 3H), 1.08 (m, 4H), 0.90 (m, 2H). **$^{13}$C NMR** (600 MHz, $CDCl_3$) *cis:* 169.20, 151.02, 139.27, 128.97, 128.51, 127.61, 81.17, 55.49, 35.70, 32.40, 32.02, 25.74, 25.22, 19.74. *trans:* 171.09, 148.55, 141.32, 129.00, 127.49, 82.33, 51.67, 38.48, 31.32, 30.72, 25.57, 25.20, 24.98, 21.26. **MS** (+ESI) Calculated *m/z* for $[M+H]^+$ = 271.16, Found *m/z* for $[M+H]^+$ = 271.12. **IR** (Thin Film, $cm^{-1}$): 3853, 3749, 3648, 2927, 2852, 2359, 1750, 1716, 1698, 1683, 1559, 1554, 1507.

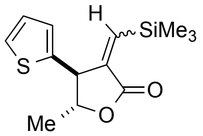

**3.17**$^a$ 80% 1.4:1 (*E:Z*)
Condition B

**(E/Z)-5-methyl-4-(thiophen-2-yl)-3-((trimethylsilyl)methylene)dihydrofuran-2(3H)-one (3.17)**: The lactone was prepared according to General Procedure B using 149 mg of *t*-2-propenethiophene, 57 mg of 3-(trimethylsilyl)propiolic acid, 13 mg of phenyl disulfide, and 4 mg of NMA $BF_4^-$. Reaction was carried out at room temperature for 3 days and purified via flash chromatography. Yield was 83 mg (78%, 1.4:1 trans: cis) of the desired adduct as a purple oil. Characterizations include *cis* and *trans* products. **$^1$H NMR** (600 MHz, $CDCl_3$) δ mixture of *cis* and *trans*: 7.28-7.22 (m, 6H *trans+cis*), 7.05 (m, 1H *cis*), 6.97 (ddd, J=3.5, 4.8, 8.6 Hz, 1H *trans*), 6.86 (d, J= 4Hz, 1H *cis*), 6.35 (d, J= 2.9Hz, 1H *cis*), 4.51 (m, 2H *trans+cis*), 4.07 (dd, J= 3, 6Hz, 1H *trans*), 4.01 (dd, J= 3, 7.8 Hz, 1H *cis*). 1.5 (m, 6H *trans+cis*), 0.22 (s, 3H *cis*), 0.02 (s, 3H *trans*). **$^{13}$C NMR** (600 MHz, $CDCl_3$) mixture of *cis* and *trans*: 169.34, 168.84, 145.59, 145.40, 143.02, 144.5, 140.94, 127.27, 127.06, 126.59, 125.45, 125.29, 125.01, 82.20, 81.51, 52.11, 49.38, 21.37, 19.80, -0.78, -1.42. **MS** (GC-MS) Calculated *m/z* for $[M]^+$ = 266, Found *m/z* for $[M]^+$ = 266. **IR** (Thin Film, $cm^{-1}$): 2952, 2899, 1763, 1385, 1307, 1245.

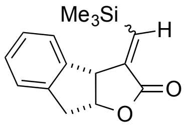

**3.18**$^a$ 76% 1.3:1 (*E:Z*)
Condition B

**(E/Z)-3-((trimethylsilyl)methylene)-3,3a,8,8a-tetrahydro-2H-indeno[2,1-b]furan-2-one (3.18)**: The lactone was prepared according to General Procedure B using 174 μL of indene, 71 mg of 3-(trimethylsilyl)propiolic acid, 16 mg of phenyl disulfide, and 5 mg of NMA $BF_4^-$. Reaction was carried out at room temperature for 4 days and purified via flash chromatography. Yield was 98 mg (76%, 1.3:1 trans: cis) of the desired adduct as a purple oil. Characterizations include *cis* and *trans*

products. **$^{1}$H NMR** (600 MHz, $CDCl_3$) δ trans: 7.29-7.20 (m, 2H), 7.19 (d, J=7 Hz, 2H), 6.9 (d, J= 1.1Hz, 1H), 5.18 (m, 1H), 4.53 (d, J=5.1 Hz, 1H), 3.37 (m, 2H), 0.35 (s, 9H). cis: 7.25 (s, 4H), 6.73 (d, J= 1.47 Hz, 1H), 5.29 (dq, J 1.6, 5.8 Hz, 1H), 4.38 (dd, J=1.3, 6 Hz, 1H), 3.34 (m, 2H), 0.22 (s, 9H). **$^{13}$C NMR** (600 MHz, $CDCl_3$) trans: 169.98, 142.45, 140.17, 138.68, 128.38, 127.43, 125.49, 125.06, 81.90, 50.33, 38.48, -0.64. cis: 169.43, 144.22, 141.03, 139.98, 128.26, 127.54, 124.17, 81.22, 53.28, 39.03, -0.78. **MS** (GC-MS) Calculated *m/z* for $[M]^+$ = 258, Found *m/z* for $[M]^+$ = 258. **IR** (Thin Film, $cm^{-1}$): 3069, 2955, 2901, 1759, 1636, 1558, 1479, 1311, 1265.

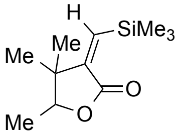

**3.19**[a] 45%
Condition B

**(E)-4,4,5-trimethyl-3-((trimethylsilyl)methylene)dihydrofuran-2(3H)-one (3.19)**: The lactone was prepared according to General Procedure B using 212 μL of 2-methyl-2-butene, 71 mg of 3-(trimethylsilyl)propiolic acid, 16 mg of phenyl disulfide, and 5 mg of NMA $BF_4^-$. Reaction was carried out at room temperature for 48 hours and purified via flash chromatography. Yield was 58 mg (55%, trans) of the desired adduct as a clear oil. **$^{1}$H NMR** (600 MHz, $CDCl_3$) δ 6.19 (s, 1H), 4.21 (q, J=6.6 Hz, 1H), 1.26 (d, J= 6.6 Hz, 3H), 1.14 (s, 3H), 1.01 (s, 3H), 0.19 (s, 9H). **$^{13}$C NMR** (600 MHz, $CDCl_3$) 170.03, 151.96, 139.96, 82.96, 43.73, 25.43, 22.68, 15.29, -0.75. **MS** (GC-MS) Calculated *m/z* for $[M+Li]^+$ = 219.14, Found *m/z* for $[M+Li]^+$ = 219.18. **IR** (Thin Film, $cm^{-1}$): 2965, 2359, 1704, 1636, 1558, 1520, 1507, 1456.

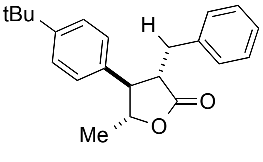

**3.20** 78% 5.8:1 dr
Condition B

**3-benzyl-4-(4-(tert-butyl)phenyl)-5-methyldihydrofuran-2(3H)-one (3.20)**: The lactone was prepared according to General Procedure B using 108.8 mg of (E)-1-fluoro-4-(prop-1-en-1-

yl)benzene, 59.2 mg of cinnamic acid, 13 mg of phenyl disulfide, and 4 mg of NMA $BF_4^-$. Reaction was carried out at room temperature for 24 hours and purified via flash chromatography. Yield was 89 mg (78%, 3.7:1 dr) of the desired adduct as a white crystalline solid. Characterizations include major and minor diastereomers. **$^1$H NMR** (600 MHz, $CDCl_3$) δ major: 7.33 (d, J= 8.4 Hz, 2H), 7.22-7.05 (m, 7H), 7.39 (dq, J=6.1, 9.7 Hz, 1H), 3.21 (dt, J= 5.55, 12.01 Hz, 1H), 3.1 (m, 1H), 2.93 (dd, J= 5.9, 14.3 Hz, 1H), 2.78 (dd, J= 9.54, 12.10 Hz, 1H) 1.23 (d, J= 6 Hz, 3H). Minor: 7.2-7.05 (m, 5H), 6.98 (d, J= 8.4 Hz, 2H), 6.92 (d, 7.35 Hz, 2H), 4.78 (dq, J= 4.2, 6.6Hz, 1H), 3.3-3.24 (m, 2H), 3.05 (d, J=4.2, 14.4 Hz, 1H), 2.36, dd, J=9.5, 14.7Hz, 1H), 1.47 (d, J= 6.6 Hz, 3H). ). **$^{13}$C NMR** (600 MHz, $CDCl_3$) δ177.79, 176.80, 150.55, 137.29, 133.63, 129.67, 128.65, 128.23, 127.65, 127.39, 126.45, 125.79, 125.61, 81.05, 77.20, 76.99, 76.79, 53.74, 49.39, 34.44, 33.42, 31.26, 31.22, 20.31, 18.05. **MS** (GC-MS) Calculated *m/z* for $[M]^+$ = 322, Found *m/z* for $[M]^+$ = 322. **IR** (Thin Film, cm$^{-1}$): 3060, 3029, 2964, 2969, 2359, 1771, 1652, 1558, 1496.

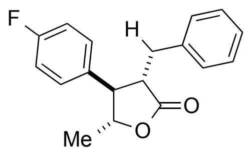

**3.21** 72% 3.6:1 dr
Condition B

**3-benzyl-4-(4-fluorophenyl)-5-methyldihydrofuran-2(3H)-one (3.21):** The lactone was prepared according to General Procedure B using 108.8 mg of (E)-1-fluoro-4-(prop-1-en-1-yl)benzene, 59.2 mg of cinnamic acid, 13 mg of phenyl disulfide, and 4 mg of NMA $BF_4^-$. Reaction was carried out at room temperature for 24 hours and purified via flash chromatography. Yield was 89 mg (78%, 3.7:1 dr) of the desired adduct as a green oil. Characterizations include major and minor diastereomers. **$^1$H NMR** (600 MHz, $CDCl_3$) δ major: 7.19-6.97 (m, 9H), 4.34 (dq, J= 6.0, 9.77 Hz, 1H), 3.17 (m, 1H), 3.06, (dd, J = 6, 14.4 Hz, 1H), 2.97 (dd, J=6, 14.4Hz, 1H), 2.79, dd (J= 9.9, 12.1 Hz, 1H), 1.23 (d, J =6.6 Hz, 3H). minor: 7.22-6.89 (m, 9H), 4.72 (dq, J=1.8, 6.4 Hz, 1H), 3.37-3.05 (m, 3H), 2.28 (dd, 10.45, 14.86 Hz, 1H), 1.48 (d, J= 6.6 Hz, 3H). **$^{13}$C NMR** (600 MHz, $CDCl_3$) δ177.43, 176.44, 138.29, 136.96, 135.69, 132.41, 130.98, 138.42, 127.71, 81.21, 81.08, 54.36, 50.39, 49.25, 44.71, 32.74, 30.93, 30.25, 20.41, 18.36. **MS** (GC-MS) Calculated *m/z* for $[M]^+$ = 284, Found *m/z* for $[M]^+$ = 284. **IR** (Thin Film, cm$^{-1}$): 3063, 3029, 2977, 2927, 2360, 2341, 1711, 1604, 1511, 1455, 1386, 1711, 1604, 1511, 1455, 1386.

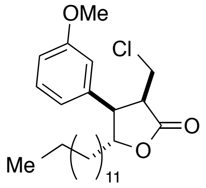

**3.24a**
*cis-trans*

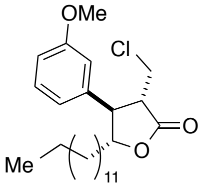

**3.24b**
*trans-trans*

***cis-trans*-3-(chloromethyl)-4-(3-methoxyphenyl)-5-tridecyldihydrofuran-2(3*H*)-one (3.24):** The lactone was prepared according to modified General Procedure C using 94.8 mg of (E)-1-methoxy-3-pentadec-1-en-1-yl)benzene, 60.8 mg of *cis*-chloroacrylic acid, 10 mg of phenyl disulfide, 3.5 μL of 2,6-lutidine, and 3 mg of NMA $BF_4^-$. Reaction was carried out at room temperature for 4 days and purified via flash chromatography. Yield was 174 mg (69%) of the desired adduct as a pink oil. **$^1$H NMR** (600 MHz, $CDCl_3$) δ *minor* (**3.24a**): 7.27-7.25 (m, 1H), 6.86-6.77 (m, 3H), 4.75-4.71 (ddd, J = 2.5, 5.7, 8.3 Hz, 1H), 3.8 (s, 3H), 3.71-3.68 (dd, J = 3.4, 11.5 Hz, 2H), 3.55-3.53 (dd, J = 2.5, 8.6 Hz, 2H), 3.37 (m, 2H), 3.05 (dd, J = 9.8, 11.5 Hz, 2H), 1.86-1.66 (m, 5H), 1.56-1.1 (m, 25H), 0.88 (m, 3H). ) δ *major* (**3.24b**): 7.29 (m, 1H), 6.87-6.0 (m, 3H), 4.46 (dt, J = 6.0, 9.8 Hz, 1H), 4.02-3.98 (dd, J = 3.4, 11, 1H) 3.82 (s, 1H), 3.55 (dd, J = 3.4, 11.7 Hz, 1H), 3.43 (dd, J – 9.8 11.7 Hz, 1H), 3.16 (dt, J = 3.3, 11.7 Hz, 1H), 1.68 (m, 5H), 1.4-1.21 (m, 24H), 0.87 (t, J = 6.8 Hz, 3H). **$^{13}$C NMR** (600 MHz, $CDCl_3$) δ *minor* (**3.24a**): 174.38, 159.91, 138.67, 130.15, 119.90, 114.00, 113.05, 85.30, 55.19, 48.41, 47.09, 39.87, 34.64, 31.86, 29.59, 29.31, 29.19, 25.57, 22.65, 10.08. *major (***3.24b**): 173.75, 160.17, 138.46, 130.37, 119.93, 114.08, 112.85, 84.32, 55.28, 50.88, 50.01, 40.66, 33.64, 31.90, 29.56, 29.46, 29.35, 29.28, 25.60, 22.68, 14.11. **MS** (+ESI) Calculated *m/z* for $[M+H]^+$ = 423.03, Found *m/z* for $[M+H]^+$ = 423.30. **IR** (Thin Film, cm$^{-1}$): 3054, 2926, 2851, 1777, 1469, 1265.

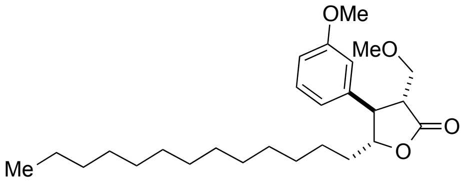

***trans-trans*-3-(methoxymethyl)-4-(3-methoxyphenyl)-5-tridecyldihydrofuran-2(3H)-one (3.27):** To a round bottom containing a *cis: trans* mixture of 3-(chloromethyl)-4-(3-methoxyphenyl)-5-tridecyldihydrofuran-2(3H)-one, (100 mg), 5 equivalents of $K_2CO_3$ (170 mg), and 0.6 $NEt_3$ were in 6mL MeOH for 1 hour. The reaction was diluted with ethylacetate and washed several times with water, then dried over $MgSO_4$, concentrated, and purified via flash chromatography. Quantitative yield was obtained.$^1$**H NMR** (600 MHz, $CDCl_3$) δ 7.35–7.27 (m, 1H), 6.88-6.79 (m, 3H), 4.45-4.68 (dt, J = 6.1, 9.5 Hz, 1H), 3.83 (s, 3H), 3.78 (dd, J = 3.30, 9.90 Hz, 1H), 3.45 (dd, J = 3.30, 9.90 Hz, 1H) 3.36 (s, 3H), 3.38-3.33 (m, 1H), 2.92-2.86 (dt, J = 3.3, 11.7 Hz, 1H) 1.71-1.64 (m, 2H), 1.56-1.47 (m, 2H), 1.18-1.37 (m, 24H), 0.93-0.86 (m, 3H). $^{13}$**C NMR** (600 MHz, CDCl3) δ 175.62, 160.00, 139.75, 130.10, 119.96, 114.02, 112.45, 84.48, 67.77, 59.22, 55.20, 50.16, 49.42, 33.83, 31.87, 29.59, 29.55, 29.45, 29.27, 29.31, 25.70, 22.64, 14.08. **MS** (GC-MS) Calculated *m/z* for $[M+H]^+$ = 419.31, Found *m/z* for $[M+H]^+$ = 419.37. **IR** (Thin Film, $cm^{-1}$): 3056, 2925, 1774, 1601, 1586, 1489, 1456, 1438, 1293, 1266.

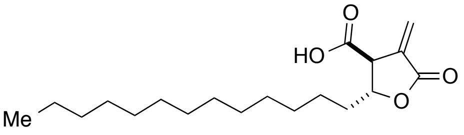

***Protolichesterinic acid***

**Protolichesterinic Acid:** 136 mg of *cis* and *trans* **3.24** were combined and stirred in 2.7 mL of EtOAc, and 2.7 mL of MeCN. To this was added 8.26 mg $RuCl_3$ and 1.022 g $NaIO_4$, dissolved in 5.3 mL $H_2O$ droppwise. Reaction was stirred for 4 hours. Following reaction completion, white precipitate was filtered through celite and was diluted with EtOAc. Washing with $Na_2S_2O_3$ (aq), and brine followed. The aqueous solution was acidified and extracted with EtOAc, which was then washed with brine. The combined organic layers were dried over $MgSO_4$ and dried. Crude material was then treated with 282 mg (5 equiv) $K_2CO_3$, 0.41 mL (1M), and 10.3 mL iPrOH. Reaction was stirred overnight. At the completion of the reaction, the solution was diluted with EtOAc, and acidified with 3 N HCl. The organics were washed with $H_2O$ and brine, and were dried over $MgSO_4$. The desired product was purified via pipet column with 100% DCM, where byproduct **3.26** was removed. Following the removal of **3.26**, the column was treated with 100% EtOAc to obtain the desired natural product as an off white solid (66mg, 54% yield). **$^1$H NMR** (600 MHz, $CDCl_3$) δ 6.47 (d, J = 2.93 Hz, 1H), 6.02 (d, J = 2.57) 4.81 (m, 1H), 3.63 (dt, J = 2.75, 5.50 Hz, 1H) 1.73 (m, 2H), 1.39 (m, 24 H), 0.88 (t, J = 7.15 Hz, 3H). **$^{13}$C NMR** (600 MHz) $CDCl_3$ d 174.39, 168.22, 132.34, 125.99, 78.84, 49.44, 35.73, 31.90, 29.66, 29.62, 29.59, 29.38, 29.34, 29.17, 24.74, 22.67, 14.11.

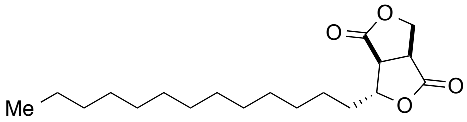

**3.26**

**3-tridecyltetrahydrofluro[3,4-c]furan-1,4-dione (3.26):** White solid **$^1$H NMR** (600 MHz, $CDCl_3$) δ 4.83–4.78 (tq, J = 1.1, 6.6 Hz, 1H), 4.72-4.66 (dd, J = 1.5, 9.5 Hz, 1H), 4.57-4.51 (dd, J = 7.7, 9.9 Hz, 1H), 3.52 (ddd, J = 1.47, 7.79, 9.45 Hz, 1H), 3.20 (dd, J = 1.47, 9.54 Hz, 1H) 1.74 (m, 2H), 1.44 (m, 2H), 1.38-1.17 (m, 23H), 0.85-0.89 (t, J = 6.97 Hz, 3H). **$^{13}$C NMR** (600 MHz, $CDCl_3$ d 175.53, 175.35, 81.86, 69.00, 45.39, 40.69, 36.31, 31.90, 29.62, 29.36, 29.01, 24.61, 22.67, 14.11.

**MS** (+ESI) Calculated *m/z* for $[M+H]^+$ = 325.23, Found *m/z* for $[M+H]^+$ = 325.24. **IR** (Thin Film, $cm^{-1}$): 3055, 2923, 2851, 1777, 1469, 1265.

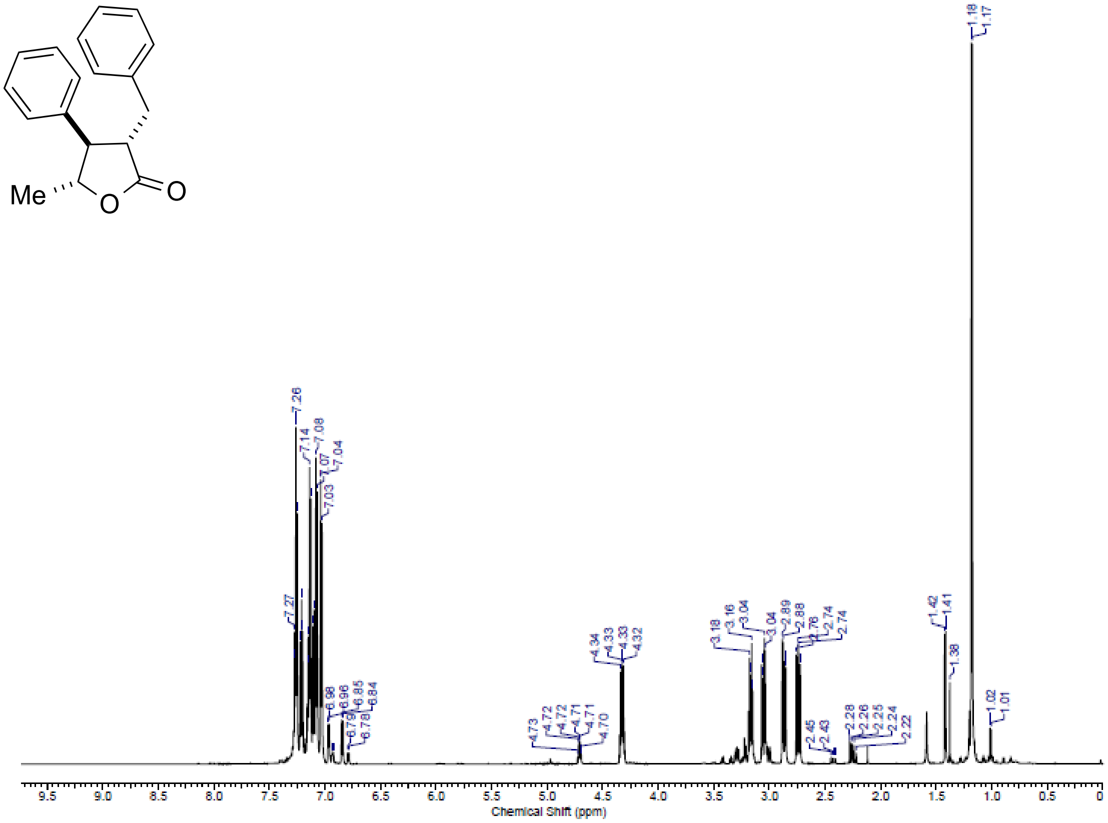
Me
O
O
7.27
7.26
7.14
7.08
7.07
7.04
7.03
6.98
6.96
6.85
6.84
6.79
6.78
4.73
4.72
4.72
4.71
4.71
4.70
4.34
4.33
4.33
4.32
3.18
3.16
3.04
3.04
2.89
2.88
2.76
2.74
2.74
2.45
2.43
2.28
2.26
2.25
2.24
2.22
1.42
1.41
1.38
1.19
1.17
1.02
1.01
9.5 9.0 8.5 8.0 7.5 7.0 6.5 6.0 5.5 5.0 4.5 4.0 3.5 3.0 2.5 2.0 1.5 1.0 0.5 0
Chemical Shift (ppm)

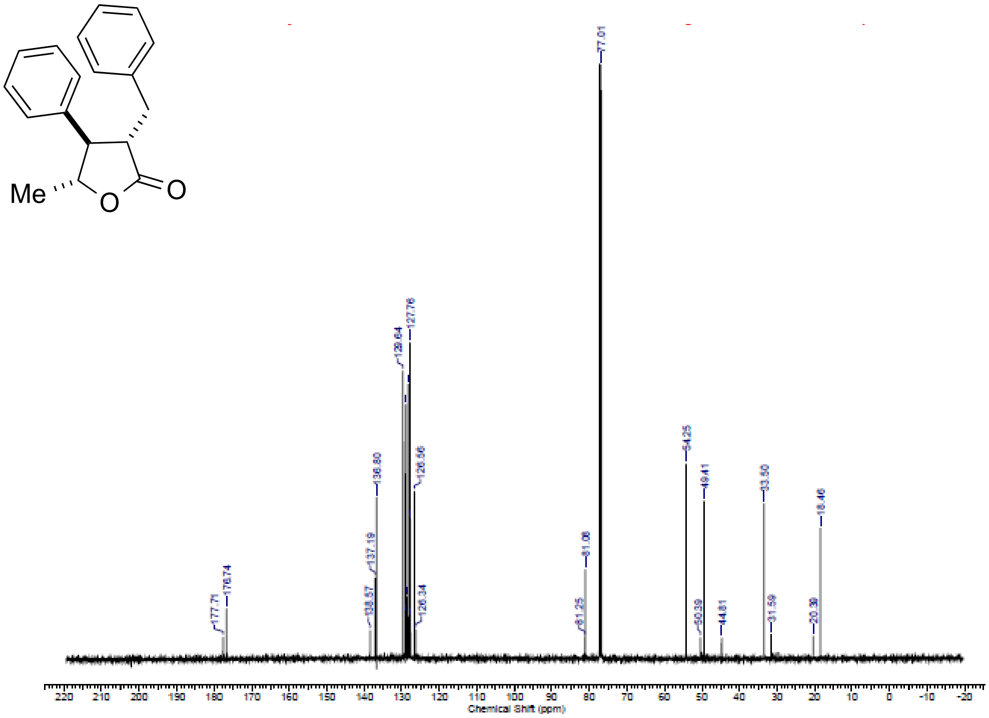
Me
O
O
177.71
176.74
138.57
137.19
136.80
128.64
127.76
126.56
126.34
81.25
81.08
77.01
54.25
50.39
49.41
44.81
33.50
31.59
20.39
18.46
220 210 200 190 180 170 160 150 140 130 120 110 100 90 80 70 60 50 40 30 20 10 0 -10 -20
Chemical Shift (ppm)

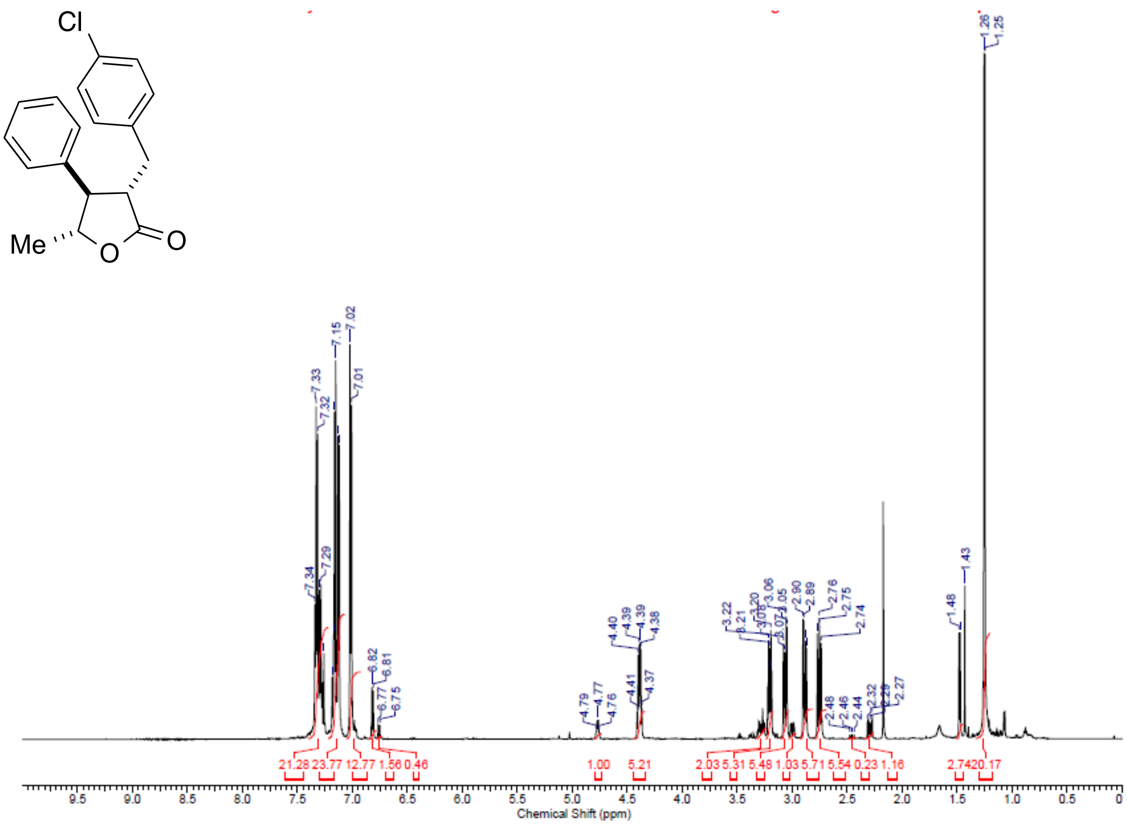
Cl
Me
O
O
7.34
7.33
7.32
7.29
7.15
7.02
7.01
6.82
6.81
6.77
6.75
4.79
4.77
4.76
4.41
4.40
4.39
4.39
4.38
4.37
3.22
3.21
3.20
3.06
3.05
2.90
2.89
2.76
2.75
2.74
2.48
2.46
2.44
2.32
2.27
1.48
1.43
1.26
1.25
21.28
23.77
12.77
1.56
0.46
1.00
5.21
2.03
5.31
5.48
1.03
5.71
5.54
0.23
1.16
2.74
20.17
9.5
9.0
8.5
8.0
7.5
7.0
6.5
6.0
5.5
5.0
4.5
4.0
3.5
3.0
2.5
2.0
1.5
1.0
0.5
0
Chemical Shift (ppm)

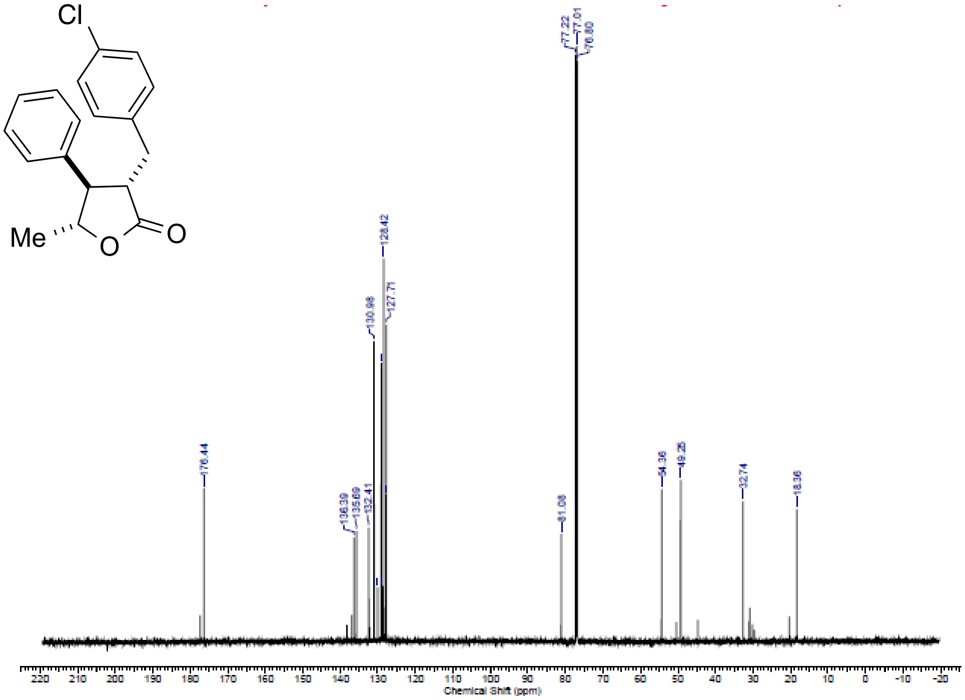
Cl
Me
O
O
176.44
136.39
135.69
132.41
130.98
128.42
127.71
81.08
77.22
77.01
76.80
54.36
49.25
32.74
18.36
220
210
200
190
180
170
160
150
140
130
120
110
100
90
80
70
60
50
40
30
20
10
0
-10
-20
Chemical Shift (ppm)

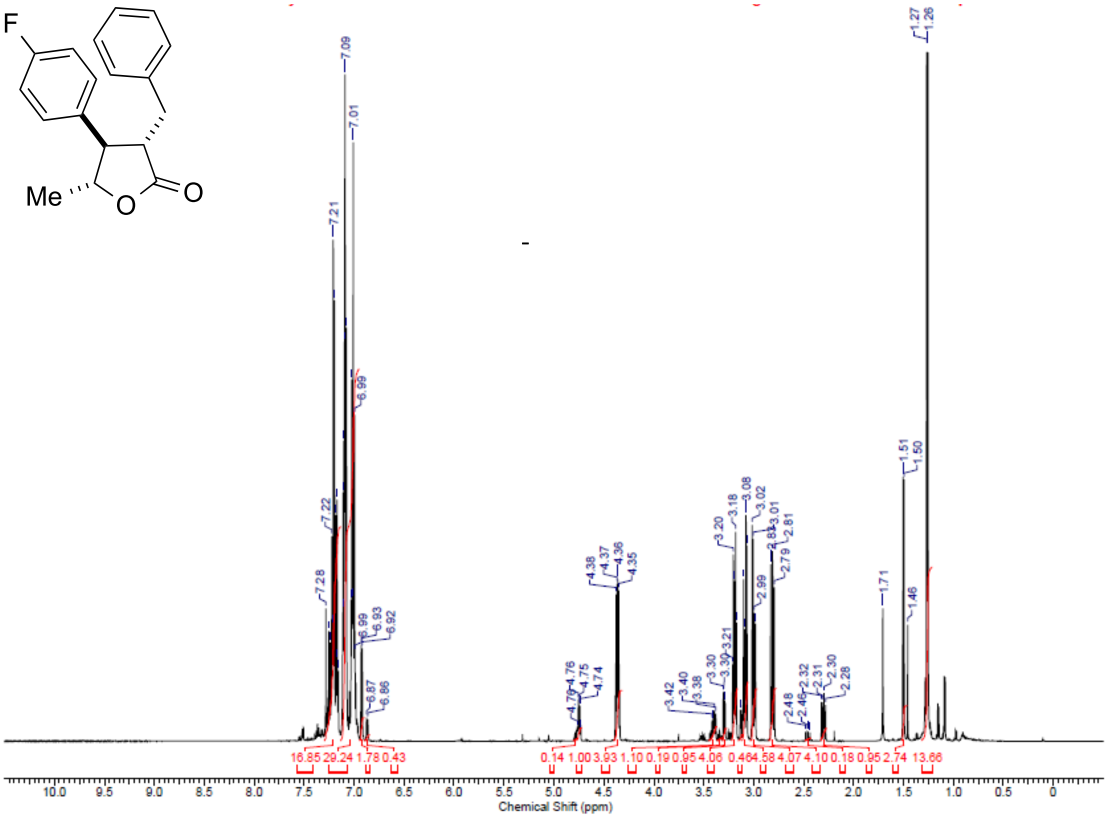
F
Me
O
O
7.09
7.01
7.21
6.99
7.22
7.28
6.99
6.93
6.92
6.87
6.86
4.76
4.75
4.74
4.38
4.37
4.36
4.35
3.42
3.40
3.38
3.30
3.30
3.21
3.20
3.18
3.08
3.02
3.01
2.99
2.83
2.81
2.79
2.48
2.46
2.32
2.31
2.30
2.28
1.71
1.51
1.50
1.46
1.27
1.26
16.85
29.24
1.78
0.43
0.14
1.00
3.93
1.10
0.19
0.95
4.06
0.46
4.58
4.07
4.10
0.18
0.95
2.74
13.66
10.0
9.5
9.0
8.5
8.0
7.5
7.0
6.5
6.0
5.5
5.0
4.5
4.0
3.5
3.0
2.5
2.0
1.5
1.0
0.5
0
Chemical Shift (ppm)

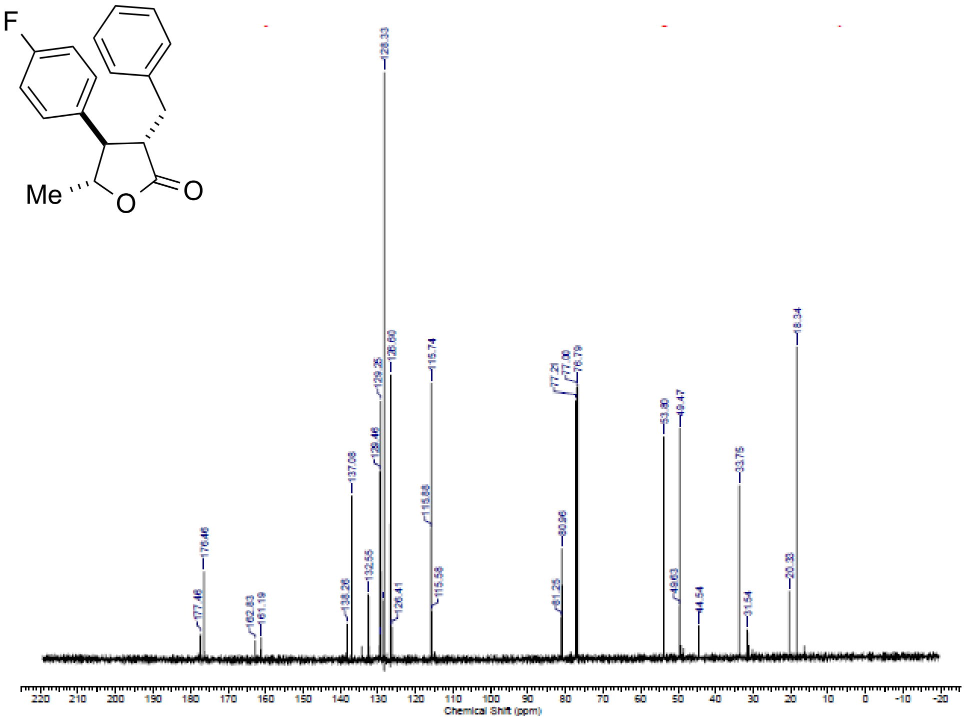
F
Me
O
O
128.33
177.46
176.46
162.83
161.19
138.26
137.08
132.55
129.46
129.25
126.60
126.41
115.88
115.74
115.58
81.25
80.96
77.21
77.00
76.79
53.80
49.63
49.47
44.54
33.75
31.54
20.33
18.34
220
210
200
190
180
170
160
150
140
130
120
110
100
90
80
70
60
50
40
30
20
10
0
-10
-20
Chemical Shift (ppm)

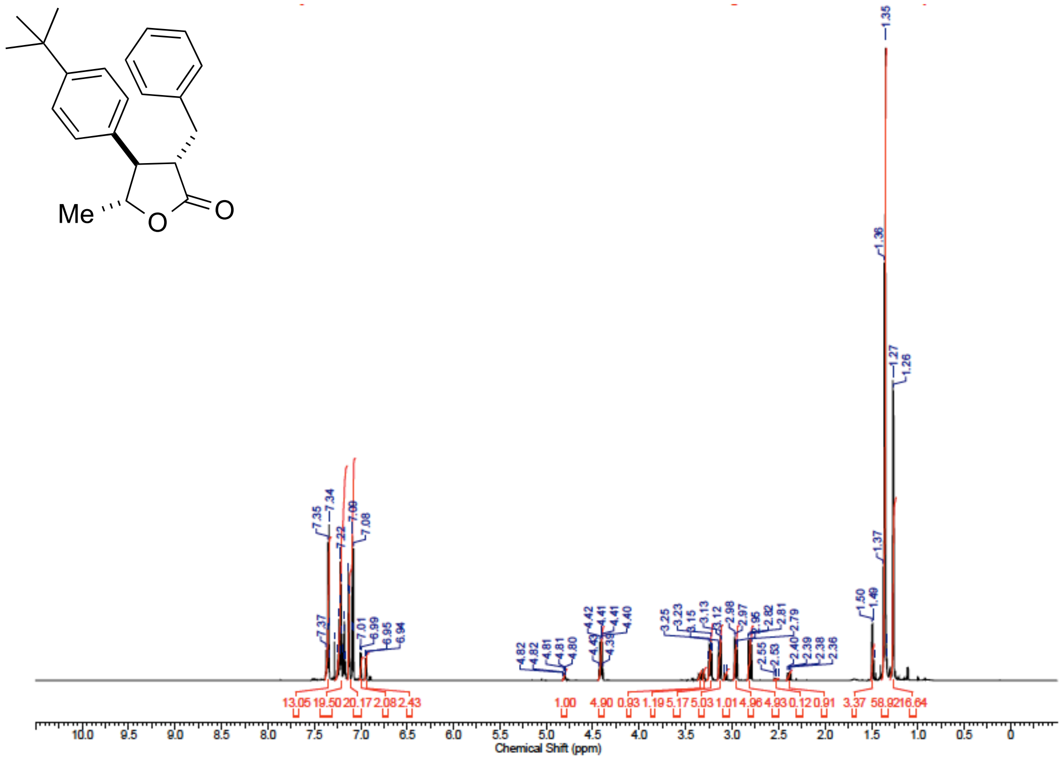
Me
O
O
7.37
7.35
7.34
7.22
7.09
7.08
7.01
6.99
6.95
6.94
4.82
4.82
4.81
4.81
4.80
4.43
4.42
4.41
4.41
4.40
4.39
3.25
3.23
3.15
3.13
3.12
2.98
2.97
2.96
2.82
2.81
2.79
2.55
2.53
2.40
2.39
2.38
2.36
1.50
1.49
1.37
1.36
1.35
1.27
1.26
13.05
19.50
20.17
2.08
2.43
1.00
4.90
0.93
1.19
5.17
5.03
1.01
4.96
4.93
0.12
0.91
3.37
58.92
16.64
10.0
9.5
9.0
8.5
8.0
7.5
7.0
6.5
6.0
5.5
5.0
4.5
4.0
3.5
3.0
2.5
2.0
1.5
1.0
0.5
0
Chemical Shift (ppm)

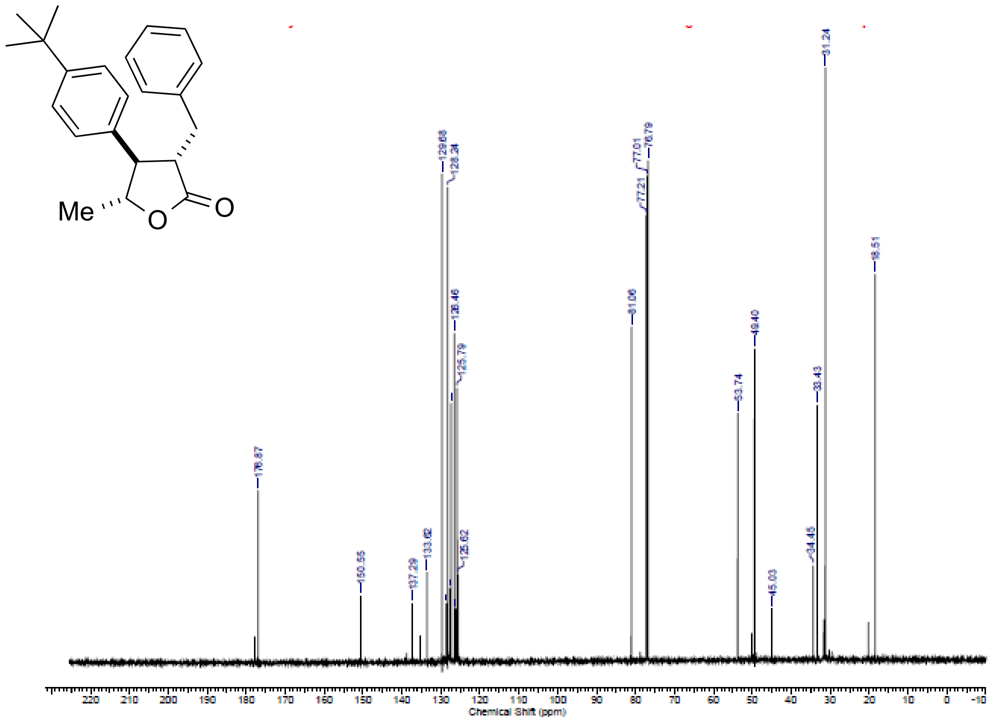
Me
O
O
176.87
150.55
137.29
133.62
129.68
128.24
126.46
125.79
125.62
81.06
77.21
77.01
76.79
53.74
49.40
45.03
34.45
33.43
31.24
18.51
220
210
200
190
180
170
160
150
140
130
120
110
100
90
80
70
60
50
40
30
20
10
0
-10
Chemical Shift (ppm)

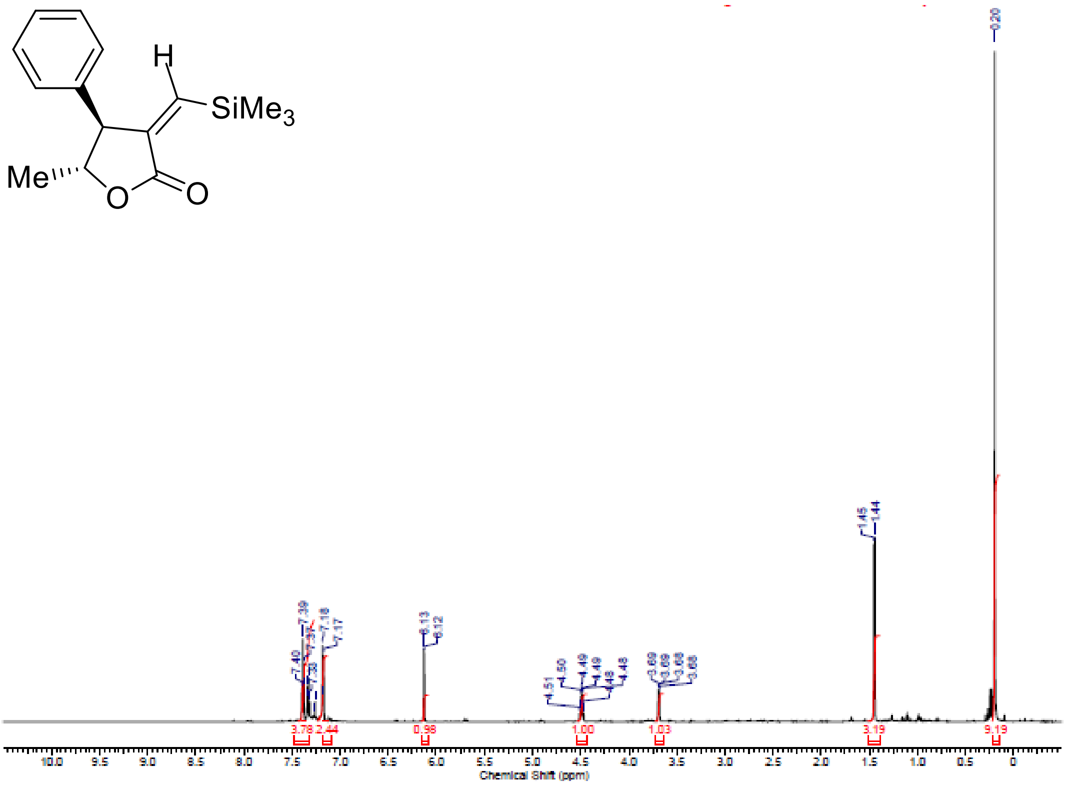
H
SiMe3
Me
O
O
7.40
7.39
7.37
7.33
7.18
7.17
6.13
6.12
4.51
4.50
4.49
4.49
4.48
4.48
3.69
3.69
3.68
3.68
1.45
1.44
0.20
3.78
2.44
0.98
1.00
1.03
3.19
9.19
10.0
9.5
9.0
8.5
8.0
7.5
7.0
6.5
6.0
5.5
5.0
4.5
4.0
3.5
3.0
2.5
2.0
1.5
1.0
0.5
0
Chemical Shift (ppm)

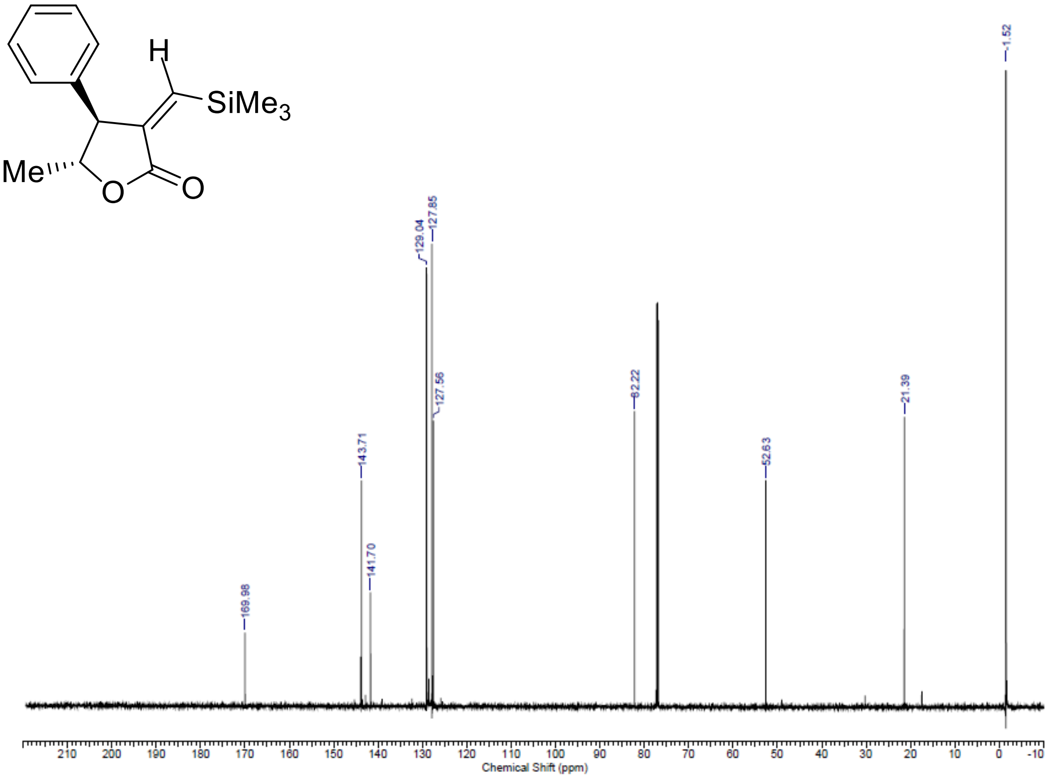
H
SiMe3
Me
O
O
169.98
143.71
141.70
129.04
127.85
127.56
82.22
52.63
21.39
-1.52
210
200
190
180
170
160
150
140
130
120
110
100
90
80
70
60
50
40
30
20
10
0
-10
Chemical Shift (ppm)

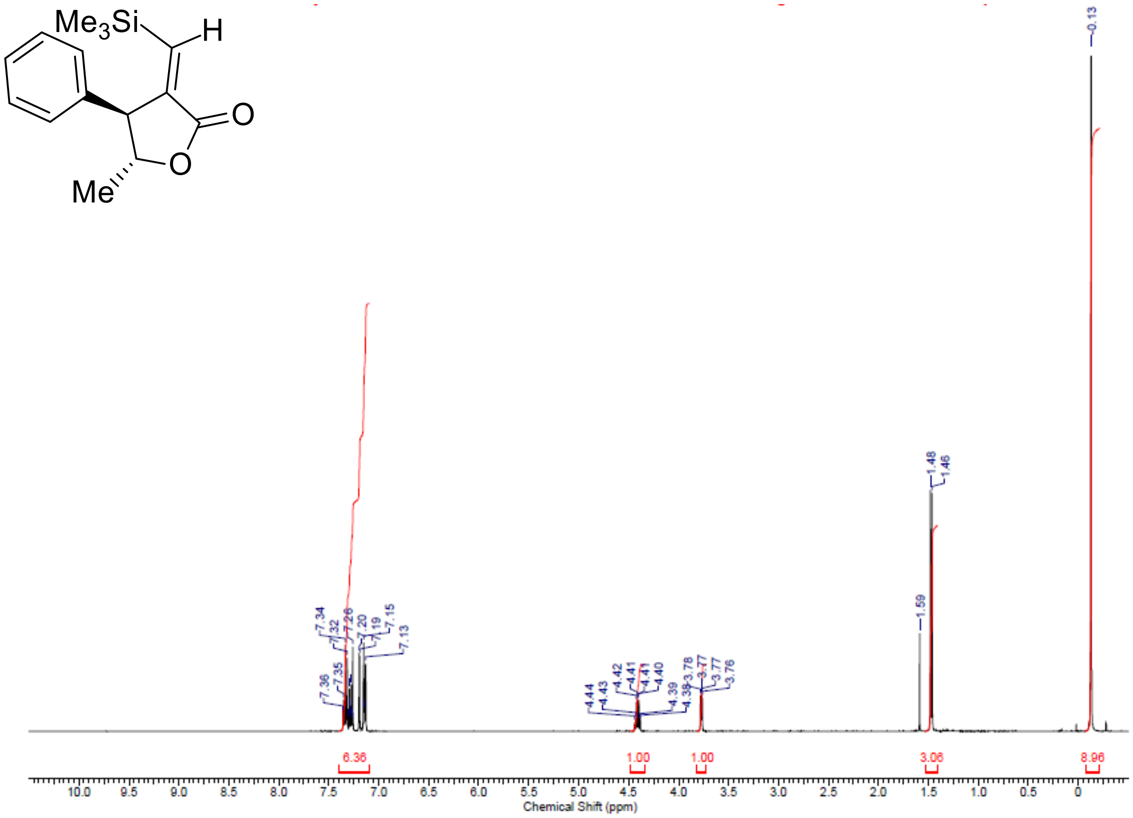
Me3Si
H
O
O
Me
7.36
7.35
7.34
7.32
7.26
7.20
7.19
7.15
7.13
4.44
4.43
4.42
4.41
4.41
4.40
4.39
4.39
3.78
3.77
3.77
3.76
1.59
1.48
1.46
-0.13
6.36
1.00
1.00
3.06
8.96
10.0
9.5
9.0
8.5
8.0
7.5
7.0
6.5
6.0
5.5
5.0
4.5
4.0
3.5
3.0
2.5
2.0
1.5
1.0
0.5
0
Chemical Shift (ppm)

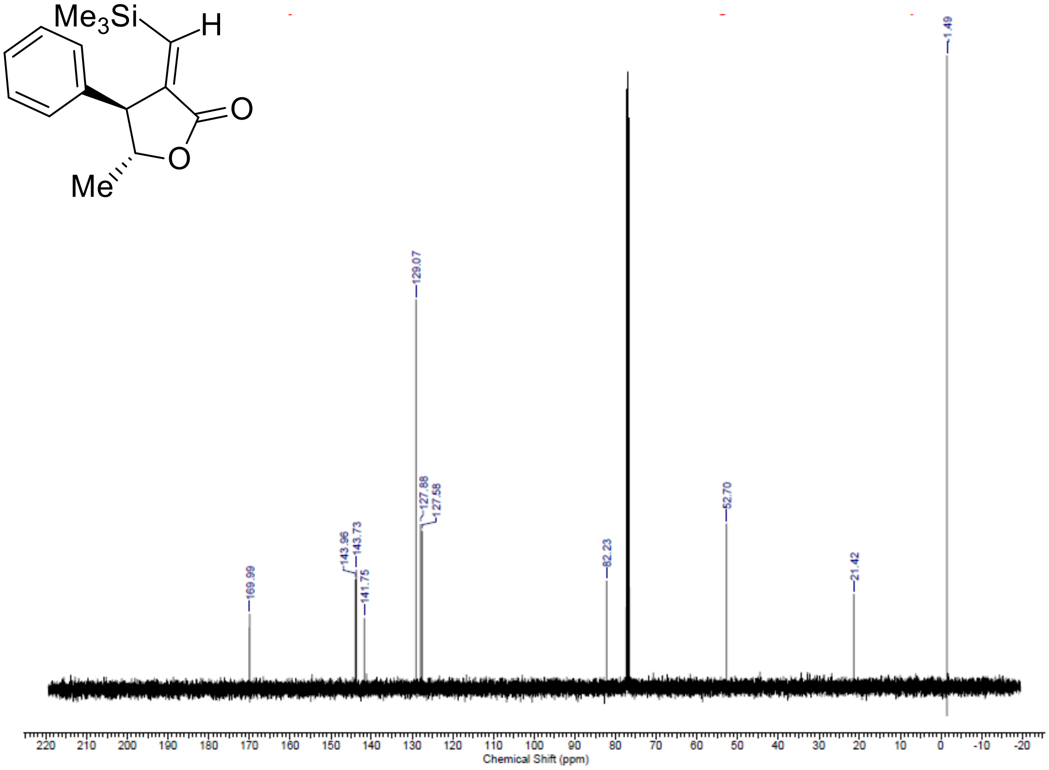
Me3Si
H
O
O
Me
169.99
143.96
143.73
141.75
129.07
127.88
127.58
82.23
52.70
21.42
-1.49
220
210
200
190
180
170
160
150
140
130
120
110
100
90
80
70
60
50
40
30
20
10
0
-10
-20
Chemical Shift (ppm)

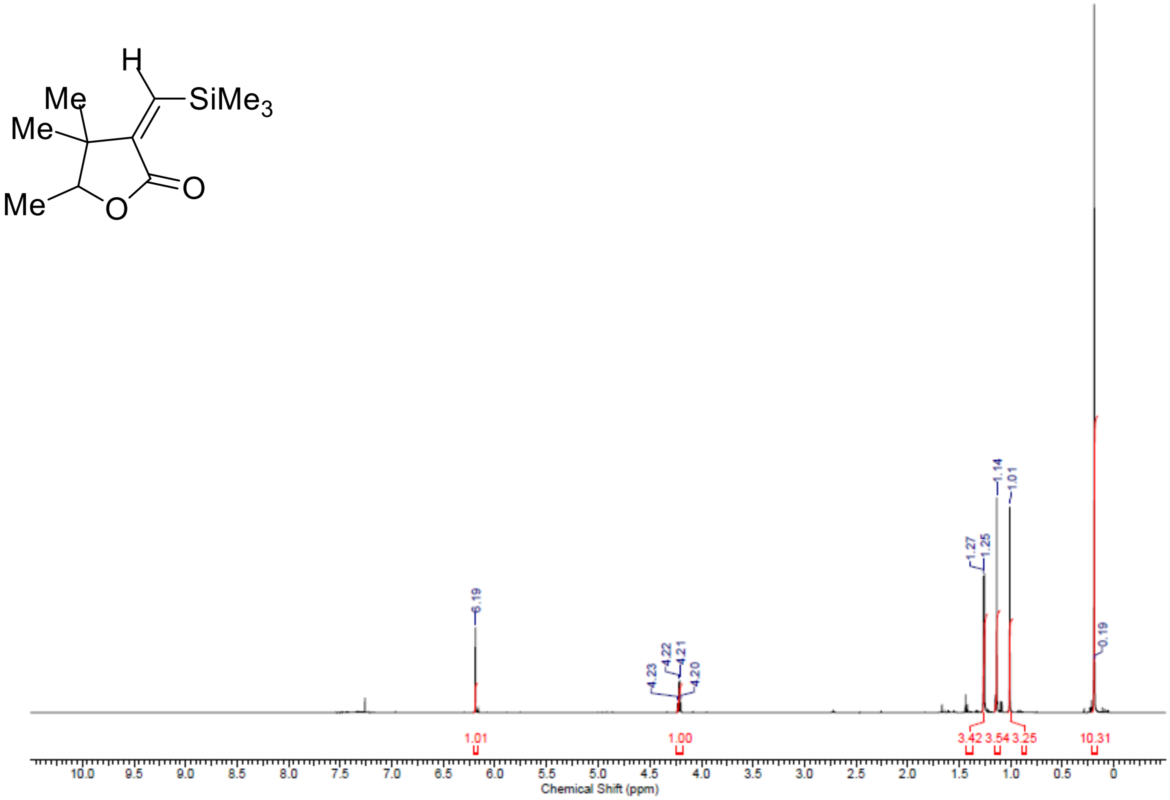
H
SiMe3
Me
Me
Me
O
O
6.19
4.23
4.22
4.21
4.20
1.27
1.25
1.14
1.01
0.19
1.01
1.00
3.42
3.54
3.25
10.31
10.0 9.5 9.0 8.5 8.0 7.5 7.0 6.5 6.0 5.5 5.0 4.5 4.0 3.5 3.0 2.5 2.0 1.5 1.0 0.5 0
Chemical Shift (ppm)

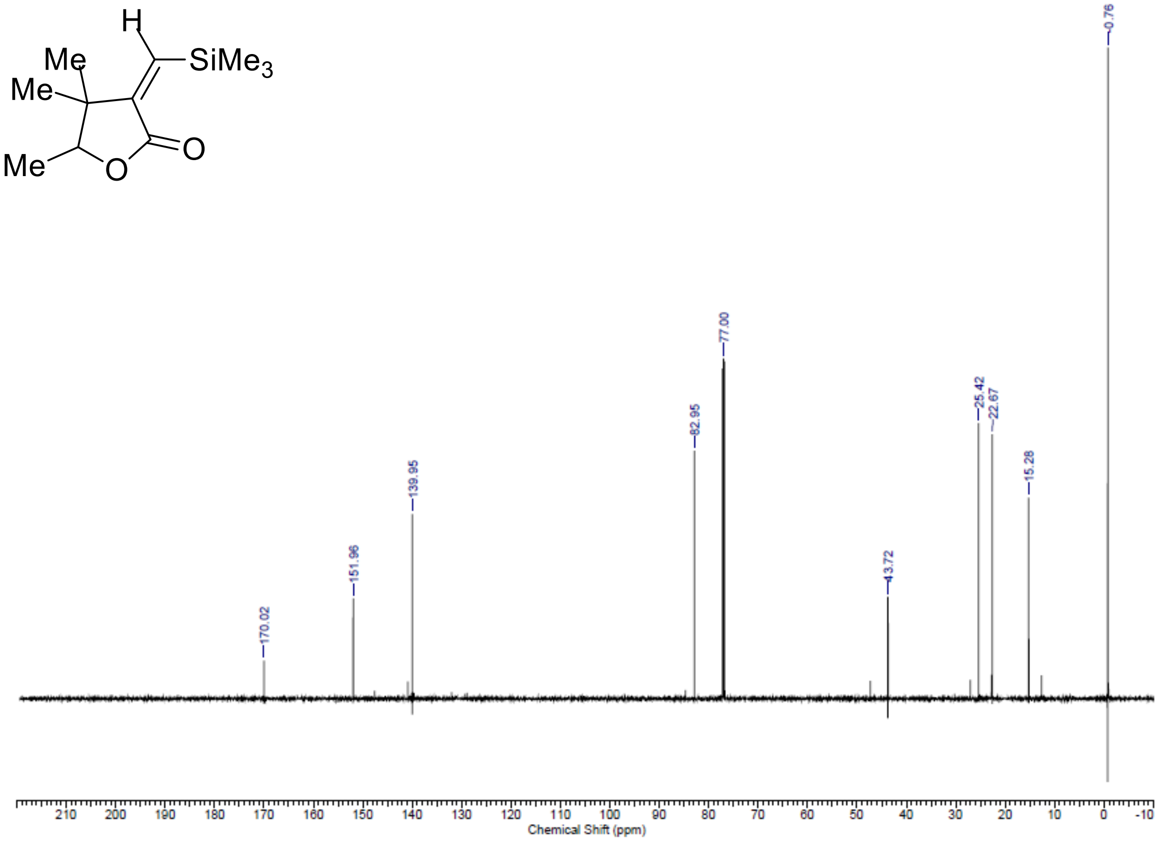
H
SiMe3
Me
Me
Me
O
O
170.02
151.96
139.95
82.95
77.00
43.72
25.42
22.67
15.28
-0.76
210 200 190 180 170 160 150 140 130 120 110 100 90 80 70 60 50 40 30 20 10 0 -10
Chemical Shift (ppm)

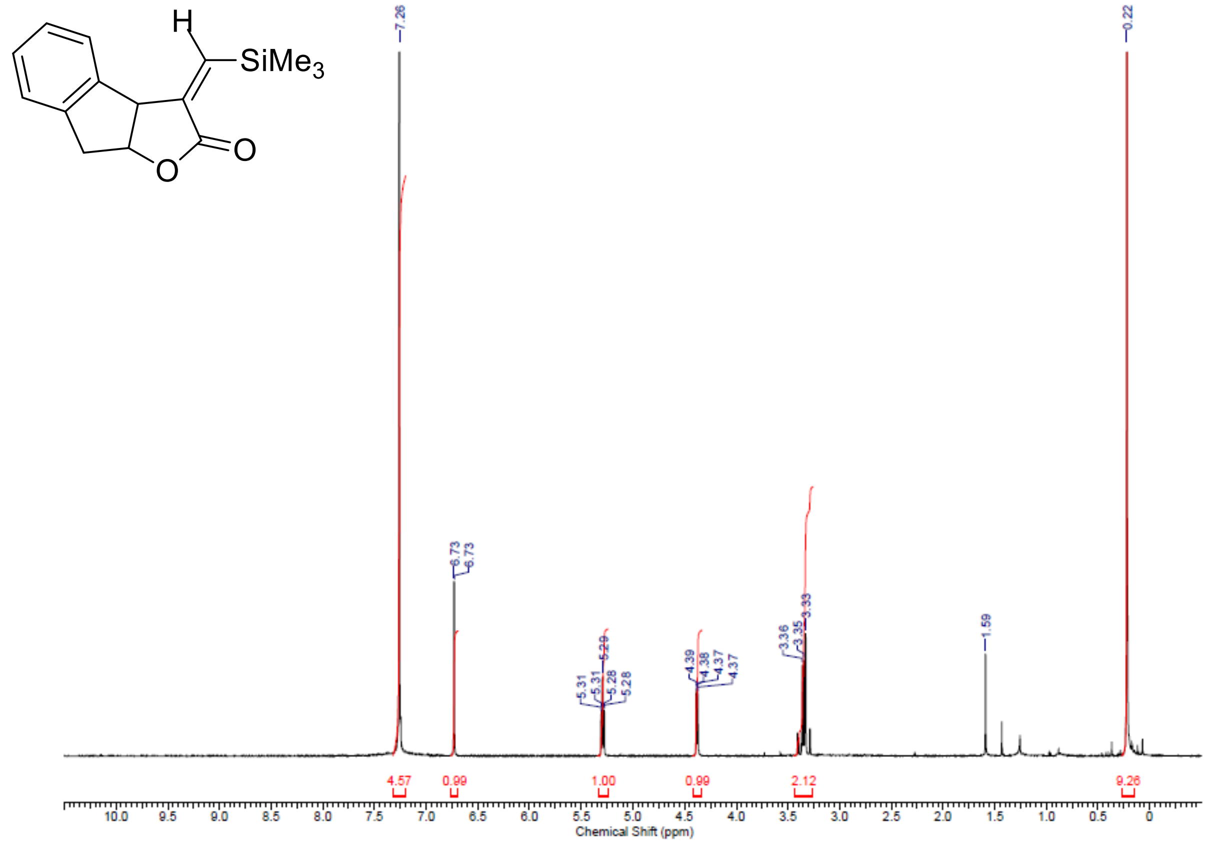
H
SiMe3
O
O
7.26
6.73
6.73
5.31
5.31
5.29
5.28
5.28
4.39
4.38
4.37
4.37
3.36
3.35
3.33
1.59
0.22
4.57
0.99
1.00
0.99
2.12
9.26
10.0 9.5 9.0 8.5 8.0 7.5 7.0 6.5 6.0 5.5 5.0 4.5 4.0 3.5 3.0 2.5 2.0 1.5 1.0 0.5 0
Chemical Shift (ppm)

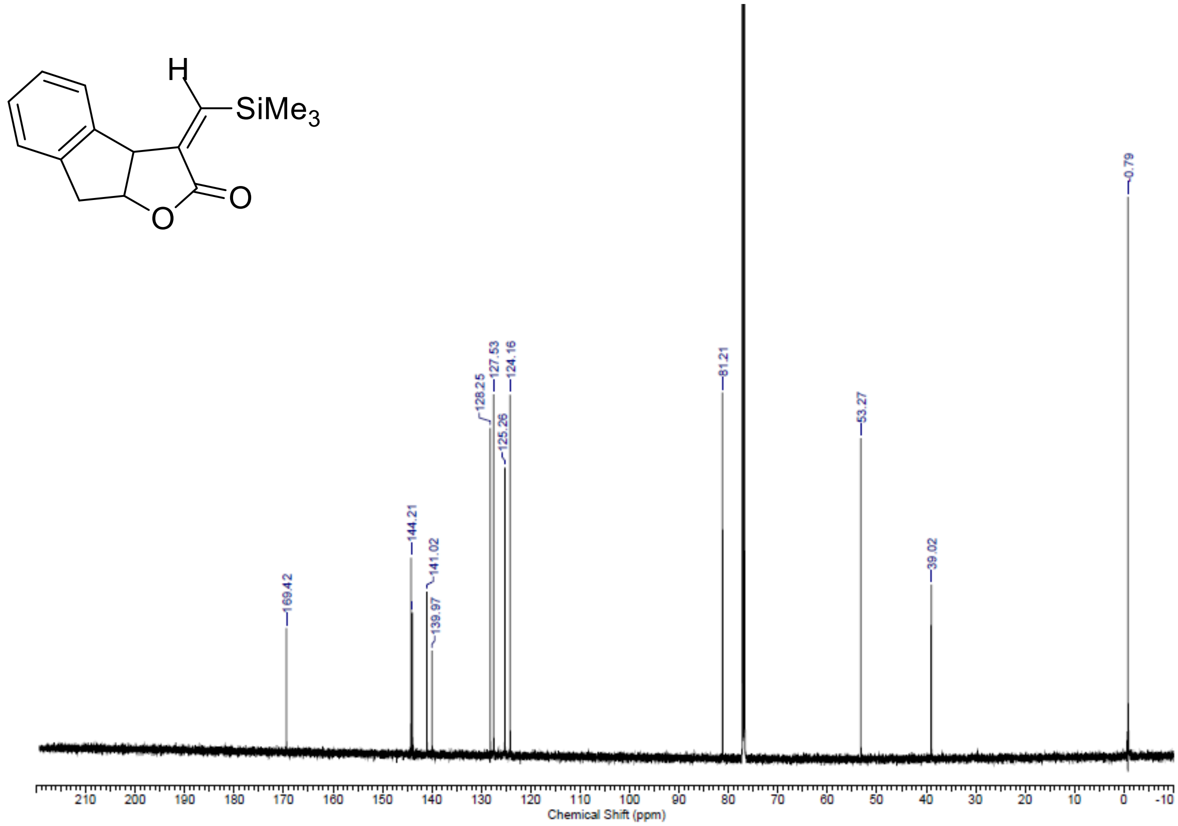
H
SiMe3
O
O
169.42
144.21
141.02
139.97
128.25
127.53
125.26
124.16
81.21
53.27
39.02
0.79
210 200 190 180 170 160 150 140 130 120 110 100 90 80 70 60 50 40 30 20 10 0 -10
Chemical Shift (ppm)

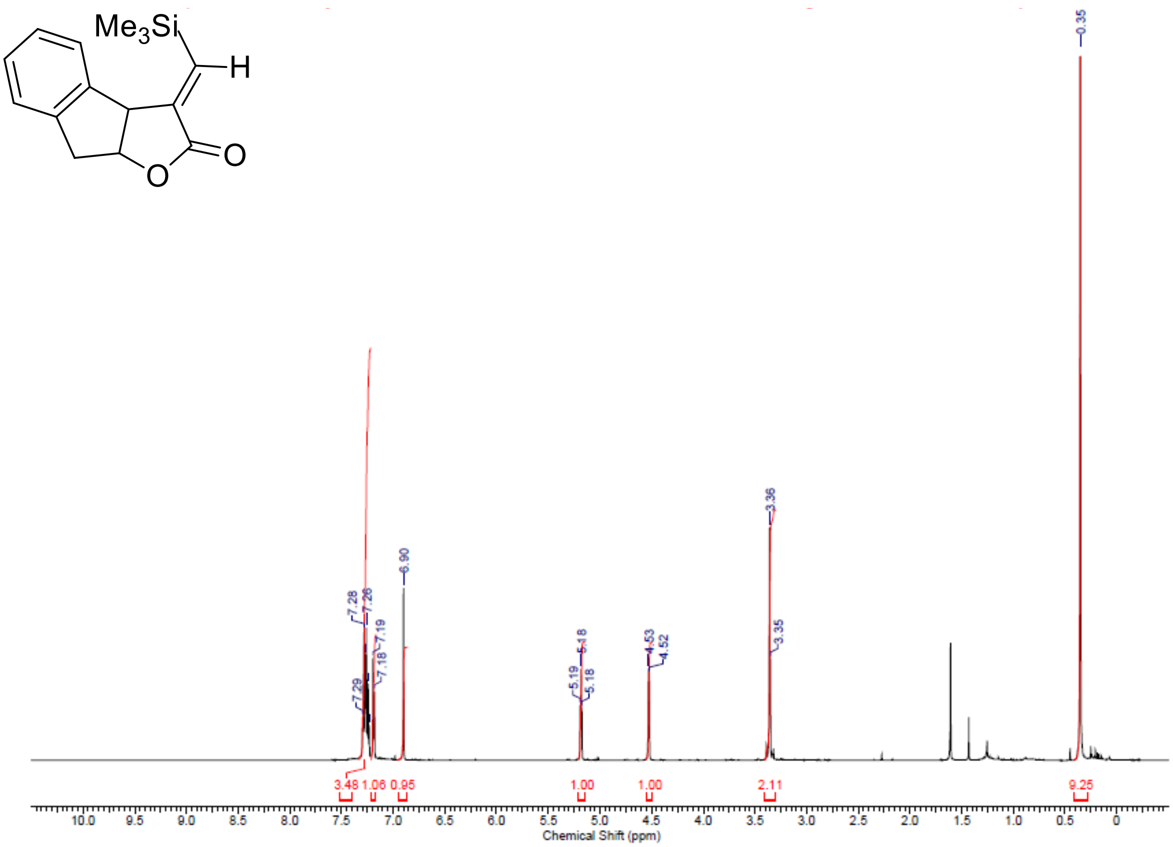
Me3Si
H
O
O
7.29
7.28
7.26
7.19
7.18
6.90
5.19
5.18
5.18
5.18
4.53
4.52
3.36
3.35
0.35
3.48
1.06
0.95
1.00
1.00
2.11
9.25
10.0 9.5 9.0 8.5 8.0 7.5 7.0 6.5 6.0 5.5 5.0 4.5 4.0 3.5 3.0 2.5 2.0 1.5 1.0 0.5 0
Chemical Shift (ppm)

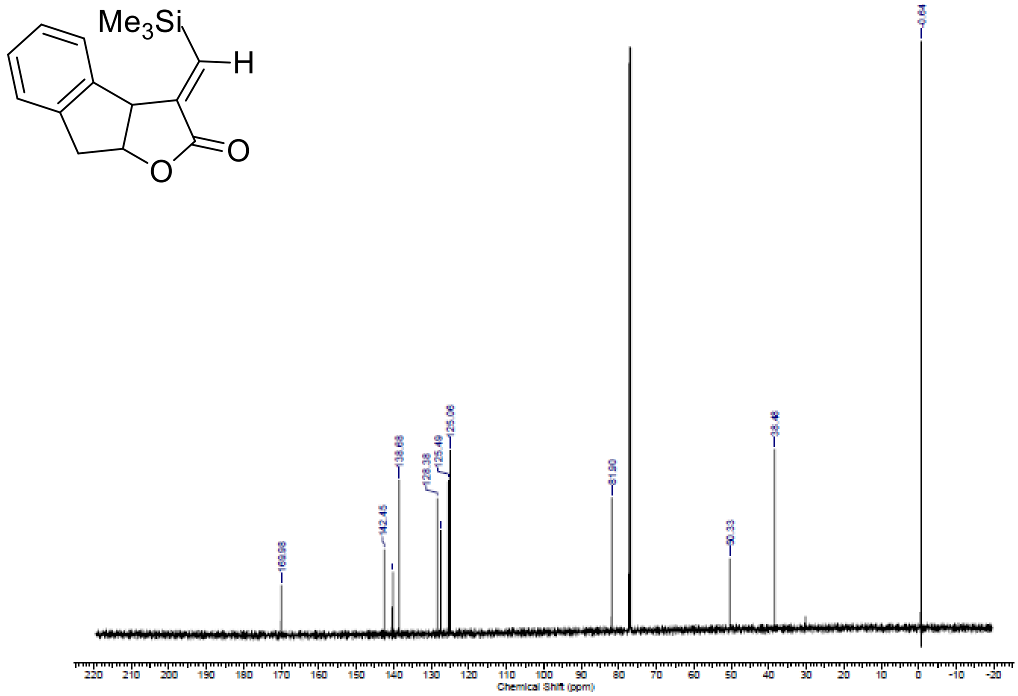
Me3Si
H
O
O
169.98
142.45
138.68
128.38
125.49
125.06
81.90
50.33
38.48
-0.64
220 210 200 190 180 170 160 150 140 130 120 110 100 90 80 70 60 50 40 30 20 10 0 -10 -20
Chemical Shift (ppm)

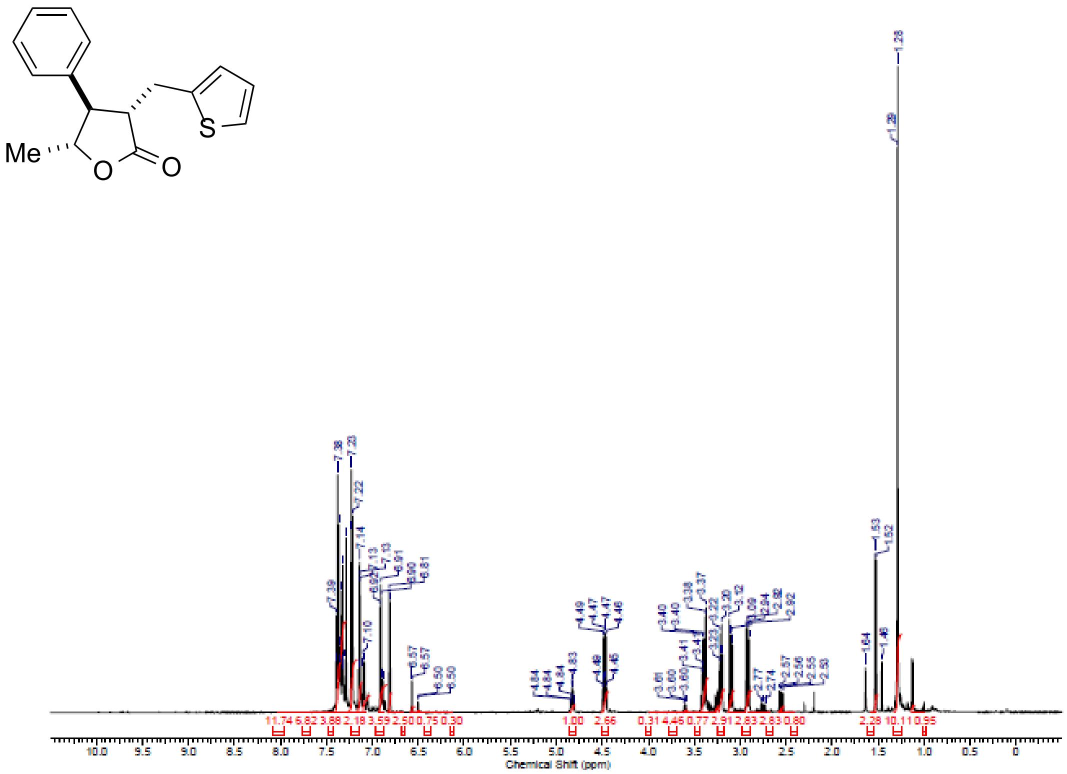
Me
O
O
S
7.39
7.38
7.23
7.22
7.14
7.13
7.13
7.10
6.92
6.91
6.90
6.81
6.57
6.57
6.50
6.50
4.84
4.84
4.84
4.83
4.49
4.48
4.47
4.47
4.46
4.45
3.61
3.60
3.60
3.41
3.40
3.40
3.38
3.37
3.23
3.22
3.20
3.12
3.09
2.94
2.92
2.92
2.77
2.74
2.57
2.56
2.55
2.53
1.64
1.53
1.52
1.48
1.29
1.28
11.74
6.82
3.88
2.18
3.59
2.50
0.75
0.30
1.00
2.66
0.31
4.46
0.77
2.91
2.83
2.83
0.80
2.28
10.11
0.95
10.0
9.5
9.0
8.5
8.0
7.5
7.0
6.5
6.0
5.5
5.0
4.5
4.0
3.5
3.0
2.5
2.0
1.5
1.0
0.5
0
Chemical Shift (ppm)

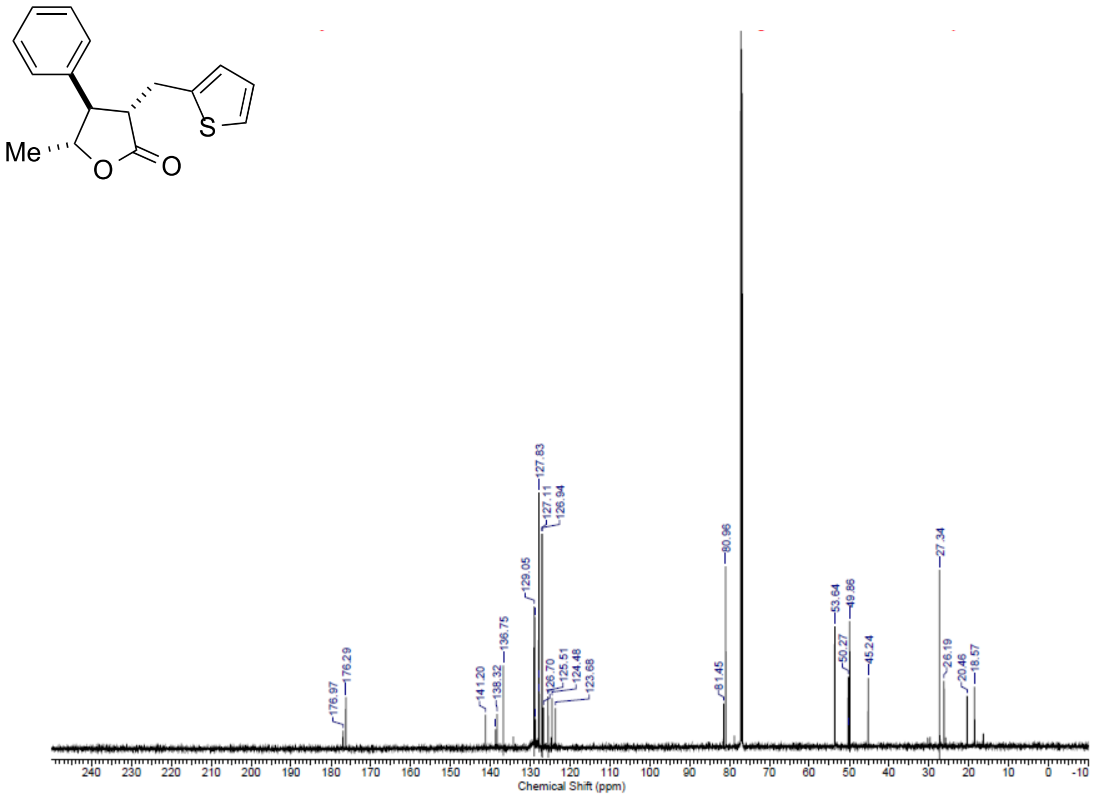
Me
O
O
S
176.97
176.29
141.20
138.32
136.75
129.05
127.83
127.11
126.94
126.70
125.51
124.48
123.68
81.45
80.96
53.64
50.27
49.86
45.24
27.34
26.19
20.46
18.57
240
230
220
210
200
190
180
170
160
150
140
130
120
110
100
90
80
70
60
50
40
30
20
10
0
-10
Chemical Shift (ppm)

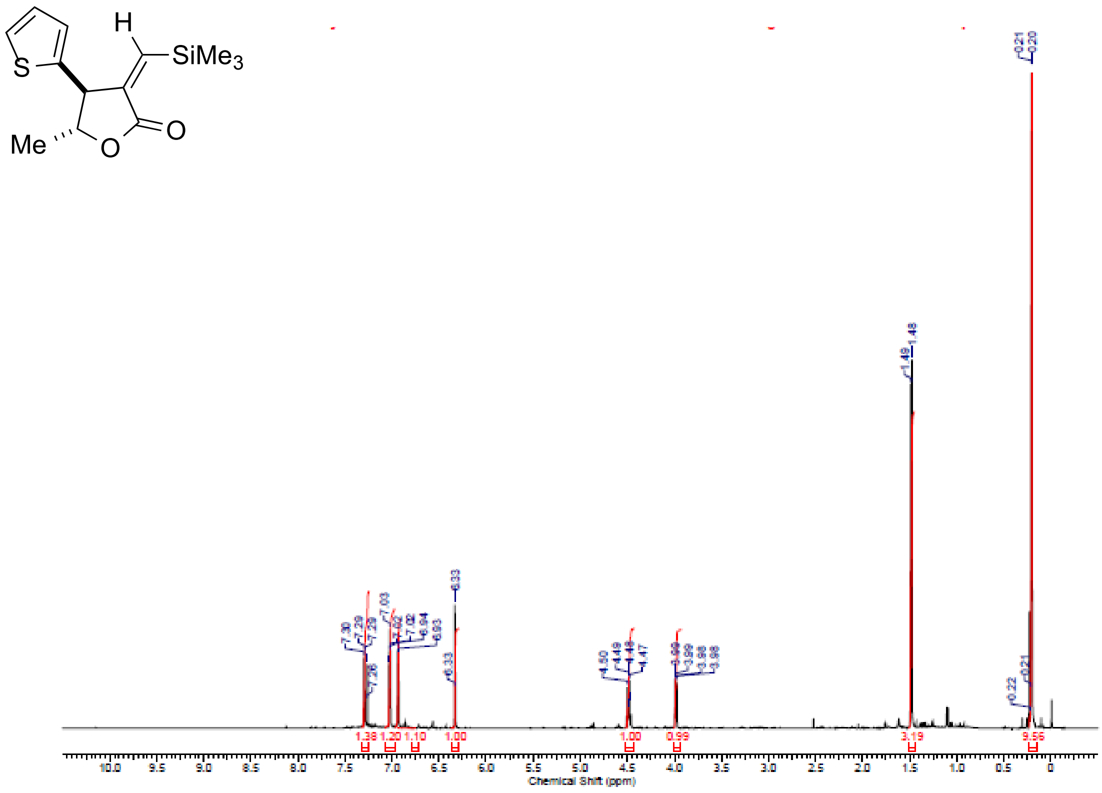
H
SiMe3
S
Me
O
O
7.30
7.29
7.29
7.26
7.03
7.02
7.02
6.94
6.93
6.33
6.33
4.50
4.49
4.48
4.47
3.99
3.99
3.98
3.98
1.49
1.48
0.22
0.21
0.21
0.20
1.38
1.20
1.10
1.00
1.00
0.99
3.19
9.56
10.0 9.5 9.0 8.5 8.0 7.5 7.0 6.5 6.0 5.5 5.0 4.5 4.0 3.5 3.0 2.5 2.0 1.5 1.0 0.5 0
Chemical Shift (ppm)

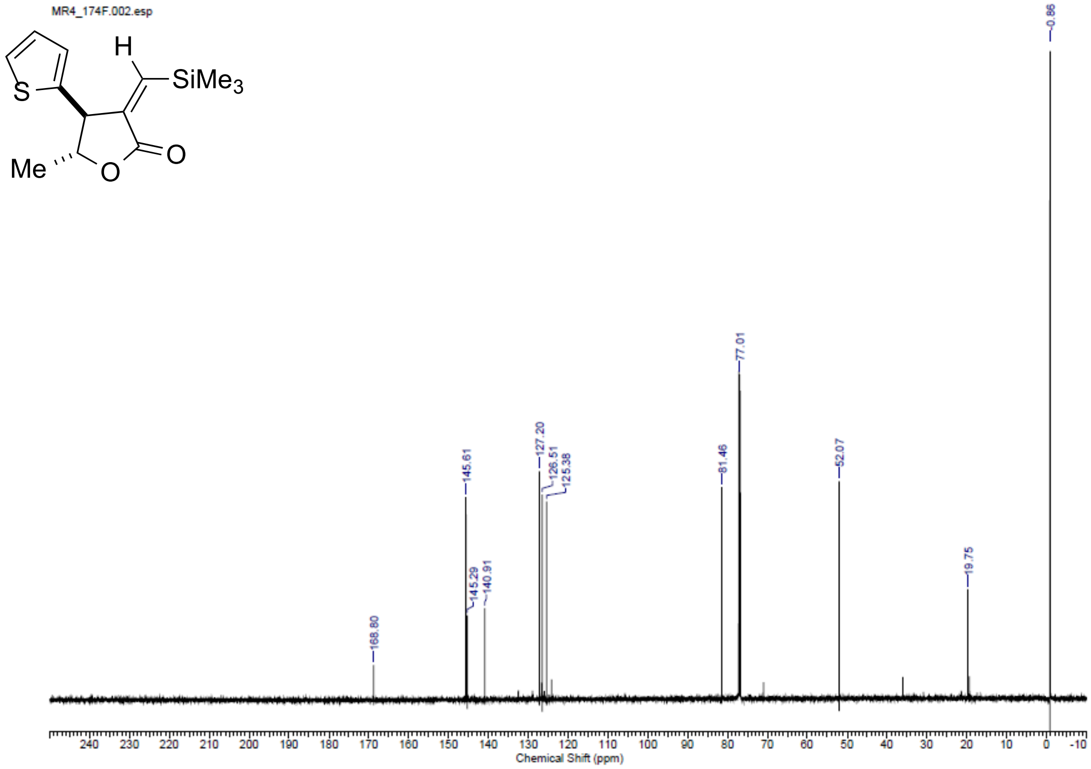
MR4_174F.002.esp
H
SiMe3
S
Me
O
O
168.80
145.61
145.29
140.91
127.20
126.51
125.38
81.46
77.01
52.07
19.75
-0.86
240 230 220 210 200 190 180 170 160 150 140 130 120 110 100 90 80 70 60 50 40 30 20 10 0 -10
Chemical Shift (ppm)

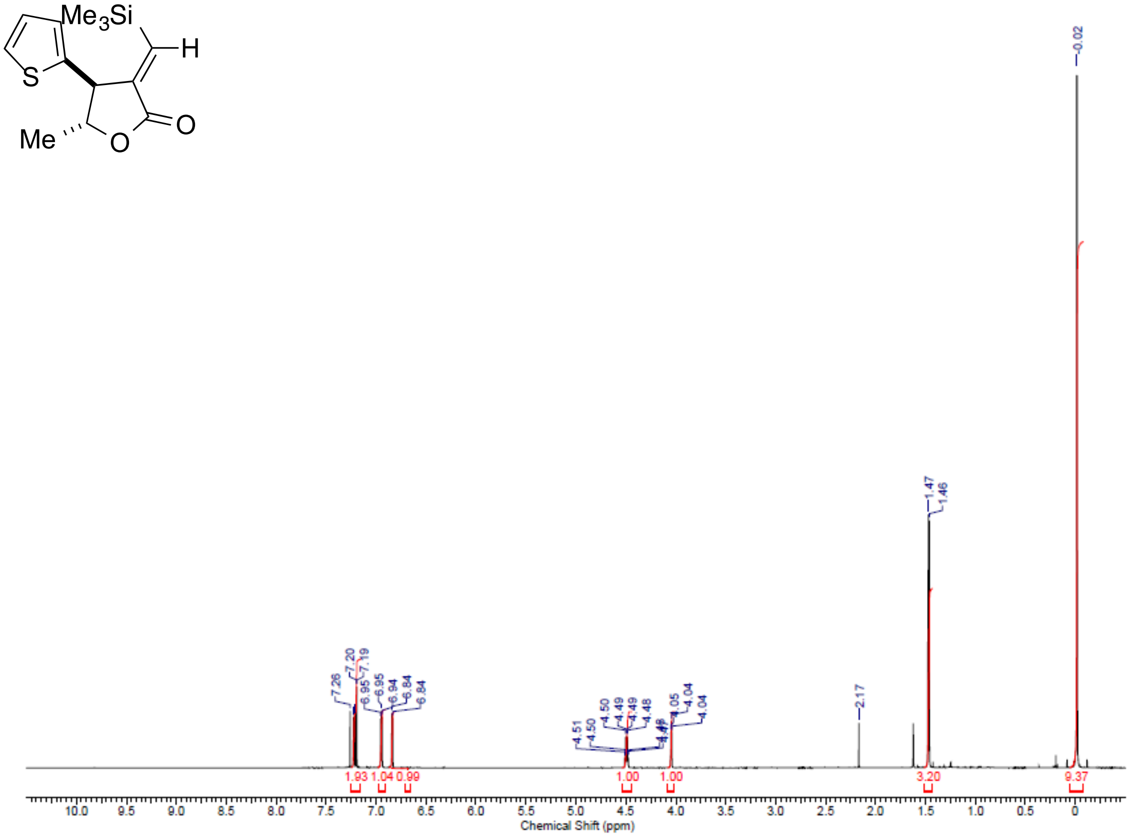

Me3Si
H
S
Me
O
O
7.26
7.20
7.19
6.95
6.95
6.94
6.84
6.84
4.51
4.50
4.50
4.49
4.49
4.48
4.48
4.05
4.04
4.04
4.04
2.17
1.47
1.46
-0.02
1.93
1.04
0.99
1.00
1.00
3.20
9.37
10.0 9.5 9.0 8.5 8.0 7.5 7.0 6.5 6.0 5.5 5.0 4.5 4.0 3.5 3.0 2.5 2.0 1.5 1.0 0.5 0
Chemical Shift (ppm)

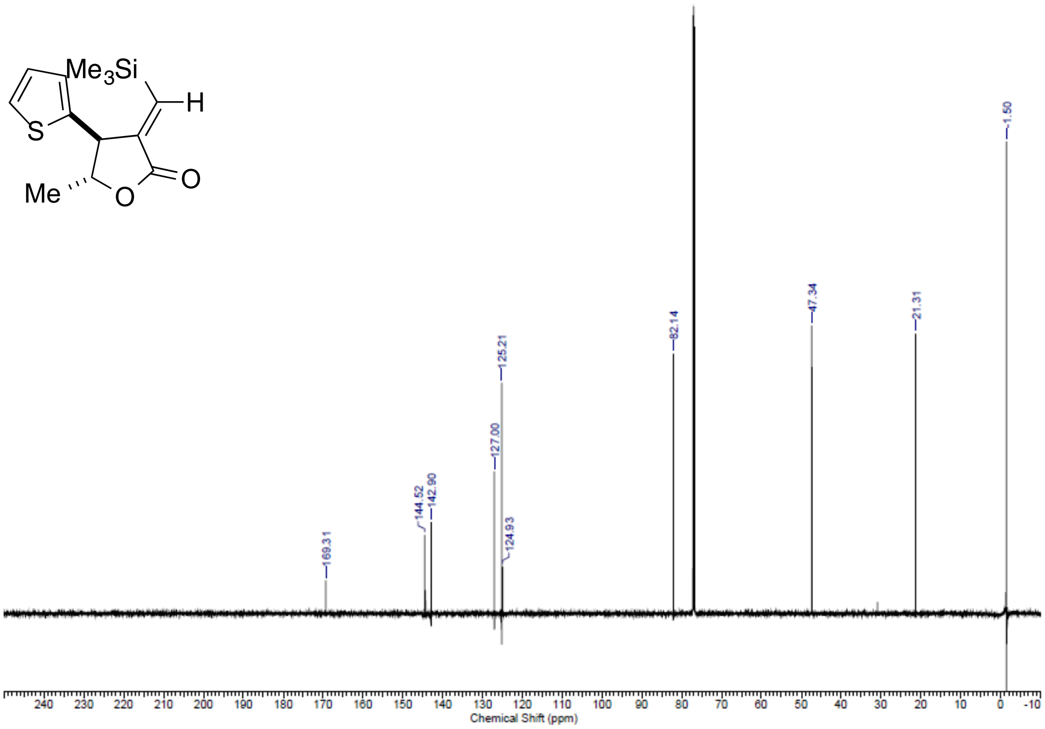

Me3Si
H
S
Me
O
O
169.31
144.52
142.90
127.00
125.21
124.93
82.14
47.34
21.31
-1.50
240 230 220 210 200 190 180 170 160 150 140 130 120 110 100 90 80 70 60 50 40 30 20 10 0 -10
Chemical Shift (ppm)

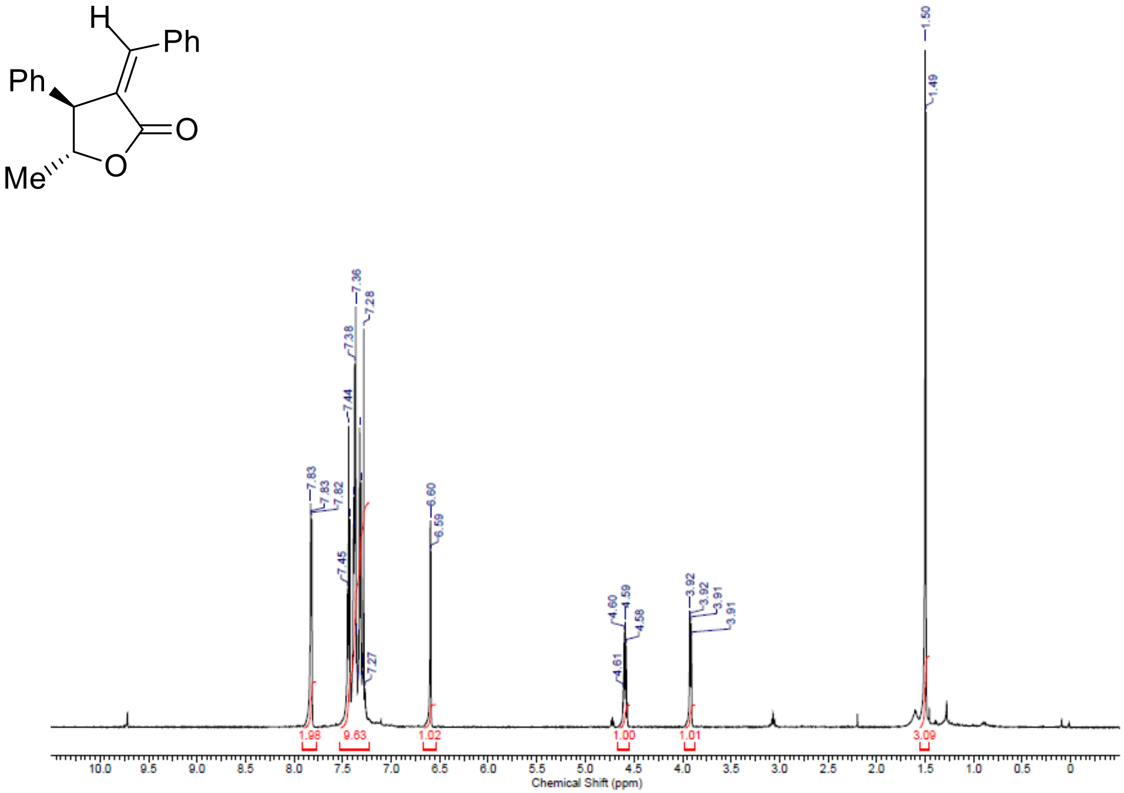
H
Ph
Ph
O
Me
O
1.50
1.49
7.36
7.28
7.38
7.44
7.83
7.83
7.82
7.45
7.27
6.60
6.59
4.60
4.59
4.58
4.61
3.92
3.92
3.91
3.91
1.98
9.63
1.02
1.00
1.01
3.09
10.0 9.5 9.0 8.5 8.0 7.5 7.0 6.5 6.0 5.5 5.0 4.5 4.0 3.5 3.0 2.5 2.0 1.5 1.0 0.5 0
Chemical Shift (ppm)

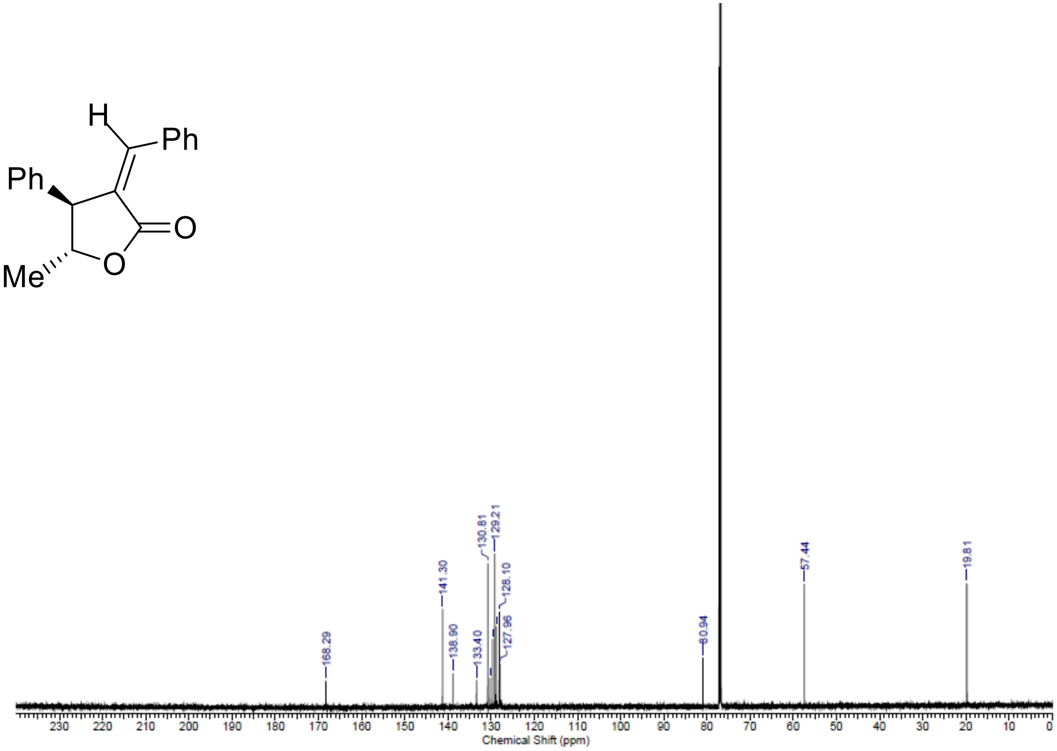
H
Ph
Ph
O
Me
O
168.29
141.30
138.90
133.40
130.81
129.21
128.10
127.96
80.94
57.44
19.81
230 220 210 200 190 180 170 160 150 140 130 120 110 100 90 80 70 60 50 40 30 20 10 0
Chemical Shift (ppm)

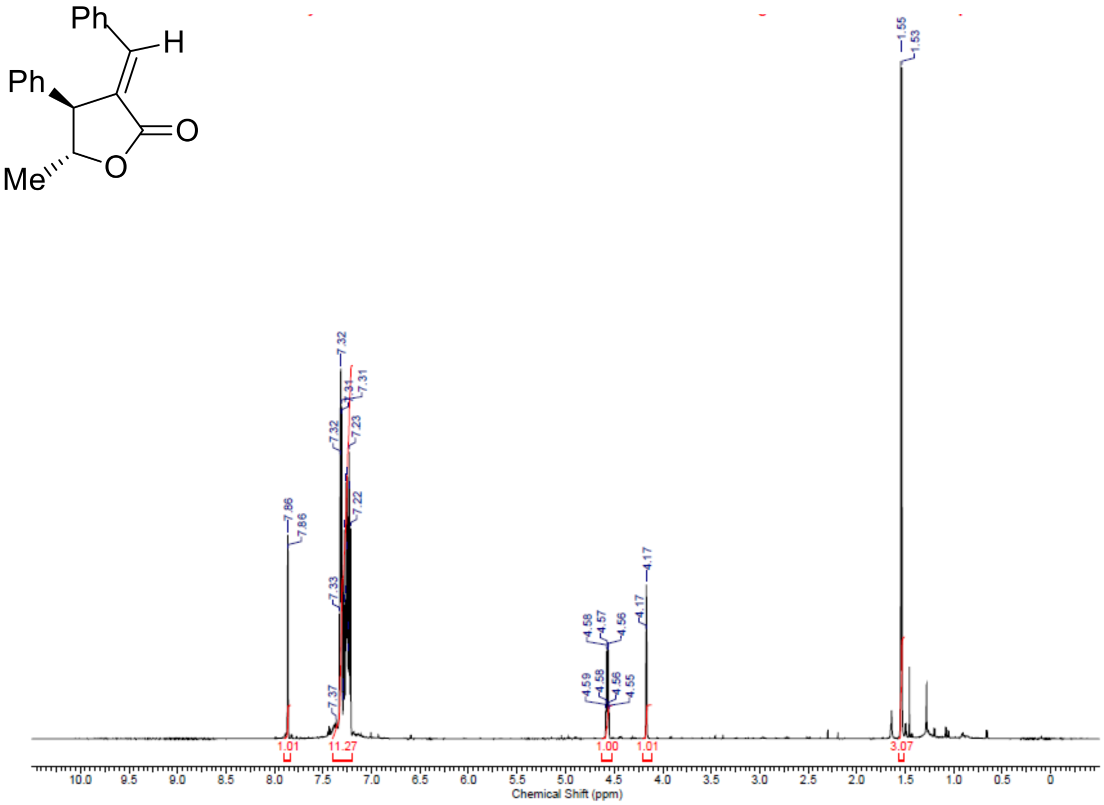
Ph
H
Ph
O
Me
O
7.86
7.86
7.32
7.32
7.31
7.31
7.23
7.22
7.33
7.37
4.58
4.57
4.56
4.59
4.58
4.56
4.55
4.17
4.17
1.55
1.53
1.01
11.27
1.00
1.01
3.07
10.0
9.5
9.0
8.5
8.0
7.5
7.0
6.5
6.0
5.5
5.0
4.5
4.0
3.5
3.0
2.5
2.0
1.5
1.0
0.5
0
Chemical Shift (ppm)

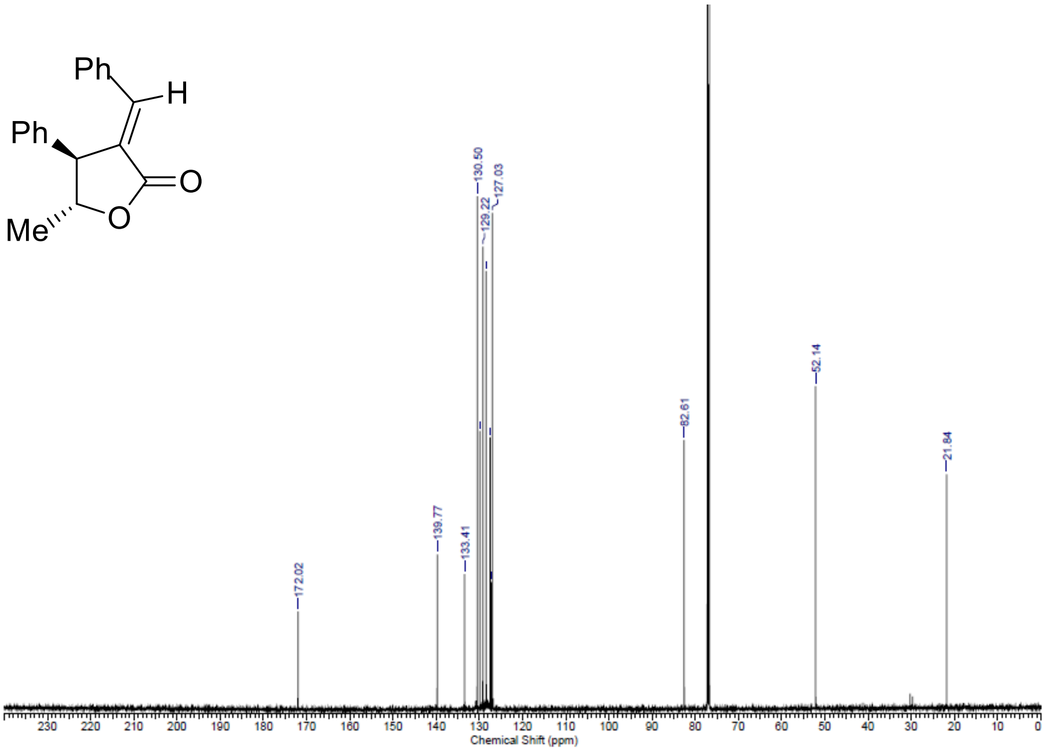
Ph
H
Ph
O
Me
O
172.02
139.77
133.41
130.50
129.22
127.03
82.61
52.14
21.84
230
220
210
200
190
180
170
160
150
140
130
120
110
100
90
80
70
60
50
40
30
20
10
0
Chemical Shift (ppm)

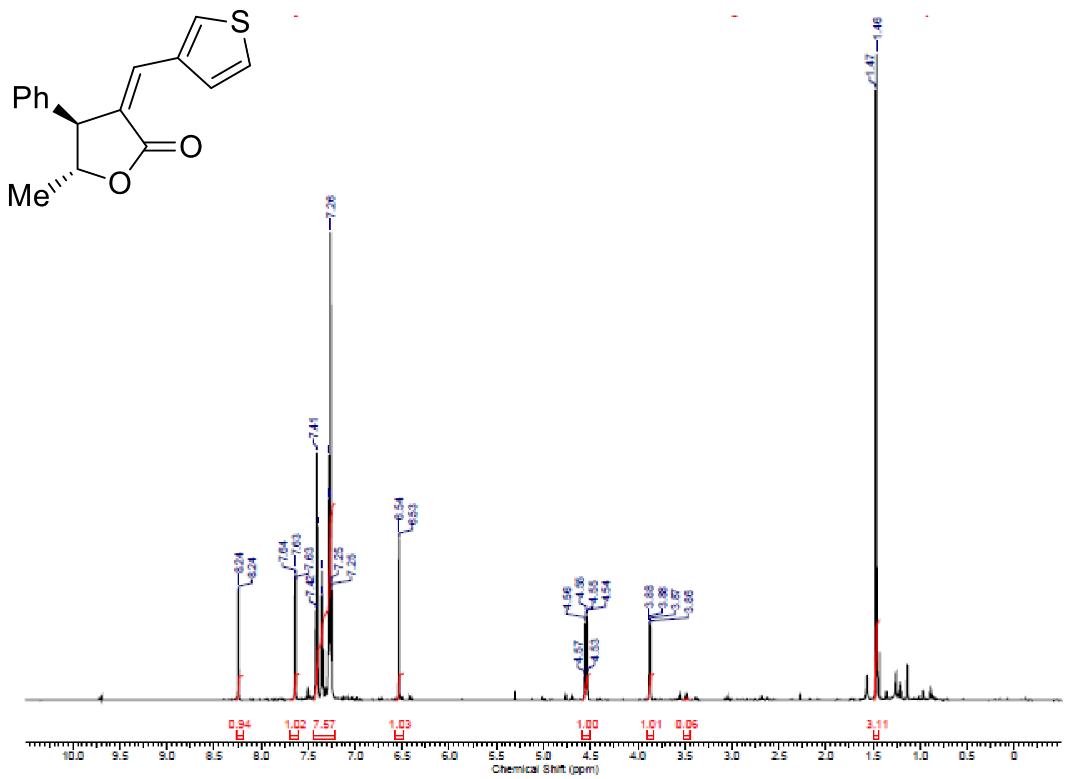
S
Ph
O
Me
O
8.24
8.24
7.64
7.63
7.63
7.42
7.41
7.26
7.25
7.25
6.54
6.53
4.56
4.56
4.55
4.54
4.57
4.53
3.88
3.88
3.87
3.86
1.47
1.46
0.94
1.02
7.57
1.03
1.00
1.01
0.06
3.11
10.0
9.5
9.0
8.5
8.0
7.5
7.0
6.5
6.0
5.5
5.0
4.5
4.0
3.5
3.0
2.5
2.0
1.5
1.0
0.5
0
Chemical Shift (ppm)

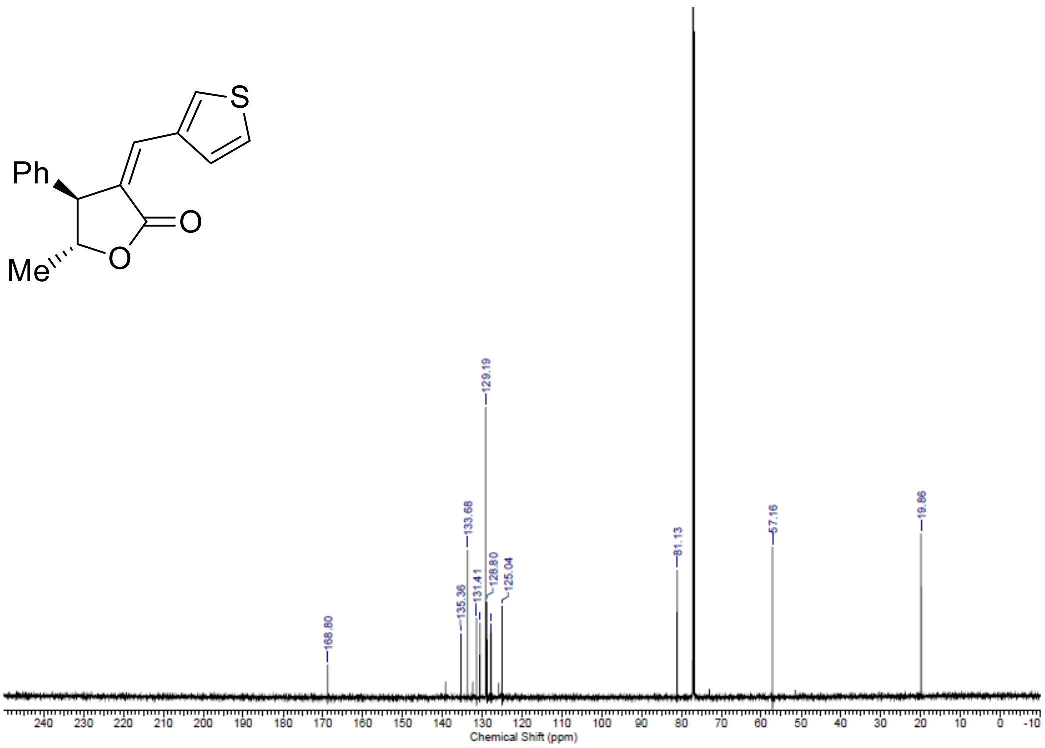
S
Ph
O
Me
O
168.80
135.36
133.68
131.41
129.19
128.80
125.04
81.13
57.16
19.86
240
230
220
210
200
190
180
170
160
150
140
130
120
110
100
90
80
70
60
50
40
30
20
10
0
-10
Chemical Shift (ppm)

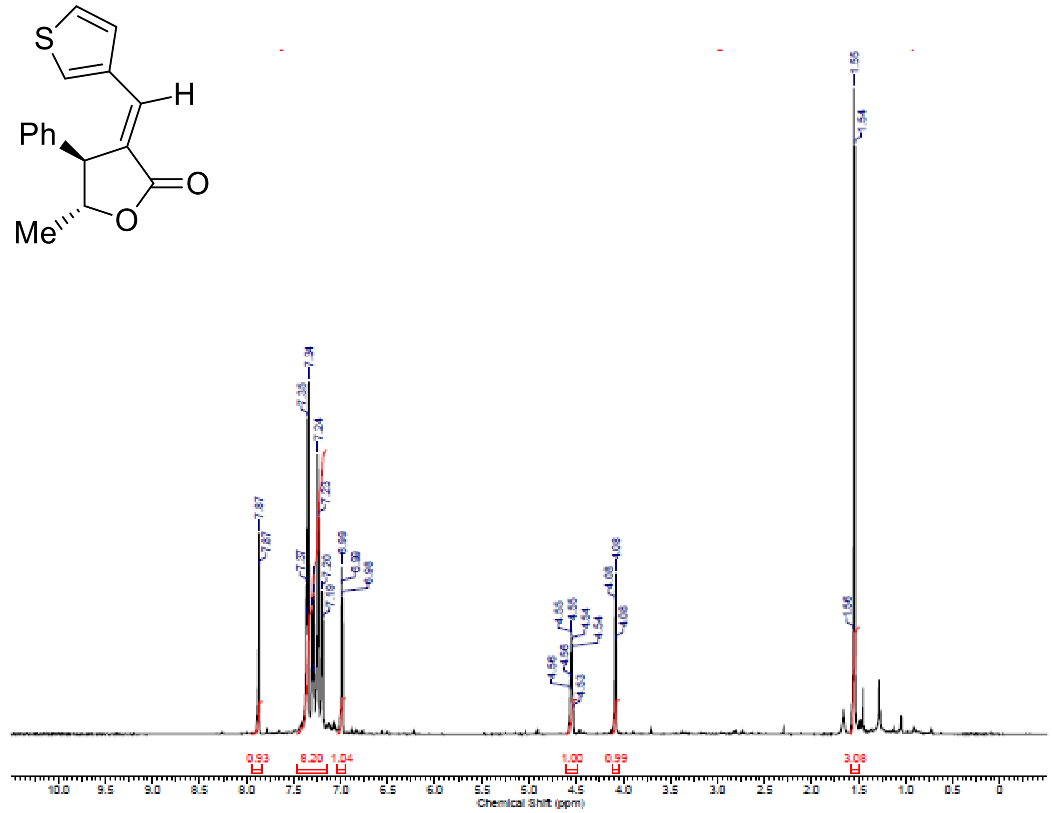
S
H
Ph
O
Me
O
7.87
7.87
7.37
7.35
7.34
7.24
7.23
7.20
7.19
6.99
6.99
6.98
4.56
4.56
4.55
4.55
4.54
4.54
4.53
4.08
4.08
4.08
1.56
1.55
1.54
0.93
8.20
1.04
1.00
0.99
3.09
10.0
9.5
9.0
8.5
8.0
7.5
7.0
6.5
6.0
5.5
5.0
4.5
4.0
3.5
3.0
2.5
2.0
1.5
1.0
0.5
0
Chemical Shift (ppm)

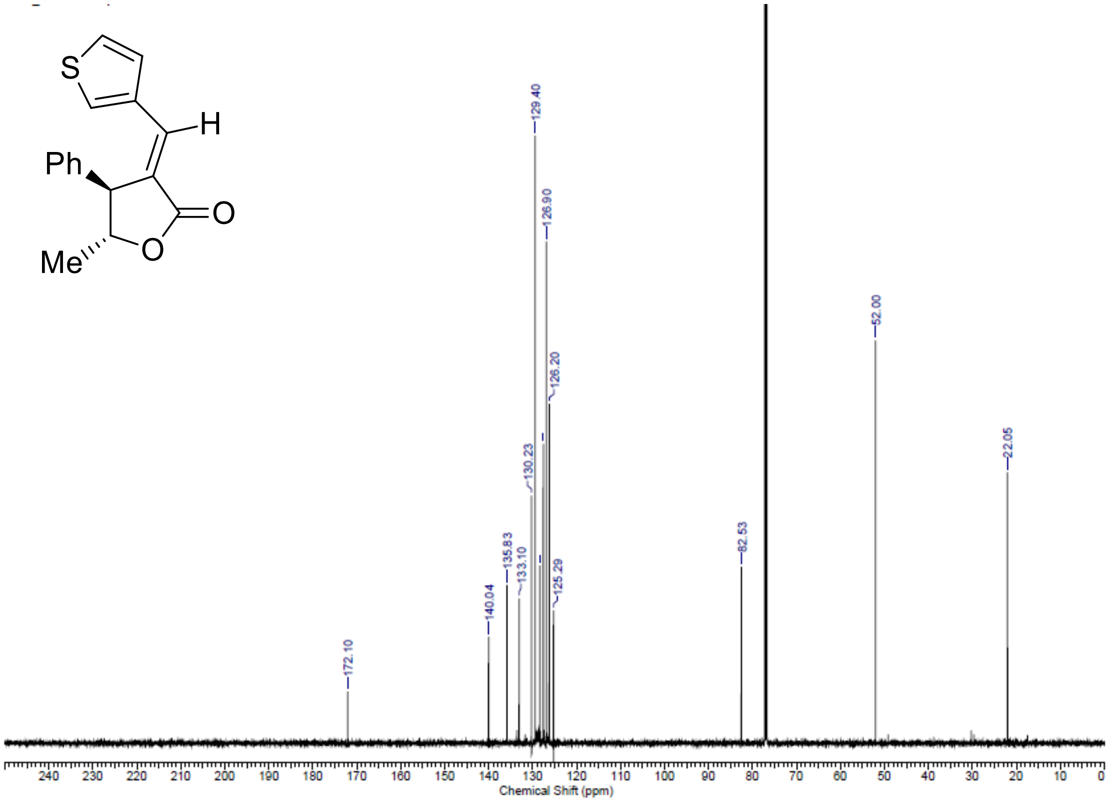
S
H
Ph
O
Me
O
172.10
140.04
135.83
133.10
130.23
129.40
126.90
126.20
125.29
82.53
52.00
22.05
240
230
220
210
200
190
180
170
160
150
140
130
120
110
100
90
80
70
60
50
40
30
20
10
0
Chemical Shift (ppm)

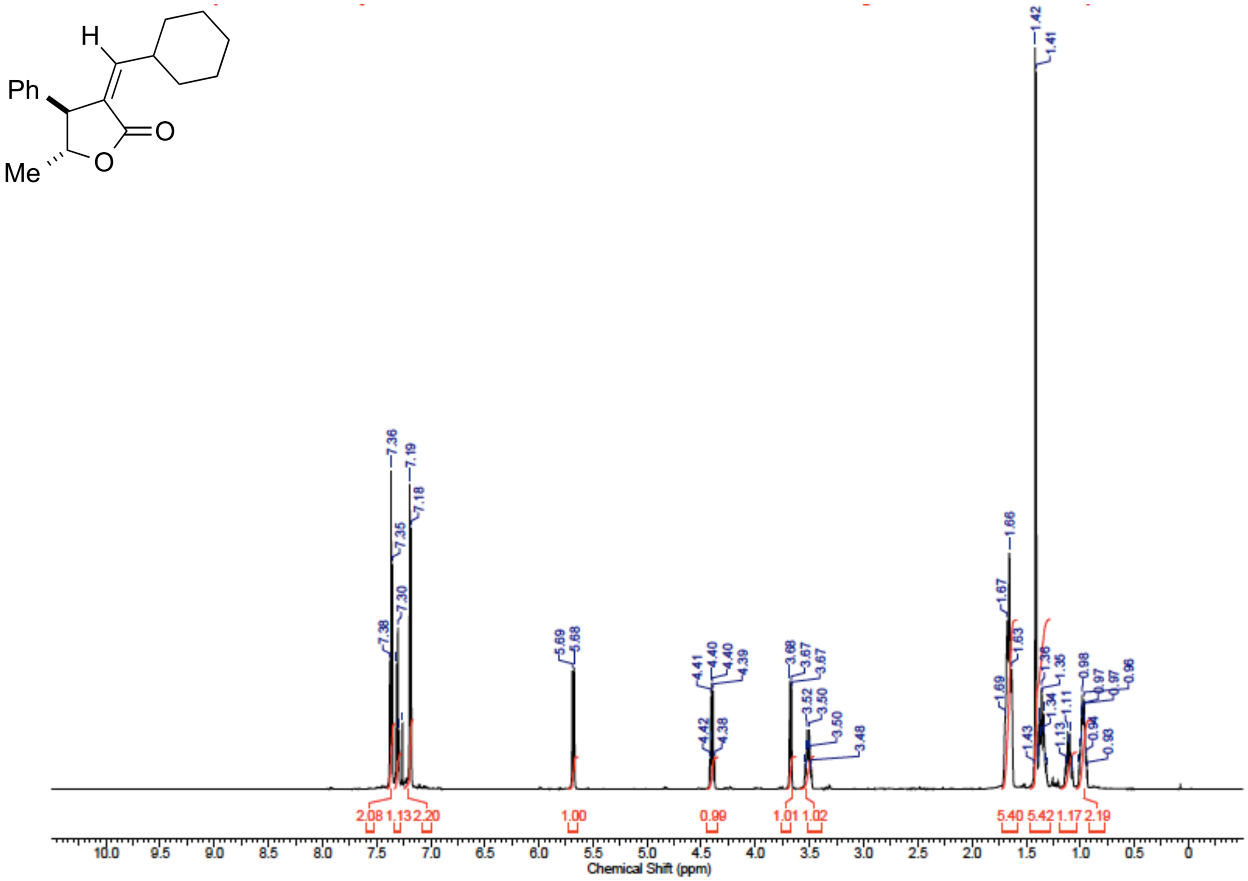
H
Ph
O
Me
O
7.38
7.36
7.35
7.30
7.19
7.18
5.69
5.68
4.42
4.41
4.40
4.40
4.39
4.38
3.68
3.67
3.67
3.52
3.50
3.50
3.48
1.69
1.67
1.66
1.63
1.43
1.42
1.41
1.36
1.35
1.34
1.13
1.11
0.98
0.97
0.97
0.96
0.94
0.93
2.08
1.13
2.20
1.00
0.99
1.01
1.02
5.40
5.42
1.17
2.19
10.0
9.5
9.0
8.5
8.0
7.5
7.0
6.5
6.0
5.5
5.0
4.5
4.0
3.5
3.0
2.5
2.0
1.5
1.0
0.5
0
Chemical Shift (ppm)

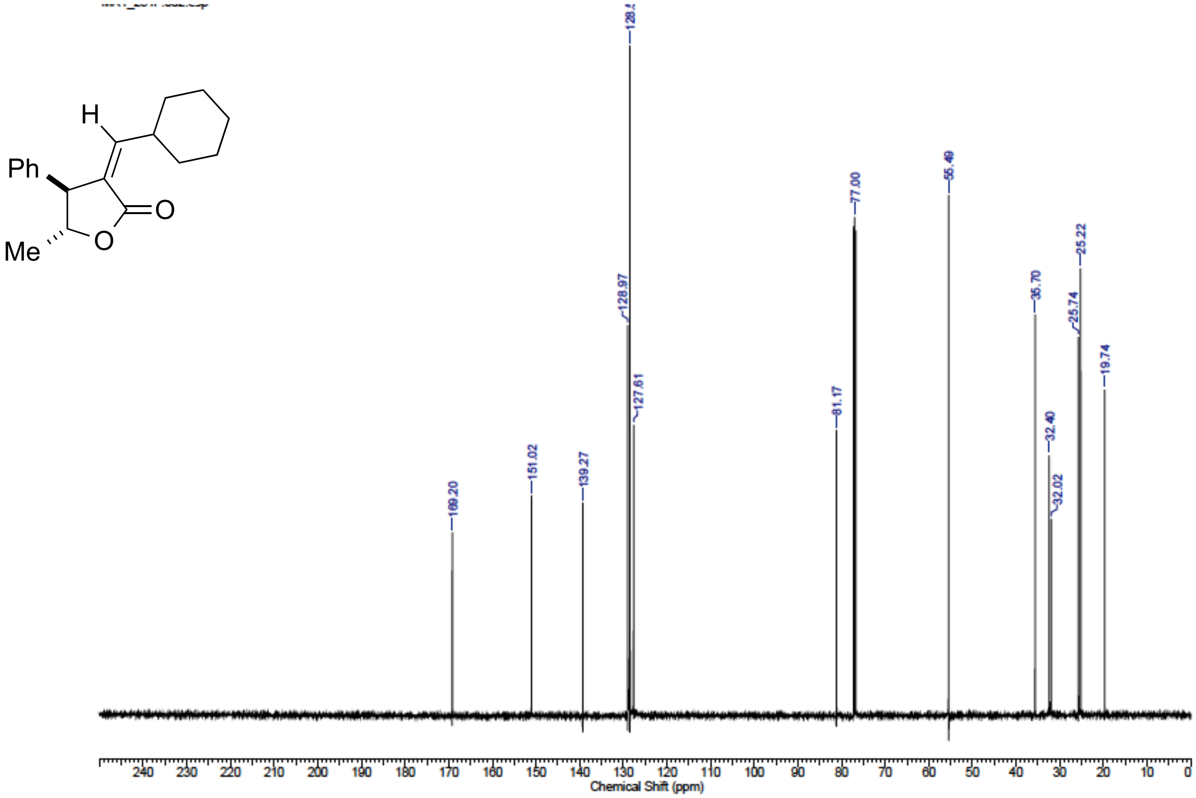
H
Ph
O
Me
O
169.20
151.02
139.27
128.97
128.5
127.61
81.17
77.00
55.49
35.70
32.40
32.02
25.74
25.22
19.74
240
230
220
210
200
190
180
170
160
150
140
130
120
110
100
90
80
70
60
50
40
30
20
10
0
Chemical Shift (ppm)

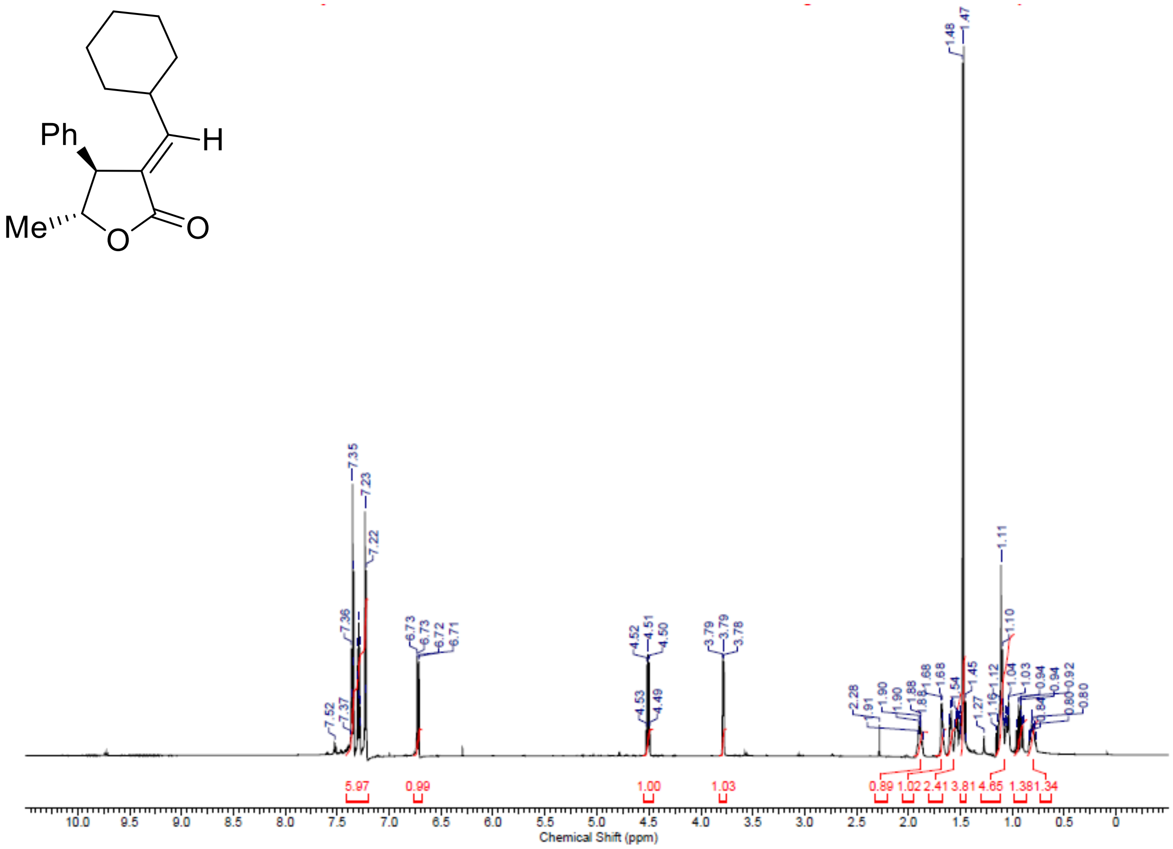
Ph
H
Me
O
O
7.52
7.37
7.36
7.35
7.23
7.22
6.73
6.73
6.72
6.71
4.53
4.52
4.51
4.50
4.49
3.79
3.79
3.78
2.28
1.91
1.90
1.90
1.88
1.88
1.68
1.68
1.54
1.48
1.47
1.45
1.27
1.16
1.12
1.11
1.10
1.04
1.03
0.94
0.94
0.92
0.84
0.80
0.80
5.97
0.99
1.00
1.03
0.89
1.02
2.41
3.81
4.65
1.38
1.34
10.0
9.5
9.0
8.5
8.0
7.5
7.0
6.5
6.0
5.5
5.0
4.5
4.0
3.5
3.0
2.5
2.0
1.5
1.0
0.5
0
Chemical Shift (ppm)

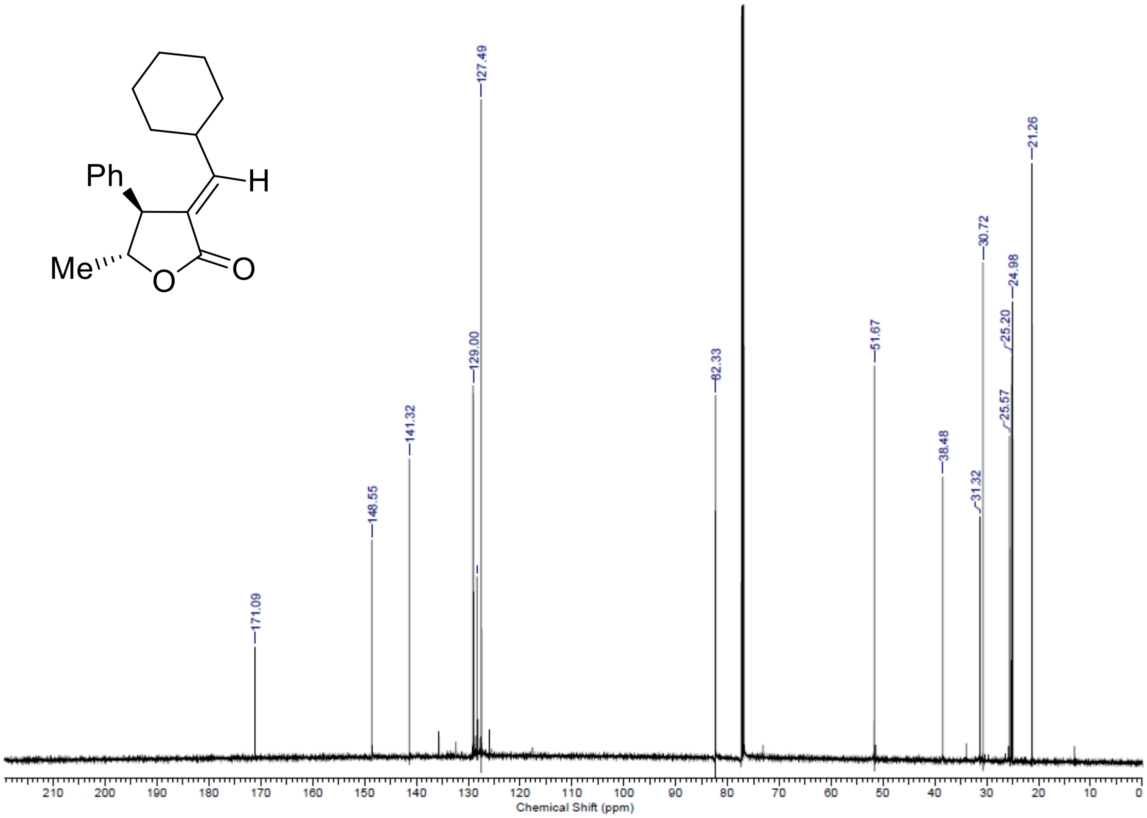
Ph
H
Me
O
O
171.09
148.55
141.32
129.00
127.49
82.33
51.67
38.48
31.32
30.72
25.57
25.20
24.98
21.26
210
200
190
180
170
160
150
140
130
120
110
100
90
80
70
60
50
40
30
20
10
0
Chemical Shift (ppm)

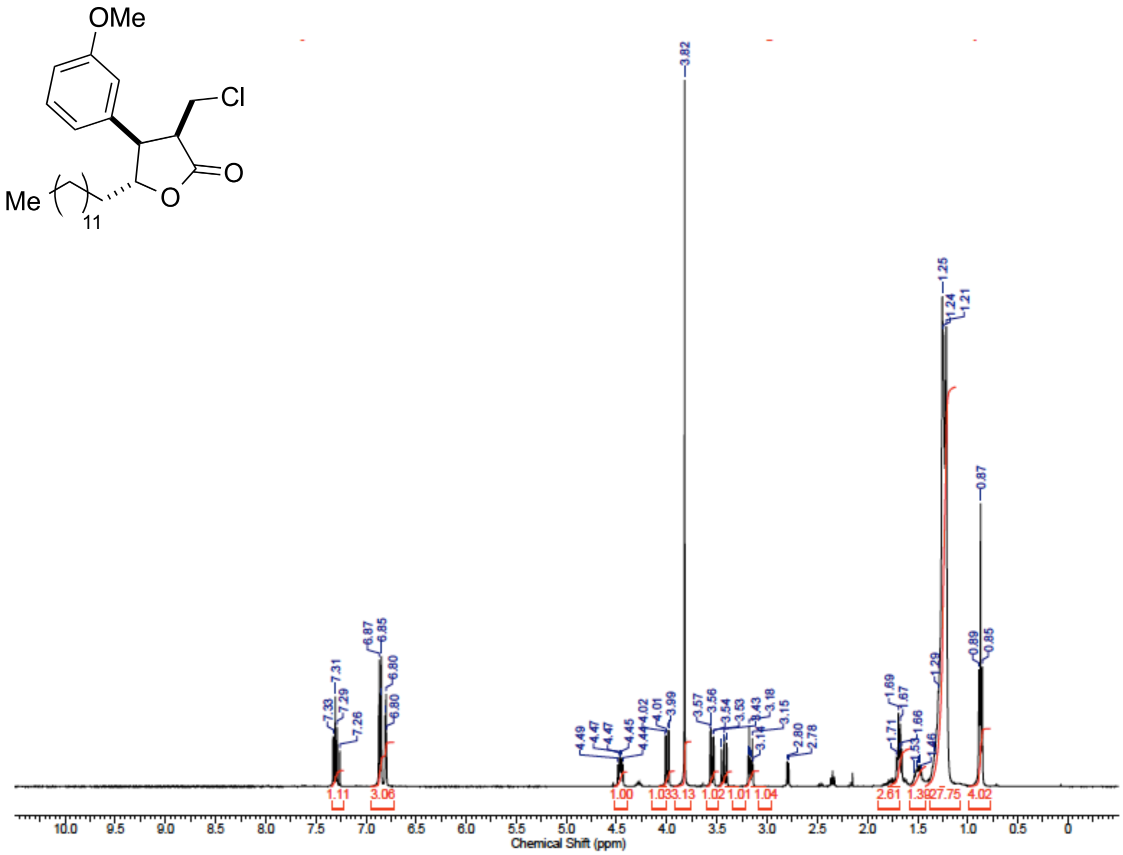
OMe
Cl
O
Me
O
11
3.82
1.25
1.24
1.21
0.87
0.89
0.85
1.29
7.33
7.31
7.29
7.26
6.87
6.85
6.80
6.80
4.49
4.47
4.47
4.45
4.44
4.02
4.01
3.99
3.57
3.56
3.54
3.53
3.43
3.18
3.15
3.14
2.80
2.78
1.71
1.69
1.67
1.66
1.53
1.46
1.11
3.06
1.00
1.03
3.13
1.02
1.01
1.04
2.61
1.30
27.75
4.02
10.0
9.5
9.0
8.5
8.0
7.5
7.0
6.5
6.0
5.5
5.0
4.5
4.0
3.5
3.0
2.5
2.0
1.5
1.0
0.5
0
Chemical Shift (ppm)

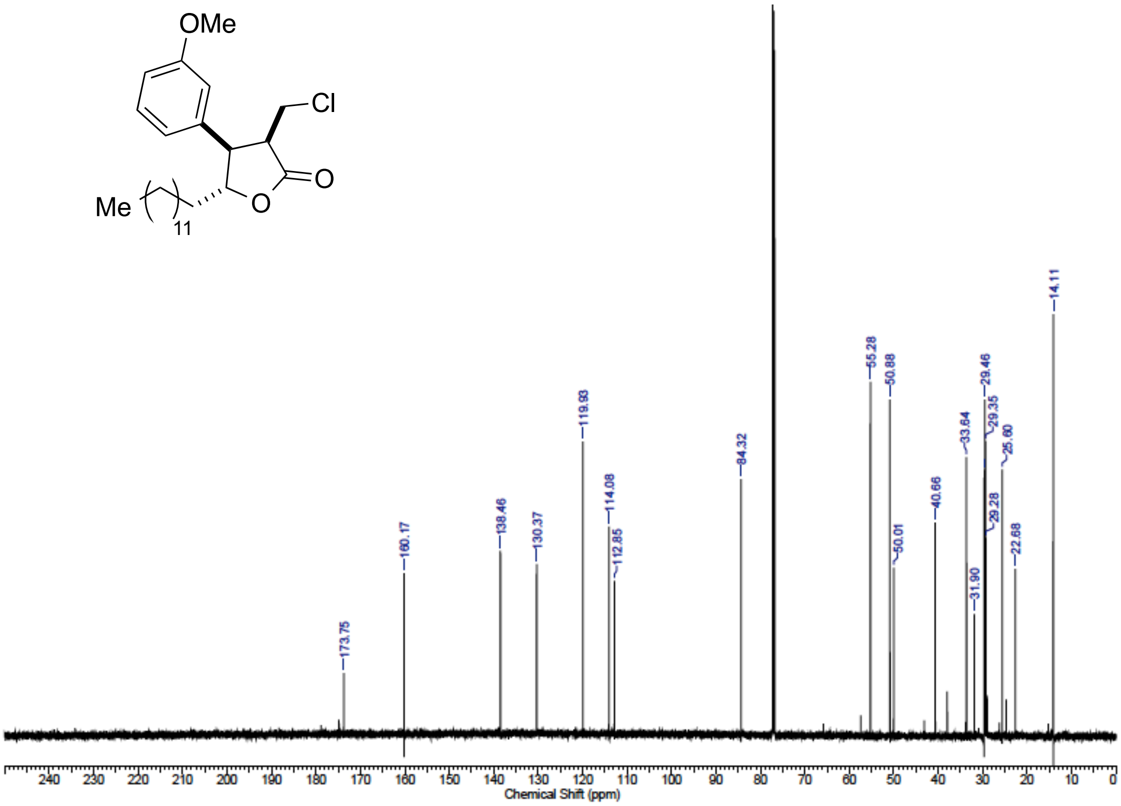
OMe
Cl
O
Me
O
11
173.75
160.17
138.46
130.37
119.93
114.08
112.85
84.32
55.28
50.88
50.01
40.66
33.64
31.90
29.46
29.35
29.28
25.60
22.68
14.11
240
230
220
210
200
190
180
170
160
150
140
130
120
110
100
90
80
70
60
50
40
30
20
10
0
Chemical Shift (ppm)

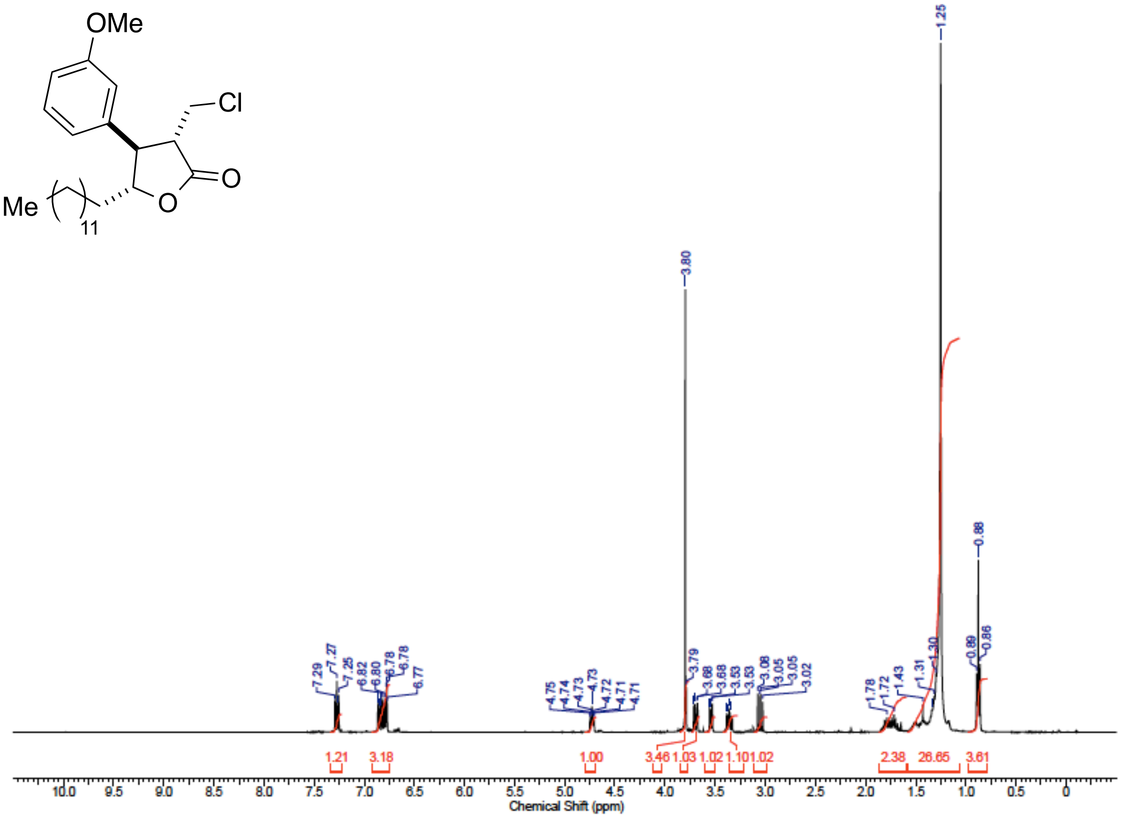
OMe
Cl
O
O
Me
11
7.29
7.27
7.25
6.82
6.80
6.78
6.78
6.77
4.75
4.74
4.73
4.73
4.72
4.71
4.71
4.71
3.80
3.79
3.68
3.68
3.53
3.53
3.08
3.05
3.05
3.02
1.78
1.72
1.43
1.31
1.30
1.25
0.89
0.88
0.86
1.21
3.18
1.00
3.46
1.03
1.02
1.10
1.02
2.38
26.65
3.61
10.0
9.5
9.0
8.5
8.0
7.5
7.0
6.5
6.0
5.5
5.0
4.5
4.0
3.5
3.0
2.5
2.0
1.5
1.0
0.5
0
Chemical Shift (ppm)

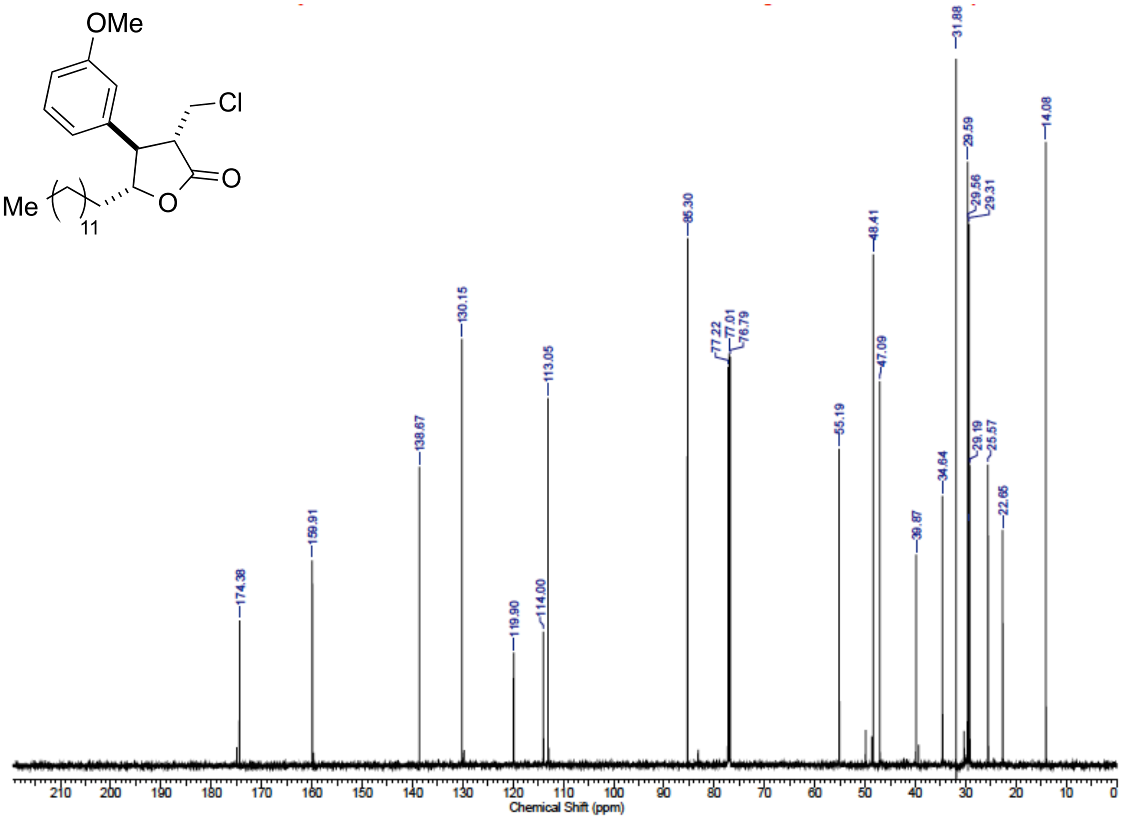
OMe
Cl
O
O
Me
11
174.38
159.91
138.67
130.15
119.90
114.00
113.05
85.30
77.22
77.01
76.79
55.19
48.41
47.09
39.87
34.64
31.88
29.59
29.56
29.31
29.19
25.57
22.65
14.08
210
200
190
180
170
160
150
140
130
120
110
100
90
80
70
60
50
40
30
20
10
0
Chemical Shift (ppm)

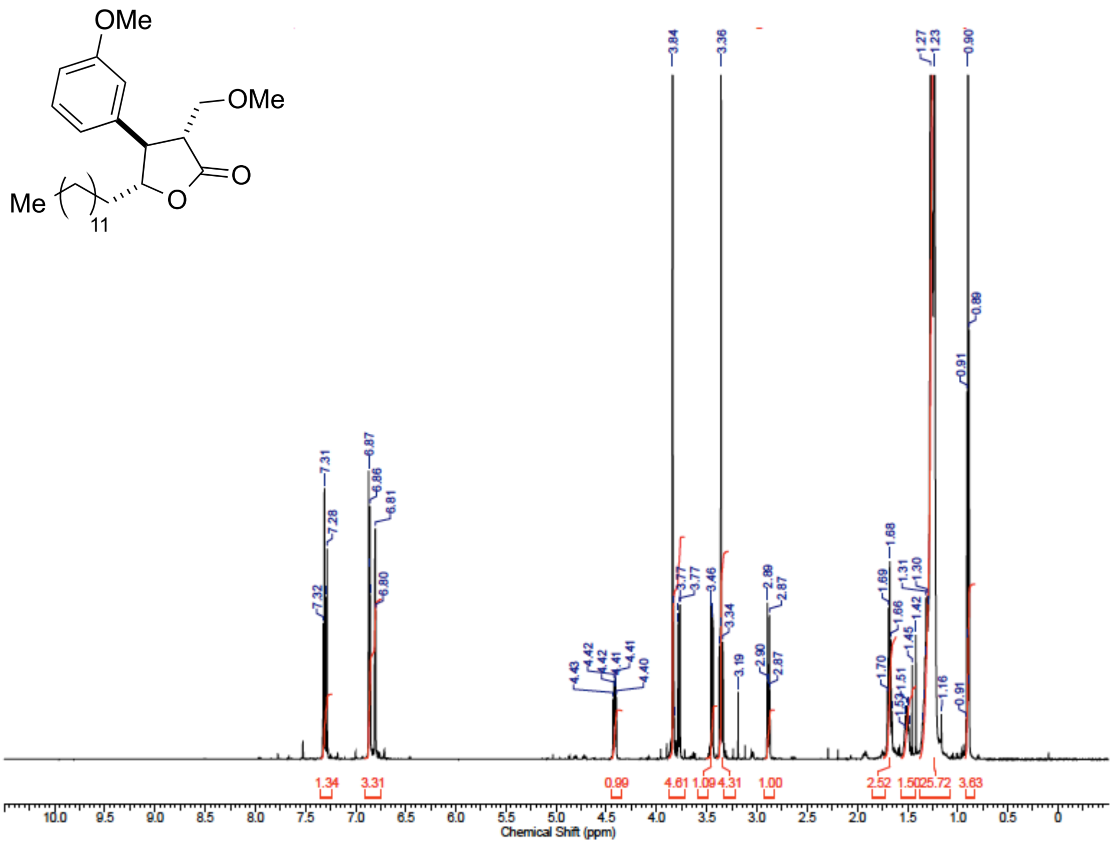
OMe
OMe
O
O
Me
11
7.32
7.31
7.28
6.87
6.86
6.81
6.80
4.43
4.42
4.42
4.41
4.41
4.40
3.84
3.77
3.77
3.46
3.36
3.34
3.19
2.90
2.89
2.87
2.87
1.70
1.69
1.68
1.66
1.53
1.51
1.45
1.42
1.31
1.30
1.27
1.23
1.16
0.91
0.91
0.90
0.89
1.34
3.31
0.99
4.61
1.09
4.31
1.00
2.52
1.50
25.72
3.63
10.0
9.5
9.0
8.5
8.0
7.5
7.0
6.5
6.0
5.5
5.0
4.5
4.0
3.5
3.0
2.5
2.0
1.5
1.0
0.5
0
Chemical Shift (ppm)

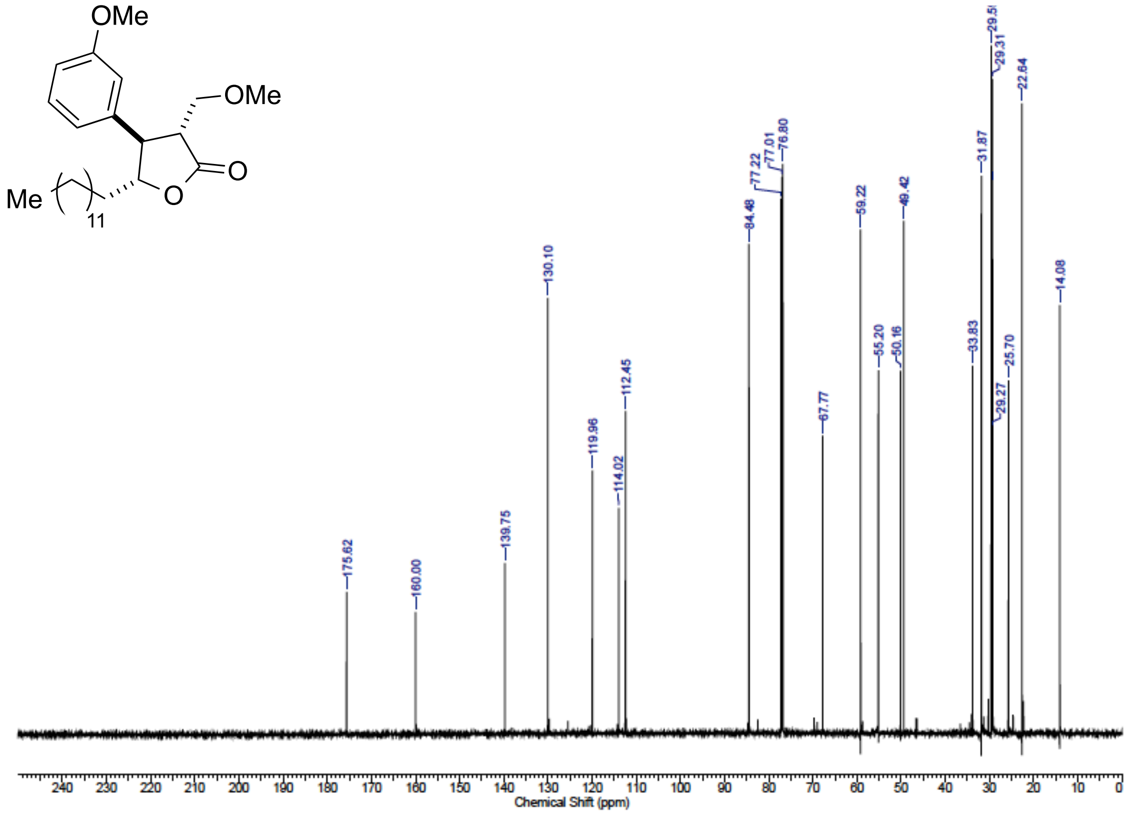
OMe
OMe
O
O
Me
11
175.62
160.00
139.75
130.10
119.96
114.02
112.45
84.48
77.22
77.01
76.80
67.77
59.22
55.20
50.16
49.42
33.83
31.87
29.5
29.31
29.27
25.70
22.64
14.08
240
230
220
210
200
190
180
170
160
150
140
130
120
110
100
90
80
70
60
50
40
30
20
10
0
Chemical Shift (ppm)

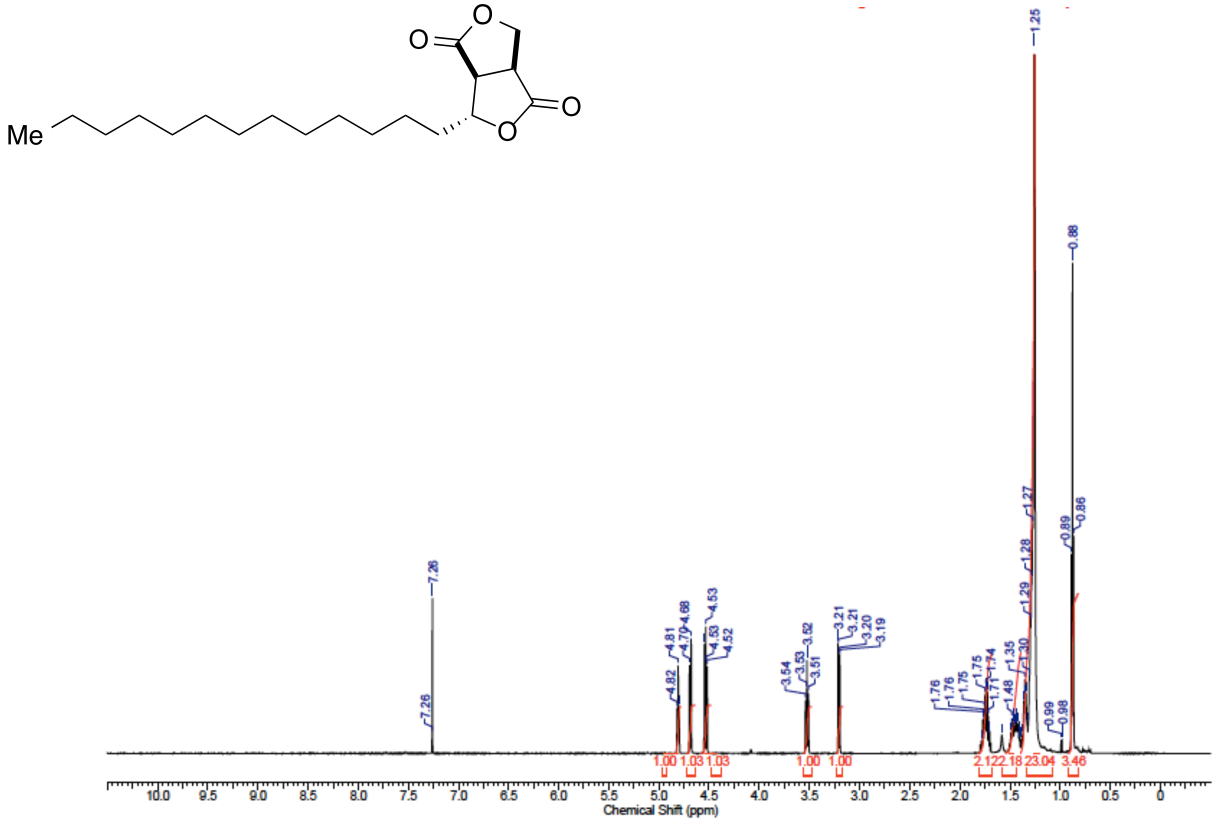
Me
O
O
O
O
7.26
7.26
4.82
4.81
4.70
4.68
4.53
4.53
4.52
3.54
3.53
3.52
3.51
3.21
3.21
3.20
3.19
1.76
1.76
1.75
1.75
1.74
1.71
1.48
1.35
1.30
1.29
1.28
1.27
1.25
0.99
0.98
0.89
0.88
0.86
1.00
1.03
1.03
1.00
1.00
2.12
2.18
23.04
3.46
10.0
9.5
9.0
8.5
8.0
7.5
7.0
6.5
6.0
5.5
5.0
4.5
4.0
3.5
3.0
2.5
2.0
1.5
1.0
0.5
0
Chemical Shift (ppm)

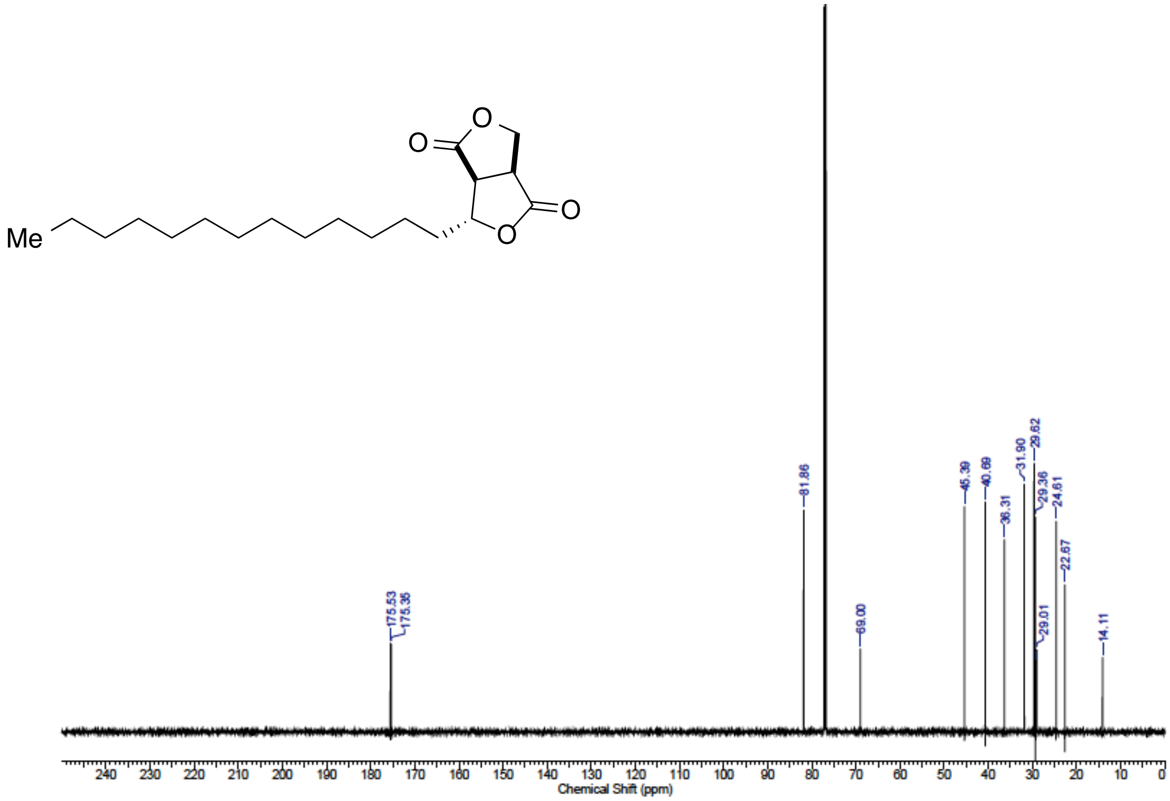
Me
O
O
O
O
175.53
175.35
81.86
69.00
45.39
40.69
36.31
31.90
29.62
29.36
29.01
24.61
22.67
14.11
240
230
220
210
200
190
180
170
160
150
140
130
120
110
100
90
80
70
60
50
40
30
20
10
0
Chemical Shift (ppm)

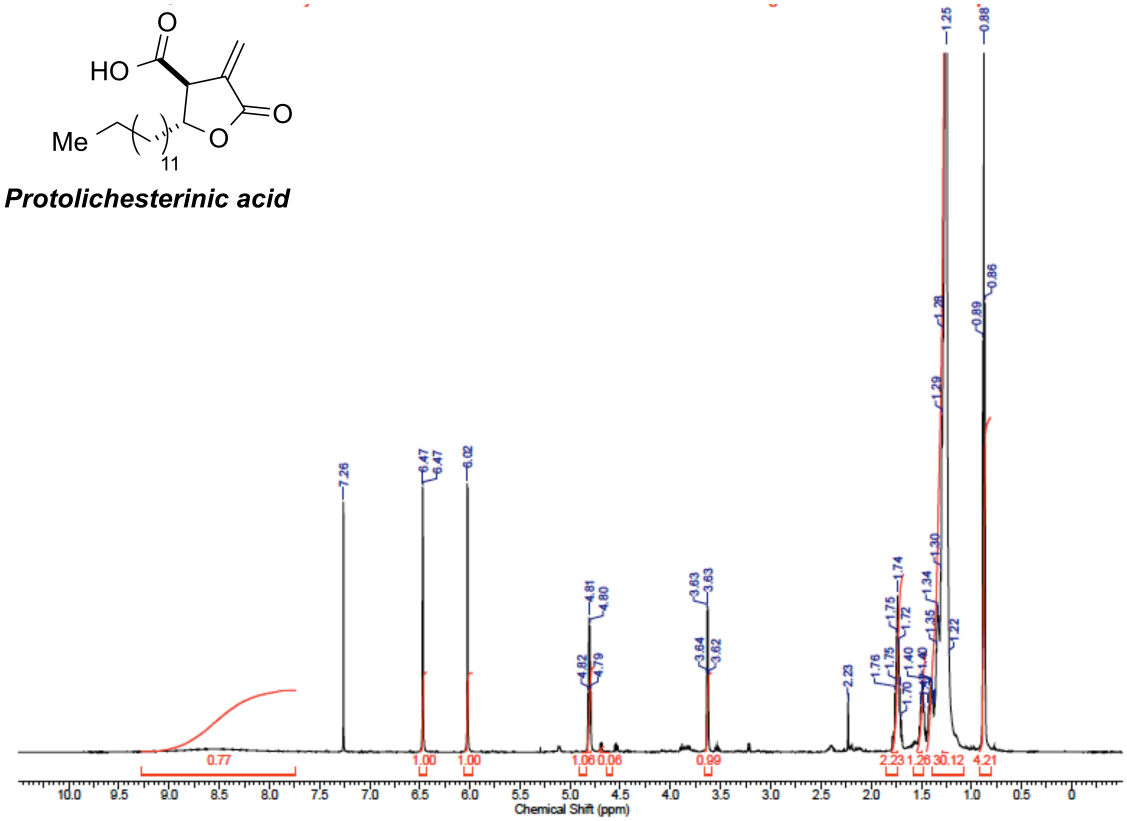
HO
O
O
O
Me
11
Protolichesterinic acid
7.26
6.47
6.47
6.02
4.82
4.81
4.80
4.79
3.63
3.63
3.64
3.62
2.23
1.76
1.75
1.75
1.74
1.72
1.70
1.40
1.40
1.35
1.34
1.30
1.29
1.28
1.25
1.22
0.89
0.88
0.86
0.77
1.00
1.00
1.06
0.06
0.99
2.23
1.26
30.12
4.21
10.0
9.5
9.0
8.5
8.0
7.5
7.0
6.5
6.0
5.5
5.0
4.5
4.0
3.5
3.0
2.5
2.0
1.5
1.0
0.5
0
Chemical Shift (ppm)

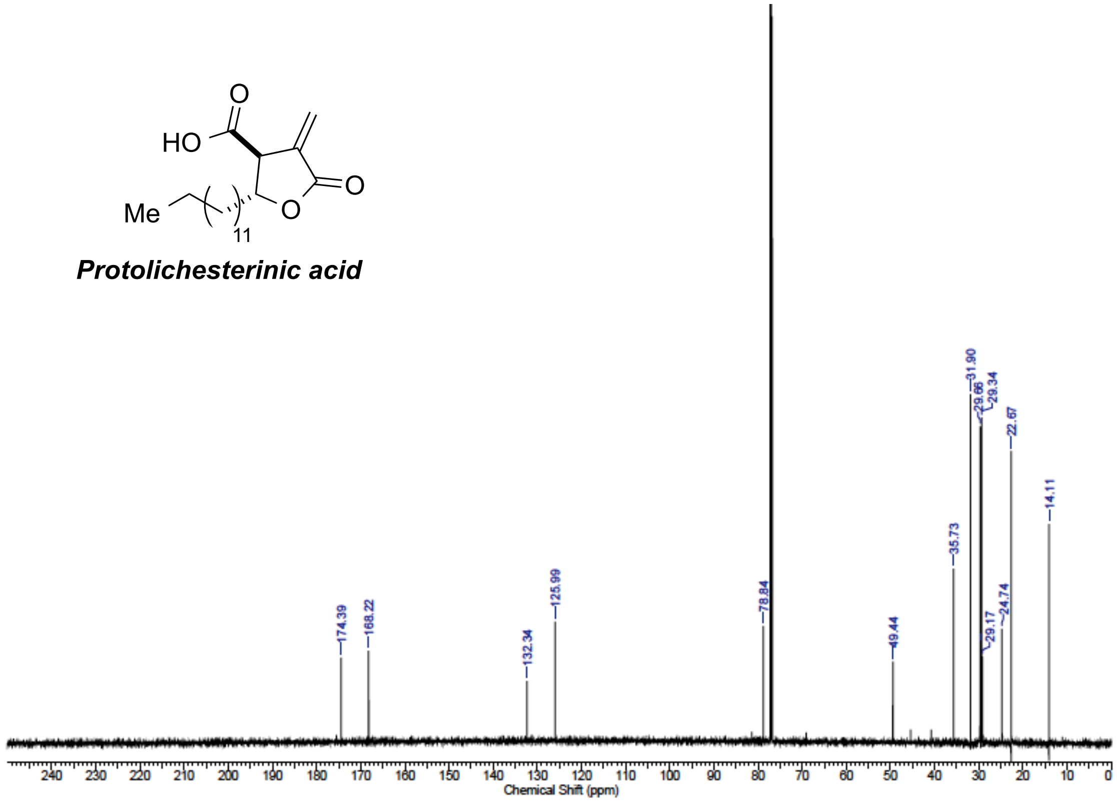
HO
O
O
O
Me
11
Protolichesterinic acid
174.39
168.22
132.34
125.99
78.84
49.44
35.73
31.90
29.66
29.34
29.17
24.74
22.67
14.11
240
230
220
210
200
190
180
170
160
150
140
130
120
110
100
90
80
70
60
50
40
30
20
10
0
Chemical Shift (ppm)

# REFERENCES

(1) Hoffmann, H.; Rabe, J. Synthesis and Biological Activity of α-Methylene-γ-Butyrolactones. Angew. Chem. Int. Ed. 1985, 24, 94–110.

(2) Kitson, R. R. A.; Millemaggi, A.; Taylor, R. J. K. The Renaissance of α-Methylene-γ-Butyrolactones: New Synthetic Approaches. Angew. Chem. Int. Ed. 2009, 48, 9426–9451.

(3) Kartnig, T. Cetraria islandica—Islandisches Moos. Z. Phytother 1987, 8, 127–130.

(4) Vartia, K. O. 1973. Antibiotics in lichens. p. 547–561. In V. Ahmadjian and M. E. Hale (ed.), The lichens. Academic Press, New York.

(5) Pengsuparp, T.; Cai, L.; Constant, H.; Fong, H. H.; Lin, L. Z.; Kinghorn, A. D.; Pezzuto, J. M.; Cordell, G. A.; Ingólfsdóttir, K.; Wagner, H. Mechanistic Evaluation of New Plant-Derived Compounds That Inhibit HIV-1 Reverse Transcriptase. *J. Nat. Prod.* **1995**, *58*, 1024–1031.

(6) Goel, M.; Dureja, P.; Rani, A.; Uniyal, P. L.; Laatsch, H. Isolation, Characterization and Antifungal Activity of Major Constituents of the Himalayan Lichen Parmelia Reticulata Tayl.†. *J. Agric. Food Chem.* **2011**, *59*, 2299–2307.

(7) Brisdelli, F.; Perilli, M.; Sellitri, D.; Piovano, M.; Garbarino, J. A.; Nicoletti, M.; Bozzi, A.; Amicosante, G.; Celenza, G. Cytotoxic Activity and Antioxidant Capacity of Purified Lichen Metabolites: an in VitroStudy. *Phytother. Res.* **2012**, *27*, 431–437.

(8) Kumar KC, S.; Müller, K. Lichen Metabolites. 1. Inhibitory Action Against Leukotriene B 4Biosynthesis by a Non-Redox Mechanism. *J. Nat. Prod.* **1999**, *62*, 817–820.

(9) Sisodia, R.; Geol, M.; Verma, S.; Rani, A.; Dureja, P. Antibacterial and Antioxidant Activity of Lichen Species Ramalina Roesleri. *Natural Product Research* **2013**, *27*, 2235–2239.

(10) Haraldsdóttir, S.; Guðlaugsdóttir, E.; Ingólfsdóttir, K.; Ögmundsdóttir, H. M. Anti-Proliferative Effects of Lichen-Derived Lipoxygenase Inhibitors on Twelve Human Cancer Cell Lines of Different Tissue Origin in Vitro. *Planta med* **2004**, *70*, 1098–1100.

(11) Park, B. K.; Nakagawa, M.; Hirota, A.; Nakayama, M. Methylenolactocin, a Novel Antitumor Antibiotic From Penicillium Sp. *J. Antibiot.* **1988**, *41*, 751–758.

(12) He, G.; Matsuura, H.; Yoshihara, T. Isolation of an α-Methylene-γ-Butyrolactogne Derivative, a Toxin From the Plant Pathogen Lasiodiplodia Theobromae. *Phytochemistry* **2004**, *65*, 2803–2807.

(13) Martin, J.; Watts, P. C.; Johnson, F. Carboxylation of Gamma-Butyrolactones with Methyl Methoxymagnesium Carbonate. New Synthesis of DL-Protolichesterinic Acid. *J. Org. Chem.* **1974**, *39*, 1676–1681.

(14) Patrick, T. M., Jr The Free Radical Addition of Aldehydes to Unsaturated Polycarboxylic Esters. *J. Org. Chem.* **1952**, *17*, 1009–1016.

(15) Mandal, P. K.; Maiti, G.; Roy, S. C. Stereoselective Synthesis of Polysubstituted Tetrahydrofurans by Radical Cyclization of Epoxides Using a Transition-Metal Radical Source. Application to the Total Synthesis of (±)-Methylenolactocin and (±)-Protolichesterinic Acid. *J. Org. Chem.* **1998**, *63*, 2829–2834.

(16) Baldwin, J. E. Rules for Ring Closure. *J. Chem. Soc., Chem. Commun.* **1976**, 734.

(17) De Azevedo, M. B.; Murta, M. M.; Greene, A. E. Novel, Enantioselective Lactone Construction. First Synthesis of Methylenolactocin, Antitumor Antibiotic From Penicillium Sp. *J. Org. Chem.* **1992**, *57*, 4567–4569.

(18) Loh, T.-P.; Lye, P.-L. A Concise Synthesis of (±)-Methylenolactocin and the Formal Synthesis of (±)-Phaseolinic Acid. *Tetrahedron Letters* **2001**, *42*, 3511–3514.

(19) Hodgson, D. M.; Talbot, E. P. A.; Clark, B. P. Stereoselective Synthesis of Β-(Hydroxymethylaryl/Alkyl)-α-Methylene-γ-Butyrolactones. *Org. Lett.* **2011**, *13*, 2594–2597.

(20) Fürstner, A.; Shi, N. Nozaki-Hiyama-Kishi Reactions Catalytic in Chromium. *J. Am. Chem. Soc.* **1996**, *118*, 12349–12357.

(21) a) Steward, K. M.; Corbett, M. T.; Goodman, C. G.; Johnson, J. S. Asymmetric Synthesis of Diverse Glycolic Acid Scaffolds via Dynamic Kinetic Resolution of Α-Keto Esters. *J. Am. Chem. Soc.* **2012**, *134*, 20197–20206. b) Steward, K. M.; Gentry, E. C.; Johnson, J. S. Dynamic Kinetic Resolution of Α-Keto Esters via Asymmetric Transfer Hydrogenation. *J. Am. Chem. Soc.* **2012**, *134*, 7329–7332.

(22) Hoppe, D. The Homoaldol Reaction, or How to Overcome Problems of Regio‐and Stereo‐Selectivity. *Angew. Chem. Int. Ed.* **1984**, *23*, 932–948.

(23) Sohn, S. S.; Rosen, E. L.; Bode, J. W. N-Heterocyclic Carbene-Catalyzed Generation of Homoenolates: Γ-Butyrolactones by Direct Annulations of Enals and Aldehydes. *J. Am. Chem. Soc.* **2004**, *126*, 14370–14371.

(24) Burstein, C.; Tschan, S.; Xie, X.; Glorius, F. N-Heterocyclic Carbene-Catalyzed Conjugate Umpolung for the Synthesis of Γ-Butyrolactones. *Synthesis* **2006**, *2006*, 2418–2439.

(25) Arduengo, A. J., III; Krafczyk, R.; Schmutzler, R.; Craig, H. A.; Goerlich, J. R.; Marshall, W. J.; Unverzagt, M. Imidazolylidenes, Imidazolinylidenes and Imidazolidines. *Tetrahedron* **1999**, *55*, 14523–14534.

(26) Yu, F.-L.; Jiang, J.-J.; Zhao, D.-M.; Xie, C.-X.; Yu, S.-T. Imidazolium Chiral Ionic Liquid Derived Carbene-Catalyzed Conjugate Umpolung for Synthesis of Γ-Butyrolactones. *RSC Adv.* **2013**, *3*, 3996.

(27) Feringa, B. L.; De Lange, B.; De Jong, J. C. Synthesis of Enantiomerically Pure. Gamma.-(Menthyloxy) Butenolides and (R)-and (S)-2-Methyl-1, 4-Butanediol. *J. Org. Chem.* **1989**, *54*, 2471–2475.

(28) Trost, B. M.; Crawley, M. L. A "Chiral Aldehyde" Equivalent as a Building Block Towards Biologically Active Targets. *Chem. Eur. J.* **2004**, *10*, 2237–2252.

(29) Shimada, S.; Hashimoto, Y.; Sudo, A.; Hasegawa, M.; Saigo, K. Diastereoselective Ring-Opening Aldol-Type Reaction of 2, 2-Dialkoxycyclopropanecarboxylic Esters with Carbonyl Compounds. 1. Synthesis of Cis 3, 4-Substituted. Gamma.-Lactones. *J. Org. Chem.* **1992**, *57*, 7126–7133.

(30) Shimada, S.; Hashimoto, Y.; Nagashima, T.; Hasegawa, M.; Saigo, K. Diastereoselective Ring-Opening Aldol-Type Reaction of 2, 2-Dialkoxycyclopropanecarboxylic Esters with Carbonyl Compounds. 2. Synthesis of Cis-2, 3-Substituted-Γ-Lactones. *Tetrahedron* **1993**, *49*, 1589–1604.

(31) Shimada, S.; Hashimoto, Y.; Saigo, K. Ring-Opening Aldol-Type Reaction of 2, 2-Dialkoxycyclopropanecarboxylic Esters with Carbonyl Compounds. 3. the Diastereoselective Synthesis of 2, 3, 4-Trisubstituted. Gamma.-Lactones. *J. Org. Chem.* **1993**, *58*, 5226–5234.

(32) Jun-Tao, F.; De-Long, W.; Yong-Ling, W.; He, Y.; Xing, Z. New Antifungal Scaffold Derived From a Natural Pharmacophore: Synthesis of ±a-Methylene-g-Butyrolactone Derivatives and Their Antifungal Activity Against Colletotrichum Lagenarium. *Bioorg. Med. Chem. Lett.* **2013**, *23*, 4393–4397.

(33) a) Jun-Tao, F.; De-Long, W.; Yong-Ling, W.; He, Y.; Xing, Z. New Antifungal Scaffold Derived From a Natural Pharmacophore: Synthesis of Î±-Methylene-Î³-Butyrolactone Derivatives and Their Antifungal Activity Against Colletotrichum Lagenarium. *Bioorg. Med. Chem. Lett.* **2013**, *23*, 4393–4397. b) Montgomery, T. P.; Hassan, A.; Park, B. Y.; Krische, M. J. Enantioselective Conversion of Primary Alcohols to A- Exo-Methylene Γ-Butyrolactones via Iridium-Catalyzed C–C Bond-Forming Transfer Hydrogenation: 2-(Alkoxycarbonyl)Allylation. *J. Am. Chem. Soc.* **2012**, *134*, 11100–11103.

(34) Öhler, E.; Reininger, K.; Schmidt, U. A Simple Synthesis of A-Methylene Γ-Lactones. *Angew. Chem. Int. Ed.* **1970**, *9*, 457–458.

(35) Csuk, R.; Schröder, C.; Hutter, S.; Mohr, K. Enantioselective Dreiding-Schmidt Reactions: Asymmetric Synthesis and Analysis of A-Methylene-Γ-Butyrolactones. *Tetrahedron: Asymmetry* **1997**, *8*, 1411–1429.

(36) Masuyama, Y.; Nimura, Y.; Kurusu, Y. Palladium-Catalyzed Carbonyl Allylation by 2-(Hydroxymethyl) Acrylate Derivatives: Synthesis of A-Methylene-Γ-Butyrolactones. *Tetrahedron Letters* **1991**, *32*, 225–228.

(37) Gagnier, S. V.; Larock, R. C. Palladium-Catalyzed Heteroannulation of 1,3-Dienes to Form A-Alkylidene-Γ-Butyrolactones. *J. Org. Chem.* **2000**, *65*, 1525–1529.

(38) Kennedy, J. W. J.; Hall, D. G. Novel Isomerically Pure Tetrasubstituted Allylboronates: Stereocontrolled Synthesis of A-Exomethylene Γ-Lactones as Aldol-Like Adducts with a Stereogenic Quaternary Carbon Center. *J. Am. Chem. Soc.* **2002**, *124*, 898–899.

(39) Hoffmann, R. W.; Schlapbach, A. *Liebigs. Ann. Chem.* **1990**, 1243-1248

(40) Kennedy, J. W. J.; Hall, D. G. Lewis Acid Catalyzed Allylboration: Discovery, Optimization, and Application to the Formation of Stereogenic Quaternary Carbon Centers. *J. Org. Chem.* **2004**, *69*, 4412–4428.

(41) Perkowski, A. J.; Nicewicz, D. A. Direct Catalytic Anti-Markovnikov Addition of Carboxylic Acids to Alkenes. *J. Am. Chem. Soc.* **2013**, *135*, 10334–10337.

(42) Grandjean, J.-M. M.; Nicewicz, D. A. Synthesis of Highly Substituted Tetrahydrofurans by Catalytic Polar-Radical-Crossover Cycloadditions of Alkenes and Alkenols. *Angew. Chem. Int. Ed.* **2013**, *52*, 3967–3971.

(43) Kelly, B. D.; Allen, J. M.; Tundel, R. E.; Lambert, T. H. Multicatalytic Synthesis of Complex Tetrahydrofurans Involving Bismuth(III) Triflate Catalyzed Intramolecular Hydroalkoxylation of Unactivated Olefins. *Org. Lett.* **2009**, *11*, 1381–1383.

(44) Clive, D. L. J.; Beaulieu, P. L. Formation of Carbon-Carbon Bonds by Ring Closure of B-Phenylselenocrotonates. *J. Chem. Soc., Chem. Commun.* **1983**, 307.

(45) Wei, X.-J.; Yang, D.-T.; Wang, L.; Song, T.; Wu, L.-Z.; Liu, Q. A Novel Intermolecular Synthesis of Γ-Lactones via Visible-Light Photoredox Catalysis. *Org. Lett.* **2013**, *15*, 6054–6057.

(46) Azam, S.; D'Souza, A. A.; Wyatt, P. B. Enantioselective Synthesis of 2-Substituted 4-Aminobutanoic Acid (GABA) Analogues via Cyanomethylation of Chiral Enolates. *J. Chem. Soc., Perkin Trans. 1* **1996**, 621.

(47) Clive, D. L. J.; Subedi, R. Radical Cyclization of O-Trityl Oximino Esters: a Ring Closure That Preserves the Oxime Function. *Chem. Commun.* **2000**, 237–238.